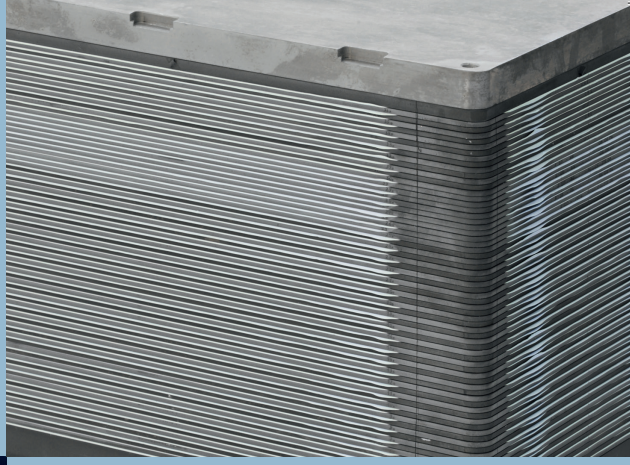

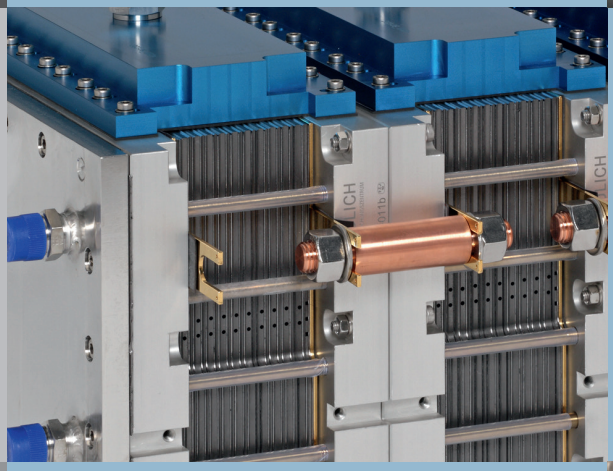

IEK-3 Report 2011

Climate-Relevant Energy Research

Member of the Helmholtz Association

JÜLICH
FORSCHUNGSZENTRUM

Schriften des Forschungszentrums Jülich
Reihe Energie & Umwelt / Energy & Environment Band / Volume 149

Forschungszentrum Jülich GmbH
Institute of Energiy and Climate Research (IEK)
Electrochemical Process Engineering (IEK-3)

IEK-3 Report 2011

Climate-Relevant Energy Research

Schriften des Forschungszentrums Jülich
Reihe Energie & Umwelt / Energy & Environment Band / Volume 149

ISSN 1866-1793 ISBN 978-3-89336-809-9

Bibliografische Information der Deutschen Nationalbibliothek.
Die Deutsche Nationalbibliothek verzeichnet diese Publikation in der
Deutschen Nationalbibliografie; detaillierte Bibliografische Daten
sind im Internet über <http://dnb.d-nb.de> abrufbar.

Herausgeber und Vertrieb:	Forschungszentrum Jülich GmbH Zentralbibliothek, Verlag D-52425 Jülich Telefon (02461) 61-5368 · Telefax (02461) 61-6103 E-Mail: zb-publikation@fz-juelich.de Internet: http://www.fz-juelich.de/zb
Umschlaggestaltung:	Grafische Medien, Forschungszentrum Jülich GmbH
Druck:	Grafische Medien, Forschungszentrum Jülich GmbH
Copyright:	Forschungszentrum Jülich 2012

Schriften des Forschungszentrums Jülich
Reihe Energie & Umwelt / Energy & Environment Band / Volume 149

ISSN 1866-1793
ISBN 978-3-89336-809-9

Vollständig frei verfügbar im Internet auf dem Jülicher Open Access Server (JUWEL)
unter http://www.fz-juelich.de/zb/juwel

Preface

The period under review here – 2009 and 2010 – is characterized by a far-reaching and radical transition to new research fields and structures. This process culminated in October 2010 with the official amalgamation of the Jülich research fields of energy and climate, and the formation of the new and dynamic Institute of Energy and Climate Research. This move united the six institutes focusing on energy and two on climate with the systems analysis with the technology evaluation project group. It aimed to focus activities in specific fields of work, identify common topics for in-depth cooperation, and to generate joint R&D results as solutions to the challenges of the future. The advantages of this concept were demonstrated in 2009 in the form of a PhD thesis jointly supervised by the two research areas on the topic of hydrogen emissions and their impacts on Arctic ozone depletion, which analyzed the risks of a global hydrogen economy. It was then decided that cooperation should be consolidated in these fields. This synergy between energy and climate research at Jülich is globally unique, and is only reflected in part in existing centers for energy and environmental research.

In this context, solutions to the growing problem of climate change are also being intensively sought. One possible solution involves the large-scale integration of renewable energy sources into the electricity market and the introduction of electric mobility in the transportation sector. However, considerable research and development efforts are required to provide the vital energy storage technologies of the next generation. These are the challenges that the Helmholtz centers address using their pertinent expertise. Within the framework of the energy storage and hydrogen initiatives, they receive additional funding from the Helmholtz Association (HGF) to implement sufficient R&D measures to help industry provide the key technologies currently lacking for a sustainable energy supply. The formal project conception and proposal for the two initiatives were completed during the period under review by the competent scientists at IEK-3, evaluated by the HGF Senate Commission and recommended for funding. R&D activities on H_2 system solutions began in January 2010 and will run for five years. Work on lithium-ion batteries began in January 2011 and will continue for four years.

Driven by the desire to adapt existing industrial infrastructure, the state government of North Rhine-Westphalia (NRW) has shown huge commitment over the last few decades to introducing new sustainable technologies. Fuel cells and hydrogen play a key role in this concept. The EnergieAgentur NRW provides substantial support in the transfer from research and development to the market and implementation. This includes assistance in relation to networking, demonstrating the state of the art in research and technology, as well as sharing information at conferences, workshops and working group meetings. After the 4th German Hydrogen Congress in 2008, the NRW Ministry of Economics appointed me Chairman of the 18th World Hydrogen Energy Conference 2010 (WHEC 2010) and entrusted me with its scientific coordination. This was a challenge that I readily accepted, as did the scientists at IEK-3 who assisted me with the detailed work. This involvement in WHEC 2010 in Essen, with almost 2,500 participants and 17 scientific contributions from IEK-3 employees, considerably increased the visibility of IEK-3 and its scientists in the field of hydrogen and fuel cells. I would like to take this opportunity to thank the employees involved in WHEC for their dedication and for their contributions to the conference, without which the 18th WHEC 2010 would not have been such a great success.

The high-temperature polymer fuel cell group, set up in 2008, continued to pursue basic research in the form of model-based simulations and the resolution of processes in phosphoric-acid-doped MEAs. It also made progress in the area of stack development with modules of the kW class. The aim of work on reformers for the catalytic conversion of middle distillates into a hydrogen-rich gas as well as work on SOFC stacks and DMFC energy systems is to achieve longer lifetimes and simultaneously lower degradation. Tests aiming to determine the maximum lifetime for the three technologies are still ongoing. Results so far are promising, indicating 3,000 hours for an autothermal reformer, approx. 27,000 hours for an SOFC stack, and almost 3,000 hours for a DMFC energy module. These values are a clear indication that the planned applications for each of these technologies will be ready for operation in the foreseeable future.

After two years of structural and thematic reforms, the focus is now on consolidating the new topics, providing them with suitable structures, appropriate infrastructure and qualified personnel. This process will be accompanied by changes in IEK-3 representing both opportunities and challenges for our employees along the way.

Jülich, September 2012

1

WHEC 2010

Contributions to the 18th World Hydrogen Energy Conference 2010

- Scientific coordination
- Coordination of accompanying events
- IEK-3 contributions
- Editing of books and publications

The World Hydrogen Energy Conference (WHEC) is an international conference with an associated trade fair and a number of accompanying events dealing with the same topic. The 18th WHEC 2010 took place from 16 to 21 May 2010 in Essen under the auspices of the International Association for Hydrogen Energy (IAHE). It was organized by the EnergyAgency.NRW and sponsored primarily by the Federal State of North Rhine-Westphalia and RWE (a leading European electricity and gas company). The aim was to provide a platform facilitating a comprehensive exchange of information between science, industry and politics in an effort to promote hydrogen as a clean energy carrier and fuel cells as clean energy converters. The conference also aimed to publicize new technologies, encourage strategic discussions and define ways of incorporating hydrogen technologies into the energy industry. As Conference Chairman, Professor Stolten was responsible for organizing the science-related aspects of the conference and for coordinating the specialist sessions and accompanying events. He was assisted by a highly efficient team of experts from the region and numerous colleagues from IEK-3. Books and series of publications on the conference documented the scientific and technical topics as well as the findings discussed and made them accessible to a wider audience.

1.1 Scientific coordination

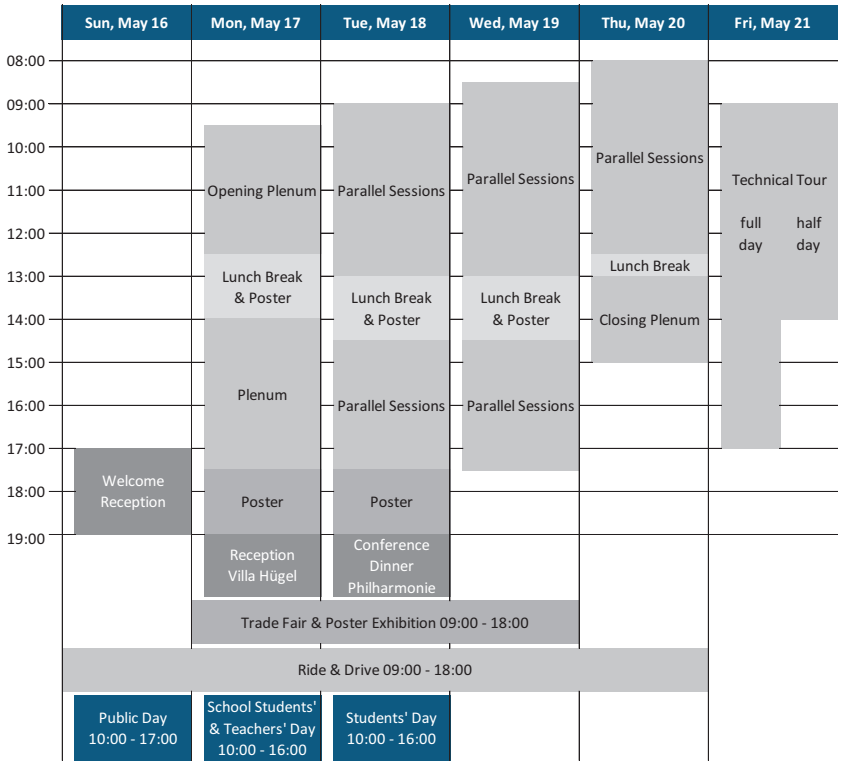

Tab. 1: Program overview

Solutions to scientific and strategic challenges in the areas of hydrogen and fuel cells on the basis of science and technology today, the specialist sessions at WHEC 2010 were divided into three separate sections over four days – opening plenum, closing plenum and parallel sessions. The timetable for these sessions and other conference events are shown in Tab. 1.

1.1.1 Opening plenum

The first day of the conference was characterized by presentations given by important decision-makers from politics and industry as well as representatives of various associations in plenary sessions. Following the opening address by Professor Stolten, IEK-3, and words of welcome from Professor Veziroglu, IAHE, and the Mayor of the City of Essen, Mr. Paß, three politicians – German Federal Minister of Transport, Building and Urban Affairs Dr. Ramsauer (see Fig. 1, top left) Minister President of North-Rhine Westphalia Dr. Rüttgers (see Fig. 1, bottom left) and Minister of Science and Technology of the People's Republic of China Professor Wan – outlined their viewpoints regarding the role of hydrogen technologies for Germany, North Rhine-Westphalia and China, respectively. Following this, high-ranking representatives from commercial enterprises and associations reported on the potential associated with the introduction of hydrogen using concrete examples.

Fig. 1: High-ranking representatives from politics (left) and industry (right)

Dr. Zetsche, Daimler (see Fig. 1, top right) spoke about hydrogen in the automotive industry, while Professor Reitzle (see Fig. 1, bottom right) Linde, outlined how the construction of a hydrogen infrastructure can be fostered in Germany. Mr. Solvay, Solvay, followed suit explaining the potential of hydrogen as a chemical raw material. Representatives from other ministries in Germany, the European Commission, the United States of America and Austria provided an overview of successful projects in the past, ongoing activities and planned projects together with their goals.

1.1.2 Parallel and poster sessions

The challenge associated with organizing the 18th WHEC 2010 was putting together an ambitious and well-structured program featuring complex topics on hydrogen and fuel cell technologies for a specialist audience, while simultaneously ensuring that separate events for the general public were also informative and interesting. The scientifically oriented part of the conference was spread out over two-and-a-half days in ten parallel sessions involving 326 speakers from 39 countries and a total of 342 presentations. An additional 176 speakers from 30 countries presented a total of 183 posters (see Fig. 2).

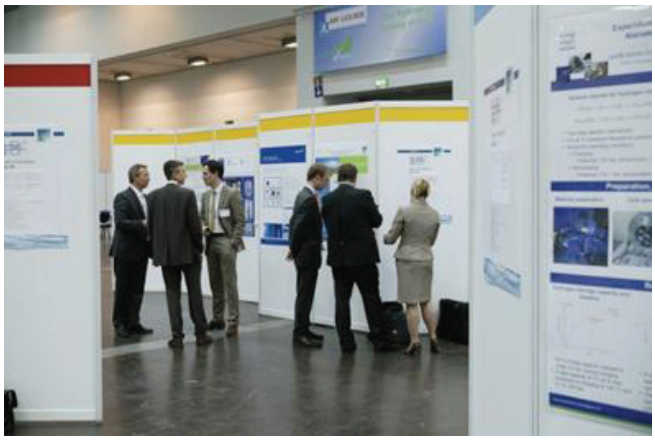

Fig. 2: Poster session

Abbr.	Main Topics	Number Sub-topics
FC	Fuel Cell Basics	5
HI	Fuel Infrastructures	3
HP	Hydrogen Production Technologies	7
HS	Storage Systems	3
IP	Policy Perspectives, Initiatives and Cooperations	3
SA	Strategic Analyses	8
SI	Safety Issues	2
SM	Existing and Emerging Markets	4
ST	Stationary Applications	2
TA	Transportation Application	6

Tab. 2: Overview of topics

The sessions were divided into ten blocks according to topic (see Tab. 2), each of which comprised two to eight subtopics. This resulted in a total of 43 blocks. Each block was

presided over by an expert who introduced the series of specialist presentations by providing an overview of the fundamentals involved and the relevant state of the art in science and technology. These review presentations were also compiled by the experts as scientific articles averaging around 20 pages each, which were published by WILEY-VCH as a book edited by Professor Stolten (see Chapter 1.4). IEK-3 made notable contributions to both sessions. It was responsible for six review presentations and six specialist presentations as well as three posters.

1.1.3 Closing plenum

With contributions from Professor Fletcher, Professor Stolten and Professor Veziroglu, the two-hour closing plenum looked back at the various conference events, assessed the progress made and predicted what developments and trends can be expected in the future. Based on the positive feedback on all parts of the conference program, we can conclude that the 18th WHEC 2010 in Essen was a resounding success.

On the very first day, the German national and federal state governments together with industry declared their intention to promote and provide new technologies starting in 2015. During the course of WHEC, it became clear that mobility is the dominant driving force for the introduction of hydrogen and fuel cell technologies. With respect to local zero-emission and highly efficient mobility by means of cars, it was shown that vehicles can be powered by batteries for short journeys but that the substitution of today's cars demands fuel cell vehicles powered by hydrogen. In discussions on reducing costs, two potential factors were identified as important: increasing production volume and improving materials and systems engineering. Basic research should continue to concentrate on identifying base metal catalysts for PEFC technology. SOFC technology necessitates a significant improvement in lifetime beyond the level that can be achieved today (30,000 hours). This is particularly important to further improve stationary applications of fuel cells, which have already generated reliable performance data in long-term field tests. As part of the German CALLUX project, around 800 devices will be installed by 2012 as fuel cell heating units for use in domestic applications.

Energy paths based on renewable energies will be dominated by hydrogen production in future. Thermochemical processes utilizing high-temperature heat from concentrated solar radiation, fermentative and photobiological processes, electrolysis combined with wind power and solar electricity, and photocatalysis are among the solutions being considered. Furthermore, generation paths based on fossil fuels must be improved in terms of efficiency and costs, and the emission of greenhouse gases must be reduced by means of CO_2 capture and storage. The question of hydrogen storage focuses on construction issues. The main solutions being discussed are pressure vessels of the fourth generation and storage systems on a hydride basis.

The conference came to a close with a reminder from Terry Kimmel of the Canadian Hydrogen and Fuel Cell Association that the 19th WHEC 2012 will take place in Toronto. Kimmel extended an invitation to all delegates present to come to the event in two years' time in Canada.

1.2 Coordination of accompanying events

Headed by Dr. Emonts, a working group of sixteen came up with ideas for one-day events targeting the general public, school students and their teachers, and undergraduates. In designing the program and selecting the various presentations and activities, great emphasis was placed on the target groups with their different expectations and requirements. The place and date of the accompanying events were carefully selected in an effort to guarantee success and to ensure that the conference itself could continue unaffected.

1.2.1 Events for the general public

On Sunday, 16 May 2010, the general public was invited to an event on the banks of Lake Baldeney in Essen. Interested visitors also had the opportunity to admire the four artificial islands in the lake known as the “Ruhr Atoll”. The artworks created by concept artist Norbert Bauer from Gelsenkirchen were exhibited under the motto of “Art is energy – energy is movement”.

The day for the general public also offered visitors an opportunity to test drive vehicles themselves or experience them as a passenger (see Fig. 3, left). The program also featured different exhibits and an information stand with employment opportunities, allowing the some 5,000 visitors to bridge gaps in their knowledge of new and emerging energy supply technologies, to experience practical applications of these technologies (see Fig. 3, right), and to network and lay the foundation for their own careers. The involvement of regional radio stations as well as competent catering companies rounded off the day, which was also blessed with warm sunny weather.

Fig. 3: Photos of the day for the general public. Left: Fuel cell vehicle with an opportunity to test drive. Right: Exhibition tent with slot cars powered by fuel cells

1.2.2 Event for school students and teachers

The program of events for school students and teachers was aimed at secondary-school students aged 15 years and over as well as trainees in technical areas and their teachers. Participants were expected to have a basic knowledge of physics and chemistry in order to understand the various lectures and presentations. On Monday, 17 May 2010, a total of 390 school students and their teachers availed of the ambitious program (see Fig. 4). The majority of participants came from North Rhine-Westphalia. In order to allow the school

students and their teachers to experience the international, scientific and technological atmosphere of the WHEC conference itself, these events were also held in the same exhibition center in Essen.

Fig. 4: School students' and teachers' day. School students (left) and teachers (right) at the exhibition showcasing practical applications and lessons

The six-hour program comprised five different blocks dealing with different topics. Under the motto "fascinating hydrogen technology", school students and teachers were treated to a warm-up session with four experts chaired by Witold Franke on conference-related topics such as the challenges associated with providing energy in the future, ideas for the first hydrogen applications by 2020, and visions for 2050. Following this, the five national champions of the global school student competition organized by the International Partnership for Hydrogen and Fuel Cells in the Economy (IPHE) presented the results of their work on hydrogen and fuel cell technologies. During the subsequent lunch break, representatives from universities and research institutions were at hand to answer questions and provide information on university courses and vocational training. The second half of the day involved separate programs for school students and teachers. Representatives from renowned German research institutions spoke to school students about research and development on fuel cell technologies. Teachers received an introduction to ways of incorporating fuel cells into lesson plans and their application in practice. The day was rounded off with a guided tour of the trade fair and exhibition and participation in a "Ride & Drive" event with numerous fuel cell and hydrogen vehicles.

1.2.3 Events for university studends

Separate parallel and poster sessions were organized for interested university students on Tuesday, 18 May 2010. The 93 students who participated also had an opportunity to visit the trade fair and exhibition as well as the "Ride & Drive" event. In addition, information was available during the breaks on possible undergraduate dissertations and PhD theses, vacant positions in industry, universities and research institutions, as well as alumni activities at RWTH Aachen University and Forschungszentrum Jülich.

1.3 IEK-3 contributions

IEK-3 also participated in past WHEC events, contributing to WHEC 2008 in Brisbane, Australia, as well as WHEC 2006 in Lyon, France. The fact that the 18th WHEC 2010 took place in Essen, which is near where IEK-3 is located in Jülich, and the technological orientation of the conference program meant that more IEK-3 employees contributed this time around. They were involved in the specialist sessions on all levels of the conference and were also represented at the trade fair and exhibition.

1.3.1 Conference papers

Session	Session Topic	Presentation Topic	Responsible Speaker
Review	Plenum Day	The Potential Role of Hydrogen as an Energy Carrier	Detlef Stolten
	FC.2 PEM/HT-PEM	High-Temperature PEM Fuel Cell: Electrolytes, Cells, and Stacks	Christoph Wannek
	FC.3 Direct Fuel Cells	Current Status of and Recent Developments in Direct Liquid Fuel Cells	Jürgen Mergel
	HP.3c Alkaline Electrolysis	Alkaline Electrolysis - Introduction and Overview	Detlef Stolten
	SM.3 APUs	Auxiliary Power Units for Light-Duty Vehicles, Trucks, Ships, and Airplanes	Ralf Peters
	TA.4 SA & WtW Studies	Systems Analysis and Well-to-Wheel Studies	Thomas Grube
Parallel	HP.4a Reforming & Gasification	Development of Fuel Cell Systems for Aircraft Applications Based on Synthetic Fuels	Joachim Pasel
	SM.4 Portables	System Technology Aspects for Light Traction Applications of Direct Methanol Fuel Cells	Holger Janßen
	FC.2 PEM/HT-PEM	Cell Resistances of ABPBI-Based HT-PEFC-MEAs: Time Dependence and Influence of Operating Conditions	Werner Lehnert
	FC.3 Direct Fuel Cells	Manufacturing Technologies for Direct Methanol Fuel Cells (DMFCs)	Andreas Glüsen
	FC.5 Advanced Modelling	Hierarchical 3D Multiphysics Modelling in the Design and Optimisation of SOFC System Components	Murat Peksen
	SM.2 Space & Aeronautic	Desulfurization of Jet Fuel for Fuel Cell-Based APU Systems in Aircraft	Yong Wang
	FC.4 HT Fuel Cells	Evaluation of the Electrical Contact Area at the SOFC Cathode	Vincent Haanappel
	SA.4 Education & Awareness	Contributrions to Education and Training made by Institutional Research	Bernd Emonts
Poster	FC.3 Direct Fuel Cells	Combined Local Current Distribution Measurements and High Resolution Neutron Radiography of Operating DMFCs	Alexander Schröder
	HP.3a H2 from Renewables	Analysis of the Impact of Hydrogen on Wind Power	Denis Krieg
	SM.4 Portables	Hybridization and Control of Direct Methanol Fuel Cell Systems for Material Handling Applications	Jörg Wilhelm

Tab. 3: Overview of IEK-3 presentations and posters

A total of 17 papers were given by scientists from IEK-3 during the opening plenum and parallel and posters sessions at WHEC. Six of the review presentations were given by scientists from the institute testifying to the outstanding excellence and broad-based competence of IEK-3. The various presentations given by IEK-3 scientists are listed in Tab. 3. Reflecting the focus on research and development and the R&D initiatives at IEK-3, five presentations dealt with DMFC technology, two looked at the HT-PEFC and two concentrated on SOFC technology. Another three presentations were on fuel processing and three dealt with hydrogen technologies. Two further presentations addressed overarching topics in the areas of systems analysis and professional development as well as public perception.

1.3.2 Trade fair and exhibitions

The WHEC trade fair and exhibition was made possible thanks to the commitment of numerous international commercial enterprises (59 %), research and development institutions (13 %), and ministries and organizations (28 %). In total, 136 exhibitors from 13 countries had stands at the 5,600 m² trade fair for relevant products, technology providers, R&D findings and a range of services. The German pavilion was divided into seven exhibition areas, each with an area of 80 m². Key German research institutes and German industry presented their current R&D activities in the area of fuel cell and hydrogen technologies. IEK-3 showcased its latest research and development results in the area of kilowatt-class fuel cells and reformers with functioning SOFC and HT-PEFC stacks as well as an autothermal reformer (see Fig. 5). Interested visitors also had an opportunity to gain detailed information on R&D priorities at IEK-3 and to assemble an HT-PEFC stack using realistic components under the guidance of the IEK-3 staff manning the stand. The exhibits were supplemented by a fuel processing module in a stand measuring 80 x 80 x 200 cm³ covering all of the conversion steps that make it possible to create a hydrogen-rich fuel gas from kerosene, water and air for an HT-PEFC with an electric power of a few kilowatts.

Fig. 5: IEK-3 booth at the trade fair

1.4 Editing of books and publications

In order to document the results of the conference and make them available to interested scientists and specialists, the organization committee developed a documentation concept and put a lot of effort into implementing it. This concept comprised three elements. The first involved the advance publication of the comprehensive review presentations given by the relevant experts as a book by WILEY-VCH, which was then distributed to each participant at WHEC together with the conference documentation. A supplement in the specialist energy journal focusing on fuel, heat and power ("BWK Das Energie-Fachmagazin") was also published in advance of WHEC by VDI Verlag. The idea was to provide information on the conference topics and advertise it in advance. The aim of the seven-volume conference proceedings on all of the parallel sessions was to provide an overview of the topics discussed at the conference.

1.4.1 Book of review articles

The first edition of the 877-page book published by WILEY-VCH and edited by Detlef Stolten appeared in May 2010 (see Fig. 6). It targeted scientists and engineers already familiar with the topics of hydrogen and fuel cells but who wanted to increase their knowledge substantially, as well as at young professionals with a background in the natural sciences. In the book, experts on hydrogen energy from science, industry and politics present the growing range of technologies offering a clean, sustainable and cost-effective alternative to non-renewable energies.

Of the 43 review presentations given at the conference, 41 were published unabridged in the book. The articles deal with separate topics including the fundamentals, the history and the current status of science and technology, as well as recommendations for future research and development. The book is a comprehensive reference work that provides those new to the field with an introduction and experts who are also involved in lecturing at universities with a basis for developing new courses and modules

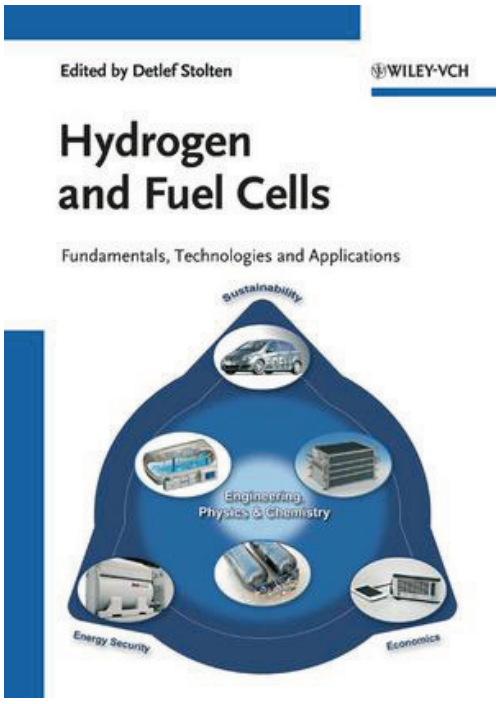

Fig. 6: WILEY-VCH book "Hydrogen and Fuel Cells"

1.4.2 Supplement on hydrogen in "BWK Das Energie-Fachmagazin"

In the run-up to the 18th WHEC 2010, the April edition of the specialist energy journal focusing on fuel, heat and power ("BWK Das Energie-Fachmagazin") contained a supplement on hydrogen with nine articles. On the topic of future energy storage systems in cars, Thomas Grube and Detlef Stolten were responsible for an article on the advantages of using hydrogen. They looked at the technical aspects of on-board power supply and derived options for fuel cells and batteries. They came to the conclusion that the advantages of zero-emission mobility for a service life and standard of comfort similar to what we are used to today will only be achievable with hydrogen-operated fuel cell vehicles. Battery operation may be a viable option for vehicles travelling short distances.

1.4.3 Conference proceedings of the plenary, session and poster sessions

Following the 18th WHEC 2010, the majority of speakers at the individual sessions submitted a three-to-six-page article for publication in the conference proceedings, which comprises seven separate volumes. The conference proceedings were edited by Detlef Stolten, Bernd Emonts and Thomas Grube and published by Forschungszentrum Jülich. Tab. 4 provides an overview of the contents covered by the individual volumes.

Volume	Scope	Pages	ISBN
78	Speeches and Plenary Talks	141	978-3-89336-658-3
78-1	Fuel Cell Basics Fuel Infrastructure	460	978-3-89336-651-4
78-2	Hydrogen Production Technologies - Part 1	400	978-3-89336-652-1
78-3	Hydrogen Production Technologies - Part 2	640	978-3-89336-653-8
78-4	Storage Systems Policy Perspectives, Initiatives and Cooperations	500	978-3-89336-654-5
78-5	Strategic Analysis Safety Issues Existing and Emerging Markets	530	978-3-89336-655-2
78-6	Stationary Applications Transportation Applications	330	978-3-89336-656-9

Tab. 4: Content and scope of the conference proceedings

The 19th WHEC 2012 will take place from 3 - 7 June 2012 in Toronto, Canada. It is being jointly organized by representatives from the Canadian Hydrogen and Fuel Cell Association and the Natural Resources Canada.

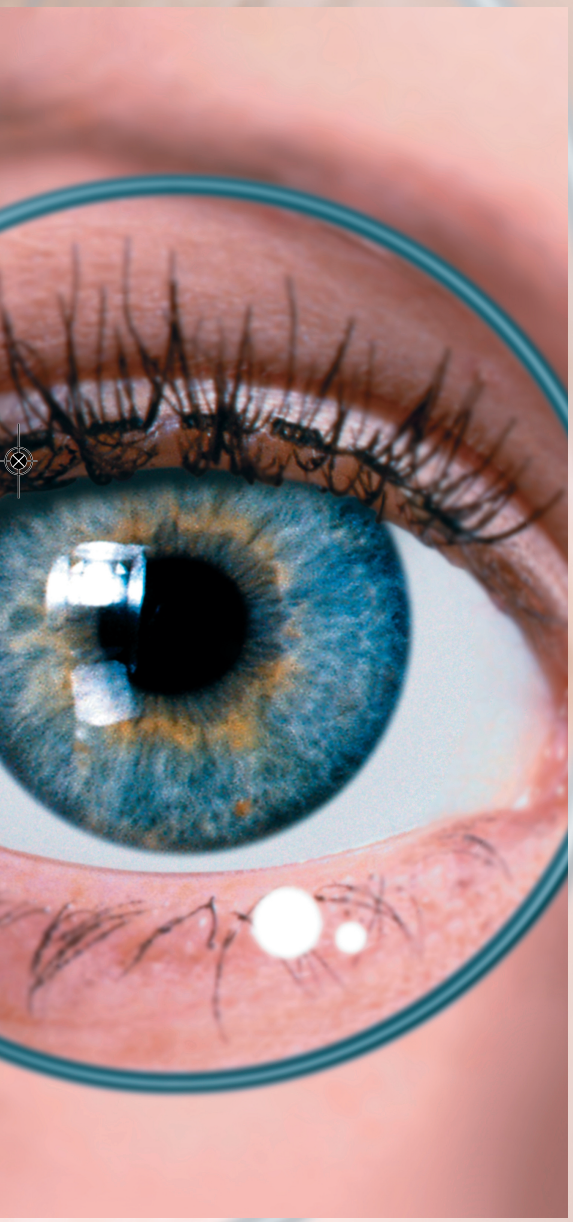

2

Education

Education and Training

- University education
- Contributions to information provision, further education and training

In addition to the priority given to research and development in the scientific institutes at Forschungszentrum Jülich, the institutes that produce new knowledge are also active in the area of training and further education. This is reflected in contributions to the education of undergraduates and PhD students as young scientists as well as to the training of qualified personnel for laboratories and mathematical and technical software developers in the form of specialized scholarships. IEK-3 employees also contribute to a range of information and further education events for different target groups.

2.1 University education

Teaching at universities is another fundamental cornerstone of the responsibilities of selected research scientists at IEK-3 in addition to research and development work. Within the framework of the Jülich model, IEK-3 also participates in a joint appointment process for professors with RWTH Aachen University, whereby Prof. Detlef Stolten (Dr.-Ing.) was appointed to a chair. Two other employees were also appointed professors at Aachen University of Applied Sciences, Campus Jülich: Prof. Ludger Blum (Dipl.-Ing.) and Prof. Ralf Peters (Dr.-Ing.). Furthermore, Dr. Werner Lehnert (PD Dr. rer. nat.) lectures at the University of Ulm and Thomas Grube (Dipl.-Ing., Dipl.-Wirt.Ing.) lectures at Aachen University of Applied Sciences, Campus Jülich (see Fig. 7).

Fig. 7: Universities where IEK-3 staff lecture

The spectrum of topics taught ranges from the fundamentals of science and theoretical modeling and simulation methods to detailed technical knowledge and the characterization of technical applications. In total, seven lectures and three tutorials are offered each semester in the form of 1.5-hour blocks. An additional half-day practical course is offered every summer semester. The number of students participating in the individual courses each semester varies between ten and fifty. The scientists at IEK-3 also play an important role in supervising term papers, diploma dissertations and PhD theses. In 2009, seven diploma/master's dissertations were successfully submitted as was one PhD thesis. In 2010, eight diploma/master's dissertations and five PhD theses were completed.

2.1.1 Courses taught by professors

The following table provides an overview of the courses taught at universities by the employees at IEK-3 (see Tab. 5).

Name	Topic	Type/extent semester		University
Prof. L. Blum	Brennstoffzellen – Die Zukunft der dezentralen Energieversorgung!? (Fuel Cells – the Future of Decentralized Energy Supply!?)	V/2	WS	Aachen Univ. of Applied Sciences, Campus Jülich
	Fuel Cells – The Future for Dispersed Power Supply!?	V/2	SS	
Prof. Dr. R. Peters	Basics and applications of Chemical Reaction Theory – Simulation of Dynamic Processes in Energy Systems with MATLAB/Simulink	V/2 Ü/2	WS	Aachen Univ. of Applied Sciences Campus Jülich
Prof. Dr. D. Stolten	Grundlagen und Technik der Brennstoffzellen (Principles and Technology of Fuel Cells)	V/2 Ü/2	WS	RWTH Aachen University

Tab. 5: Courses taught by professors

2.1.1.1 Brennstoffzellen – Die Zukunft der dezentralen Energieversorgung!? (Fuel Cells – the Future of Decentralized Energy Supply!?)

Prof. Ludger Blum teaches the specialist subject of fuel cell technology at Aachen University of Applied Sciences, Campus Jülich. The optional subject “fuel cells for stationary applications” in the undergraduate course on energy and environmental technology and the master’s course on energy systems covers the function, construction, behavior, and advantages and disadvantages of different types of fuel cells. It also lays the groundwork for the process engineering design of fuel cell systems. The topics include: basic principles of fuel cells; fuel supply; efficiency, function and construction of different types of fuel cells; fuel cell system requirements; process engineering of various fuel cell systems for different applications; energy balance of a fuel cell system; and modern plant engineering. An average of twelve students takes the course each semester.

2.1.1.2 Basics and Applications of Chemical Reaction Theory – Simulation of Dynamic Processes in Energy Systems with Matlab/Simulink

Prof. Dr.-Ing. Ralf Peters is responsible for teaching energy process engineering at Aachen University of Applied Sciences, Campus Jülich. The course “Basics and applications of chemical reaction theory – Simulation of dynamic processes in energy systems with

Matlab/Simulink" links the basic principles of chemical process engineering with dynamic simulations of reactors. The lectures and tutorials use the following as examples: fuel processing and fuel cell system technology for methanol fuel cell drive systems and for diesel-based on-board power supply. The course is compulsory for the 30 - 40 students enrolled in the Master of Science in Energy Systems.

2.1.1.3 Grundlagen und Technik der Brennstoffzellen (Principles and Technology of Fuel Cells)

Prof. Dr.-Ing. Detlef Stolten is head of the Chair for Fuel Cells at RWTH Aachen University. The courses offered deal with the conversions of renewable and fossil energy carriers for use in fuel cells for portable, stationary and mobile applications. The process engineering and systems technology aspects cover high-temperature and low-temperature fuel cells, as well as the processing of specific fuels for fuel cells. These elements are accompanied by an examination of the basic physical and chemical principles involved. Systems analysis studies on energy process engineering, including cost estimates, provide a holistic coverage of the subject with a view to future market launch. During the 2009/2010 winter semester, just under 50 students attended the lectures and seminars. As part of the existing cooperation with Forschungszentrum Jülich, the chair offers students the chance to work on term papers and diploma dissertations and also provides them with an opportunity to work on projects as research assistants.

2.1.2 Courses taught by university lecturers

The following table provides an overview of the courses taught at universities by members of staff at IEK-3 (see Tab. 6).

Name	Topic	Type/hours	semester	University
Th. Grube	Basics and Applications of Chemical Reaction Theory – Simulation of Dynamic Processes in Energy Systems with Matlab/Simulink (Description see 2.1.1.2)	Ü/2	WS	Aachen Univ. of Applied Sciences, Campus Jülich
Dr. W. Lehnert (Privatdozent)	Brennstoffzellen – von den Grundlagen bis zur Anwendung (Fuel Cells – From the Basics to Applications)	V/2	SS	University of Ulm
	Elektrochemische Verfahrenstechnik (Electrochemical Process Engineering)	V/2	WS	

Tab. 6: Courses taught by university lecturers

2.1.2.1 Brennstoffzellen – von den Grundlagen bis zur Anwendung (Fuel Cells – from the Basics to Applications)

Dr. Werner Lehnert (Privatdozent) lectures at the University of Ulm. His lecture “Fuel cells – From the basics to applications” is part of the interdisciplinary course on energy technologies for students enrolled in science and engineering. It takes place during summer semester. The course provides an introduction to the different fuel cell technologies before looking at the electrochemical, chemical and physical principles. One of the key aspects is a description of modern methods of investigation, such as synchrotron and neutron radiography and tomography, which are used to non-invasively image liquid water in situ in cells and stacks. Technologies that produce hydrogen, entire fuel cell systems and their applications are also taken into consideration. An average of 30 students attends the lectures.

2.1.2.2 Elektrochemische Verfahrenstechnik (Electrochemical Process Engineering)

Dr. Werner Lehnert targets chemists in the final years of their studies with his lectures on “Electrochemical process engineering” at the University of Ulm. The lectures are held during winter semester and are attended by between six and ten students. The main issues addressed are mass and heat transport processes in electrochemical process engineering and the energy balance of reactors. Different types of electrochemical reactors and their applications in an industrial setting are also dealt with.

2.2 Contributions to information provision, further education and training

The range of events organized in relation to the provision of information and further education is just as diverse as the needs of the groups themselves. In order to adequately meet the demands made on a research institute for training and information, a variety of different events are organized by IEK-3. IEK-3 is also involved in external events on various levels and it works with other institutions preparing, coordinating and offering support.

2.2.1 Organization of tours, seminars, practical courses, information events and visits to the institute

The topics dealt with at the events depend on the requirements and requests of each target group. In other words, the events range from information events and training courses for secondary-school students, university students, teachers, tradesmen, technicians, engineers and scientists to practical courses on career choice and work experience for secondary-school students, as well as vocational training and study-related placements for undergraduates and postgraduates. The length of each of the events ranges from a half day to a number of weeks depending on the situation. The tasks assigned to secondary-school students and university students during a placement include shadowing technical and scientific staff at the institute as well as supervised independent work on selected practical projects.

- Information events and visits to the institute for individuals interested in Jülich's contribution to research and development on fuel cell technology. Every year, an average of 60 guided tours is organized at IEK-3 with approximately 20 people per tour, each of which is headed by two PhD students.
- Work experience and placements for secondary-school students from local schools focusing on specialist careers in fuel cell technology (2009: 6 students and 2010: 6 students on placement). The range of activities offered covers a broad interdisciplinary spectrum of topics. Placements for secondary-school students are generally for one or two weeks depending on requirements.
- Seminar for highly motivated and talented school students involved in the school forum organized by RWE Germany (a leading European electricity and gas company) as part of a project promoting young talent run by the umbrella organization of the industrial associations in Düren, Jülich, Euskirchen and the surrounding area focusing on the topic of hydrogen as a future energy carrier in February 2009
- Information stand on the topic of fuel cells and a hands-on experiment on H_2 as a method of storing energy as part of the Jülich School's Laboratory Energy Week for school students in the region in March 2009
- Presentation on the how scientists work together with the in-house Language Services at Forschungszentrum Jülich for participants of a CAT Reloaded workshop for translators and interpreters in May 2009
- Seminar on energy from fuel cells for students involved in the ProMINat academy as part of the research placements offered at Jülich in June 2009.
- Information stand on the R&D topics of fuel cells and hydrogen at Forschungszentrum Jülich's Open Day in September 2009

- Lecture on hydrogen as a storage medium for the provision of energy on a renewable basis for members of the PhD students' initiative "Studium Universale" in April 2010
- In cooperation with the Jülich Schools Laboratory and Jülich's Vocational Training Centre, IEK-3 offered placements for ten school students from the region. For one week during their school holidays, the school students on placement had the opportunity to learn about various scientific and technical professions connected with fuel cells (see Fig. 8)

Fig. 8: School students on placement working on aspects associated with fuel cells

2.2.2 Involvement in external events

Several scientists from IEK-3 gave review presentations and more in-depth specialized presentations on fuel cells and hydrogen at a number of external events as invited experts.

- The internationally acclaimed achievements of IEK-3 employees in this field proved beneficial for the 18th World Hydrogen Energy Conference 2010 in Essen (see section 1.2). IEK-3 was also involved in the day for the general public along with other actors showcasing numerous exhibits and providing selected information. In collaboration with the nearby secondary school Haus Overbach, the Fuel Cell Research Center (ZBT) and the Fuel Cell Education and Training Centre Ulm WBZU, IEK-3 organized presentations, a panel discussion and outlined practical tips for lessons at the day for school students and their teachers at the exhibition center in Essen. The school students' day offered students an opportunity to attend the conference itself and to gather information on university studies and further training in the field.During WHEC, the status of on-board power supply with fuel cells was reported to reprensentatives from companies in NRW
- Workshop for developers and users of fuel cells entitled "Polymer Electrolyte Fuel Cell Introduction Course (PEFC)" as part of the WBZU events in Ulm. The course was run twice during the year and included detailed presentations by an IEK-3 scientist on "Lifetime Aspects of PEFC" and "Porous Media"

- Participation in the lecture series on energy and the environment in June 2009 for master's students at Aachen University of Applied Sciences, Campus Jülich, with a presentation entitled "Fuel Cells - Energy conversion processes for the different energy carriers"
- Conference for school directors and specialist teachers on hydrogen and fuel cell technology as a technology of the future with 41 participants from schools in the Emscher-Lippe region in May 2009
- Lecture on hydrogen as a storage medium for the provision of energy on a renewable basis for delegates at the conference on sun and wind organized by the episcopal academy of the diocese of Aachen in November 2009
- Lecture on hydrogen as a storage medium for the provision of energy on a renewable basis for secondary-school students in Bergheim in June 2010 at the invitation of the Year of Science research forum
- Lecture on fuel cells for school students participating in the schools' cinema week in Asbach near Cologne in November 2010 upon invitation at the invitation of the Year of Science research forum

2.3 Collaboration with other organizations

More and more attention is being devoted to designing, launching and implementing training and further education measures and qualification programs focusing on fuel cell technology both in the manufacturing industry and in the relevant educational establishments. In order to cater for this demand, special initiatives have been launched. The combination of specialist technical knowledge and existing opportunities provide an excellent basis for collaboration.

- Involvement in the Fuel Cells Qualification Initiative (IQ-BZ), working to implement information and training measures for fuel cell and hydrogen technologies
- Promotion and sale of a “Fuel Cells” CD-ROM through the Federal Technology Centre for Electrical Engineering and Information Technology, Oldenburg, and Vogel Industrie Medien GmbH, Würzburg, which is designed to provide information, increase the acceptance of fuel cells, and promote further training and education
- Adaptation of existing teaching modules to meet consumer demands
- Support and incorporation of training centers and centers of excellence (WBZU and RAG Bildung) in the planning and realization of joint training events held at the respective center
- Involvement in the school student competition “Fuel Cell Box”, organized annually by the EnergyAgency.NRW: assessment of the theoretical and practical results of 20 teams of students in the final round of the competition (see Fig. 9)

Fig. 9: **Minister Thoben (2009; left photo) and State Secretary Baganz (2010; right photo) award certificates to the winning teams of students**

The Jülich Schools Laboratory has set itself the task of introducing students to the world of science, including hydrogen and fuel cells, by encouraging them to conduct their own experiments. Five experiments have been developed for this purpose, and students perform them in order to find theoretical and practical solutions to the following:

- generation of hydrogen from water
- construction of a low-cost fuel cell
- characterization of a fuel cell
- determination of the efficiency of an electrolyzer and a fuel cell

Experiments are conducted under supervision in the well-equipped Schools Laboratory (see Fig. 10). Students must be familiar with how to conduct experiments from chemistry and physics class. For this reason, they are performed with senior secondary-school students. Approximately three 1.5-hour blocks are required to complete the experiments.

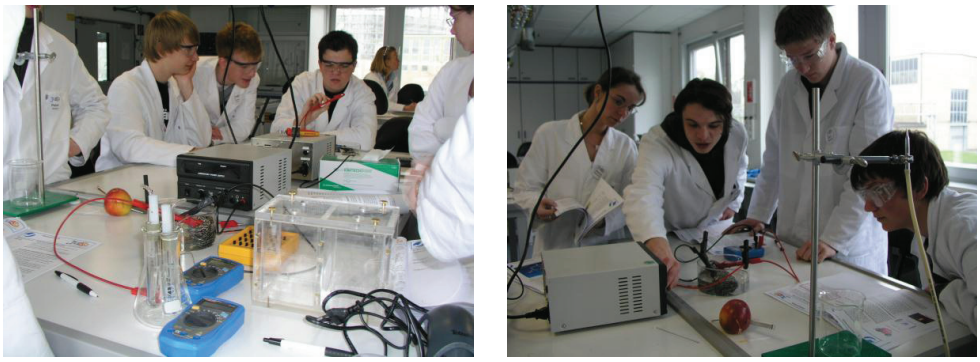

Fig. 10: **Students conduct experiments in the Schools Laboratory on the topics of "hydrogen" and "fuel cells"**

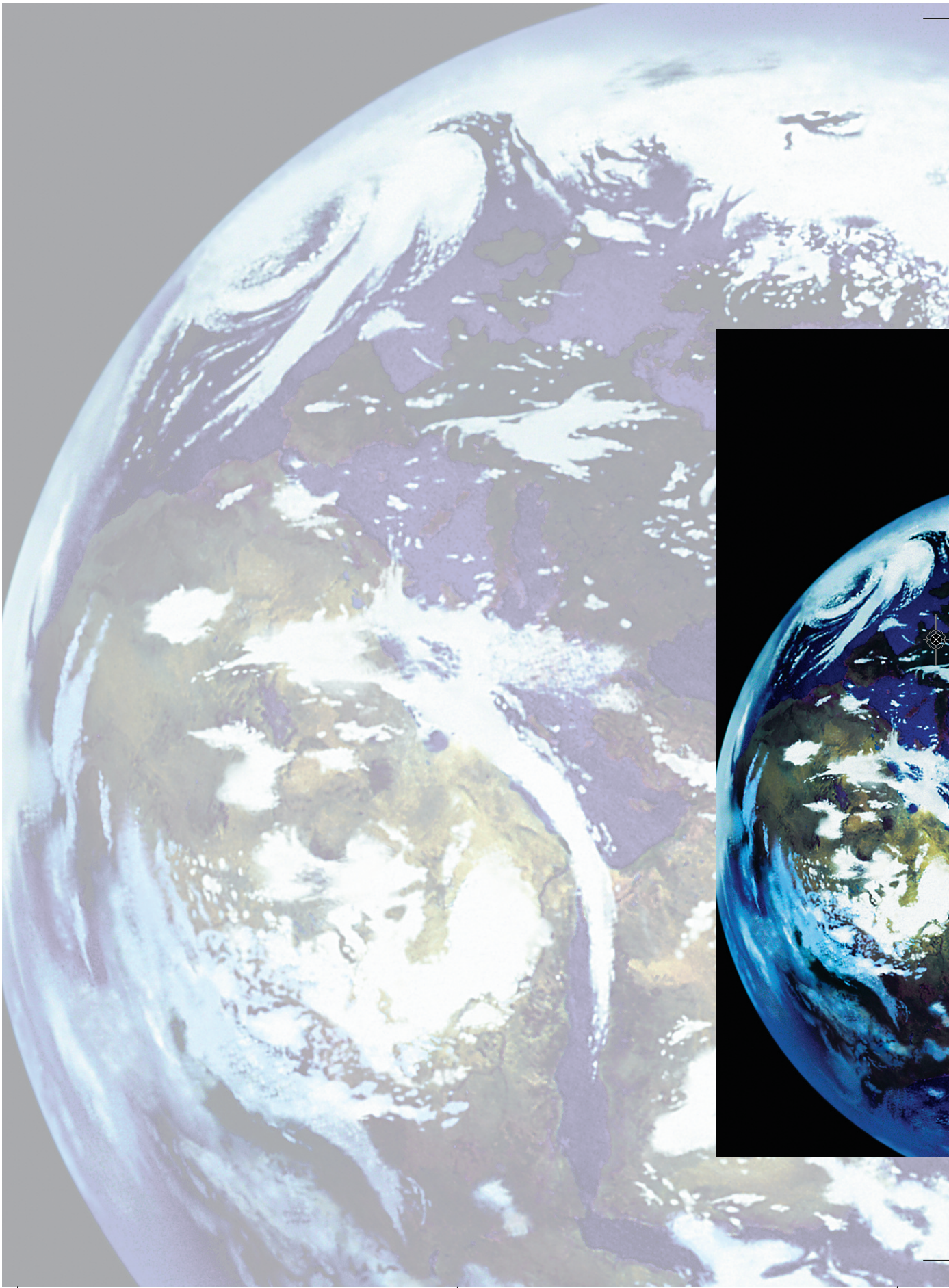

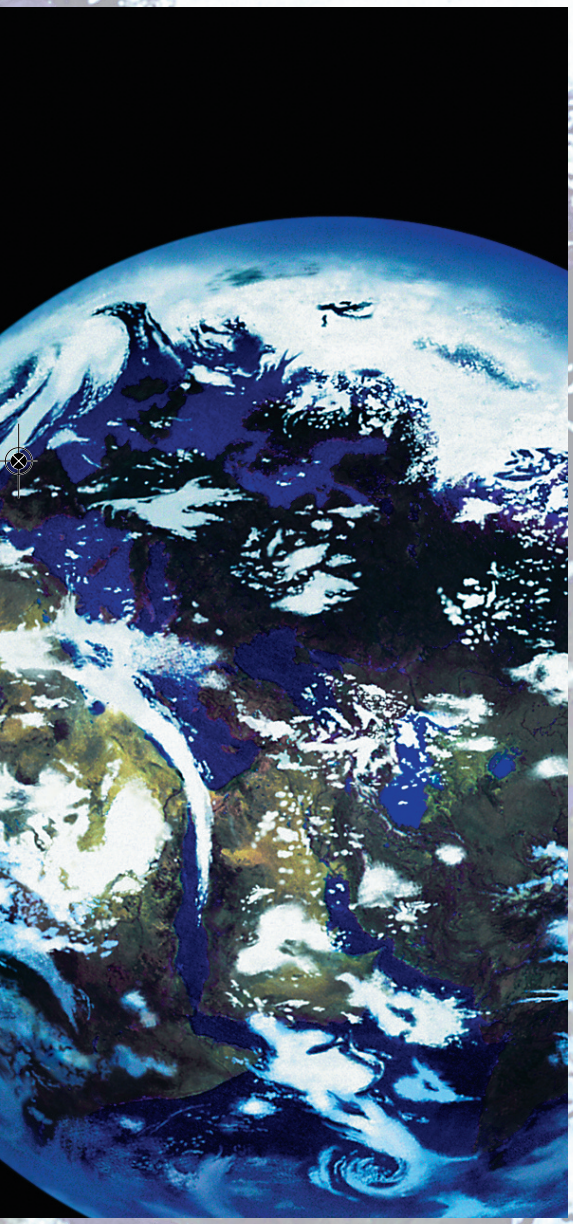

3

Reports

Scientific and Technical Reports

- Direct methanol fuel cells
- High-temperature polymere electrolyte fuel cells
- Solid oxide fuel cells
- Fuel processing and systems
- Process and systems analysis
- Analysis
- Quality management

3.1 Direct methanol fuel cells

3.1.1 Objectives and fiels of activity

Direct methanol fuel cells (DMFCs) provide an interesting alternative in the short-to-medium term to lead-acid batteries, which are currently used for small mobile applications (e.g. in the field of material handling) thanks to their large range and the fact that they are easy to refuel. IEK-3 has therefore made the research and development of DMFC technology one of its main priorities.

Activities focus on increasing the overall efficiency, power density, and lifetime of fuel cells, while simultaneously decreasing the manufacturing costs. In order to achieve these objectives, degradation mechanisms must be identified, material and manufacturing costs must be reduced for stack components and MEAs, the quality must be increased, and a highly integrated fabrication technique must be applied. The challenge in terms of applications lies in optimally integrating fuel cells into energy (hybrid) systems and implementing a closed water cycle during system operation. Important supporting activities are pursued in the area of analysis in studies on the structure-activity relationships of functional layers and the spatially resolved electrochemical and physiochemical characterization of fuel cell components.

3.1.1.1 MEA development and fabrication

Prerequisites for launching DMFCs on the market in the area of portable and small mobile applications not only include high power density and sufficient long-term stability but also a cost level that is comparable to existing technologies. The specific electric power of the MEA directly influences the size of the fuel cell stack and thus the power density and cost of the entire system. The major cost drivers are the noble metal catalysts for electrocatalysis in the electrodes.

Work on the further development of MEA components therefore concentrates on optimizing media transport and the electrical properties in the individual functional layers in order to improve the power output and efficiency of MEAs, and thus facilitate stable DMFC operation under load, even for low air flow rates (and balanced heat budget).

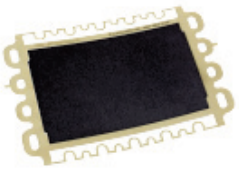

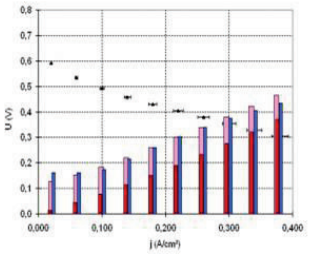

These activities are supported by electrochemical and structural studies. The electrochemical characterization of an MEA focuses particularly on analyzing the relationships between input parameters, such as operating parameters, and observed parameters, such as cell voltage, and on describing system performance. The characterization must incorporate interactions between the physicochemical processes occurring in the MEA, such as electrochemical reactions, methanol permeation and water evaporation, and it must be able to mathematically describe relationships with the operating parameters.

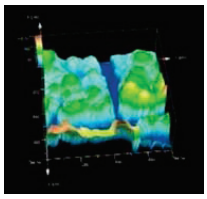

Particular attention is paid to the development, configuration and application of special measuring techniques for the structural analysis of components in the MEA and for the characterization of stacks and single cells. Highest priority is given here to clarifying degradation effects in the MEA.

In terms of the further development of manufacturing processes for MEA components, work focuses on continuous mechanized methods of manufacturing gas diffusion electrodes (GDEs) and catalyst-coated membranes (CCMs.). Priority is given to developing suitable catalyst inks for applying the catalyst layer on different substrates using different coating techniques on a pilot plant scale.

3.1.1.2 Stack and system development

DMFC stack development is pursued at the interface between MEA development, MEA characterization and systems technology. An important field of work here is communicating and balancing the development objectives among the various spheres of work. Practical work can be broken down into the following fields: layout, design, fabrication, assembly and testing with the aim of developing high-performance DMFC stacks with long-term stability, which can be operated with low excess air.

System development focuses on designing and constructing efficient fuel cell energy systems using DMFCs as a basis. This requires in-depth knowledge not only of the cell but also of the entire system, which represents a challenge for development work. Priority is given here to developing new system concepts, testing and evaluating them, developing system components in cooperation with industry, and testing and developing control system concepts.

3.1.1.3 Modeling

DMFC modeling aims to gain a basic understanding of the physicochemical processes on different time and length scales, and then to use this knowledge for the further development of DMFCs. The numerical and analytical models for cells and stacks are based on fundamental fluid dynamics laws and electrochemical laws. Modeling aims to increase our understanding of the physical processes that occur during cell and stack operation and to test optimization measures.

3.1.2 Important results

3.1.2.1 MEA development

Membrane electrode assemblies (MEAs) are composed of a number of layers, each of which must perform its respective task optimally. Furthermore, they must also function in interaction with each other. The development objective is twofold: on the one hand, a high power density must be achieved for a comparably high single cell voltage, while on the other, a stable voltage level must be ensured under load, particularly for low air flow rates, in order to allow the DMFC system to be operated in a water-autonomous manner at ambient temperatures of up to 35 °C.

Gas diffusions layers

At the moment, carbon tissue forms the basis for gas diffusion layers. It has very good diffusion characteristics while also being extremely flexible, which means that it contributes little to the mechanical stability of the membrane electrode assembly. The swelling of the membrane during fuel cell operation therefore brings with it a danger of deforming the MEA, causing it to penetrate into the channels of the bipolar plates. These channels provide the electrodes with air or methanol (see Fig. 11). The resulting decrease in the channel cross-section and the related higher loss in pressure mean that the affected area cannot be optimally supplied with reactants. In order to mitigate this effect, very deep channels must be used, which in turn leads to an increased stack volume and higher material costs.

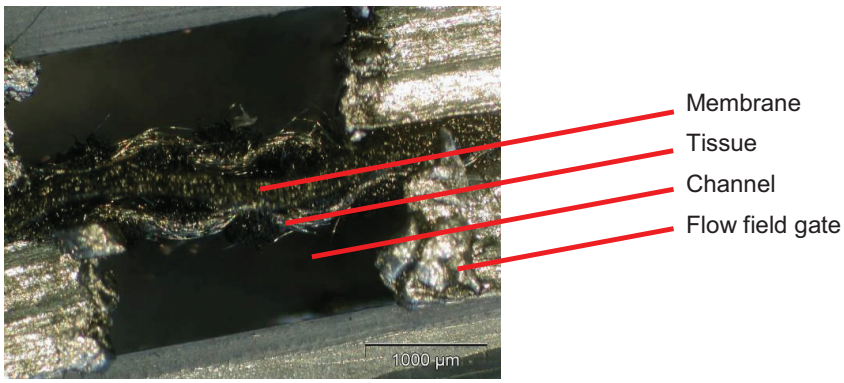

Fig. 11: Deformation of an MEA with gas diffusion layers made of carbon tissue. The MEA is much thicker in the channel area than in the gate area and is wave-like

As a result, the fabrication of gas diffusion electrodes based on carbon fleece substrates was developed as an alternative. As shown in the IEF-3 Report 2009, the use of carbon fleece as a substrate allows a cell voltage to be achieved over the entire current density range which is comparable to that achieved using conventional tissue materials. At the same time, the MEA is dimensionally more stable, thus reducing swelling of the MEA in the channel area, which otherwise causes a narrower channel cross-section leading to an undersupply of the corresponding area.

However, as was the case for MEAs based on carbon tissue, these MEAs could not be operated stably at the low air flow rates (10 ml/(cm²min)) required for water-autonomous operation in real systems.

Freudenberg FCCT supplies different types of fleece materials: in some, the fleece is hydrophobic, while others are coated with a microlayer, and some have both a hydrophobic finish and a microlayer. The fleece materials with microlayers are much denser than those with no microlayer, which in Gurley units, is expressed in an air permeability of approximately 10-50 µm/Pas (with a microlayer) and 500-1000 µm/Pas (no microlayer). Part of the development of MEAs based on fleece involved investigating which combination is more suitable. Very different requirements must be reconciled, particularly in the anode. On the one hand, the anode must be optimally supplied with methanol (made easier by the high permeability of the fleece material), while on the other, the MEA must have as low water permeability as possible (made easier by a dense fleece material).

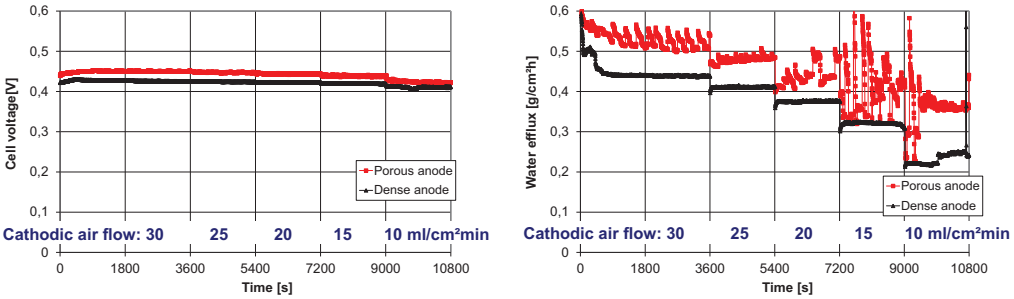

Fig. 12: Comparison of fleece-based MEAs with a dense anode substrate (with a microlayer) and an open-pored anode substrate (no microlayer). Cell voltage (left) and water discharge (right) at 0.14 A/cm². Measurement at 70 °C, 0.75 M methanol solution

Fig. 12 compares the cell voltages and water discharge on the cathode side for two different anode substrates. It can be seen that the cell voltage is higher for all air flow rates when a more open fleece material (no microlayer) is used at the anode. The water discharge, however, is lower when a denser fleece (with a microlayer) is used as an anode substrate.

In short-stack measurements in the single-cell areas required for the application of material handling, both anode substrates demonstrated approximately the same behavior as in the single-cell measurements. The two variants with cathodic volume flow rates of 10 ml/(cm²min) were operated stably. However, the measurements revealed that the MEAs with dense anodes functioned slightly better in terms of power density and water discharge than the MEAs with open anodes, i.e. with no microlayer.

Influence of catalyst loading on the cell performance

The most expensive component in an MEA is the noble metal platinum, which is used as a catalyst in the cathode and in the platinum-ruthenium alloy in the anode. It is therefore important to know how much catalyst is required to ensure optimal fuel cell performance. Electrodes with different levels of noble metal loading were therefore fabricated and the cell

voltage in the MEA was measured at different current densities. The anodes were deposited together with a catalyst on a carbon substrate (72 % PtRu on C) on an impregnated carbon fleece with no microlayer. Fig. 13 shows the cell voltages for MEAs with different levels of anodic noble metal loading at a current density of 0.1 A/cm². There is a marked increase in the cell voltage up to 2.5 mg/cm². After this, it continues to increase, albeit to a lesser degree. Similar behavior is also observed at higher current densities.

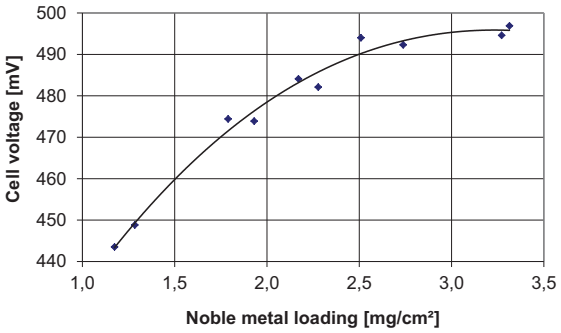

Fig. 13: Influence of anode loading on cell voltage at 0.1 A/cm². Cathode loading: 2.1 mg/cm² platinum, measurement at 70 °C, 1 M methanol solution, air flow rate 37 ml/(cm²min). The curve is only intended to visualize the trend

The series of tests revealed that increasing the noble metal loading on the anode above the conventional 2.0 mg/cm² to approximately 3.0 mg/cm² with the materials currently used (72 % PtRu on C) also increases the cell voltage and thus leads to an increase in efficiency.

Use of hydrocarbon membranes to improve the level of methanol utilization

The DMFC systems constructed at IEK-3 (see Section 3.1.2.4) are operated at moderate current densities ($j < 150$ mA/cm^2) in order to achieve high cell efficiencies and to minimize aging effects. Under these conditions, only 60–70 % of the fuel (methanol) is currently actually used to generate power. The remaining proportion is diffused and is carried with the proton current through the perfluorinated sulfonic acid membrane (Nafion115) presently used to the cathode, where it is oxidized.

In an effort to significantly increase fuel utilization, two publicly funded projects have been focusing on developing MEAs based on new sulfonated polyarylsulfones (FuMA-Tech) as well as on sulfonated polyaryl ether nitriles (National Research Council Canada) since 2009 and 2010, respectively, as fluorine-free hydrocarbon membranes. By carefully adjusting the balance between chemical structure (intermolecular interactions, degree of swelling) and the degree of sulfonation (possible carrier concentration), oxidative and mechanically stable membranes can be manufactured with a high proton conductivity and a low transfer of methanol and water from the anode to the cathode.

As shown on the left in Fig. 14, such MEAs were constructed within a short period of time. At a current density of 140 mA/cm^2 and at a low cathodic air flow rate as desired for DMFC

system operation (10 ml/(cm^{2}min) or below), these MEAs show a cathodic water discharge that is only half as great as that for the Nafion-based reference MEA. Differences in the water discharge, which is easy to measure, can be regarded as a good indication of changes in the methanol permeation. The reason for this is that the membranes currently used are either not selective or only slightly selective towards water or methanol. However, in these new hydrocarbon-based MEAs, the cell voltage at present is still approx. 30 % lower than for conventional MEAs under the conditions shown in Fig. 14.

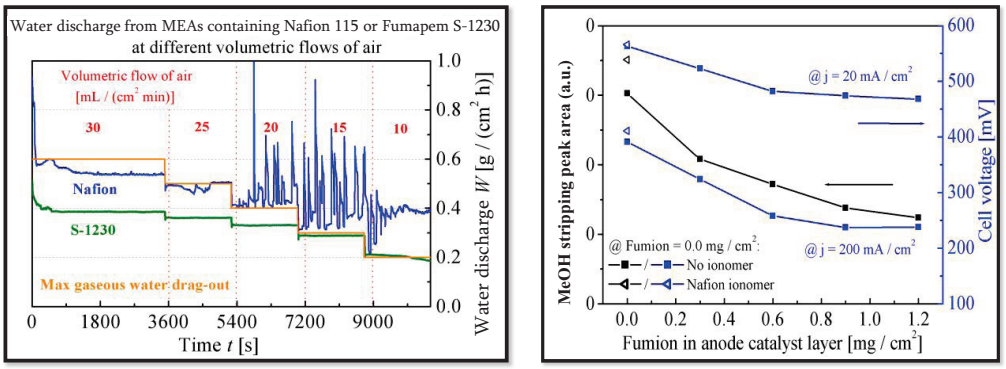

Fig. 14: **Left: Cathodic water discharge from MEAs with a Nafion 115 and hydrocarbon membrane (sulfonated polyarylsulfone, type S-1230) at a current density of j = 140 mA/cm^2 (0.5 molar aqueous methanol solution / air, T = 70 °C,); Right: Using cyclovoltammetry (methanol stripping) selected active catalyst surfaces of the anode and DMFC cell voltage (1.0 molar aqueous methanol solution / air, T = 70 °C) for different concentrations of hydrocarbon (HC) ionomer in the anodic catalyst layer**

When Nafion is also replaced with hydrocarbon materials as the proton-conducting phase in the anode during catalyst layer fabrication, significant losses in cell performance are observed. Classifications of the active catalyst surface suggest that in the contemporary method of fabricating the electrodes, the hydrocarbon materials precipitate onto the catalyst in such a way that they inhibit the fuel supply to the platinum-ruthenium particles (see Fig. 14, right).

At the moment, these new MEAs do not yet perform as well as the existing technology. This is predominantly due to the fact that despite higher membrane permeabilities, comparatively high cell resistances were measured in these MEAs. One of the reasons for this is that the MEAs are still assembled by hot pressing of the gas diffusion electrodes and the membrane. When Nafion is used as a membrane material, this hot pressing leads to a sound bond between the electrode and electrolyte at the interface (e.g. since parts of the membrane material flow into the cracks of the catalyst layers; Fig. 15, left). However, this does not happen with hydrocarbon polymers as they usually do not possess a glass-transition temperature below 250 °C, which is necessary for hot pressing. (In the image on the right in Fig. 15, the material visible in the cracks of the catalyst layer is investment material from the sample preparation for microscopy – the interface to the membrane can be clearly recognized). For this reason, electrode manufacturing concentrates on developing a direct coating for membranes in the medium term.

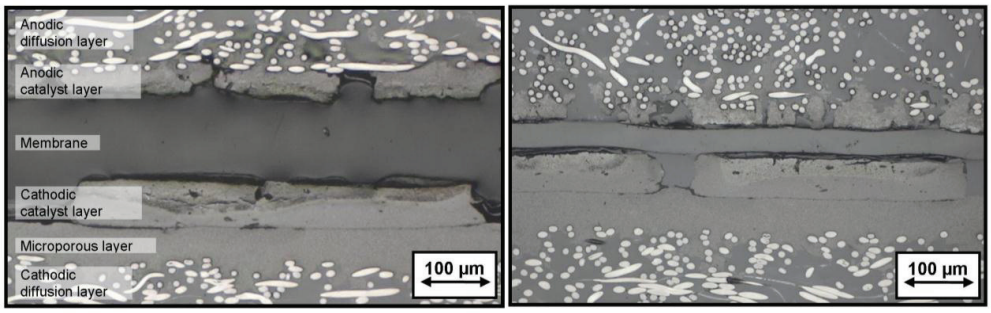

Fig. 15: Micrographs of cross-sections through MEAs with different membranes (left: Nafion 115; right: sulfonated polyaryl ether nitrile) after hot pressing of the membrane and gas diffusion electrodes at 130 °C

In addition to optimizing the electrodes by varying the experimental parameters, work concentrates on adjusting the electrochemical operating parameters as well as on the use and further development of special characterization methods. In future, MEA activation procedures will be adjusted, the methanol permeation of MEAs in operation will be at least approximated, impedance measurements will be implemented to identify the different resistance values in the cell, and new tensile shear tests will be used to quantify the strength of the MEA bonding.

Instead of optimizing the MEA performance under abstract laboratory conditions, the aim is to look at how the use of these hydrocarbon membranes impacts on the regulated operating state and the efficiency levels of an autothermally operated DMFC system of the kW class as soon as possible.

Electrochemical MEA characterization

Electrochemical MEA characterization aims to support MEA development in identifying new materials and new fabrication methods for MEA production in order to better address the requirements for DMFC stack and system development. If new techniques or new materials are to be used for the assembly of MEAs, then test measurements must first be made using small samples, which will subsequently be electrochemically characterized in test stands. The problem with these measurements is that the behavior of the MEA in a DMFC system cannot be directly deduced from the test stand measurement data. The data must first be mathematically processed. The methods required here have already been developed and successfully tested. An important prerequisite for the applicability of the process is that the MEAs are operated in a stable state during the tests.

In the past, however, the operating conditions of the majority of MEAs investigated often did not stabilize in the test stands, therefore ruling out further data preparation. Water transport through the MEA is specifically affected by this. As shown in Fig. 16, it fluctuates enormously for small air flow rates. The signal noise is often so large that evaluation is impossible.

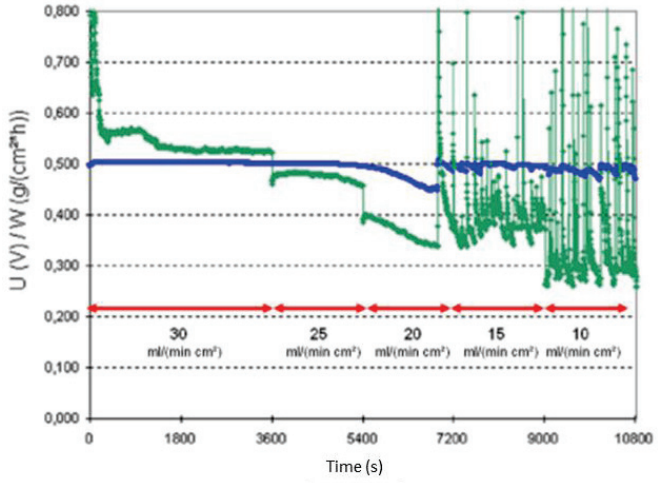

Fig. 16: **Graph showing the cell voltage (blue) and water transport (green) through the MEA for different air flow rates of 30 to 10 ml/(min cm²) (red arrows). Operating conditions: cell temperature = 70 °C, current density = 0.1 A/cm²**

As the cause of this behavior has not yet been clearly identified, further analyses were undertaken focusing on water transport through MEAs.

The water balance in the MEA is a complicated function of the operating parameters and also depends on the electrochemical processes as well as methanol permeation. As the simultaneous analysis of a large number of processes is very difficult due to unknown coupling between the processes, a new method was developed for the analyses. In this case, the water transport through a sample comprising a gas diffusion layer (GDL) and a membrane is measured in relation to the temperature T and the air flow rate in the cathode as a process-specific criterion (PSC). The analysis of the data obtained in this way permits conclusions to be drawn on the diffusive water transport through an MEA, as the GDL at the anode and the electrolyte membrane are predominantly responsible for this.

The analysis of a GDL with a Nafion 115 membrane in a test cell resulted mathematically in a two-dimensional scalar field when the cell temperature and air flow rate were varied (see Fig. 17). The aim of the studies was to work with a selection of GDLs and identify the GDL with the lowest water transport. The GDL thus selected should also allow less water to permeate from the anode to the cathode. However, comparing the measurement results in order to identify such a GDL proved difficult using graphs such as that shown in Fig. 17. It is intended for comparisons at each operating parameter point, and the illustrated area can be distorted within certain limits for different samples. As a result, a technique was developed to determine six characteristic variables from the measurement data using mathematical routines. These variables can then be used as a basis to compare the samples.

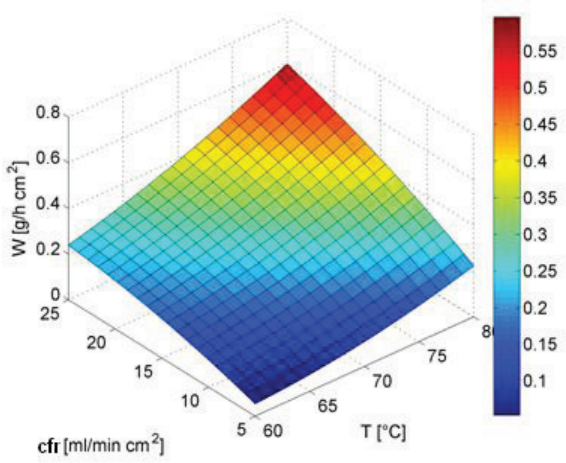

Fig. 17: Representation of water transport W through a GDL/Nafion 115 membrane sample as a function of cell temperature T and the air flow rate PSC

During the period under review, the test stand required for these investigations was constructed and the mathematical procedures required determining the characteristic variables were integrated into the evaluation concepts. The field shown in Fig. 17 was calculated using the characteristic variables of this sample determined from the measurement data. These variables can be used, for example, to easily calculate the volume under the area in Fig. 17, from which a mean value can then be derived for the operating parameter interval. The values measured in the experiments can therefore be reduced to a single parameter and the comparison of several samples can be considerably simplified. In future measurement series, this procedure will be used to systematically analyze water transport for GDLs.

3.1.2.2 MEA production

In 2008, IEK-3 acquired a new line coater. Prior to this, gas diffusion layers and gas diffusion electrodes were fabricated for direct methanol fuel cells using a desk coater. The desk coater was designed as a compact system, which allowed a number of different process steps to be performed. However, these steps were not flexible enough for research purposes because of the rigid installation in a certain order. For example, only one process step could be performed for each machine run. The material then had to be sent back again before the next process step could be performed. This involved sending the material back through the entire machine repeatedly, which in certain cases led to applied layers that were of a lower quality. In 2008, a flexible line coater was installed as an alternative. By clicking together the necessary modules, a coating process can be performed in one run.

After the new line coater was put into operation (Click and Coat), the first objective was to transfer the coating techniques developed on the desk coater to the new coating facility using the same materials. Fig. 18 shows Uj curves for MEAs with electrodes fabricated using the desk coater and MEAs with electrodes fabricated using the line coater.

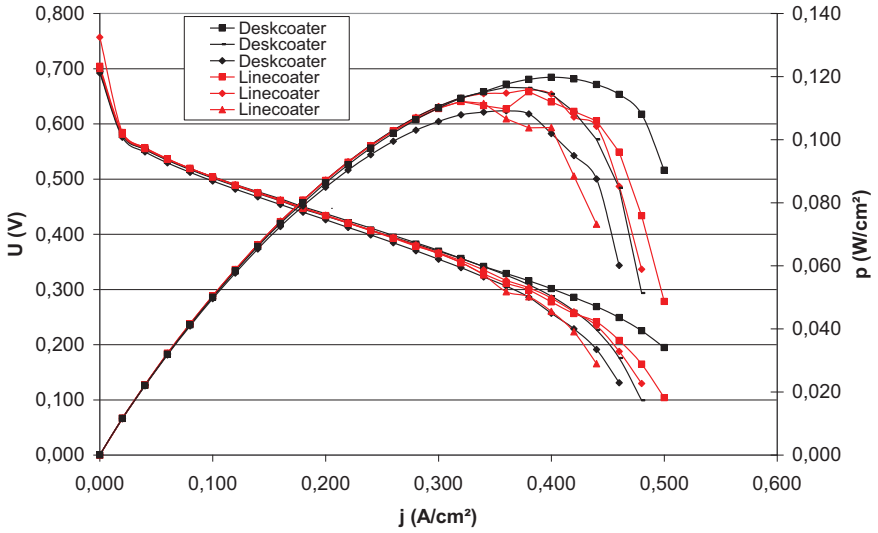

Fig. 18: **Current-voltage characteristics for MEAs with desk-coater electrodes (black) and line-coater electrodes (red)**

The results of the electrochemical characterization show that for operation with high air flow rates at the cathode (in terms of presently achievable reproducibility) the MEAs with electrodes fabricated using the line coater have current-voltage characteristics that are almost the same as MEAs with electrodes fabricated using the desk coater. The fabrication of gas diffusion electrodes could therefore be transferred from the desk coater to the new line coater facility.

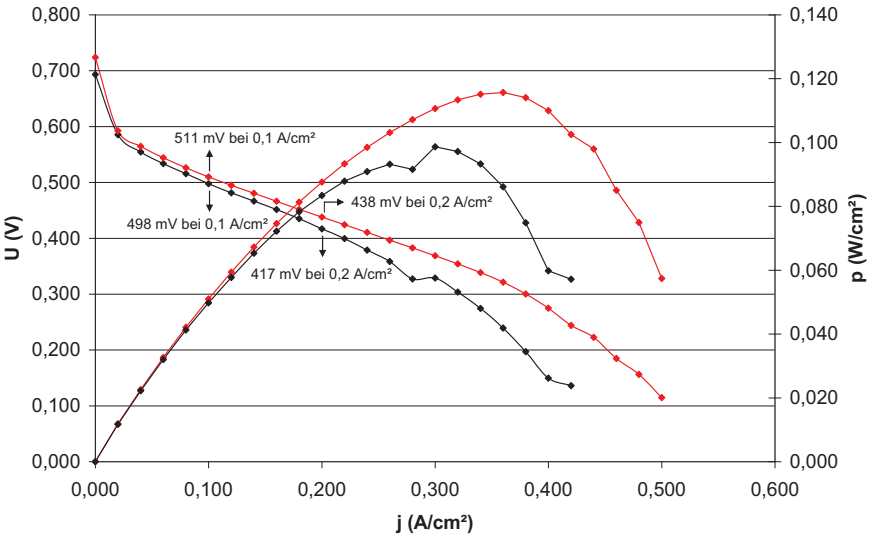

Fig. 19: **Current-voltage characteristics of MEAs produced in the same manner**

For the numerous MEAs investigated, which were produced using tissue as well as fleece, frequent differences were observed in the characteristics. Fig. 19 shows the Uj characteristics for two MEAs which were produced in the same manner and electrochemically characterized under identical conditions. The results illustrate the occurrence of fluctuations of up to 13 mV at 0.1 A/cm² and fluctuations of up to 21 mV at 0.2 A/cm². As the experimental results suggest that the problems are associated with inhomogeneities in the electrodes, the electrode fabrication process was investigated.

As a possible cause of the differences in the characteristics, fluctuations in catalyst loading were assumed. They can occur as a result of the blade process used. The blade process facilitates the simple and cheap production of electrodes. However, the disadvantage is that it can also compensate for unevenness of the substrate and thus lead to fluctuations in loading.

Fig. 20 illustrates the influence of unevenness in the substrate on the catalyst loading. In order to determine the influence of the homogeneity of the substrate on the catalyst loading, the substrate thickness and weight per unit area were analyzed. To calculate the catalyst loading, the weight per unit area of the substrate was determined both before and after coating (see Fig. 21).

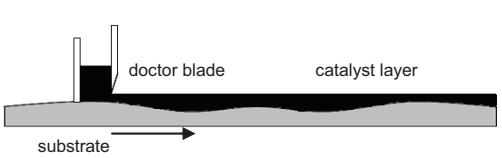

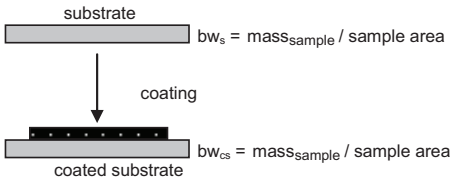

Fig. 20: Influence of substrate unevenness on catalyst loading

Fig. 21: Determination of the weight per unit area

The catalyst loading was determined by multiplying the difference between the two values by the noble metal fraction. This subtraction leads to the inaccuracies in the substrate weight per unit area being transferred to the catalyst loading.

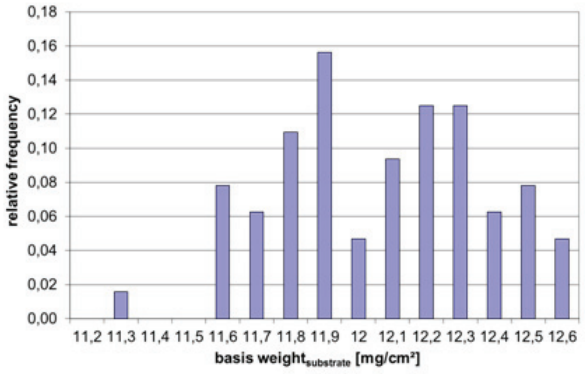

Fig. 22: Relative frequency distribution of the weight per unit area

A frequency distribution was calculated using the measured values (see Fig. 22). The statistical analysis shows that a normal distribution can be assumed. The expected value of the weight per unit area was derived as 1.8 mg/cm² +/- 0.3 mg/cm². The calculation of the impact of these fluctuations resulted in an expected distribution for the catalyst loading of 2.0 mg/cm² ± 0.3 mg/cm².

In order to answer the question of whether these results can explain the observed fluctuations in the Uj characteristics, another measurement series was performed. It investigated the dependence of cell voltage on catalyst loading. The loading at the anode was varied while cathode loading was kept constant. The reason for this approach is that fluctuations in the weight per unit area were greater for the anode substrate while they were significantly smaller for the cathode substrate. Using these results, the expected value of the cell voltage and its standard deviation could then be calculated in a statistical analysis for 0.1 A/cm².

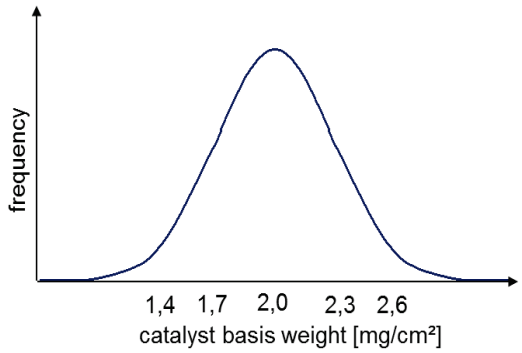

Fig. 23: Expected distribution of the catalyst loading of 2.0 mg/cm² ± 0.3 mg/cm² due to fluctuations in the weight per unit area of the substrate before coating

On the basis of the catalyst loading distribution (Fig. 23), a cell voltage distribution of 490 +/- 10 mV can be assumed (Fig. 24).

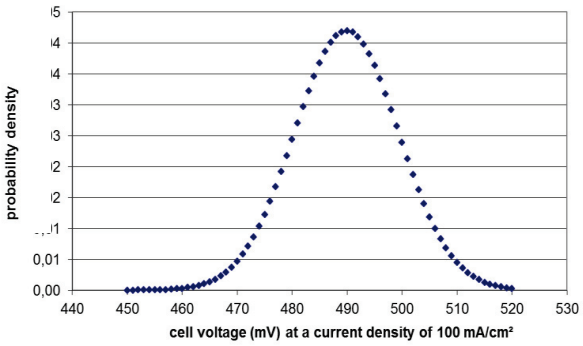

Fig. 24: Expected voltage distribution of U=(490 ± 10) mV due to fluctuations in the catalyst loading of 2.5 ± 0.3 mg/cm²

The results thus show that the measured voltage differences in the Uj characteristics of between 486 mV and 504 mV for j=0.1 A/cm² are within the range of values expected because of fluctuations in the catalyst loading. Fluctuations in the weight per unit area in the substrate used can consequently be assumed to be the cause of fluctuations in the Uj characteristics.

The results presented here involved the use of different methods from inductive statistics in an effort to identify the possible causes of measured reproducibility difficulties. The greater the degree to which these methods can be adapted to the actual production processes, the more precisely the causes of fluctuations can be determined. An important factor here is knowing certain statistical variables from the production process, the covariance matrices. The elements in these matrices can be determined once the production processes are understood in depth.

Current experiments aim to improve our understanding of the blade process. However, other production methods for MEA fabrication are also being investigated as alternatives in order to reduce scattering and meet the demands of DMFC stack developers more effectively.

3.1.2.3 Stack development

Stack development is divided into two development lines: stacks based on graphitic components and stacks based on metallic components. Design and construction work is being carried out for both development lines, fabrication techniques are being developed and adjusted to the meet the various requirements, and electrochemical measurements are also being performed. The objective in terms of the development of graphitic stacks is based on the requirements for a stable and economically efficient system operation for light traction:

Lifetime	> 3,000 h
Specific power in stack	> 75 mW/cm²
Air requirement	< 10 ml/(cm²min) @ 0.14 A/cm²
Efficiency in system	≥ 30 %

The construction and fabrication of stack components were improved and a stack suitable for actual use was created. It will be used as the basis for launching DMFC systems for light traction on the market. In order to improve the lifetime of stacks, mechanisms that could cause damage must first be understood. For this reason, the impact of cationic contamination of the fuel on cell performance was quantitatively investigated. The anode material was selectively and systematically contaminated in order to ascertain the impact on the performance efficiency of fuel cells. This method was used to quantify the influence of iron, nickel and chromium (the typical components of stainless steel) on cell performance. Fig. 25 shows the decrease in performance as a function of loading the membrane with the sulfonic acid group. It is clear that the deposition of ions in the membrane affects the degradation to a varying degree depending on the type of membrane used. The dotted red line is a rough approximation of the measured dependences, which allows further cationic contamination to be evaluated.

The maximum permissible level of impurities in the anodic fuel was derived based on these investigations and the desired operating life. These limits are particularly important for the use of metallic bipolar plates and system components. In other tests, however, it was also shown that cations were stripped out of expanded natural graphite, which is the bipolar plate

material in a graphitic stack design. These cations accumulate in polymer electrolytes and the catalyst layers and therefore also reduce the performance efficiency of MEAs.

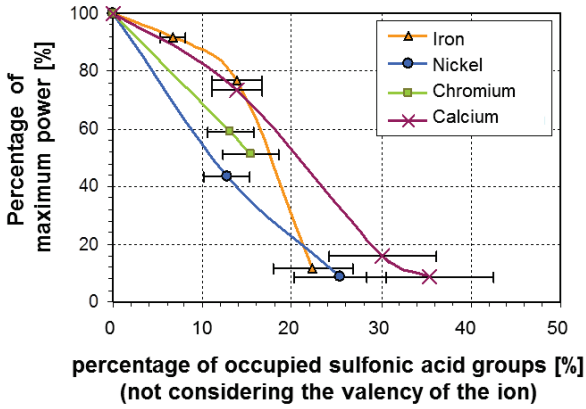

Fig. 25: Impact of ion contamination of the membrane on cell performance

In order to reduce the loading of expanded graphite with cationic impurities, particularly with iron, the existing purification procedure was extended to include an additional purification step with oxalic acid. The oxalic acid treatment strips the iron oxide out of the material. The purification mechanism can be described by the following reaction equation:

$$6\ C_2H_2O_4 + Fe_2O_3 \rightarrow 2\ [Fe(C_2O_4)_3]^{3-} + 6\ H^+ + 3\ H_2O$$

Suitability was verified in preliminary tests using Sigraflex contaminated with iron. This material was purified in a water/oxalic acid solution at a temperature of around 70 °C. After approx. 35 min, the red-brown discoloration had almost completely disappeared (see Fig. 26). This test and other analyses were used to prove the effectiveness of the purification procedure.

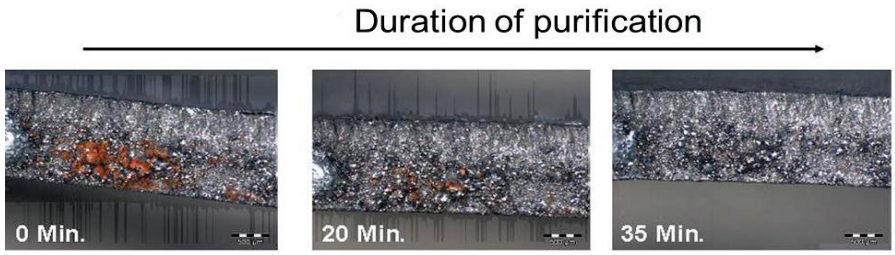

Fig. 26: Purification of the Sigraflex material using an oxalic acid/water mixture

In order to simplify stack assembly and to facilitate additional quality controls, the preassembly of bipolar plate units was investigated in several steps. The following issues were addressed:

- How can subcomponents be integrated?
- How can the plates be joined?
- Is automation possible?

The bipolar plate system comprises the cathode and anode flow field, the actual bipolar plate and a wick. First of all, possible joining methods were identified. Then, promising methods were tested, evaluated and examined in terms of suitability for automation. Amongst the variety of techniques investigated, the use of adhesives proved a promising method of joining graphite plates. In the tests performed, a low-viscous polymer electrolyte adhesive was identified as particularly suitable for the assembly of bipolar plate units. The application of adhesive dots is shown in Fig. 27. In order to ensure that the components do not move during operation, the adhesive strength was determined under shear stress. In a tensile shear test, sufficient adhesive strength was demonstrated with 0.31 N/mm². No significant increase in the contact resistance of 11 mΩcm² between two graphite plates that were not glued was measured when polymer electrolyte adhesive was used. Polymer electrolyte adhesive thus causes no electrical losses. These adhesive bonds were also tested under DMFC operating conditions. First, these conditions were simulated using a one-molar methanol solution heated to 70 °C in an ultrasonic bath. The adhesive bond withstood the test in the ultrasonic bath and proved that the gates of the cathode and anode flow fields are also protected against displacement during DMFC operation.

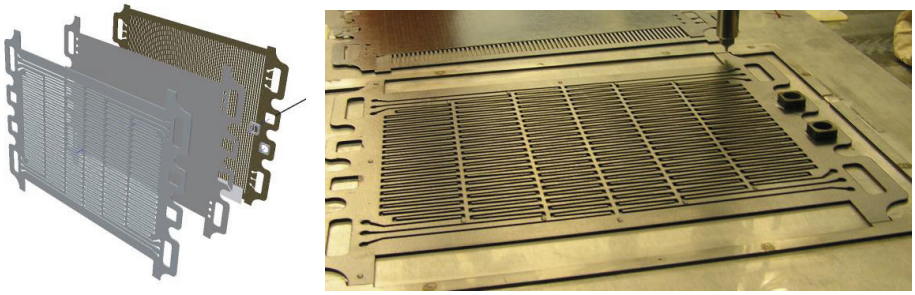

Fig. 27: Application of adhesive dots to the anodic flow distributor

The automation of bipolar plate assembly was also shown to be possible. An articulated robot with six axes, an application unit attached to the robot, and a hot press was used for these experiments. The application unit allows the polymer electrolyte adhesive to be applied as a spray or as individual dots. Dots were applied in order to prevent adhesive from seeping into the channels. The bipolar plate was sprayed with the adhesive as the surface area of the gates of the cathode flow field, which was to be joined with the bipolar plate, was too small for the application of dots. The polymer electrolyte adhesive was hardened in the hot press at 137 °C under a pressure of 50 kN. A short stack was assembled in this manner using the bipolar plate units and put into operation. The values measured for the current-voltage characteristics corresponded to the values of short stacks with non-glued bipolar plate units. The concept developed is therefore suitable for use in DMFCs. To summarize, preassembly has the following advantages:

- reduction in the number of components for stack assembly
- subdivision of the fabrication process

– additional quality control before stack assembly

In addition, a stack was automatically assembled using the existing six-axis robot (see Fig. 28). The automated assembly reduced the possibility of error, decreased the time required for assembly, and further improved the dimensional accuracy of the stack.

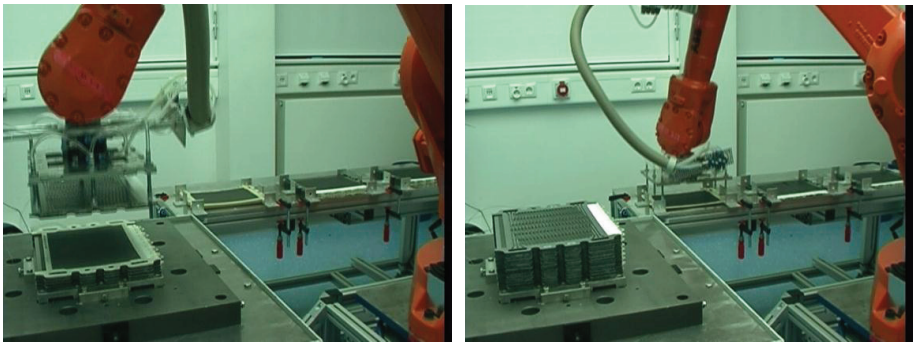

Fig. 28: Automated assembly of stacks

The preassembled bipolar plates described above were also used to construct several stacks (see Fig. 29). A quality assurance program was developed to check the dimensional accuracy of all bipolar plates before assembly by means of an automated non-contact measurement technique.

Fig. 29: Photo of a 90-cell stack with an active area of 315 cm² per cell

Once the stacks had been assembled, they were put into operation and their performance efficiency was determined under defined conditions in a stack test stand. The cathode was supplied with non-tempered ambient air via an air compressor which fed air into the stack (30 ml/(cm²*min)). The stack anode was supplied with a tempered (70 °C) water/methanol mixture. Here, instead of the methanol concentration, the methanol permeation was set at a value of around 0.1 A/cm². Under the conditions described, a power of three kilowatts was achieved in a stack with 88 cells (see Fig. 30). In this stack, an optimized wick system was used. It allowed stable operation for low excess air and low pressure losses of less than two millibar on the cathode side.

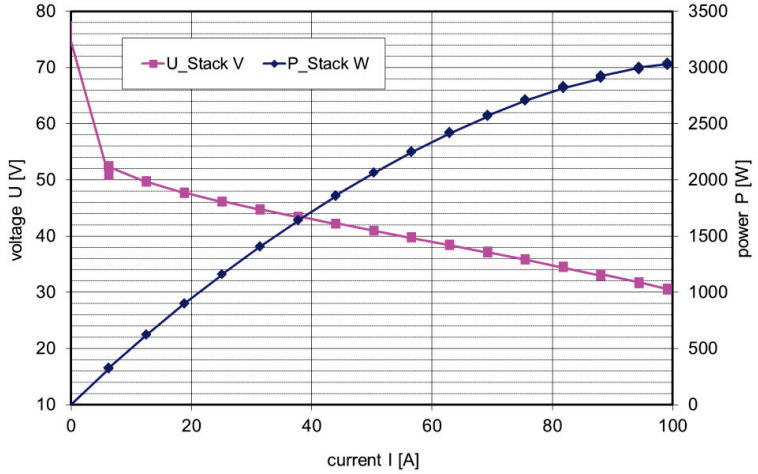

Fig. 30: Voltage and power of the stack (MM-44)

In addition to the current-voltage characteristics, the frequency distribution of the cell voltages at a certain load is an important criterion for evaluating the quality of the stack. Refining the wick system during the fabrication of a second mechanically identical stack (Stack 1 → Stack 2) allowed the scattering of the cell voltages to be reduced. At a load of 0.1 A/cm², the difference between the largest and smallest cell voltage in Stack 1 was 46 mV, whereas in the second stack the difference between the largest and smallest cell voltage was only 20 mV (see Fig. 31).

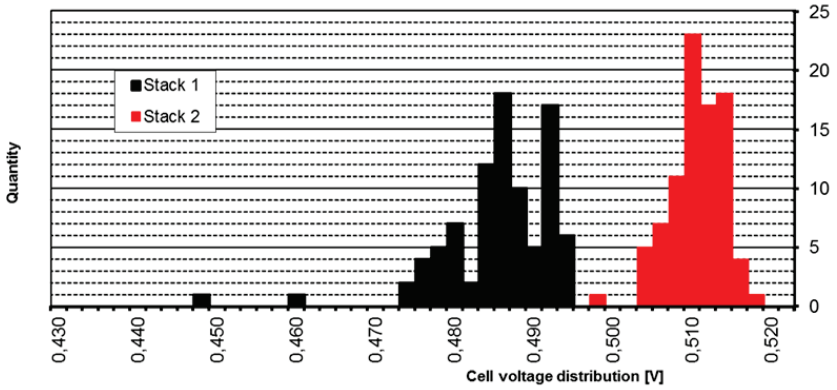

Fig. 31: Cell voltage distribution at 0.1 A/cm² for two stacks

As mentioned earlier, metallic stacks are also being developed for the DMFC in addition to graphitic stacks. The objectives in terms of lifetime, power density and efficiency are similar but other challenges must be addressed by the fabrication techniques.

In addition to the segmented coating technology described in previous reports, the focus lay on further developing the sealing technology. The use of metallic and rigid graphitic bipolar

plates necessitates the integration of a separate sealing element in the plates. In order to perform this precisely, the existing robot was expanded to include an additional dispenser (see Fig. 32). This allows sealants made of silicone or other materials to be applied to the bipolar plates.

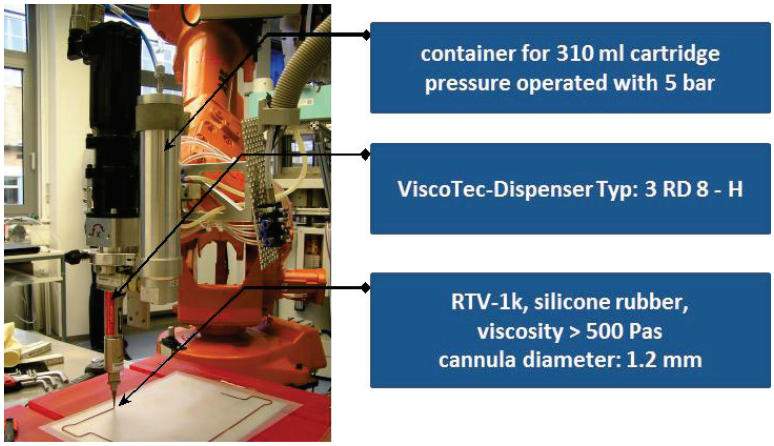

Fig. 32: Dispersion unit for the articulated six-axis robot

Future work will concentrate on achieving a lifetime of 5,000 hours with stacks in the kilowatt range. Such lifetimes have already been demonstrated in a short-stack test. The power density of the stack also has to be increased. This involves increasing the performance efficiency of the MEA while simultaneously constructing the stack in more compact manner. The metallic concept could prove important in this regard. The efficiency of the stack must also be improved to values in excess of 35 %. The key to this lies in improving the fuel utilization.

3.1.2.4 System development and verification

DMFC systems technology focuses on the development of concepts, the layout, design, construction and testing of fuel cell systems in relation to the respective application. Work is structured according to different applications. Within the framework of a project funded by BMWi, an energy supply system for forklift trucks has been developed and tested over the last two years in cooperation with partners from industry. In addition to creating operating strategies for processes, control systems and safety monitoring, another priority was component development for DMFC hybrid systems. The key objective here was to demonstrate robust, long-term stability for operation under realistic conditions. In 2009 and 2010, two systems of the DMFC V3.3 series were constructed.

Process development; hybridization

Fig. 33 shows the flow chart for the DMFC V3.3. The system as a whole has been implemented as an active serial hybrid. The base load required to supply the electric motors (drive and lift motor) in the vehicle is covered by fuel cell A1. Battery A2 stores energy to bridge the fuel cell's warm-up phase when the stack provides no electrical output, and to

smooth the high load dynamics (start-up and braking peaks). The DC/DC converter A3 decouples stack and battery.

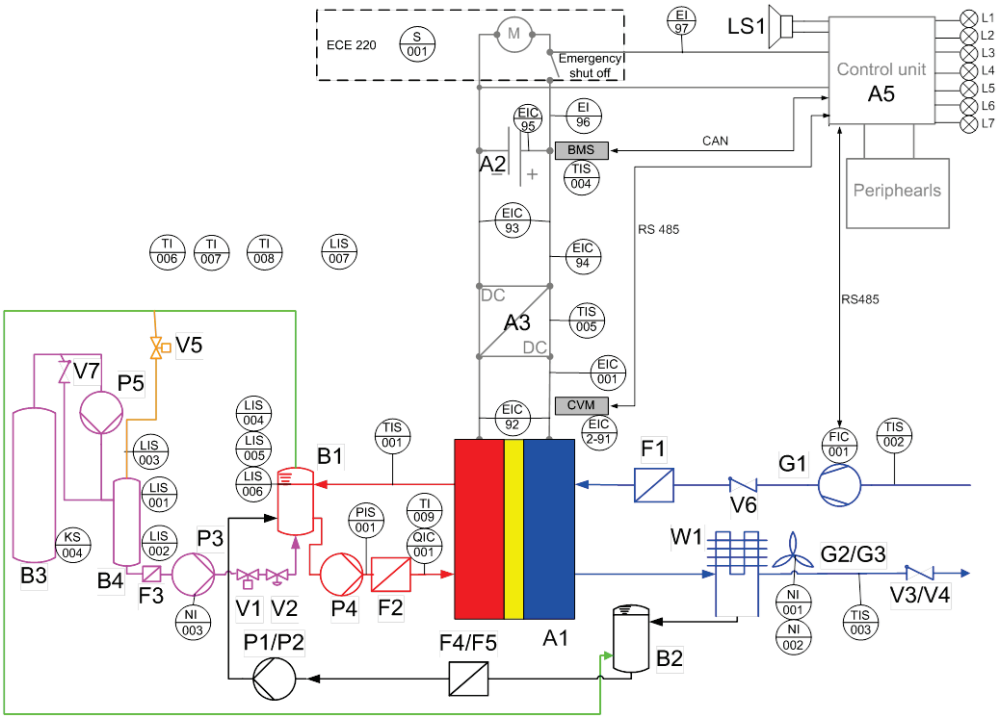

Fig. 33: DMFC V3.3 process flow chart with the actuators and sensors necessary for system operation

The system is started using the key switch S-001 in the vehicle. If the vehicle emergency stop is pressed, the energy system is turned off. This ensures full compatibility with a conventional energy system (lead-acid batteries). The following features are unique to the system:

- Use of a licensed and readily available methanol cartridge B3 from ACC beku/SFC. Methanol surge tank B4 as a reserve tank for approx. 20 minutes of operation
- High-performance Li-ion battery as hybrid energy storage unit A2. Preliminary tests have shown that this technology is the only one suitable for such an application (in terms of energy and power densities as well as lifetime)
- Adapted power electronics A3 and control system A5
- System of valves (V3/V4) to shut off the cathode supply system when not in operation; measure to counteract stack aging
- Anode exhaust gas (green line) fed into the condensate (B2, stripping) and then into the cathode exhaust gas (condensation in W1); measures to reduce organic emissions (incl. methanol)

The first system (DMFC V3.3-1) was constructed with a few prototype versions of the components (control system, DC/DC converter, data logging, some sensors). Long-term

operation in a test-stand environment was still possible under a realistic electrical load (see Chapter 4.1).

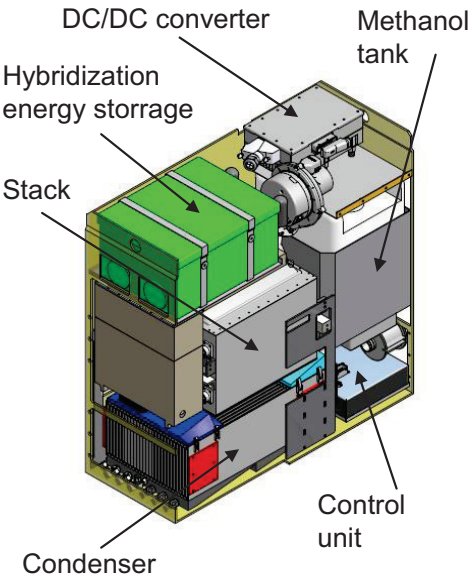

Technical data		
Drive module	Peak power	7 kW (fuel cell battery hybrid system)
		water autonomous @ 35 °C
	MeOH cartridge	20 L, 20 h operation time
	battery	lithium ion high power (45 Ah, 7s)
Stack	Nominal power	1.3 kW
	Number of cells	90
	Lifetime	25 % power loss @ 3,000 h
MEA	Power density	75 mW/cm² @ 450 mV
	Pt/PtRu loading	4.5 mg/(cm² cell)

Fig. 34: System setup and technical data of DMFC V3.3-2

The DMFC V3.3-2 system shown in Fig. 34 comprises all of the original parts and was successfully demonstrated in a vehicle on 14 July 2010. At the moment, it is running in a realistic operating cycle in the system test stand (as of 17 February 2011: 2,850 operating hours).

Monitoring and control system

The control software includes the procedures for operating and monitoring the energy system (see Fig. 35, left). When the supply voltage is switched on (battery switch on), the control system is booted and goes into “stand-by” mode. When the key switch is activated, the program goes into “start-up” mode. In this mode, procedures are run to check the system (tank level is checked, minimum methanol concentration is checked, tests are run on the sensors and actuators, plausibility checks are run, etc.) and to prepare the system for normal operation (nominal concentrations are set, standard settings are activated for actuators, system is warmed up, etc.). When all start-up criteria have been fulfilled, the program automatically goes into the “normal operation” mode. Here, the regular load operation of the energy system is controlled and monitored.

The control structure of DMFC V3.3 is shown as a cascade controller in Fig. 35, top right. The control structure basically comprises controller 1, which controls the battery voltage and calculates the setpoint for the stack voltage, and controller 2, which regulates the stack voltage and calculates the setpoint for the current at the DC/DC converter output.

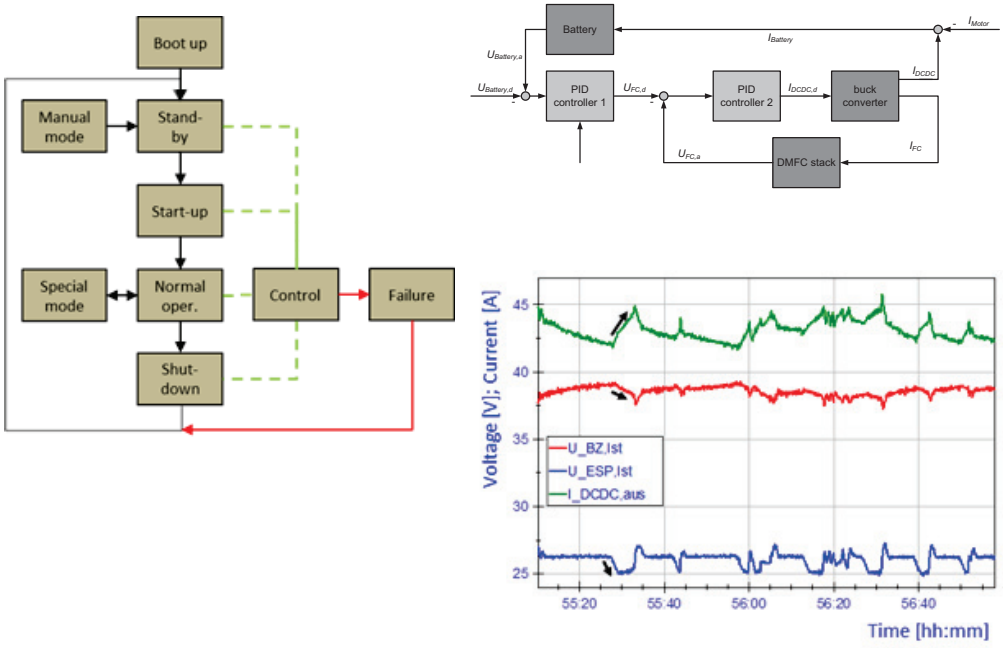

Fig. 35: Program flow (left); controller structure (right)

The graph shows how the controllers work. It shows the progression of battery voltage (U_ESP_Ist), stack voltage (U_BZ_Ist) and the DC/DC converter outlet current (I_DCDC_aus) over a period of around half an hour. When the battery voltage falls below the setpoint (= 26.3 V), it needs a higher charge. This is achieved by increasing stack performance (decreasing stack voltage, increasing stack power and/or increasing the DC/DC converter output current).

In normal operation, various additional modes are automatically activated:

- "Cyclic load disconnection": Regular shut down (every 30 minutes at the moment) of the stack load and the air supply for around 30 seconds; procedure ensures performance efficiency of the stack is maintained
- "Purging": Cathode blower should be set to maximum speed for a set time for certain deviations of the single cell voltages from their mean values; prevention of automatic shutdown because of water blockages in the cathode flow field
- "Refueling": The fuel level sensors in the surge tank register when the cartridge needs to be changed. The suction procedure (filling of the surge tank and supply lines after the cartridge has been changed) is initiated by a contact switch on the tank filler flap

Diverse monitoring processes are in place – both within each of the operation modes and centrally – to ensure the safety of the system and the durability of the stack. A malfunction immediately leads to system shutdown and a return to stand-by mode.

Depending on the authorization rights of the user, the “manual operation” mode can be selected in the stand-by mode. All actuators can be turned on and off manually or operated with various partial loads. This mode is required to start up the system in particular. Stand-by mode comprises both sleep and wake phases. As soon as the system goes into stand-by mode, the sleep phase begins, where only the timer runs. When the timer switches off and the system is still in stand-by mode, the wake phase is activated. Here, procedures are run to ensure performance efficiency of the stack (nominal fuel level and concentration in the anode system are checked and corrected if necessary).

3.1.2.5 Modeling

One of the main problems with the direct methanol fuel cell is the relatively rapid aging of the catalyst layer on the anode side (ACL). In the ACL of a DMFC, methanol is split into protons and electrons on a Pt/Ru catalyst (methanol oxidation reaction, MOR). Ru prevents the poisoning of the catalyst surface as a result of reaction by-products. The experiments conducted at IEK-3 have indicated that the dissolution of Ru is the dominant mechanism in the aging of the anode catalyst layer. A post mortem analysis showed a loss of 15 % ruthenium in the anode. Most of the corroded ruthenium collects on the cathode, which comprises a pure platinum catalyst before operation (see IEF-3 Report 2009).

Since ruthenium corrosion and deposition also occur on the surface of the catalyst particles, the effect is considerably greater and leads to high overvoltage losses at both electrodes. The electrochemical mechanism of Ru dissolution is still inadequately understood.

In 2010, a general model of the performance of the catalyst layer was developed [1, 2]. The model contains the conservation of the ion current derived from the Butler-Volmer equation of the electrochemical reaction, Ohm’s law for ion current, and the mass balance equation for the transport of the added molecules (methanol). Estimated values show that the methanol is transported rapidly through the ACL while proton transport is usually poor. Fig. 36 shows the operating range of the ACL under these conditions.

The analysis of the model equations shows that the thickness l_* of the reaction layer is equal to

$$l_* = \frac{s_t b}{j_0}$$

Where s_t is the ACL proton conductivity, $b = RT/(a\,F)$ is the Tafel slope and j_0 is the current density in the cell. Usually, l_* is much thinner than the ACL, which leads to an interesting scenario when Ru is dissolved. Qualitatively, the dissolution of Ru is a subordinate electrochemical process with a course that is similar to that of the overvoltage of MOR. The curve of the rate of dissolution of Ru is therefore similar to the curve of MOR; both achieve a maximum at the membrane interface. The catalyst in the conversion area (shaded area in Fig. 36) is initially destroyed while the rest of the ACL remains functional. The curves in Fig. 36 would clearly move towards the right and reach their maximum at the dotted line (Fig. 36).

---

[1] Kulikovsky, A.A.:. Analytical Modelling of Fuel Cells, Elsevier, Amsterdam, 2010

[2] Kulikovsky, A.A.: The regimes of catalyst layer operation in a fuel cell, Electrochim. Acta 55 (2010), 6391-6401

If this occurs, a new area of the reaction layer is subjected to Ru dissolution. This mechanism leads to the formation of a progressive wave moving towards the interface between anode catalyst layer and diffusion layer. This mechanism is currently being analyzed.

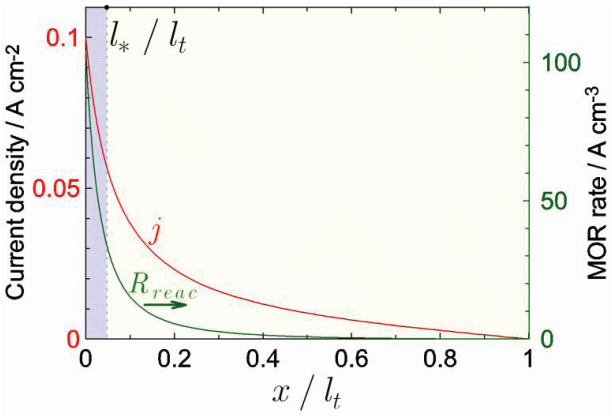

Fig. 36: **Curves of the proton current density j and the speed of the methanol oxidation reaction in the anode catalyst layer [1, 2]. The membrane is $x = 0$ and the substrate layer $x / l_t = 1$, whereby l_t is the thickness of ACL. The conversion mainly occurs in a small conversion area with a thickness of l_* close to the membrane (area shaded violet)**

Modeling of stacks

The modeling of DMFC stacks is still in its infancy. In 2010, the focus lay on improving our understanding of the most important phenomena of heat and current transport in small and large stacks. Experiments at IEK-3 have shown that small stacks have a much longer lifetime than large stacks. Modeling should help to explain this difference.

The model of heat regulation in stacks includes both the heat created by electrochemical reactions and the heat contributed by the direct catalytic combustion of methanol, which penetrates the membrane, as well as heat loss caused by the evaporation of liquid water [3]. The electrochemical model is based on analytical expressions for the half-cell overvoltage in DMFCs [4].

The model was designed for a small part of the stack, namely for a section containing a bipolar plate with air and water channels. The bipolar plate is so thin that a 3D Laplace equation for the heat transport in the plate can be replaced by a 2D Poisson equation [5].

---

[3] Kulikovsky, A.A.: Optimal temperature for DMFC stack operation, Electrochimica Acta 53 (2008), 6391–6396

[4] Kulikovsky, A.A.: On the nature of mixed potential in a DMFC, J. Electrochem. Soc., 152 (2005), A1121–A1127

[5] Kulikovsky, A.A.: Efficient parallel algorithm for fuel cell stack simulation, SIAM J. Appl. Math. 70 (2009), 531–542

Each cell in the stack is “cut” into N_{elem} elements and the code is replicated on $N_{elem}N_{cell}$ processors. In every approximation step, these elements exchange data with their neighbors in the stack. In a stack with 32 cells of 8 elements each, this code requires 8 x 32 = 256 processors. The code exhibits excellent parallel scalability.

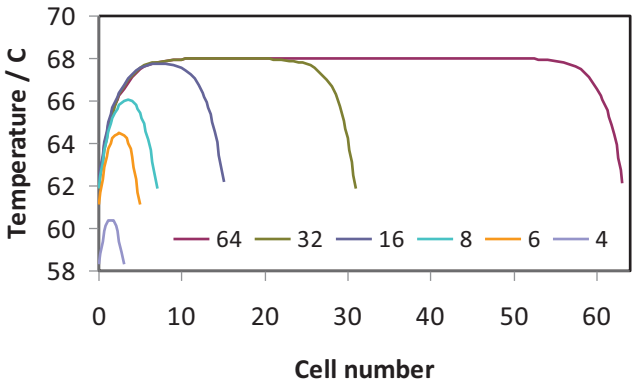

Fig. 37: Calculated axial temperature profiles of stacks with 4, 6, 8, 16, 32 and 64 cells

Fig. 37 shows the calculated temperature profile on the axes of stacks with 4, 6, 8, 16, 32 and 64 cells. Each temperature value is averaged across the surface of the respective cell. The figure shows that the axial variation of T in the small stack with 4 cells is much lower than in the large stacks. Another interesting property is the length of the “thermal boundary layer”, which comprises almost 10 cells on both sides of the large stacks. In a stack with 64 cells, the “inner” cells (11–53) have the same temperature and are insensitive to cooling by the end plates.

Further work will concentrate on investigating the uneven temperature distribution in the stacks caused by the “resistance points” in the stacks, as well as on analyzing changes to these irregularities over time. The latter problem does not just necessitate this model but also requires an expansion that includes the non-stationary terms in the appropriate equations.

3.1.3 Staff members and fields of activity

Name	Tel. (+49 2461-61-) E-mail address	Field of activity
J. Mergel	5996 j.mergel@fz-juelich.de	Head of Direct Methanol Fuel Cells
R. Elze	1902 r.elze@fz-juelich.de	Development of membrane electrode assemblies for DMFCs with high fuel utilization levels
Dr. A. Glüsen	5171 a.gluesen@fz-juelich.de	Performance optimization of MEAs for the DMFC and development of their mechanized fabrication
M. Hehemann	5431 m.hehemann@fz-juelich.de	Emission measurements on DMFC systems. Component development, setting up and operating test stands
S. Hürter	1902 s.huerter@fz-juelich.de	Development of membrane electrode assemblies for DMFCs with high fuel utilization levels
Dr. H. Janßen	5082 h.janssen@fz-juelich.de	Head of the DMFC System Development Group, development of components, system design, construction and testing of DMFC systems
D. Kalkreuth	2378 d.kalkreuth@fz-juelich.de	General quality management, quality assurance in the area of standardized electrochemical testing procedures
N. Kimiaie	6484 n.kimiaie@fz-juelich.de	Technical and organizational project coordination for DMFC system development, development of automated production and assembly techniques for fuel cell components and stacks
I. Konradi	4832 i.konradi@fz-juelich.de	Development of continuous mechanized processes for fabricating MEA components
Prof. A. A. Kulikovsky	5396 a.kulikovsky@fz-juelich.de	Development of analytical and numerical models of PEFCs and DMFCs, interpretation of experimental data, designing new cell and stack setups
A. Löhmer	8731 a.loehmer@fz-juelich.de	Clarification of physical/chemical degradation mechanisms in direct methanol fuel cells
J. McIntyre	8731 j.mcintyre@fz-juelich.de	Development of numerical models of DMFC stacks

Dr. M. Müller	1859 mar.mueller@fz-juelich.de	Head of the DMFC Stack Development Group, technical and economic optimization of DMFC stacks, selection and testing of materials for stack parts, plant design and verification
H. Schmitz	4113 hei.schmitz@fz-juelich.de	Performance optimization of diffusion layers and catalyst layers for the DMFC
Dr. M. Stähler	2775 m.staehler@fz-juelich.de	Head of the MEA Fabrication Group, standardized fabrication and characterization of DMFC membrane electrode assemblies
Dr. Chr. Wannek	4013 c.wannek@fz-juelich.de	Head of the New Materials and Processes Group, development of membrane electrode assemblies for DMFCs
M. Wannert	5590 m.wannert@fz-juelich.de	Development of mathematical procedures for magnetic imaging, reconstruction of current density distributions using 2D and 3D models and single cells
Dr. J. Wilhelm	1573 j.wilhelm@fz-juelich.de	Hybridization and control of DMFC systems, modeling and simulation of DMFC systems
W. Zwaygardt	2109 w.zwaygardt@fz-juelich.de	Design and construction of DMFC plant components, setting up and operating test stands

3.1.4 Important publications and patents

Important publications

Mergel, J.; Glüsen, A.; Wannek, C.

Current Status of and Recent Developments in Direct Liquid Fuel Cells

Hydrogen and Fuel Cells, Fundamentals, Technologies and Applications, / ed.: D. Stolten, Wiley-VCH, 2010, Weinheim. - 978-3-527-32711-9. - pp. 41 - 60

Direct liquid fuel cells, such as the direct methanol fuel cell (DMFC) or the direct ethanol fuel cell (DEFC), convert liquid fuel directly into electric current. In comparison to fuel cell systems that operate with pure hydrogen or hydrogen-rich gases from reforming processes, the fuel in the DMFC is supplied directly via liquid methanol. Apart from the very high energy density of methanol, the DMFC is characterized by easy handling and trouble-free refueling. As the reforming step is by-passed in direct fuel cells, compensation in the form of higher overvoltages (i.e. electrochemical losses) is acceptable. Despite the resulting moderate power densities, direct fuel cells are more attractive for a variety of applications in the low to medium power range than PEM fuel cells powered by hydrogen. Examples of their use include replacement of batteries in portable applications and for light traction, as there is no need for the relatively expensive and time-consuming charging of batteries or for a spare battery

for multiple-shift operation. Furthermore, the high energy density of the liquid energy carrier permits much longer operating times than batteries or fuel cell systems based on hydrogen.
This paper outlines the level of development of different direct liquid fuel cells based on current research findings and trends.

Wannek, C.; Nehr, S.; Vahlenkamp, M.; Mergel, J.; Stolten, D.

Pseudo-half-cell measurements on symmetrical catalyst-coated membranes and their relevance for optimizing DMFC anodes

Wannek, C.; Glüsen, A.; Stolten, DThe preparation of catalyst-coated membranes (CCMs.) with two anodic catalyst layers (60 % PtRu/C as catalyst) using a decal technique and their characterization by pseudo-half-cell measurements using both sides of the CCMs. by simply turning the test cell around, allows the characterization of quasi-identical CCMs. with a much smaller experimental uncertainty than observed for the classical direct methanol fuel cell (DMFC) testing of membrane electrode assemblies under similar working conditions (5 mV vs. 12 mV at a current density of 140 mA cm^{-2}). With this new sensitive tool, we study the influence of the dispersing technology and the Nafion content on the performance of DMFC anodes. While the ionomer content shows a broad optimum between 20 and 40 %, the dispersing technology does not have a strong impact on the fuel cell performance under the experimental conditions of this study, but influences strongly the stability of the catalyst slurries and the homogeneity of the electrode coatings.

Wannek, C.; Glüsen, A.; Stolten, D.

Materials, manufacturing technology and costs of fuel cell membranes

Desalination 250 (2010) 1038-1041

We give an overview about the status and current trends for fuel cell membranes. The paper highlights aspects of material design but also provides details concerning membrane manufacturing technology and the costs estimated or projected for polymer electrolyte fuel cells (PEFCs) developed for different types of applications. In addition to the description of membranes for the most common type of fuel cells, which is operated with pure hydrogen as fuel at temperatures around 80 °C and relies on perfluorosulfonic acid type membranes such as Nafion®, special focus is given to two auspicious subcategories of proton-exchange membrane fuel cells: high temperature PEFCs with phosphoric acid-doped polybenzimidazole type membranes and direct methanol fuel cells (DMFCs) with perfluorosulfonic acid or hydrocarbon type membranes. Where applicable, this is being illustrated with relevant details from the fuel cell research at Forschungszentrum Jülich's IEF-3.

Kulikovsky, A.A.

Analytical Modelling of Fuel Cells

Elsevier, Amsterdam, 2010, ISBN: 978-0-444-53560-3

Generally speaking, there are two levels of FC research: (i) study of the fundamental physical and electrochemical processes (reaction kinetics, ionic transport, capillary phenomena etc.) and (ii) engineering design of cells, stacks and FC systems. The coupling between these two levels is provided by the *physical modelling of fuel cells*. This new discipline aims at understanding the basic transport and kinetic phenomena in a real cell and stack environment. Physical modelling uses fist-level data to pave the way for better cell, stack and system designs. This discipline is the subject of this book.

A numerical result represents just one point in the multidimensional space of parameters determining FC operation. What happens in the system if we change one parameter? To answer this question another calculation has to be done. Since the number of parameters is large and each variant is a time-consuming procedure, a parametric study with the numerical models is exhausting.
Analytical solutions resulting from a good model simply show the parametric dependencies. These solutions may significantly advance our understanding of FC operation; sometimes they predict novel effects. The goal of analytical modelling is to derive simple relations describing different aspects of FC operation in special cases. The book considers these special cases. In this book we demonstrate the basic analytical solutions describing coupled kinetic, transport and electric phenomena in catalyst layers, cells and stacks. However, the aim of this book is not a simple collection of results, but rather a step-by-step demonstration of how they are derived.

Kulikovsky, A.A

The regimes of catalyst layer operation in a fuel cell

Electrochimica Acta, ***55*** *(2010) 6391- 6401*

In this work, we report the exact solutions to a generalized Perry—Newman—Cairns model for the catalyst layer (CL) operation. The model includes the ionic current conservation equation with the Butler—Volmer rate of the electrochemical conversion, the Ohm's law for ionic current and the mass balance equation for the feed molecules (oxygen, hydrogen or methanol). The exact solutions for this system are obtained for the cases of poor reagent, or poor ionic transport in the CL. In the case of poor feed transport, the electrochemical conversion runs in a small conversion domain at the CL/GDL interface. In the case of poor ionic transport, the thin conversion domain resides at the membrane/CL interface. For DMFC studies most interesting is the case of poor ionic transport, which takes place in DMFC anode. The key finding of this work is the equation for the conversion domain thickness:, where j_{s_t} is the CL proton conductivity, b is the Tafel slope of the half—cell reaction and j_0 is the cell current density. This equation helps to formulate the model of Ru dissolution on the anode side of DMFC; this work is in progress.

Janßen, H.; Blum, L.; Hehemann, M.; Mergel, J.; Stolten, D.

System Technology Aspects for Light Traction Applications of Direct Methanol Fuel Cells

18th World Hydrogen Energy Conference 2010 – WHEC 2010 Proceedings, Parallel Sessions Book 5, Schriften des Forschungszentrums Jülich, Reihe Energie & Umwelt, Vol. 78-5, ISBN: 978-3-89336-655-2, pp. 497-502

Due to extended driving range and quick refuelling time the Direct Methanol Fuel Cell (DMFC) is advantageous for special niche applications compared to the traditional battery propulsion technology. The system setup is adapted to the boundary conditions of the particular unit. Usually there are guidelines for maximum space, weight and of course costs. Additionally technical rules are given concerning gaseous and noise emissions. Safety requirements for the electric drive system and the fuel must be fulfilled.
In this contribution the results of a system analysis on the basis of a first prototype system for the energy supply of a horizontal order picker will be discussed. The key topics are as follows:
Does it make sense to pressurise the system to simplify the water management? The discussion will also include energetic aspects.
In liquid operated DMFC systems the heat and water household is directly coupled. The actual system setup uses the water crossover through the proton conducting membrane to remove the waste heat from the stack by evaporating water. To get a

water autonomous system a particular part of the evaporated water must be recycled. What are the requirements for such a unit and how can it be sized and constructed? To minimize the system volume a big effort was made. Especially the integration of the anodic sub system into the stack is promising. Different concepts and detail constructions were realised over the last years.

Wilhelm, J.; Blum, L.; Janßen, H.; Mergel, J.; Stolten, D.

Control Strategy for a Direct Methanol Fuel Cell Hybrid System

3rd European and International Conference eHydrogenia, Bukarest (Romania), 2009

Direct methanol fuel cells (DMFCs) directly convert liquid methanol into electric energy. DMFC systems are characterized by easy handling and unproblematic refuelling. Since they permit longer operating times due to the high energy density of methanol, these systems are attractive for various applications as replacements for batteries. The results of a market analysis show that the best potential for DMFC systems in the kW class is found in the material handling sector. Therefore, a DMFC system was designed for a horizontal order picker. This paper describes the process engineering and the hybridization concept of this DMFC hybrid system. The main focus will be on the control strategy for the power flow between the DMFC stack und the energy storage facility.

Wilhelm, J.; Blum, L.; Janßen, H.; Mergel, J.; Stolten, D.

Hybridization and control of direct methanol fuel cell systems for material handling applications

18th World Hydrogen Energy Conference 2010 – WHEC 2010 Proceedings, Parallel Sessions Book 5, Schriften des Forschungszentrums Jülich, Reihe Energie & Umwelt, Vol. 78-5, ISBN: 978-3-89336-655-2, pp. 523–528

Direct methanol fuel cells (DMFCs) directly convert liquid methanol into electric energy. In addition to the very high energy density of methanol, they are characterized by easy handling and unproblematic refuelling. Since they permit longer operating time, they are attractive for various applications as replacements for batteries. The results of a market analysis show that the best potential for DMFC systems in the kW class lies in the material handling sector. Therefore, a DMFC system was designed for a horizontal order picker and will be described here in terms of hybridization and control strategy. The system sizing with respect to DMFC stack dimensions, which are kept as small as possible, will be described. Because of the highly fluctuating load profile suitable energy storage for the hybrid system must be identified. The requirements for energy storage systems and the pros and cons of different types will be discussed. For the hybridization there are several possible concepts which will be compared regarding the requirements of the considered application. Result is an active series hybrid, where the DMFC and the energy storage are connected with a buck converter. To control the power flow between the DMFC and the energy storage there is a need for a control strategy, which will be described here. With this control strategy, consisting of a cascade controller and map controller, a control signal for the buck converter according to the actual states of the DMFC and the energy storage will be calculated.

Wilhelm, J.; Janßen, H.; Mergel, J.; Stolten, D.

Energy storage characterization for a direct methanol fuel cell hybrid system

Journal of Power Sources (2010), article in press, doi: 10.1016/j.jpowsour.2010.09.088

This paper describes the energy storage characterization for a direct methanol fuel cell (DMFC) hybrid system for light traction applications. In a first step, the DMFC stack and the energy storage were dimensioned. To dimension the energy storage, the required energy density and power density were calculated. These are influenced by the operating states of the vehicle as well as the highly fluctuating load profile. For this kind of application a high energy density as well as a high power density is needed. Therefore, super capacitors are not the energy storage of choice. As an alternative, suitable batteries were analyzed in terms of their behavior in the DMFC hybrid system. Therefore, a characterization procedure was developed consisting of five different tests. These tests were developed adapted to the requirements of the application. They help to characterize the battery in terms of energy content, high power capability during charge and discharge, thermal behavior and lifetime. The tests showed that all batteries have to be operated on a partial state of charge (pSOC) and a thermal management is very important. Especially lead-acid battery show an decrease in lifetime under a pSOC operation. Therefore, a lithium battery was identified as the suitable energy storage for the considered application.

Wilhelm, J.; Janßen, H.; Mergel, J.; Stolten, D.

Energy management for a fuel cell/battery hybrid system

Emobility – Electrical Power Train (IEEEXplore), 8. - 9. November 2010, doi: 10.1109/EMOBILITY.2010.5668030

Direct methanol fuel cells (DMFCs) convert liquid methanol directly into electric energy. Due to the high energy density of methanol, they permit a longer operating time. Therefore, DMFC systems are attractive in various applications as replacements for batteries. A market analysis showed that the best application potential is to be found in the material handling sector. A DMFC system was designed for a horizontal order picker, which is in this application class. To fulfill the requirements of a highly fluctuating load profile, the DMFC has to be hybridized. The hybridization concept for the DMFC energy system is described, as well as the dimensioning of the DMFC stack and the battery. The main focus will be placed on the energy management for this fuel cell/battery hybrid system. The energy management strategy is used to control the power flow between the DMFC stack and the battery according to their actual states. Additionally, this strategy has three different aims. The first is to maintain the state of charge of the battery at a constant level. The other two concern avoiding and identifying aging of the DMFC stack. Several control strategies will be analyzed with simulations and experiments.

PhD theses:

Wilhelm, J.

Hybridisierung und Regelung eines mobilen Direktmethanol-Brennstoffzellen Systems (Hybridization and Control of a Mobile Direct Methanol Fuel Cell System)

Schriften des Forschungszentrums Jülich, Reihe Energie & Umwelt, Vol. 73, ISBN 978-3-89336-642-2, RWTH Aachen 2010

Direct methanol fuel cells (DMFCs) are characterized by the fact that they directly convert the chemical energy of the liquid fuel methanol into electrical energy. Methanol has a high energy density and can be stored relatively easily. Due to these advantages, direct methanol fuel cell systems are suitable, for example, as a battery replacement for light-traction applications in the kW class. Since refueling is much faster than recharging a battery, almost interruption-free operation is possible. The aim of this thesis is therefore to develop a direct methanol fuel cell system for light-traction applications. The systems technology development and characterization of a mobile direct methanol fuel cell system is initially examined in general and then applied to the example of a horizontal order picker, a type of forklift truck. A hybridization and control concept is developed for this type of truck. The procedure is structured into the characterization of the application, the development of theoretical concepts and a concluding systems analysis using data from the test stand and simulations. The characteristic driving cycle of the application results from the characterization. The concept development is based on key data such as maximum peak performances during acceleration and braking as well as average power output. The two-stage theoretical development of a hybridization concept is based on a vehicle that is exclusively powered by fuel cells. A systems analysis of all possible concepts with respect to the criteria of fuel cell performance, total system efficiency and dynamic fuel cell loading eventually leads to the preferred concept of indirect coupling. A cascade controller with map control, the control concept developed for this purpose, keeps the energy storage unit at a constant charge and provides for aging protection as well as aging detection. The driving cycle, operational states of the vehicle and the efficiencies of the individual components play a decisive role for the dimensioning of the fuel cell as well as of the energy storage unit. Variation of parameters shows that a minimum fuel cell performance of 1.3 kW is required as is a minimum energy density of 66 Wh/l or a minimum power density of 355 W/l for the energy storage unit, respectively. The high energy density required and the fact that the energy storage unit must always be operated in a partial charge state leads to faster aging, particularly of lead storage batteries, so that a lithium battery is eventually chosen as an energy storage unit.

Trappmann, C.

Metallische Bipolarplatten für Direkt-Methanol-Brennstoffzellen (Metallic bipolar plates for direct methanol fuel cells)

Aachen, RWTH Aachen University, PhD thesis, 2010

Direct methanol fuel cells (DMFCs) efficiently convert the chemical energy of the liquid energy carrier methanol into electric power. A key component of DMFCs is the bipolar plate, which supplies and removes the process media of the electrochemically active surface of the fuel cell, separates the anode compartment from the cathode compartment and discharges the electric power generated in the cell. Traditionally, bipolar plates are fabricated from graphitic materials, because graphite is electrically conductive and is stable under the chemical conditions of DMFCs. Since graphite is extremely brittle, the structures have comparatively large wall thicknesses, resulting in less efficient utilization of installation space and in greater weight. As a result of their

mechanical properties, metallic materials in contrast allow much more compact bipolar plates. The problem, however, is the limited corrosion resistance of most metallic materials. The few corrosion-resistant metallic materials are either too expensive or form a passivation layer, which increases contact resistance and thereby electric losses.
The goal of the present work was the development of a volume-and weight-reduced bipolar plate made out of corrosion-resistant sheet metal and an inexpensive coating to reduce contact resistance.
The influence of metal ions from the non-inert materials on the DMFC was first evaluated in fundamental investigations. These investigations showed, on the one hand, that metallic contaminations of the anode fluid in the ppm range significantly damage the DMFC and, on the other hand, that iron and nickel ions do more damage than chromium ions.
Subsequently, a nickel-base alloy was identified as a corrosion-resistant material for the DMFC bipolar plate and so a metallic bipolar plate for DMFCs was developed. This bipolar plate, fabricated by hydroforming, saves 30 % installation space and 50% weight compared to graphitic bipolar plates. The development of a unique partial coating with laser build-up welded gold points allowed the contact resistance of the metallic bipolar plates to be reduced by a factor of five and the maximum electric power to be increased by 30 %. Since the gold used in this process only amounts to 1 % of the all-over coating, this partial coating is particularly economical.
Finally, the functionality of these new metallic bipolar plates was demonstrated in long-term tests. The metallic bipolar plates developed as part of this work therefore fulfill all prerequisites for use in portable DMFC applications. This represents an important step towards achieving market maturity for the DMFC.

Important patents

Patent applications:

Principal inventor	PT	Description
Prof. A.A. Kulikovsky	1.2394	A method for detection and location of current—free spots in a fuel cell stack.
Dr. M. Müller	1.2398	Heat exchanger device
Prof. A.A. Kulikovsky	1.2426	Optimal shape of catalyst concentration across the active layer of a fuel cell

Patents granted

Principal inventor	PT	Description
Dr. J. Divisek	1.1770	Alkaline direct methanol fuel cell
J. Mergel	1.854	Fuel cell stack with circuit
H. Schmitz	1.858	Methode for depositing a catalyst
H. Schmitz	1.865	Method for depositing a catalyst
Th. Bewer	1.873	Low-temperature fuel cell stack
J. Mergel	1.936	Device for cleaning waste gases for a direct alcohol fuel cell or for a fuel cell stack constructed therefrom
D. Stolten	1.1962	Catalyst layer, method for the fabrication thereof and the use of such a catalytic layer in a fuel cell
H. Schmitz	1.1982	Microstructured Diffusion Layer in Gas Diffusion Electrodes
Dr. J. Bringmann	1.2948	Method of Separation of highly active Catalyst particles
J. Mergel	1.2062	Fuel cell and method for operating the same
J. Mergel	1.2067	Cathode for a direct methanol fuel cell and method for operating the same
J. Mergel	1.2202	Fuel cell and method for operating the same
M. Stähler	1.2326	Exhaust gas purification for fuel cell stacks
Prof. A.A. Kulikovsky	1.2394	A method for detection and location of current—free spots in a fuel cell stack
Prof. A.A. Kulikovsky	1.2426	Optimal shape of catalyst concentration across the active layer of a fuel cell
Dr. M. Müller	1.2502	Methode and device for the assembling of membrane electrode assemblies for fuel cells

3.2 High-temperature polymer electrolyte fuel cells

3.2.1 Objectives and fields of activity

Commercial vehicles, construction machines, ships and aircraft will continue to be run on diesel and kerosene in the long term. Substantial energy savings can be made by increasing electrification due to more efficient on-board generation of power. From a practical point of view and in the interests of the end user, these auxiliary power units (APUs) must be run on the fuel that is already available on board. This means that these “middle distillates” must be reformed. If the high-temperature polymer electrolyte fuel cell (HT-PEFC) is combined with an appropriate reforming technology on board, it becomes possible to efficiently generate electricity, even when the engine is not running.

The HT-PEFC, based on polybenzimidazole membranes doped with phosphoric acid, has a typical operating temperature of 160 °C. As a result of the high temperature level, it has a high CO tolerance, which makes it particularly suitable for operation in combination with reformers. In contrast to Nafion-based polymer electrolyte membrane fuel cells, water is not required for the ionic conductivity of the membrane; therefore the gases do not need to be humidified. Another advantage of HT-PEFC technology is that the considerable temperature difference between the stack and the ambient temperature facilitates a more compact cooling design than is necessary in classical PEMFC systems.

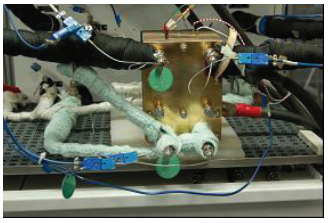

However, for all these advantages, prevention measures must be in place to ensure that the acid is not discharged from the membrane. Operating conditions that could create liquid water in the cells should be avoided. Furthermore, it was found that the membrane resistance increases significantly at a temperature below 60 °C. Operation in low temperature ranges should therefore be avoided. This has been taken into account by the operating strategies and the specific areas of application.

Since 2005, research projects have been pursued at IEF-3 in the field of the HT-PEFC. These include activities in the field of electrode development, on the one hand, and activities related to stack development, on the other. Due to positive experience with this technology and the appraisal of possible application potential, it was decided to establish this area as a new key topic within fuel cell research. Following this decision, the new High-Temperature Polymer Electrolyte Fuel Cells Group was set up in 2008. Currently, the group focuses on three topics. These are electrode development, stack development in the 5-kW power range, and modeling and simulation.

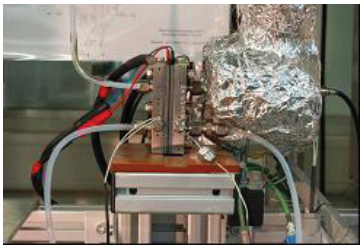

The institute's many years of experience in SOFC and DMFC research and development have given rise to synergy effects, which will accelerate HT-PEFC development. Fundamental methods in electrode, cell and stack technology, which have already been established in the DMFC area, were adapted. With respect to process engineering simulations of the design of cells and stacks, recourse was made to experience in the SOFC area. This allowed the new area to be effectively expanded into a new key topic over the last few years

This process was supported by sizeable investments in the laboratory. Some of the existing individual test stands were modified. Furthermore, two new test stands specially designed for HT-PEFC technology were acquired and put into operation. These two test stands mean that stack powers up to 5 kW_{el} are now covered.

3.2.2 Important results

3.2.2.1 HT-PEFC stack develompment

The objective of stack development is to design, construct and test HT-PEFC stacks with a power of 5 kW. Development focuses specifically on applications in the area of on-board power supply, as the HT-PEFC is particularly suitable for such applications when combined with a reformer. The HT-PEFC becomes even more relevant when the fuel that is already in the vehicle can be used. As both diesel and kerosene will continue to be used in the future, the stacks are designed for reformate gas typically containing 33 % hydrogen and 1 % carbon monoxide in the wet reformate. Due to the operating temperature between 140 °C and 180 °C, stacks are capable of withstanding the high CO content in the reformate gas. Stacks are designed for operation at ambient pressure and as PBI membranes doped with phosphoric acid are used, they require no external humidification, which leads to a simplified system layout. Both in-house MEAs and MEAs from cooperation partners were incorporated into the stacks.

Once concepts had been successfully developed for an HT-PEFC stack of the 5 kW class, several short stacks were assembled and electrochemically characterized. These tests analyzed long-term stability, power output and efficiency, as well current density distribution and temperature distribution in the stack. The basic data of the short stack developed are given in Fig. 38. The stack was operated at ambient pressure. The cell stack was tested in hydrogen operation as well as in reformate operation. The behavior of the stack in reformate operation is interesting with respect to its planned use as an auxiliary power unit. Here, the cell stack is supplied with a hydrogen-rich gas by means of a coupled fuel processing system. Further components of this gas mixture are nitrogen, carbon dioxide and carbon monoxide.

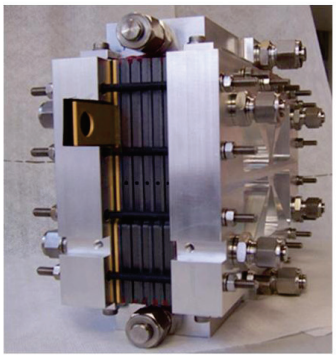

Efficiency	η_{BZ} = 40 – 55%
Operating temperature	T = 140 – 180 °C
MEA	BASF Celtec®-P1000
Cell area	200 cm²
Fuel	Hydrogen, reformate
Cooling	Oil

Fig. 38: HT-PEFC short stack

Long-term stability

Two aspects are relevant for lifetime. The first is the aging behavior of the membrane electrode assembly (MEA) and the second is the lifetime of the other stack components. Here, the choice of sealing concept is particularly important.

The aging curves of two short stacks are shown in Fig. 39. StackII2009-5 was operated with synthetic reformate, while the other was run with hydrogen at the anode. The average aging rates for the tests, each of which lasted approx. 1,000 hours, were 70 µV/h for operation with synthetic reformate and 60 µV/h for operation with hydrogen.

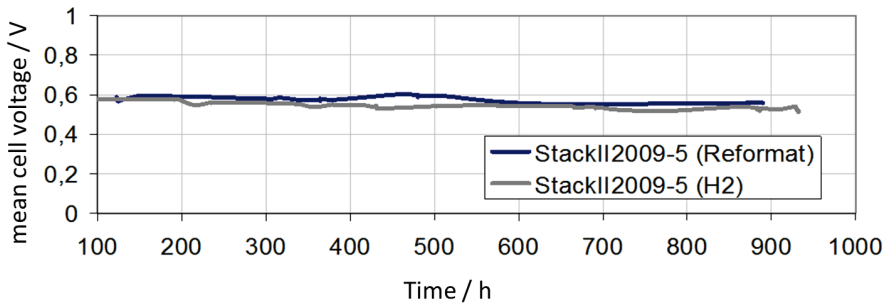

Fig. 39: Lifetime of BASF Celtec®-P1000 MEA in stack operation

Initial operating experience showed that with increasing operating time the stack leaks oil. For this reason, the sealing concept was further developed. First of all, a concept with O rings was abandoned in favor of Sigraflex surface sealing. In a second step, the graphite plates were additionally sealed with adhesive at the edges. In this configuration, a short stack was operated continuously for 2,500 hours with no oil loss.

Power output and efficiency

The power output and efficiency were determined by recording the current-voltage characteristics (Fig. 40). The short stacks were operated with pure hydrogen on the anode side as well as with reformate. On the cathode side, air was added in all tests. Operation with reformate led to poorer current-voltage characteristics because of catalyst poisoning with carbon monoxide and a lower hydrogen concentration. Comparing the polarization curves recorded for pure hydrogen and reformate also revealed that the cell voltage depends more strongly on temperature for reformate operation. Details of the design and results of the operating test of the stacks demonstrated from 2008 to 2010 were published in [6].

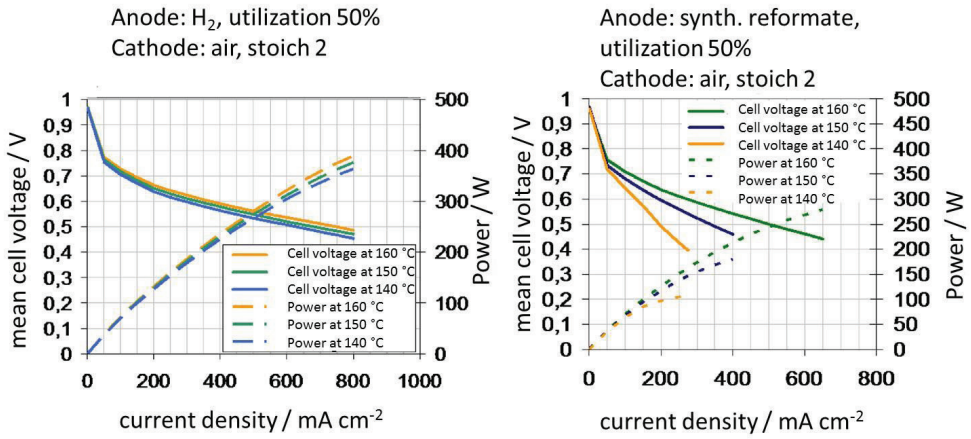

Fig. 40: Polarization curves hydrogen (left) and reformate (right)

Current density and temperature distribution

To evaluate the short stack concept and to show the potential for optimization, current density and temperature distribution were measured across the cell area. Local problem areas, recognizable by strong variations in local current densities or temperature increases, can cause accelerated aging of the fuel cell stack. A product designed especially for this stack manufactured by S++ was used to measure current density and temperature distribution. The central component is a segmented measuring plate. The local current is measured in 390 segments distributed over the cell area and temperature is measured at 65 locations. The advantage of this measuring system compared to other methods is that the design of the stack did not have to be changed for the measurements. The measuring plate was installed between cells three and four in a five-cell short stack. In order to monitor the temperature inside the stack and to calibrate the temperature sensors in the measuring plate, additional graphite plates with channels for the introduction of thermocouples were installed before the first and after the last cell in the stack.

---

[6] Bendzulla A. Von der Komponente zum Stack: Entwicklung und Auslegung von HT-PEFC-Stacks der 5 kW-Klasse, Schriften des Forschungszentrums Jülich, Vol. 69, ISBN 978-3-89336-634-7, 2010

Fig. 41 shows the measured current density and temperature distribution at an operating point for operation with hydrogen and air. The local current density decreased from the cathode inlet (top right) to the cathode outlet (bottom left). This drop is due to the depletion of oxygen in the cathode air. The cell temperature increases from the area around the coolant inlet (top) to the coolant outlet (bottom). This temperature rise occurs in the top half of the cell area. In the bottom area, a more even temperature distribution was observed.

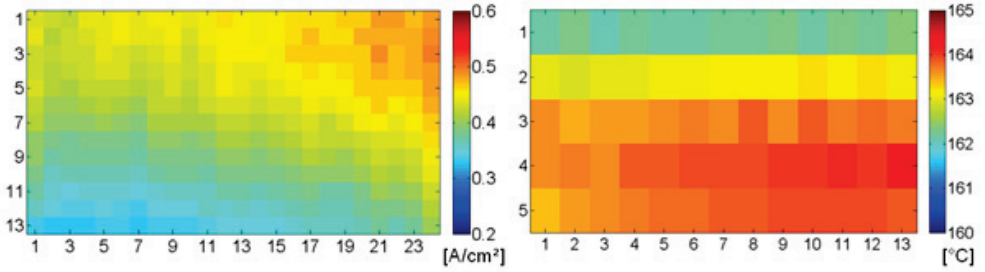

Fig. 41: Current density distribution (left) and temperature distribution (right) for StackII-2010-4 operated with hydrogen and air

The even spread in both diagrams demonstrates the quality of the stack concept. No local problem zones with discontinuities in current density and temperature distribution were visible. At the moment, research is concentrating on optimizing the flow configuration in reformate operation using current density and temperature distribution measurements.

3.2.2.2 Electrode and MEA development

In HT-PEFCs, ABPBI (poly(2,5-benzimidazole) doped with phosphoric acid is used as the electrolyte in membrane electrode assemblies (MEAs). The electrolyte is characterized by a high protonic conductivity at operating temperatures of around 160 °C. In order to increase the power and lifetime of HT-PEFCs, MEAs must be fabricated that allow the precise adjustment of the distribution of phosphoric acid within the membrane, the catalyst layers and the gas diffusion layers. Only ex situ measurements or averaging procedures currently exist for determining the distribution of phosphoric acid inside MEAs. In situ measurements with a high spatial and temporal resolution were therefore performed with synchrotron radiation. The aim was to image the local distribution of phosphoric acid inside the MEA without interrupting fuel cell operation.

Fig. 42 shows the normalized radiographs (normalized in relation to a reference image at the beginning of the measurements) of the MEA cross section of an HT-PEFC for different current densities. The membrane can be seen in the center of the image. Directly beside the membrane on the left and the right are the anode and cathode catalyst layers, respectively. They were blade coated on the tissue gas diffusion layers (GDLs). Fig. 42 a) and e) show the cells in a power-free state (OCV), while b), c) and d) show cell operation for different current densities. An increase was observed in the membrane thickness as a function of current density. The dry undoped ABPBI membrane has a thickness of 30 ± 2 µm (not shown here). After the membrane has been assembled with the electrodes doped with phosphoric acid, it swells to approx. 55 ± 3 µm (Fig. 42 a) because it adsorbs phosphoric acid from the

electrodes. Switching from OCV to 140 mA cm^{-2} leads to a further swelling of the membrane to 65 ± 3 µm after an operating time of around 15 min (Fig. 42 b and inset). Further increases in current do not cause any significant further swelling of the membrane. This could be explained by the fact that the spatial resolution does not allow very small expansions to be visually detected.

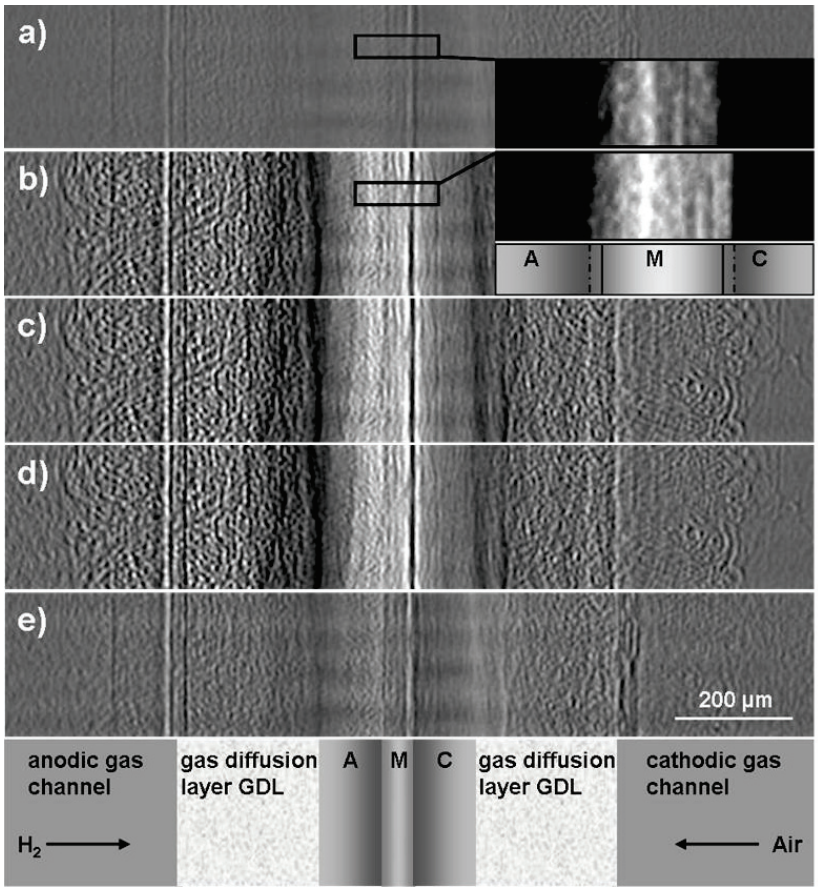

Fig. 42: **Normalized radiographs of the MEA cross section for different current densities j: a) 0 mA cm^{-2} (OCV before), b) 140 mA cm^{-2}, c) 300 mA cm^{-2}, d) 550 mA cm^{-2} and e) 0 mA cm^{-2} (OCV after). Inset: Non-normalized enlarged radiographs of the membrane and parts of the catalyst layers for OCV and 140 mA cm^{-2}. (GDL: gas diffusion layer, A: anode, M: membrane, C: cathode [7]**

The increase in membrane thickness could be due to a number of reasons: I) dilution/hydration of phosphoric acid in the membrane by means of product water; II) the transport of more phosphoric acid from the pores of the electrode layers into the membrane;

[7] Maier, W.; Arlt, T.; Wannek, Ch.; Manke, I.; Riesemeier, H.; Krüger, Ph.;. Scholta, J.; Lehnert, W.; Banhart, J.; Stolten, D.: In-situ synchrotron X-ray radiography on high temperature polymer electrolyte fuel cells, Electrochemistry Communications 12 (2010), 1436-1438

III) a combination of the first two possibilities. In order to ascertain which of these possibilities causes the swelling, transmission (and/or gray values) must be examined inside the MEA.

Fig. 43 shows the transmission inside the MEA for different states of operation. The gray values were taken from normalized radiographs and reflect changes in transmission. The radiographs in question were divided by a reference radiograph. A gray value > 1 represents an increase in transmission in the radiograph at hand compared to the reference image, while a gray value < 1 means a transmission decrease in the radiograph. If the gray value is equal to 1, the transmission is the same for the real and the reference radiographs.

The results in Fig. 43 show that switching from OCV to 140 mA cm^{-2}, 300 mA cm^{-2} or 500 mA cm^{-2} leads to increased transmission in the membrane (M). This transmission increase can be explained by the formation of product water. The product water leads to dilution/hydration of the phosphoric acid and thus causes the membrane to swell. The corresponding attenuation coefficient of water (0.157 cm^{-1} at 30 keV) is around one order of magnitude smaller than that of phosphoric acid (1.020 cm^{-1} at 30 keV). The transmission increase can therefore only be caused by an increase in water inside the membrane and the build-up of phosphoric acid hydration products.

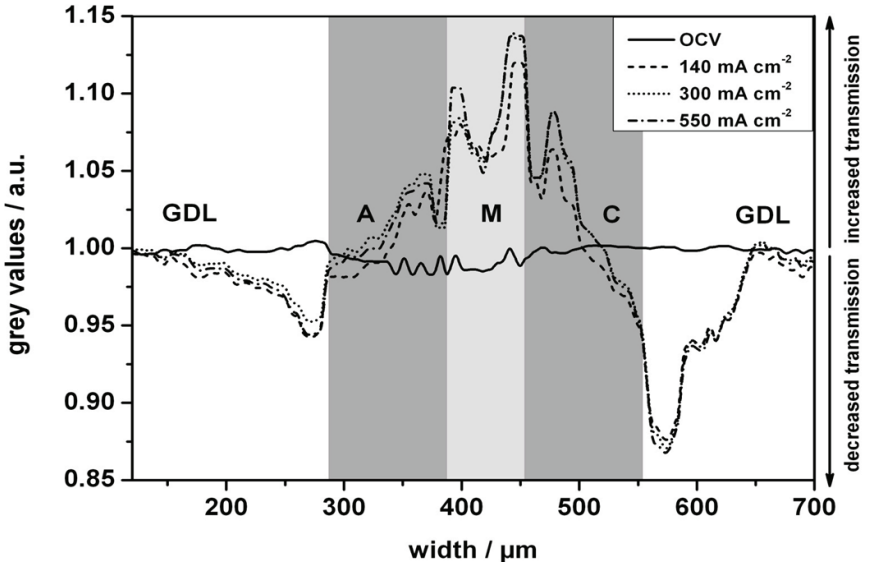

Fig. 43: Gray values inside the MEA for different operating conditions: OCV (continuous line), 140 mA cm^{-2} (dashed line), 300 mA cm^{-2} (dotted line) and 550 mA cm^{-2} (dash-dotted line). The membrane thickness for different operating conditions was derived from the non-normalized radiographs and is shown here as a gray shaded area [7]

Another effect was observed inside the cathode catalyst layer (C). At the membrane/electrode interface, an increase in transmission can also be observed. The phosphoric acid, which is also found in the pores of the catalyst layer near the membrane, is also diluted/hydrated here by product water. Due to the fact that approx. 20 % of the product water diffuses on the anode side (A), these dilution/hydration processes are also visible

there. At the electrode/GDL interface, a decrease in transmission can be observed. This decrease can be explained by the filling of previously empty pores in the catalyst layers. During the running-in process, a large fraction of the phosphoric acid previously located in the catalyst layers diffuses into the membrane. The pores in the catalyst layer located at the interface to the GDL thus remain partially empty. Filling these pores with phosphoric acid leads to a decrease in transmission.

The results presented here show that synchrotron radiography is an efficient method for determining the local composition of MEAs in HT-PEFCs during operation. It allows us insights into the processes occurring at different operating conditions and therefore helps us to improve our understanding of fuel cell operation. It also allows the MEA design to be optimized, the cell performance to be increased and degradation mechanisms to be better understood.

In the future, further synchrotron measurements will be conducted in order to quantitatively analyze the water balance in MEAs for different operating conditions as well as during the running-in process. They will also allow us to investigate the influence on the performance and lifetime of HT-PEFCs.

3.2.2.3 Modeling/simulation

The development of fuel cells and fuel cell stacks at IEK-3 is based on both solid engineering approaches as well as basic scientific principles. Both aspects are equally as important since current distribution in the media and electrochemical processes strongly influence each other. In combination with electrochemical models, computational fluid dynamics (CFD) is a tool suitable for describing processes on both a cell level and a molecular level. In the following, two selected examples will show what insights can be gained from modeling.

Modeling a test cell

The basic behavior of new materials (e.g. new catalyst layers) and the behavior for different operating conditions can be experimentally verified in “test cells”. These cells have an active area of approx. 16 cm^2. Their uncomplicated structure (Fig. 44) means that they can be prepared quickly for different types of tests.

Despite its relatively simple construction, the processes that occur inside the test cell are fairly complex. The interplay between electrochemical reactions, flow and overall heat balance, in particular, can only be measured with a limited spatial resolution. On the other hand, the test cell can be adequately characterized in experiments and can therefore be used to validate complex models. For this reason, a CFD model was created to initially visualize the existing test cell.

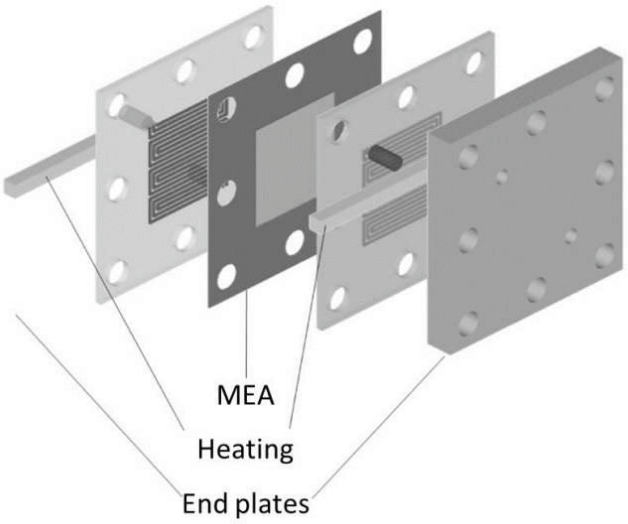

Fig. 44: Schematic of a test cell

The temperature distribution of the test cell in operation is shown in Fig. 45 as an example. The dominant influence of the two heating rods can be clearly seen. The maximum temperature difference between different points on the surface is approx. 7 K. This was verified with the aid of an infrared camera.

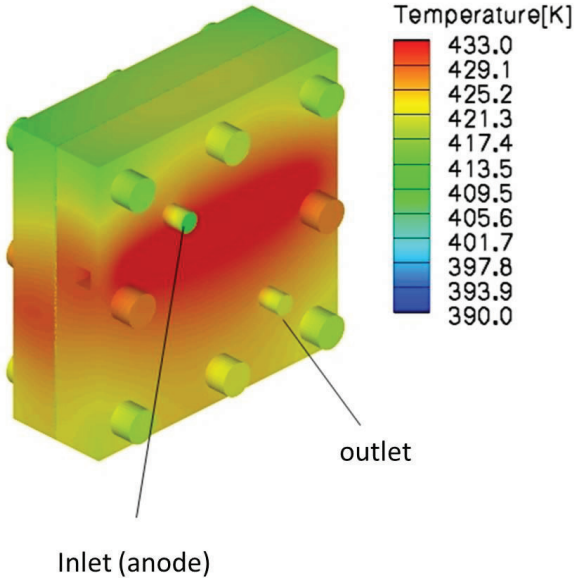

Fig. 45: Temperature of the test cell in operation (simulation) – H_2/air for stoichiom. 2.0/2.0 and j = 200 mA/cm^2

An important issue is the relation between current density distribution and temperature distribution as the electrochemical reaction does not just provide heat but the kinetics of the reaction itself depends on the temperature. Fig. 46 shows the temperature and current density distribution on the active area of the MEA. It can be clearly seen that temperature distribution and current density distribution are very weakly coupled. The emerging temperature gradients are too small to have a significant impact on the operation of the fuel cell with pure hydrogen. However, operating the cell with reformate is expected to give rise to a much stronger coupling. The different scales in Fig. 46 indicate that the differences in temperature are very small. The distribution of current density, in contrast, appears to behave independently of the operating point.

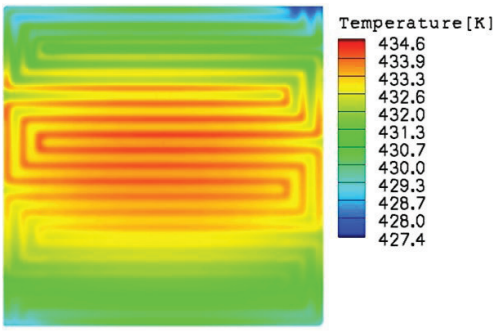

a) Temperature distribution on the MEA at j = 200 mA/cm^2

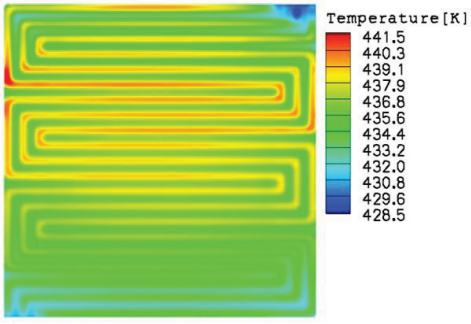

b) Temperature distribution on the MEA at j = 700 mA/cm^2

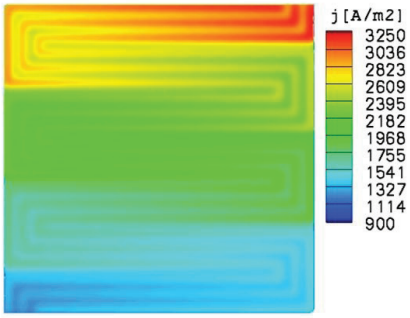

c) Current density distribution on the MEA at j = 200 mA/cm^2

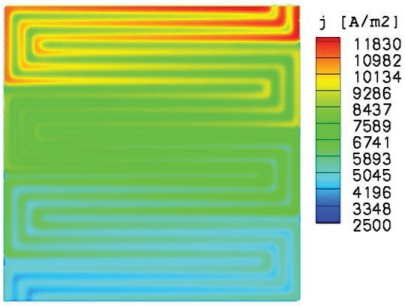

d) Current density distribution on the MEA at j = 700 mA/cm^2

Fig. 46: Temperature and current density distribution (simulation) – H_2/air operation for stoichiom. 2.0/ 2.0

Modeling of fuel cell modules

As mentioned in the previous section, single test cells are heated externally in order to maintain the operating temperature of approx. 160 °C. Large fuel cell modules therefore have more complex requirements in terms of heat management. In order to heat these modules up and to operate them with low electric power, they must be externally heated. In the medium

and high power range, in contrast, excess heat has to be removed from the module. The operating temperature should be kept as constant as possible at all times. For this reason, a cooling system (which both supplies and removes heat) is an important component in larger modules.

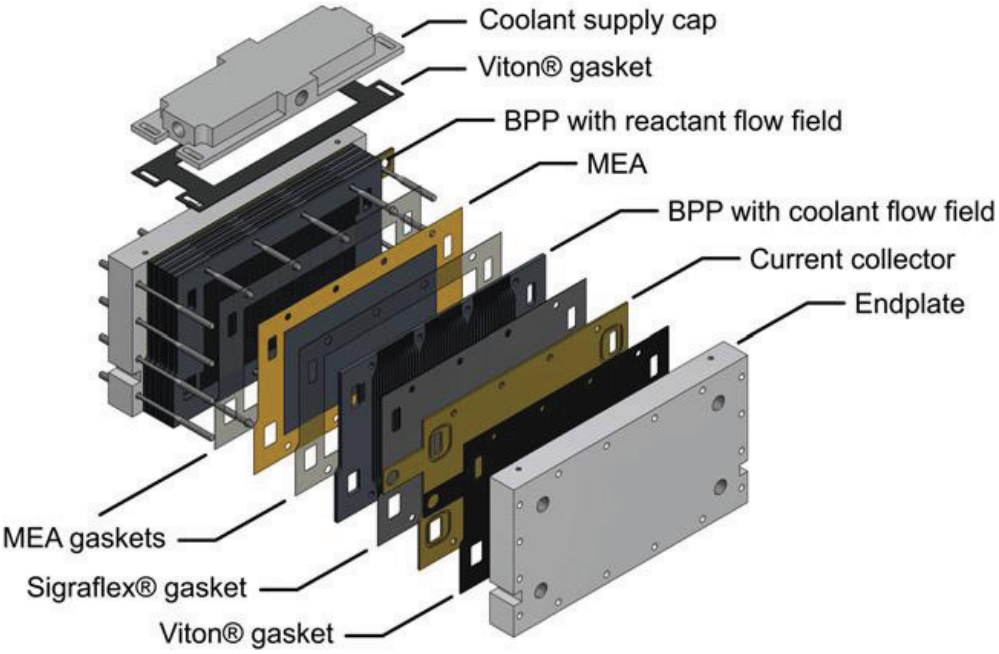

a) Exploded view of an HT-PEFC fuel cell module

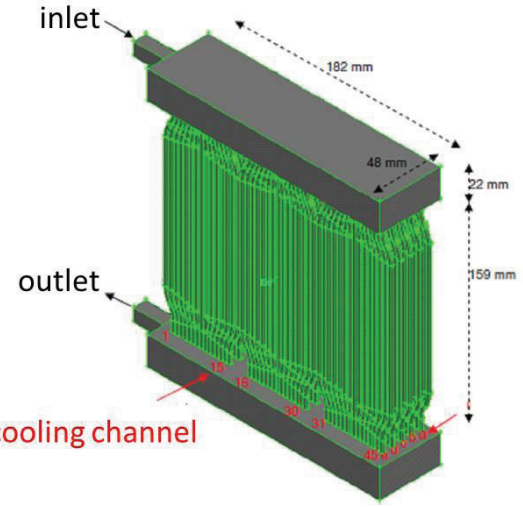

b) CFD model for a five-cell module (not insulated)

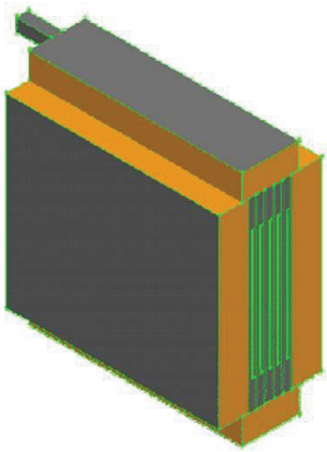

c) CFD model for a five-cell module (insulated)

Fig. 47: Schematic and CFD model of an HT-PEFC fuel cell module

Within the framework of a diploma dissertation [8], the cooling system of an existing module was reproduced as a CFD model and a possible strategy for improving it was outlined. Due to the very complex geometry of the module, an appropriate model reduction must first be performed. The flow channels are therefore represented as an effective porous medium, thus considerably simplifying the computational fluid dynamics and making it possible to simulate such modules. Fig. 47 shows the structure of such a module and the resulting CFD model.

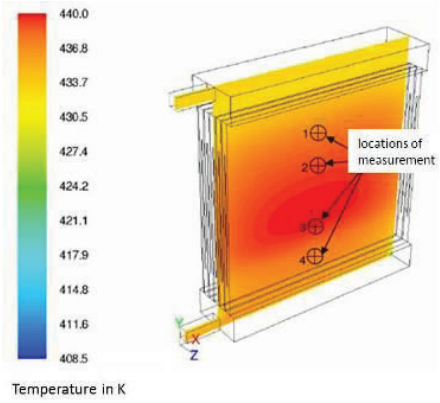

a) Position of the temperature sensors

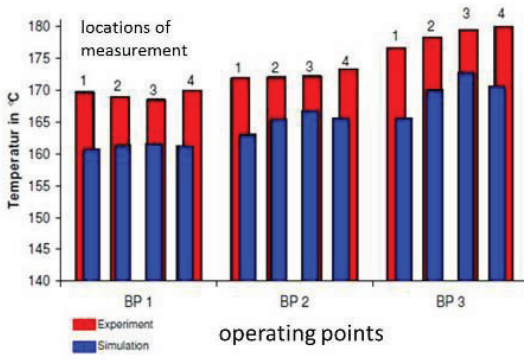

b) Comparison of temperatures from experiments and simulations

Fig. 48: Temperature distribution of the module for different operating points (OP 1: j = 100 mA/cm^2; OP 2: j = 300 mA/cm^2; OP 3: j = 500 mA/cm^2)

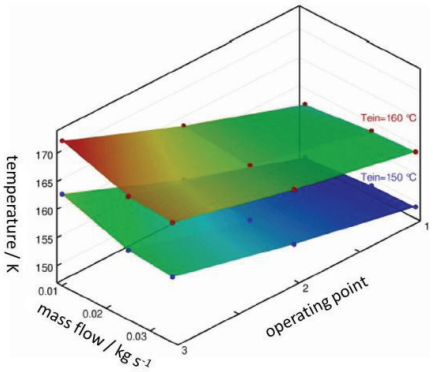

Fig. 49: Mean temperatures on the active area of the HT-PEFC module as a function of mass flow rate and the coolant inlet temperature (OP 1: j = 100 mA/cm^2; OP 2: j = 300 mA/cm^2; OP 3: j = 500 mA/cm^2)

[8] Supra, J.: Aktive Kühlung von Brennstoffzellen in Flugzeugsystemen - CFD Simulationen für den Typ HT-PEFC, RWTH Aachen University, 2010

To validate the model, experimental temperature measurements were compared with the simulation results. The comparison shows adequate accuracy for the selected model (see Fig. 48).

The main finding was that the selected configuration of the cooling system ensures a very homogeneous temperature distribution. However, the inlet temperature of the coolant must be actively controlled as a function of the operating point in order to ensure that the maximum allowed temperature is not exceeded at high current densities. If a constant coolant temperature is selected for pragmatic reasons, there is a certain operating window within which such modules can be run without any damage (see Fig. 49).

3.2.3 Staff members and fields of activity

Name	Tel. (+49 2461-61-) E-mail address	Field of activity
Dr. W. Lehnert	3915 w.lehnert@fz-juelich.de	Head of High-Temperature Polymer Electrolyte Fuel Cells
J. Bohner	5172 j.bohner@fz-juelich.de	HT-PEFC stack development
J. Brinkmann	2177 j.brinkmann@fz-juelich.de	Modeling on the cell component level
D. Froning	6676 d.froning@fz-juelich.de	Modeling of fuel cells, computer science, software engineering
B. Kohnen	5406 b.kohnen@fz-juelich.de	Technical support for HT-PEFC test stands and examination of HT-PEFCs
Prof. Dr. A. Kulikovsky	5396 a.kulikovsky@fz-juelich.de	Development of analytical and numerical models of HT-PEFCs, DMFCs and SOFCs
M. Kvesic	5396 m.kvesic@fz-juelich.de	Stack modeling
F. Liu	9036 f.liu@fz-juelich.de	Electrode characterization
L. Lüke	8965 l.lueke@fz-juelich.de	Operating behavior of HT-PEFC stacks
W. Maier	9073 w.maier@fz-juelich.de	Electrode characterization
A. Majerus	3018 a.majerus@fz-juelich.de	Membrane and electrolyte characterization
Dr. M. Nullmeier	9074 m.nullmeier@fz-juelich.de	Principles of electrochemistry HT-PEFC
M. Prawitz	2574 m.prawitz@fz-juelich.de	PEFC, testing and characterization of HT-PEFCs
Dr. U. Reimer	3537 u.reimer@fz-juelich.de	Head of the HT-PEFC Modeling and Simulation Group

B. Schumacher	5406 b.schumacher@fz-juelich.de	Development of designs for test stands for HT-PEFCs, testing of HT-PEFCs
J. Supra	6029 j.supra@fz-juelich.de	Development of HT-PEFC stacks, benchmarking of stack materials
R. Zeis	1923 r.zeis@fz-juelich.de	Head of the Principles of Electrochemistry HT-PEFC Group

3.2.4 Important publications and patents

Important publications

Wannek, Ch.; Konradi, I.; Mergel, J.; Lehnert, W.

Redistribution of Phosphoric Acid in Membrane Electrode Assemblies for High Temperature Polymer Electrolyte Fuel Cells

*Int. J. Hydrogen Energy **23** (2009) 9479*

> We demonstrate that the performance of a high-temperature polymer electrolyte fuel cell with a phosphoric acid-based electrolyte is almost independent of the way of introducing the acid into the membrane electrode assembly (MEA). The same power densities were obtained with different MEAs in which the poly(2,5-benzimidazole) membrane was either pre-doped or not and in which either one or two catalyst layers were impregnated with H_3PO_4. Chemical analysis after shut down revealed that in all these MEAs the phosphoric acid distribution between the membrane and the electrodes was nearly the same. An MEA with acid impregnation via the electrodes was started up rapidly from room temperature, delivered a power density of 120 $mWcm^{-2}$ at 600 mV (H_2/air, 160 °C, ambient pressure) after only 11 min and was operated for 1,000 h (degradation rate: 0.06 mV/h). Based on the analysis of the H_3PO_4 content in the MEA components, reflections on the kinetics of the redistribution of phosphoric acid within the MEA are provided.

Wannek, Ch.; Lehnert, W.; Mergel, J.

Membrane electrode assemblies for high-temperature polymer electrolyte fuel cells based on poly(2,5-benzimidazole) membranes with phosphoric acid impregnation via the catalyst layers

J. Power Sources 192 (2009) 258-266

> A novel strategy for introducing phosphoric acid as the electrolyte into high-temperature polymer electrolyte fuel cells by using acid impregnated catalyst layers instead of pre-doped membranes is presented in this paper. This experimental approach is used for the development of membrane electrode assemblies based on poly(2,5-benzimidazole) (ABPBI) as the membrane polymer. The acid uptake of free-standing ABPBI used for this work amounts to ABPBI×3.1 H_3PO_4 which has a specific conductivity of ~80$mScm^{-1}$ at 140 °C. Rather thick catalyst layers (20 % Pt/C, 1mg Pt cm^{-2}, 40 % PTFE as binder, d = 100–150 µm) are prepared on gas diffusion layers with a dense hydrophobic microlayer. After impregnation of the catalyst layers with phosphoric acid and assembling them with a mechanically robust undoped ABPBI

membrane a fast redistribution of the electrolyte occurs during cell start-up. Power densities of about 250 mWcm^{-2} are achieved at 160 °C and ambient pressure with hydrogen and air as reactants. Details of membrane properties, preparation and optimization of gas diffusion electrodes and fuel cell characterization are discussed. We consider our novel approach to be especially suitable for an easy and reproducible fabrication of MEAs with large active areas.

Kulikovsky, A.A.

Efficient Parallel Algorithm for Fuel Cell Stack Simulation

*SIAM J. Appl. Math., **70** (2009) 531—542*

A planar fuel cell stack is a layered structure consisting of repeated modules — membrane-electrode assemblies (MEAs) separated by bipolar plates (BPs). Generally, the distributions of voltage and temperature over the BP volume are described by three-dimensional Laplace equations. However, the thickness of a BP is much smaller than its in-plane size. This enables us to reduce a three-dimensional Laplace equation to a two-dimensional Poisson equation and to develop an efficient parallel algorithm for stack simulation. In the simplest variant, each individual module "MEA + BP" is solved on a separate processor. Typically, the number of cells in a stack is 10 to 100; this algorithm is thus most suitable for small- and medium-scale parallel machines. A much faster method is to cut every module into a number of "stripes" and to solve each stripe on a separate processor. Numerical tests with this method show that with eight stripes per module the solution of the electric problem is obtained roughly ten times faster than expected. Evidently, the striping algorithm provides much faster convergence of the iterative Poisson solver. The effect is presumably due to fast damping of high-frequency modes of potential in the iteration process. This algorithm may open up possibilities for fast simulation of real 100-cell stacks using massively parallel machines.

Thiedmann, R.; Hartnig, Ch.; Manke, I.; Schmidt, V.; Lehnert, W.

Local Structural Characteristics of Pore Space in GDLs of PEM Fuel Cells Based on Geometric 3D Graphs

*J. Electrochem. Soc **156** (2009) B1339 – B 1347*

Physical properties affecting transport processes inside the gas diffusion layer (GDL) in polymer electrolyte membrane (PEM) fuel cells mainly depend on the microstructure of its pore space. The presented characterization of the complex structure of the pore space is based on geometric three-dimensional (3D) graphs, which are marked to display transport-related properties such as pore diameters. This representation of the open volume allows for an investigation of local structural characteristics by considering local tortuosity characteristics, pore sizes, and connectivity characteristics, respectively. The notion of local shortest path length through the pore space of the GDL is introduced and the probability distribution of this random variable is computed. Its mean value is related to the (physical) tortuosity, which is given by the ratio of the mean effective path length through the GDL and its thickness. The developed methods are applied to simulated and to real (experimentally measured) 3D data. The used stochastic 3D model for the GDL is an extended version of the multilayer model proposed by Thiedmann et al. (J. Electrochem. Soc., 155, B391 (2008)), including a more flexible modeling of binder. The numerical results show the sensitivity of the proposed local characteristics to varying binder modeling.

Wippermann, K.; Wannek, Ch.; Oetjen, H.-F.; Mergel, J.; Lehnert, W.

Cell Resistances of ABPBI-based HT-PEFC-MEAs: Time Dependence and Influence of Operating

*J. Power Sources **195** (2010) 2806–2809*

Time-dependent measurements of cell impedance of a HT-PEFC based on ABPBI were performed at constant frequencies close to the high-frequency (h.f.) intercept of the corresponding Nyquist plots with the real axis. The h.f. impedances approximate the ohmic resistance of the cell and they decrease, when current (140 $mAcm^{-2}$) is switched on. Steady-state values are attained after 10 min. Vice versa, when current is switched off (OCV), the h.f. impedances instantaneously increase but reach steady-state values only after about 1 h. These values rise with increasing gas flow rates. The results are discussed in terms of hydration/dehydration processes, changing the equilibrium between orthophosphoric and pyrophosphoric acid and thus the conductivity of the electrolyte as well as the mobility of molecules and charge carriers. Impedance spectra were recorded after each time-dependent measurement under OCV conditions. The fit of these impedance data based on an equivalent circuit revealed ohmic resistances corrected by h.f. inductances and low frequency impedances associated with the cathode oxygen exchange reaction. The charge transfer resistances deduced from the low frequency impedances strongly depend on both air and hydrogen flow rates.

Kulikovsky, A.A.

The regimes of catalyst layer operation in a fuel cell

Electrochimica Acta, 55 (2010) 6391–6401.

A generalized Perry–Newman–Cairns model for performance of a generic catalyst layer (CL) with the Butler–Volmer conversion function is considered. The CL polarization curve, the rate of electrochemical conversion S(x) and the thickness of the conversion domain $l*$ are derived for the cases of ideal transport of ions or feed molecules. In both cases, the CL may work in the low- or high-current regime. In the low-current regime with poor ionic transport, $l*$ is given by the Newman's current-independent reaction penetration depth. In the high-current regime, $l*$ is inversely proportional to the cell current, regardless of the origin of transport loss. The position and width of the transition region between the low- and high-current branches of the polarization curve are calculated. Based on these results, the features of catalyst layer performance in PEMFC, HT-PEMFC, DMFC and SOFC are discussed.

Wang, Y.; Cho, S.; Thiedmann, R.; Schmidt, V.; Lehnert, W.; Feng, X.

Stochastic Modeling and Direct Simulation of the Gas Diffusion Media for Polymer Electrolyte Fuel Cells

*Int. J. Heat and Mass Transfer, **53** (2010) 1128–1138*

This paper combines the stochastic-model-based reconstruction of the gas diffusion layer (GDL) of polymer electrolyte fuel cells (PEFCs) and direct simulation to investigate the pore-level transport within GDLs. The carbon-paper-based GDL is modeled as a stack of thin sections with each section described by planar two-dimensional random line tessellations which are further dilated to three dimensions. The reconstruction is based on given GDL data provided by scanning electron microscopy (SEM) images. With the constructed GDL, we further introduce the direct simulation of the coupled transport processes inside the GDL. The simulation considers the gas flow and species transport in the void space, electronic current

conduction in the solid, and heat transfer in both phases. Results indicate a remarkable distinction in tortuosities of gas diffusion passage and solid matrix across the GDL with the former ~1.2 and the latter ~13.8. This difference arises from the synthetic microstructure of GDL, i.e. the lateral alignment nature of the thin carbon fiber, allowing the solid-phase transport to occur mostly in lateral direction. Extensive discussion on the tortuosity is also presented. The numerical tool can be applied to investigate the impact of the GDL microstructure on pore-level transport and scrutinize the macroscopic approach vastly adopted in current fuel cell modeling.

Maier, W.; Arlt, T.; Wannek, Ch.; Manke, I.; Riesemeier, H.; Krüger, Ph.;. Scholta, J.; Lehnert, W.; Banhart, J.; Stolten, D.

In-situ synchrotron X-ray radiography on high temperature polymer electrolyte fuel cells

Electrochemistry Communications ***12*** *(2010) 1436*

In contrast to classical low temperature polymer electrolyte fuel cells (LT-PEFCs), the membrane conductivity in high temperature polymer electrolyte fuel cells (HT-PEFCs) (operating temperature ~160 °C) is based on proton transport within phosphorus-oxygen acids at different levels of hydration, orthophosphoric acid (H_3PO_4) being the simplest example. We present for the first time in-situ synchrotron X-ray radiography measurements applied to a HT-PEFC to gain insight into the local composition of the membrane electrode assembly (MEA) under dynamic operating conditions. Transmission changes during the radiographic measurements exhibit a clear influence of the formation of product water on the membrane composition.

Steinberger-Wilckens, R.; Lehnert, W.

Innovations in Fuel Cell Technology

RSC Publishing, Cambridge, 2010, ISBN: 978-1-84973-033-4

This book reviews the state-of-the-art in fuel cells (low and high temperature) across all the types applied in the field today and assesses current trends in development. The main technology problems are discussed and current gaps to market success identified. The innovations covered in the book deliver new answers to pertinent problems and/or offer new opportunities, be it in operating conditions, application area, extension of lifetime, new fuels, exciting new diagnosis and analysis methods. The volume gives an insight not only to the key developments within the next few years, but also shows perspectives in the mid-term. Readers receive an overview of cutting edge, challenging research and development that can be used in future developments, both of personal careers, as well as in company technology planning.

Kulikovsky, A.A.

Analytical Modelling of Fuel Cells

Elsevier 2010, ISBN: 978 0-444-53560-3

This book summarizes advances in the new and rapidly evolving field of analytical modeling of fuel cells, cell components and stacks. Analytical solutions to fundamental problems ranging from catalyst layer performance to thermal stability of stack operation are given. In fuel cell research, the gap between fundamental electrochemical processes and the engineering of fuel cell systems is bridged by the physical modeling of fuel cells. This relatively new discipline aims to understand the basic transport and kinetic phenomena in a real cell and stack environment, paving the way for improved design and performance. The author presents a unique approach to fuel cell modeling in this essential reference for energy technologists.

Key features of the book:
Covers recent advances and analytical solutions to a range of problems faced by energy technologists, from catalyst layer performance to thermal stability
Provides detailed graphs, charts and other tools to maximize R&D output while minimizing costs and time spent on dead-end research.
Presents Kulikovsky´s signature approach (and the data to support it) – which uses "simplified" models based on idealized systems, basic geometries, and minimal assumptions – enabling qualitative understanding of the causes and effects of phenomena.

Bendzulla, A.

Von der Komponente zum Stack: Entwicklung und Auslegung von HT-PEFC-Stacks der 5 kW-Klasse. (From the Components to the Stack: Developing and Designing 5 kW HT-PEFC Stacks)

Schriften des Forschungszentrums Jülich, Reihe Energie & Umwelt / Energy & Environment Band / Vol. 69, ISSN 1866-1793, ISBN 978-3-89336-634-7, 2010

Numerous areas of application, such as aviation or heavy goods transport, have no medium-term alternative to the middle distillates currently in use, namely diesel and kerosene. For both economic and environmental reasons, optimizing the efficiency of the systems in use is therefore a key objective. In achieving this objective, fuel cells are a promising option. Due to the lacking hydrogen infrastructure, fuel cells are equipped with an on-board supply system. The hightemperature polymer electrolyte fuel cell (HT-PEFC) is particularly suitable for such applications due to its high CO tolerance, simple water and heat management, and moderate material loads. The aim of the present project is to develop a stack design for a 5-kW HT-PEFC system. First, the state of the art of potential materials and process designs will be discussed for each component. Then, using this as a basis, three potential stack designs with typical attributes will be developed and assessed in terms of practicality with the aid of a specially derived evaluation method. Two stack designs classified as promising will be discussed in detail, constructed and then characterized using short stack tests.

Important patents

Patent applications:

Principal inventor	PT	Description
Dr. H. Dohle	1.2375	High-temperature polymer electrolyte fuel cell system (HT-PEFC) and a method for operating the same

Patents granted

Principal inventor	PT	Description
J. Mergel	1.2334	Cooling cell for a fuel cell

3.3 Solid oxide fuel cells

3.3.1 Objectives and fields of activity

Solid oxide fuel cells (SOFCs) generate electricity and can be operated not just with pure hydrogen but also with a number of other fuels including natural gas, biogases and diesel reformate. This makes this type of fuel cell suitable for various stationary and mobile applications – for example, in the field of decentralized energy supply for single-family houses and multifamily dwellings or for industrial consumers, as well as in the area of mobile applications for on-board power supply in vehicles, ships and aircraft.

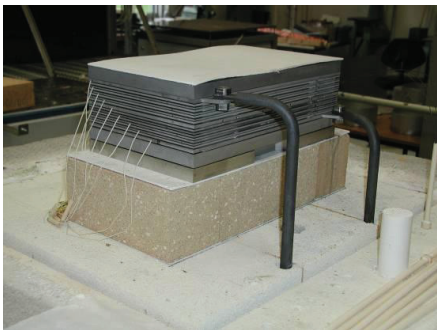

In the field of research and development, the Electrochemistry of Solid Oxide Fuel Cells Group tests stacks, as well as single cells, in order to investigate the impact of a wide range of operating conditions. The experimental facilities are equipped to facilitate a number of fuel gas compositions – from pure hydrogen to biogases with impurities such as hydrogen cyanide or hydrogen sulfide. In addition, special test facilities are being developed and built to allow the interaction between different stack components to be investigated. An example of this is the interaction between the metallic interconnect and the glass or metal sealant in different fuel cell atmospheres, whereby the electrically insulating function of the glass sealant is simultaneously tested using resistance measurements. A similar setup also exists for the interaction between the contact layer or protective coating and the cathode material, whereby the conductivity is continuously measured. The interaction between interconnect materials (with and without a protective coating) and cells is also currently being studied, whereby the influence of metallic components on the cell performance is being selectively investigated.

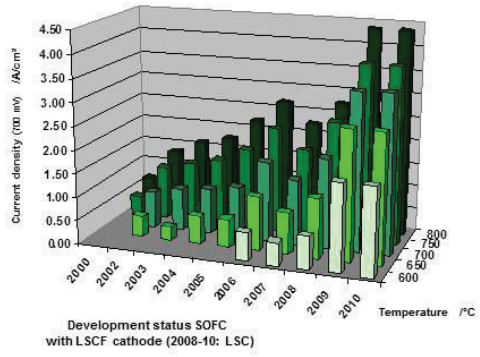

Different applications make different demands on the lifetime of a fuel cell. For stationary applications, a minimum lifetime of 5 years is essential. During this time, the fuel cell must not lose more than 10 % of its initial power output. Long-term tests are being carried out on both single cells and stacks and performance is being measured as a function of electrical load over time. In addition to the strength of the current, the operating temperature and the fuel gas composition are also important parameters whose influence on performance is being investigated. Another topic related to development and optimization is the comparability of measurement results for different types of cells and the analysis of the influence of materials and/or fabrication techniques.

In the area of mobile applications, the demands made on stacks are much more stringent than those in the area of stationary applications due to dynamic operation. Changes in load occur very often, thus causing the current strength to vary considerably. In real systems, the temperature of the stack decreases in stand-by mode. When it is restarted, the stack must be brought to operating temperature as rapidly as possible. This places great demands on the materials used and on their thermomechanical stability. These processes are also being investigated in stacks in order to characterize technologically relevant systems. The stack must retain its power output, for example losing no more than 10 % after 100 cycles.

In addition to experimental studies, SOFC operation is also analyzed by mathematical modeling. The processes in the SOFC (charge, heat and mass transfer) are described by mathematical (partial differential) equations. The models can describe the structures and processes in a very detailed (3D) or very simplified (1D) manner. The latter models are not as complex and thus easier to solve, which means that they can be used in generic system simulations. Current, temperature and concentration distributions are determined by solving all model equations numerically (simulation calculations). The operating behavior of an SOFC can thus be predicted, providing optimized approaches for layout and design, which in turn accelerates development.

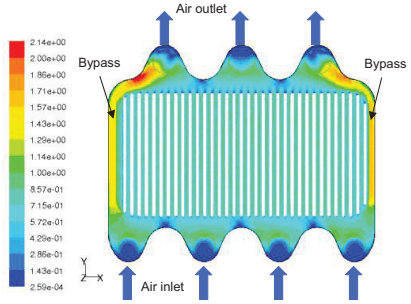

Modeling work is supported in certain areas by experimental work, either to determine the input parameters for the calculations or to verify the calculation results. Thus, for example, mass transfer parameters in porous bodies (anode substrate, cathode layer) are selectively determined by diffusion and permeation measurements, which are then incorporated into simulation calculations. Moreover, in special measurement setups, the flow distribution can be determined in the gas distribution channels inside the cell by measuring pressure loss and pressure distribution. The measurement setup allows the manifolds to be varied simply and quickly. This in turn means that the geometry for homogeneous mass distribution can be optimized.

The Fuel Cell Process Engineering Group is involved in the layout, design, and construction of test setups and their components, as well as process engineering system analyses. The main fields of work are described below:

Construction, modeling and testing of plant components: The key components of an SOFC system, such as the recuperative heat exchanger, prereformer or afterburner, are not commercially available. For this reason, test facilities are set up to characterize products developed in-house and by third parties and to examine their suitability. Development work is supported by the use of CFD and FEM to analyze component behavior, and to make suggestions for optimizing design and operation.

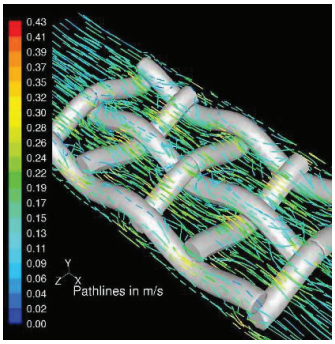

Testing and optimizing the control and regulating concepts of SOFC systems: Fuel cells require complex plant and process engineering. In order to reliably operate the plants, to safely control the different operating modes and to prevent damage to the plant and the fuel cells, special control and regulating concepts are essential. These are derived on the basis of experience acquired testing cells and stacks, and are then tested and further developed in the existing plants.

Development and construction of plants: In order to demonstrate the feasibility of the technology and test the interplay of all components, an SOFC demonstration plant is being developed and built. It will run on natural gas and should achieve an electric power of 20 kW.

Calculation and evaluation of plant concepts: Based on experience gained in experiments, steady-state and dynamic simulation calculations are carried out using different tools, with which different plant concepts can be evaluated and individual plant components designed.

3.3.2 Important results

3.3.2.1 Cell and stack development

Optimizing the performance of cells

The performance of SOFC cells developed and fabricated in IEK-1 and electrochemically characterized in IEK-3 is very good today thanks to the targeted modification of materials and (micro)structures. The performance of cells with (La,Sr)MnO_3 (LSM) cathodes, which are standard for the operation of stacks at temperatures of 700 - 800 °C, was shown to have very good reproducibility in quality assurance measurements taken over the years (Fig. 50, left).

In order to decrease the operating temperature, cells with (La,Sr)(Co,Fe)O_3 (LSCF) cathodes were refined at IEK-1. However, these cells require a diffusion barrier between the yttria-stabilized zirconia (YSZ) electrolyte and the cathode in order to avoid the formation of

strontium zirconate at the interface. This diffusion barrier is made from gadolinium-doped cerium oxide (CGO). It was found that the use of special techniques such as physical vapor deposition (PVD) for the diffusion barrier and the omission of iron in the cathode composition (LSC) led to very high power densities being achieved at temperatures of 600 °C (see Fig. 50, right). The next step involves investigating the long-term stability of these cells.

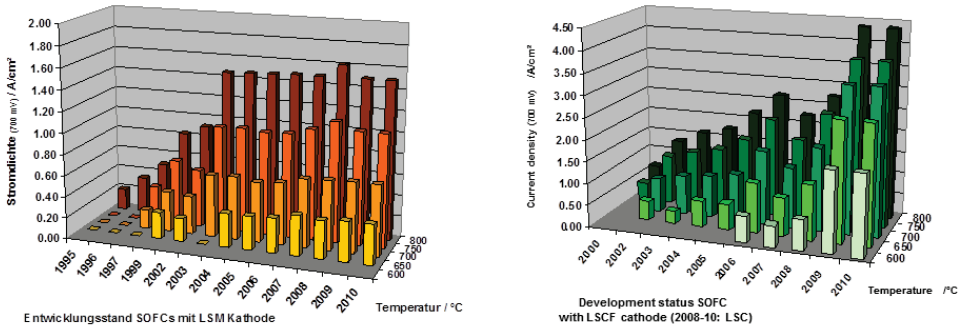

Fig. 50: Power densities of cells with LSM (left) and LSC(F) (right) cathodes over the years

Chromium poisoning of the cathode

Within the scope of extensive research in a collaboration between the institutes IEK-1 and IEK-3 on single cells and cells in real stacks, progress was made in clarifying the influence of volatile chromium compounds on the SOFC cathode [9]. Volatile chromium compounds are created by evaporation from the chromium-containing oxide layers to the chromium-containing steels used as interconnects in the stacks. The chromium compounds are either reduced at the electrolyte/cathode three-phase boundary or they interact with the cathode material.

By means of electrochemical tests with cells with (La,Sr)MnO_3 (LSM) cathodes and using wet-chemical and scanning electron microscopy post-examinations, the influence of these volatile chromium species was almost completely elucidated. The high-temperature steel Crofer22APU was used as the chromium source. It was varied by gradually adding the chromium vaporization protective layer Mn_3O_4 and the perovskite cathode contact layer LCC10. The degradation curve over time of cells with a chromium source when being assembled and in operation under current load is divided into three phases: a running-in regime, a linear regime of weak degradation, and a linear regime of strong degradation. Reducing the dissolution rate of chromium by means of the different coatings stretched the degradation curve in relation to time (see Fig. 51).

Based on the results obtained in the cell tests, three interactions between chromium species and LSM were identified.

- Gaseous chromium species form chromium-manganese spinels due to interaction with manganese oxide phases in the current collector. This interaction gives rise to

[9] Neumann, A.: Chrom-bezogene Degradation von Festoxid-Brennstoffzellen, PhD thesis, Ruhr University Bochum, 2010. Schriften des Forschungszentrums Jülich, Reihe Energie & Umwelt, Vol. 98

most of the chromium content but does not cause measurable performance degradation

- Gaseous chromium species adsorb on the surface of the LSM and prevent oxygen from adsorbing and diffusing in the electrochemically active zone. This increases the activation losses of the cathode but does not cause any permanent chromium deposition
- Gaseous chromium species are reduced in the electrochemically active zone and form Cr_2O_3. In the long term, the reduction of chromium species leads to accumulation in the cathode. This leads to the pores being filled. The interaction of Cr_2O_3 with LSM leads to the formation of chromium-manganese spinel. The continuous removal of manganese from the LSM perovskites leads to stoichiometric modification of the perovskites until the stability limit has been reached. This point in time marks the beginning of gradual decomposition. The decomposition influences both the microstructure of the cathode as well as the conductivity of the LSM matrix and represents the onset of strong degradation

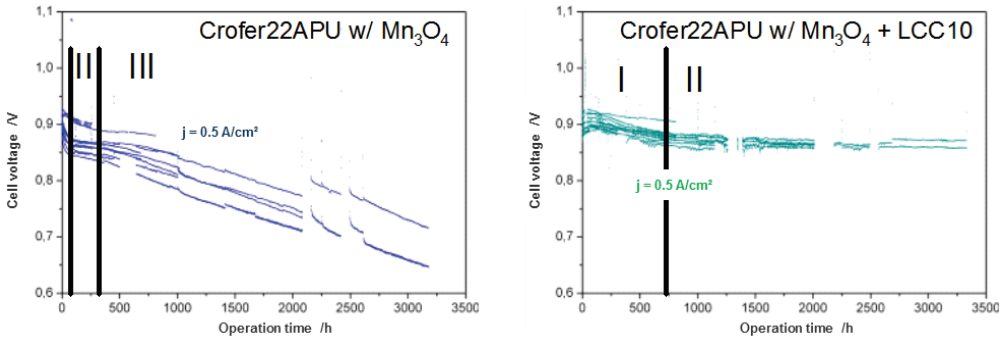

Fig. 51: **Degradation of SOFC single cells when a chromium source is present on the cathode side. Left: Crofer22APU with an Mn_3O_4 protective coating. Right: Crofer22APU with an Mn_3O_4 protective coating and an LCC10 contact layer. Areas of strong (I), weak (II) and renewed strong (III) voltage degradation as a function of time and of the coating**

Optimizing the lifetime of stacks

The priorities for stack development are mainly in the areas of lifetime/degradation, gas tightness (see Section “Stack joining”), and contacting. Important progress has been made in relation to degradation/lifetime using what are known as third-generation (G3) short stacks. These stacks were put into operation back in August 2007 within the EU project Real-SOFC. In September 2009, one stack was shut down after two years of operation (17,500 hours). In the cell voltage curve over time (Fig. 52), progressive degradation can be seen over the last 3,000 - 4,000 hours. This eventually led to the stack being shut down. In the same period of time (August to October 2009), the voltage curves for the two cells in stack F1002-97 exhibited a marked change in slope. However, the voltage drop remained almost linear. This stack achieved the milestone of 30,000 operating hours in the first week of 2011 (see Fig. 52).

In Fig. 53 the degradation rates for the cells in the two stacks F1002-95 and -97 are shown as a function of operating time. During the first 5,000 hours of operation, the degradation rates steadily decline from 6 mV/kh to 8 mV/kh. The degradation rates for stack F1002-97 remain constant at this level over the next 10,000 hours of operation. However, after 10,000 hours of operation, the degradation rates begin to increase for stack F1002-95 and they do not appear to achieve a constant level after this point in time. This means that the degradation is progressive, which agrees with the deviation from linearity observed in Fig. 52. After 15,000 operating hours, the degradation rate also appears to increase for the cells in the stack. In this case, however, the degradation rates reach a new constant level at 10 mV/kh after around 20,000 operating hours (see Fig. 53).

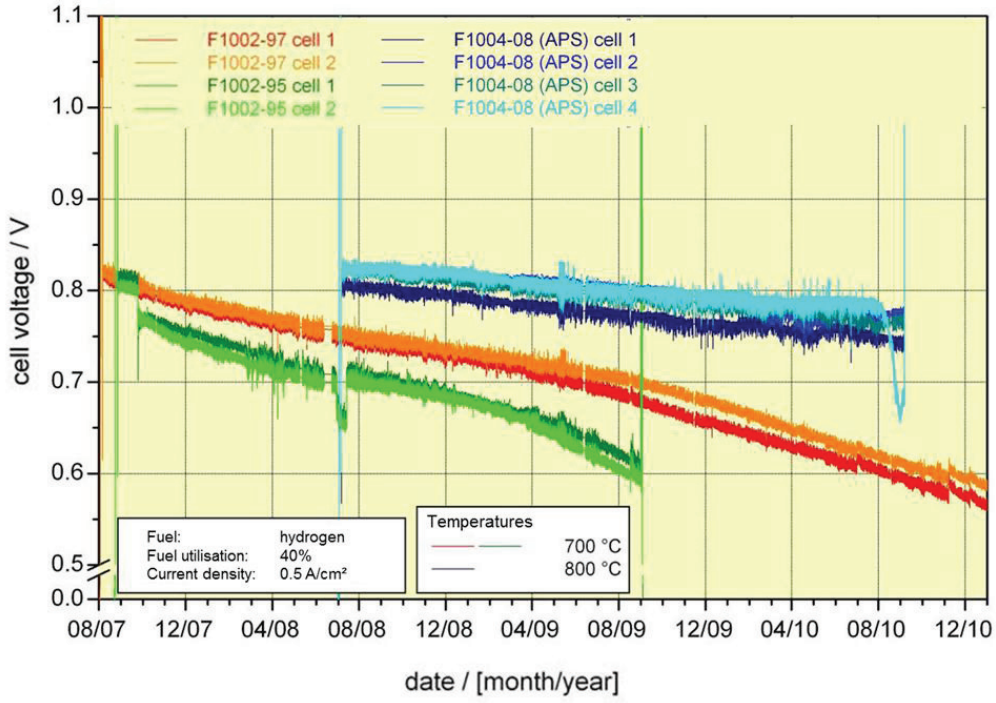

Fig. 52: Cell voltages over time in three stacks for the period from August 2007 to January 2011

In another stack, F1004-08, in which the interconnect plates were equipped with a protective coating using a special technique, the degradation rate was reduced to about 4 mV/kh even when this stack was operated at the higher temperature of 800 °C. However, the collapse of the cell voltage on one of the four layers led to the experiment being terminated after 19,000 hours of operation (see Fig. 52).

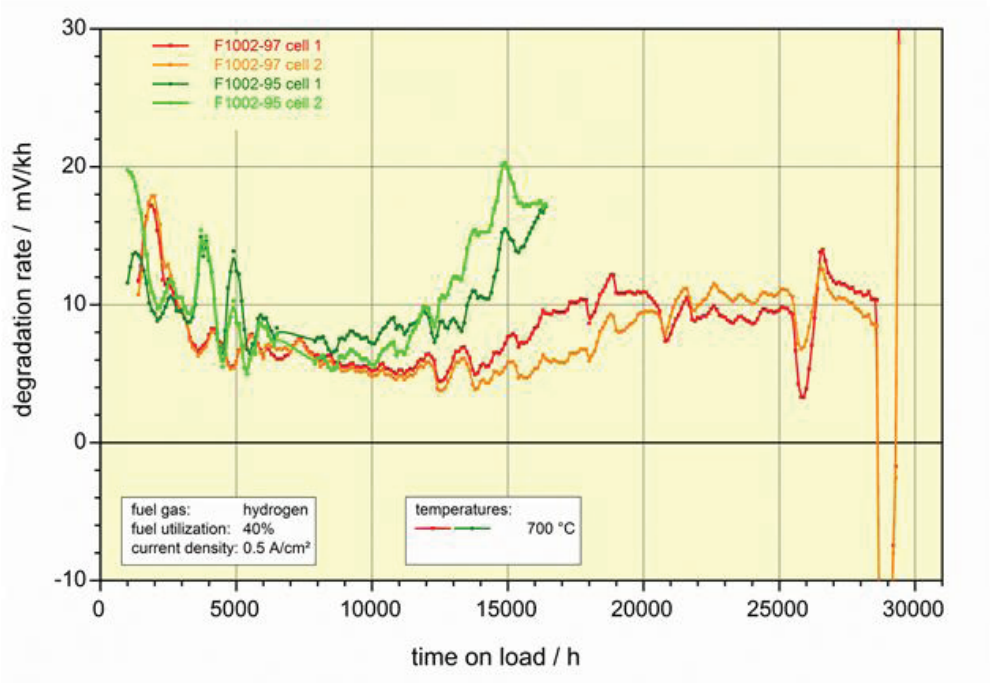

Fig. 53: Degradation rates over operating time for the cells in stacks 1002-95 and -97 shown in Fig. 52

3.3.2.2 System development and verification

Component development for the 20 kW system

The SOFC system components operated at high temperatures of between 500 °C and 950 °C must be able to withstand these operating conditions and simultaneously perform their tasks as efficiently as possible, i.e. with small amounts of material. In order to optimize the components, they were individually modeled using CFD.

The 3D continuum model developed for the prereformer used in the integrated module in the 20 kW system was validated using measurement results. Fig. 54 compares the temperature distribution in the reformer and the fuel composition after reforming with the measurement data as an example. The CFD results show good agreement with the experimental studies. Only in case C is the consumption of methane too high in the CFD simulation. This suggests that the kinetics of the methane-steam reaction is severely inhibited for low reaction temperatures in the test. The simulations performed improved our understanding of the processes occurring in the reformer. The model was used to optimize the design. For example, it was used to identify the parameters with the biggest impact on reformer weight and construction volume.

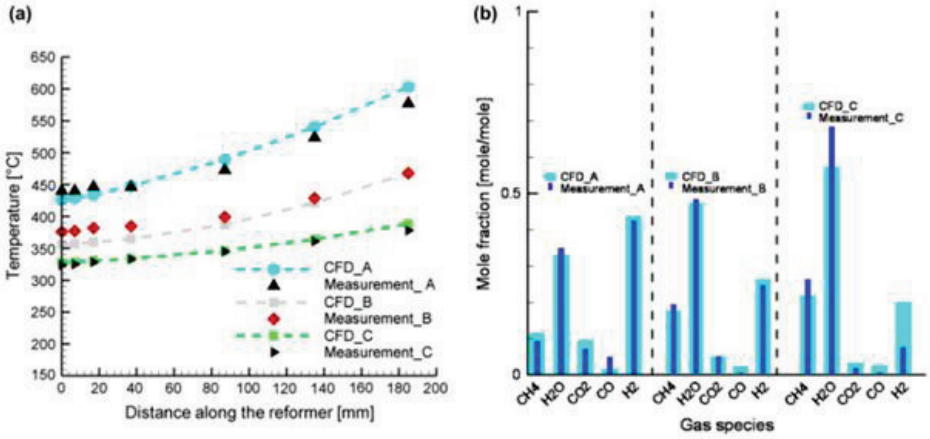

Fig. 54: CFD analysis and experimental validation of the prereformer: (a) reformer temperature distribution, (b) fuel composition

The recuperative air preheater (AP) used in the integrated module was characterized in the heat exchanger test stand set up in 2009 (for experimental parameters, see Fig. 55; test results see below: heat exchanger tests). The asymmetrical flow necessitated by integration into the module gave rise to different temperatures in the two flow channels. This was confirmed by CFD calculations for 100 %, 75 % and 50 % of the nominal flow (see Fig. 56). Based on this temperature distribution, FEM calculations were performed in order to identify the critical areas from a thermomechanical point of view. They will then be taken into account in a redesign (see Fig. 57).

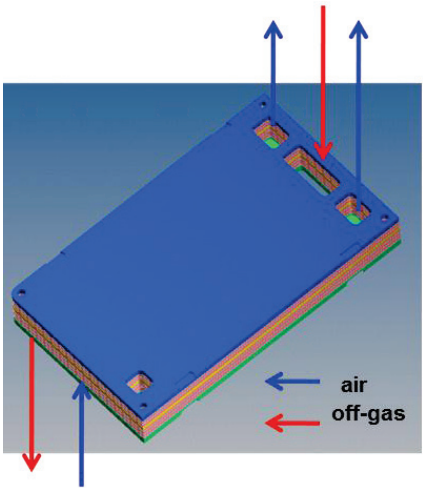

Operational parameter

Air inlet	Mass flow/ kgh^{-1}	Temperature / °C
Case_1 (100%)	60.8	40
Case_2 (75%)	45.6	37
Case_3 (50%)	30.4	33
Off-gas inlet	Mass flow/ kgh^{-1}	Temperature / °C
Case_1 (100%)	50.2	886
Case_2 (75%)	37.7	876
Case_3 (50%)	25.0	854

Fig. 55: AP of the integrated module: design and experimental parameters

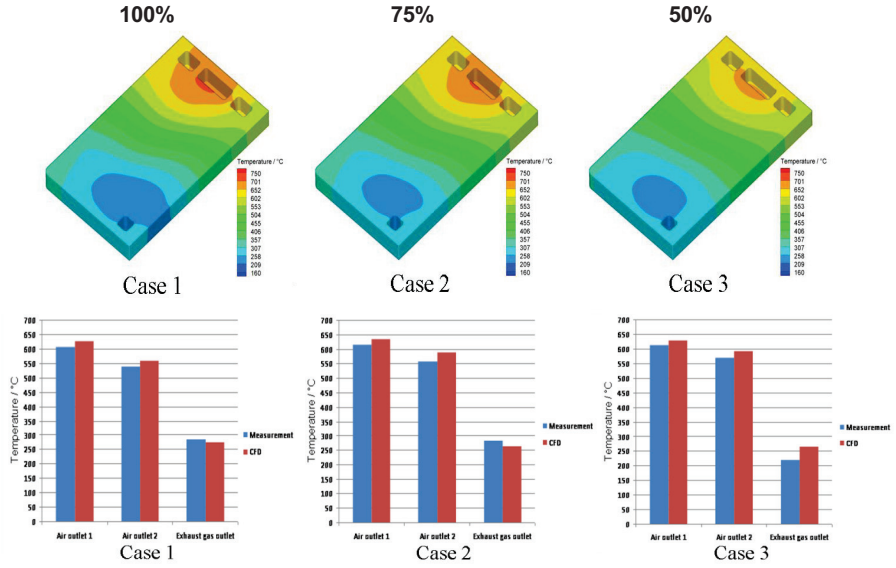

Fig. 56: **AP of the integrated module: calculated temperature distribution compared to that measured for 100 %, 75 % and 50 % of the nominal flow**

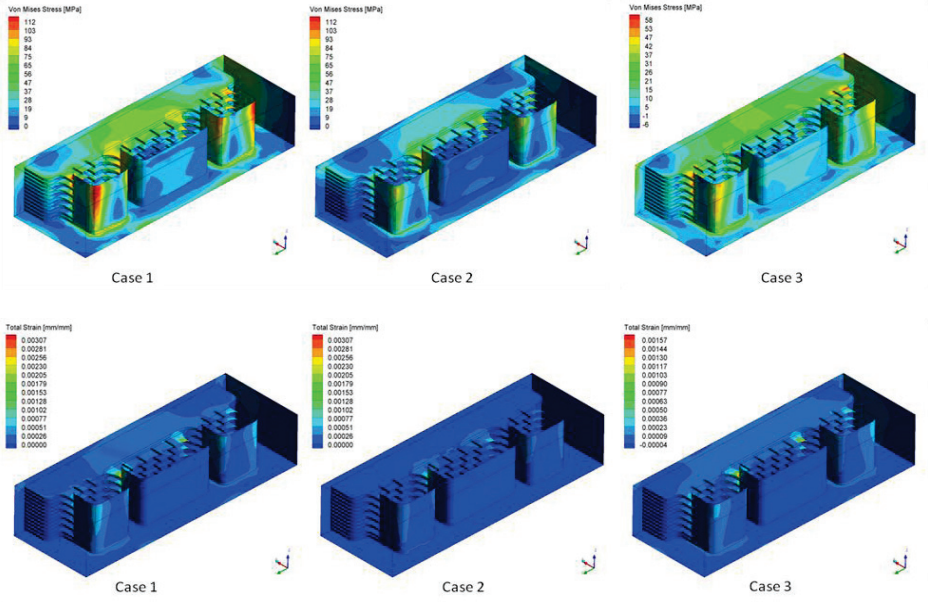

Fig. 57: **AP of the integrated module: calculated equivalent stresses and total deformations at the critical manifold area with temperature profiles resulting from 100 %, 75 % and 50 % of the nominal flow**

A 3D CFD model was also created for the third component of the integrated module, the afterburner, and the computational grid was optimized. Work began on optimizing the afterburner. The afterburner model was calculated for a geometrical variant including the chemical reactions. Here, the mixing of the gaseous reaction partners was shown to have a large impact on the combustion process. This point is being further investigated.

An essential aim of CFD modeling is the analysis of the operating behavior of the complete integrated module comprising the AP, reformer, afterburner and stack, in order to optimize the system construction and system control. This requires information on how the components influence each other, particularly in terms of their thermal behavior. An initial partial model was created and integrated for the reformer and the AP (see Fig. 58). A macro was written to incorporate reforming kinetics according to the Hinschelwood approach and the equations experimentally determined by Drescher were implemented. Initial calculations were performed for the integrated module.

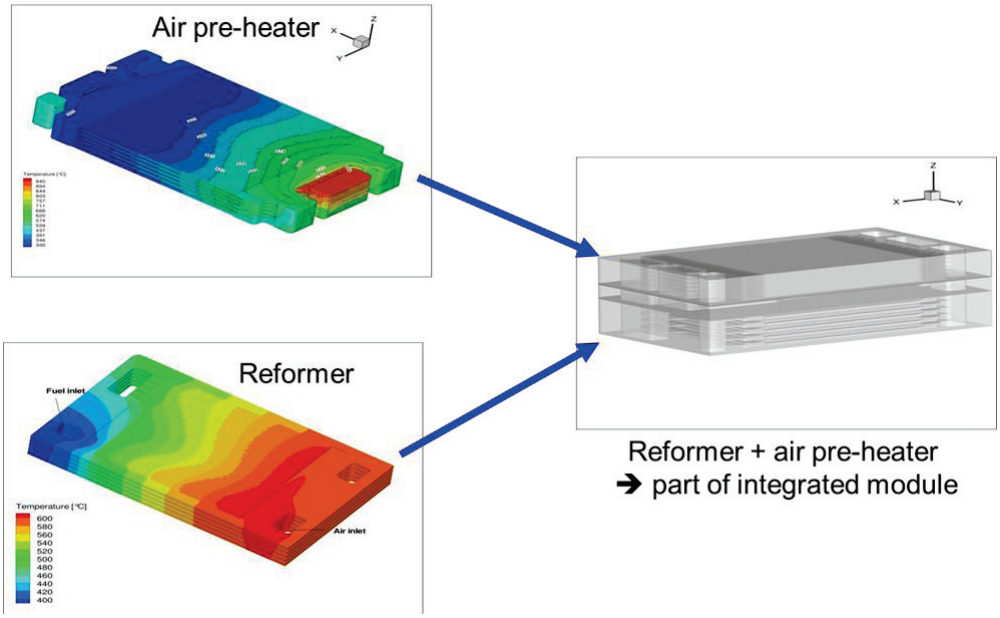

Fig. 58: CFD analysis of interaction between reformer and air pre-heater

Heat exchanger tests

The test stand developed and set up for high-temperature heat exchangers as part of the EU project LargeSOFC was adapted for tests on the air preheater in the integrated module (see Fig. 59). A fatigue test was conducted over 1,000 hours and stationary tests were performed for load conditions of 100 %, 75 %, 50 % and 25 %. The analysis showed that the transfer behavior was almost independent of mass flow rates (at a constant ratio of hot to cold mass flow rate) and that partial loads tended to cause the temperature of the heated medium (“cold out”) to increase slightly, which is desirable for operation in a fuel cell system (see Fig. 60).

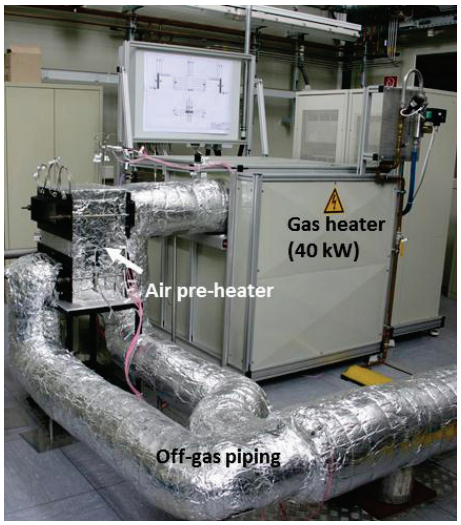

Fig. 59: **Setup of the air preheater test stand**

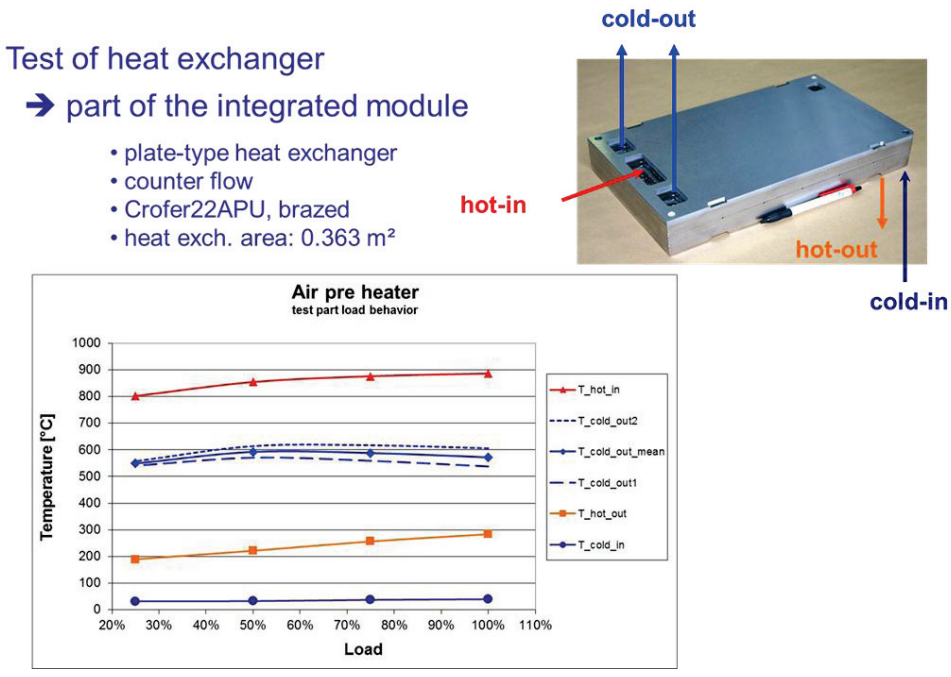

Fig. 60: **Partial load behavior of the air preheater in the 20 kW system**

Test of stack and reformer with mine gas

A test stand for the operation of a reformer coupled with an SOFC with mine gas as a fuel was set up at Evonik New Energies (formerly Saarenergie) in Saarbrücken. After a lengthy operating phase, the first reformer began to leak. A new reformer was fabricated with optimized joining and integrated into the test stand (see Fig. 61). Its functionality was verified in further tests, and the measurement data obtained were used to validate the reformer model.

Following these tests, a 1 kW SOFC stack was integrated into the test stand. This stack was the first stack developed by Forschungszentrum Jülich to be operated outside a furnace with no heating. After approx. 24 hours of heating using preheated air, a mean temperature of around 630 °C was achieved at the stack and of approx. 430 °C at the prereformer. When mine gas containing approx. 28 % methane was supplied, a strong decrease in temperature occurred in the stack because for the given temperatures, reforming occurs mainly in the stack and to a lesser degree in the prereformer. This limits the stack temperature. The stack exhibited sufficient tightness after heating. The low stack temperature of 680 °C only allowed a power of 420 W to be reached. The tests were discontinued after 130 hours due to disturbances in the test stand.

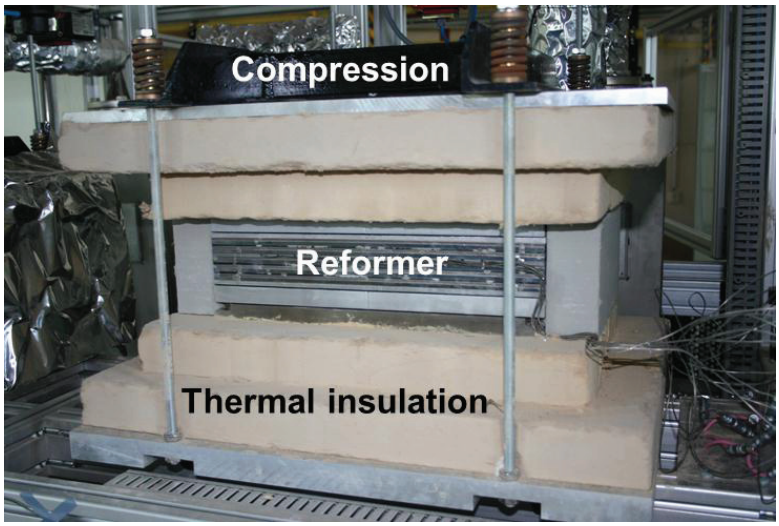

Fig. 61: New reformer in the mine gas test stand

Stack joining

Work continued on improving the tightness of stacks joined with glass sealant. CFD and FEM simulations of a heating experiment (“heating dummy”) with heating to medium temperatures of up to 500 °C were compared to the results of the post-examination of the thirteen heating dummy tests conducted to date. The damage pattern was shown to agree well with the stress calculations. However, the components failed at very different stress levels. Failure occurred in some instances at a shear stress of only 100 MPa (no tensile stresses), as shown in Fig. 62, while in individual heating tests no leaks were detected at shear stresses of

up to 185 MPa and tensile stresses of 18 MPa. Glass 48, in particular, exhibited large scattering, which can most likely be attributed to the extreme sensitivity of the glass sealant joints on the surface of the metal, as demonstrated in other experiments. As the heating dummies can currently only be tested up to 500 °C, it was decided not to pursue any further tests of this type for the time being, as the glasses under such conditions are loaded below the glass transition temperature, which does not correspond to real operating conditions.

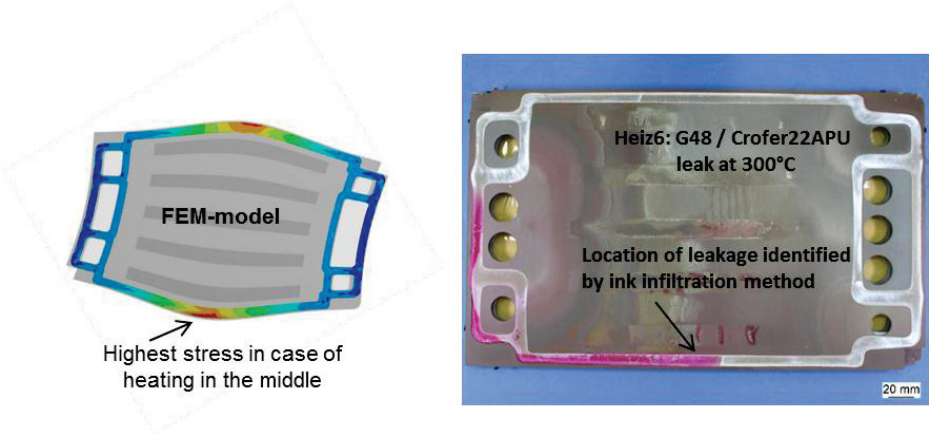

Fig. 62: Leakage in the heating dummy compared to the stress level in FEM calculations

The test with a ten-layer stack (F'''2010-13), which was thermally cycled once and then operated after reheating with methane (incl. internal reforming), produced the following results:

- The power density and the homogeneity of the characteristics at 800 °C are very good (also for methane operation)
- Implemented structural modifications were successful
- No "outliers" among the layers, even for 65 % fuel utilization with methane

However, there was a massive short circuit in layer 9, which was still present after disassembly. The subsequent post-examination showed that:

- A metal particle had welded the layer and the frame together (QA problem during assembly)
- The stack was sufficiently tight after the first phase of cooling; after re-installation and a new thermal cycle, it became untight on the short face sides (manifold area)
- The temperature differences near the manifold were much higher during the second operating phase (after re-installation) in methane operation with low fuel utilization (39 %) than in the furnace environment of 800 °C (see Fig. 63)
- Thermomechanical stresses in the manifold area destroyed the joining

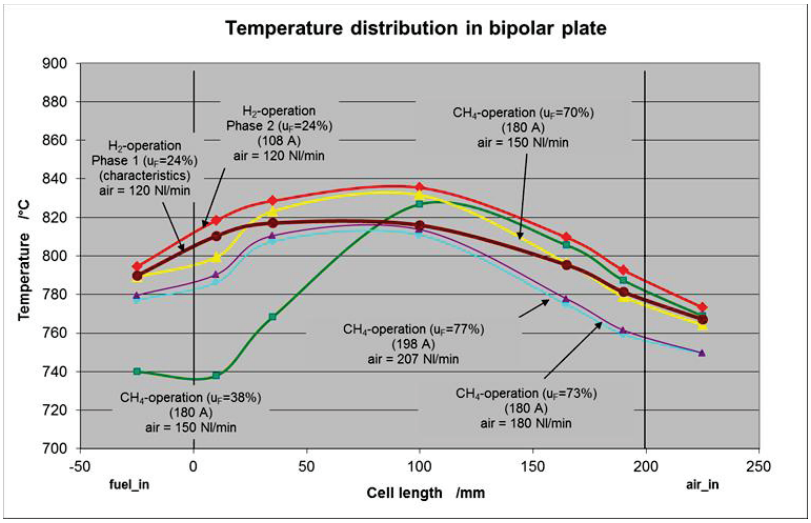

Fig. 63: **Stack F'''2010-13: Temperature distribution in the stack from $fuel_{in}$ to $fuel_{out}$ (= air_{in}) for different fuels and fuel utilization u_F**

New stack design/stack modeling

The new stack design (Y1-20) was thermodynamically simulated with heat sources intended to simulate the heat production of the stack. Calculations were performed for a six-layer stack as well as for a thirty-six-layer stack. The coupled thermodynamic and thermomechanical calculations took account of elastic and plastic expansion as well as deformations caused by creep. The temperature profile (see Fig. 64) was derived from the coupled CFD calculations and included in the mechanical calculation.

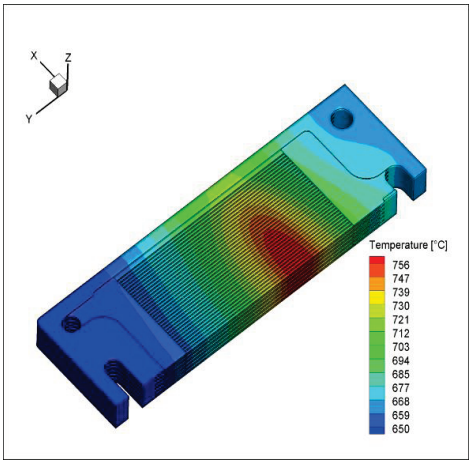

Fig. 64: **Temperature distribution of the Y1 design in stationary operation calculated using CFD**

A transient 3D simulation of the joining process in the furnace was created using CFD heating calculations. The heat emitted by the furnace via radiation was modeled using a ramp function. The natural convection of the air in the furnace was also incorporated into the model. The simulation results were then compared to the measurement results.

Analysis of different SOFC system configurations

As part of an EU project, the advantages and disadvantages of different system configurations were analyzed. Six circuits (flow diagrams) were selected, from which four system configurations were analyzed at IEK-3 with four different gases. A total of 130 system calculations were performed. The following criteria were identified as critical:

- Formation of carbon in the reformer
- Pinch point of the heat exchanger and heated reformer (minimum 50 K)
- Outlet temperature afterburner (maximum 1000 °C)
- Oxygen utilization (maximum 50 %)

A total of 70 system parameter combinations fulfill all requirements. Some of these results are presented here as examples.

Based on the flow diagram for concept 1.2 (see Fig. 65), the results for natural gas operation (GUS Gas H) are shown in Fig. 66.

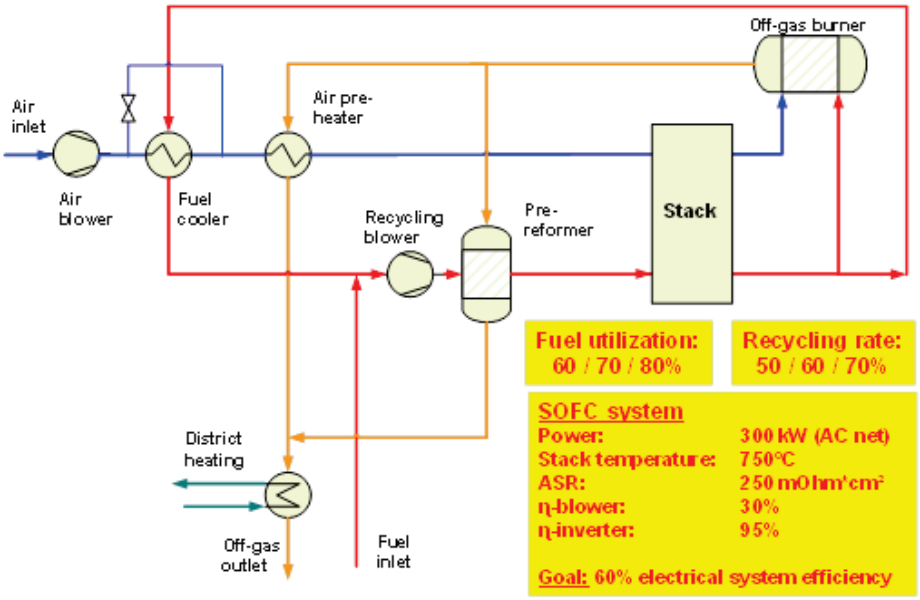

Fig. 65: Flow diagram concept 1.2

Calculations were performed for three recycling rates (50 %, 60 % and 70 %) and three fuel utilizations (60 %, 70 % and 80 %). It was shown that increasing fuel utilization and increasing recycling rates led to a decrease in system efficiency (see Fig. 66). This is due to the fact that the increased fuel utilization is overcompensated from a certain point onwards by the increased need for compression power, which is caused by the increased need for

cooling as less heat is removed by internal reforming because of the small amount of fuel. The dotted red line in Fig. 66 shows the limit for carbon deposition. A good operating range with electrical system efficiencies of up to 60 % was found for fuel utilizations in the stack of 60 % to 70 % and for recycling rates of 65 % to 70 %.

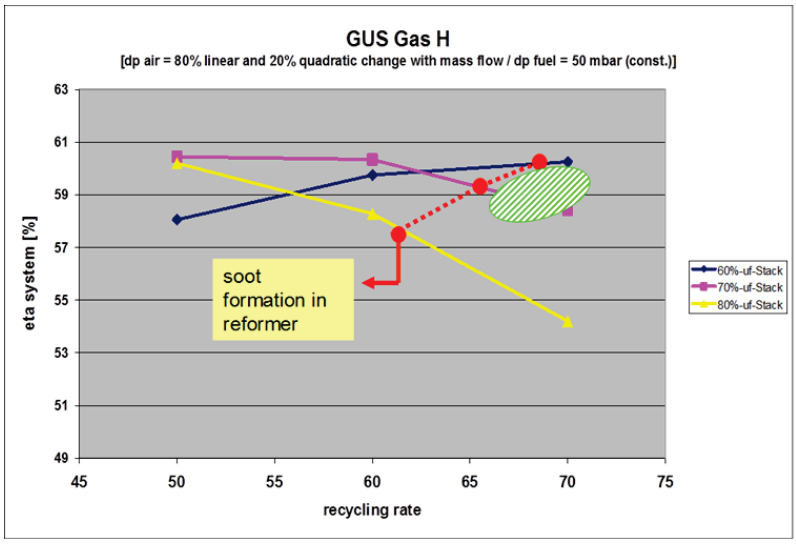

Fig. 66: Flow diagram concept 1.2: System efficiency as a function of the recycling rate for GUS Gas H

The results of the calculation for Biogas 2 (40 % methane) are shown in Fig. 67.

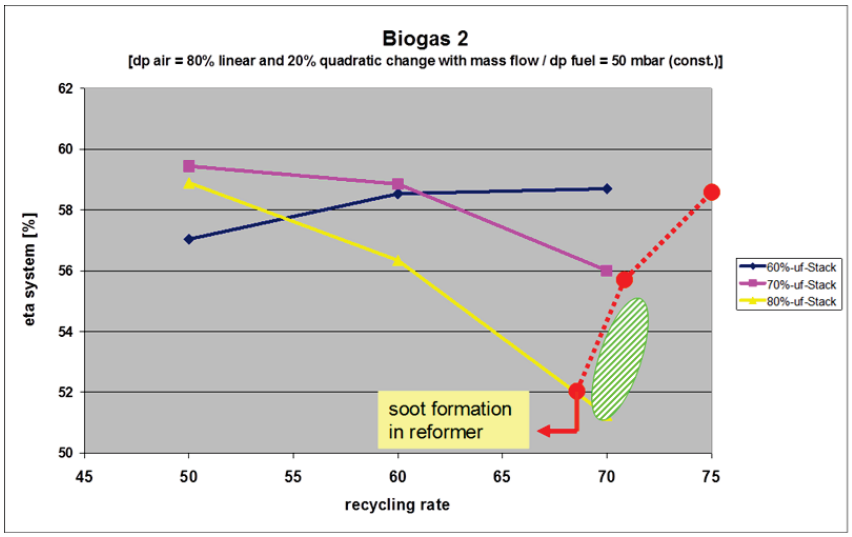

Fig. 67: Flow diagram concept 1.2: System efficiency as a function of the recycling rate for Biogas 2

In general, the shape of the graph is similar to that for calculations with natural gas. A good operating range with electrical system efficiencies of up to 53 % was found for fuel utilizations in the stack of 70 % to 80 % and for recycling rates of 70 % to 75 %. The high recycling rates are necessary to avoid carbon deposition.

The electrical and thermal system efficiencies are shown in Fig. 68 for all calculations. With the exception of system 0.1, all systems have anode gas recycling.

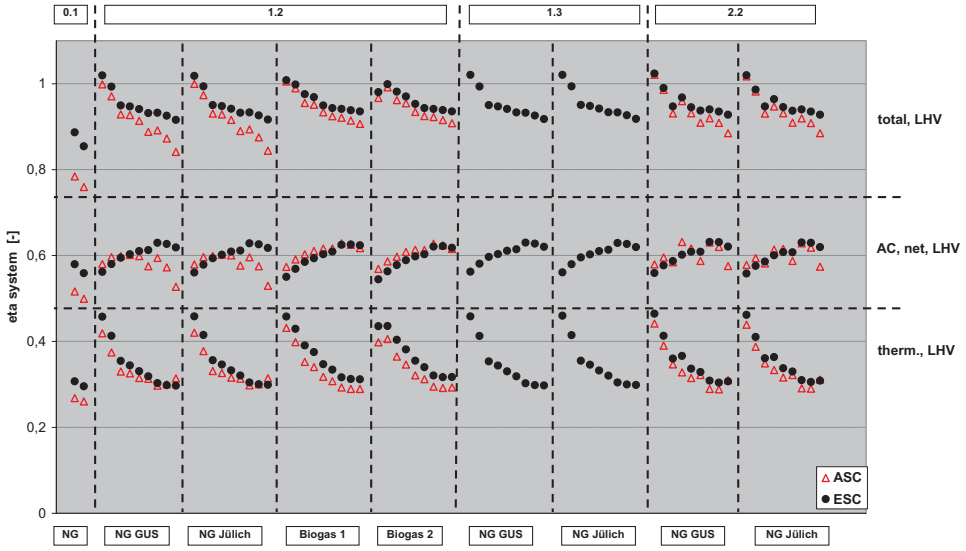

Fig. 68: System efficiencies of the simulated systems (concepts 0.1, 1.2, 1.3, 2.2) for nominal operation

The efficiencies are generally of a high level and depend only to a limited extent on the system configuration, the type of gas and the type of cell. However, recycling rates of 50 % and 60 % often lead to soot formation in the reformer. The recycling rate should therefore be higher than 60 %. In general, net electrical efficiencies of 50–63 % are achievable.

3.3.3 Staff members and fields of activity

Name	Tel. (+49 2461-61-) E-mail address	Field of activity
S. Berns	6697 s.berns@fz-juelich	Software development, modeling
Prof. L. Blum	6709 l.blum@fz-juelich.de	Head of Fuel Cell Process Engineering (VBZ)
Dr. K. Cerny	5170 k.cerny@fz-juelich.de	Software development, modeling

P.H. David	4652 p.h.david@fz-juelich.de	Electrical engineering, measurement data acquisition and systems control
R. Deja	5291 r.deja@fz-juelich.de	System simulation, development and testing of SOFC system components
Dr. V.A.C. Haanappel	4656 v.haanappel@fz-juelich.de	Chemical technology, (high-temperature) corrosion
Dr. L.G.J. de Haart	6699 l.g.j.de.haart@fz-juelich.de	Head of SOFC Electrochemistry and Simulation
I. Hoven	4053 i.hoven@fz-juelich.de	Electrical engineering, measurement data recording and systems control
A. Kind	3850 a.kind@fz-juelich.de	Software development, modeling
J. Kuhl	6697 j.kuhl@fz-juelich.de	Software development, modeling
U. Packbier	5170 u.packbier@fz-juelich.de	Tests on SOFC stacks and evaluation of results
Dr. M. Peksen	8732 m.peksen@fz-juelich.de	Testing and simulation of system components
R. Peters	4664 ro.peters@fz-juelich.de	Head of the SOFC Systems Technology Group, component development, plant design, construction and testing
Dr. I.C. Vinke	6688 i.c.vinke@fz-juelich.de	Electrochemistry, solid-state ionics, high-temperature electrochemistry

3.3.4 Important publications and patents

Publications:

Blum, L.; Peksen, M.; Peters, Ro.; Vinke, I.C.; Malzbender, J.; Groß, S.M.; Pabst, U.

Investigation of SOFC sealing behavior under stack relevant conditions at Forschungszentrum Jülich

Journal of Power Sources (2010), doi:10.1016/j.jpowsour.2010.09.041

Hermetic sealing is a key requirement for the operation of solid oxide fuel cell (SOFC) stacks in a system environment. The sealant material has to withstand stresses due to mechanical loading, mismatch in thermal expansion coefficient and thermal gradients that arise during operation. Based on leakage tests performed at Forschungszentrum Jülich it was obvious that stacks, having been operated successfully in a furnace, are not necessarily usable in a system, e.g. because of deviating pressure differences and temperature gradients. Thorough investigations including stack and stack dummy tests, and finite element modelling (FEM) were

performed to get a comprehensive understanding of the various parameters, influencing the leak tightness of the sealing material. It was found that even small temperature differences especially in the area of gas and air manifolds can create excessively high tensile stresses. Based on initial FEM analyses, a better understanding of the problem has been obtained and a tool was developed that can assist in the design of more robust stacks. These investigations and modelling activities will be continued with a main focus on thermal cycling, which is the next step in the list of requirements.

Blum, L.; Riensche, E.

Solid Oxide FCs: System

In: Juergen Garche, Chris Dyer, Patrick Moseley, Zempachi Ogumi, David Rand and Bruno Scrosati, editors. Encyclopedia of Electrochemical Power Sources, Vol 3. Amsterdam: Elsevier; 2009. pp. 99-119. ISBN 9780444520937

In this paper some basic arrangements for SOFC systems are described, starting with atmospheric systems using a catalytic burner or a thermal burner and anode gas recycling. For illustrating the potential for electrical efficiency of SOFC systems, the combinations with a gas turbine and in addition with a steam turbine are also described. To be able to evaluate the potential of the different systems firstly the essential efficiencies relevant to fuel cell systems are defined and the basics for doing energy balance calculations are illustrated. Equations are given to describe e.g. the effect of fuel recycling on system fuel utilisation or the effect of internal reforming on the necessary air flow for cooling the stack.
It becomes obvious, that there is a strong dependency of the electrical efficiency on cell voltage and on fuel utilisation. If cells are available allowing operation with a high fuel utilisation at cell voltages of 800 mV a net electrical efficiency above 55 % can be achieved. The combination in a pressurized system with a gas turbine enables efficiencies of up to 70 % and combining this system with an additional steam turbine allows efficiencies of up to 75 %. But as an investigation of the size of these steam turbines shows, such combined systems only make sense above a gas input of 10 MW.

Blum, L.; Riensche, E.; Stolten, D.; Menzer, R.; Grube, Th.

Technologiebewertung stationärer Erdgas-basierter Brennstoffzellen,

Das EduaR&D-Projekt: Energie-Daten und Analyse R&D, Forschungszentrum Jülich GmbH, Projektträger Jülich (Hg.), Umwelt- und Ressourcenökonomik, Vol. 27, LIT-Verlag Berlin, Münster, 2009, ISBN 978-3-8258-1956-9

This study takes recourse to the extensive fuel cell know-how, which the Institute for Energy Research at Forschungszentrum Jülich has consistently built up since 1990. For each of the four fuel cell systems dealt with here
– PEFC (polymer electrolyte fuel cell)
– MCFC (molten carbonate fuel cell)
– tubular SOFC (solid oxide fuel cell) and
– planar SOFC
updated and comprehensive simulation calculations were carried out within the framework of the EduaR&D project to reflect the current state of the art of fuel cell systems. The in-depth knowledge thus gained, particularly the dovetailing of electrochemistry and process engineering in the “electrochemically active” center of the system, which remains hidden to the outside observer, was then used as the basis to perform a temporal analysis of the development paths already explored and those yet to be pursued. This led us to an important question, which every fuel cell developer is continuously faced with, namely how to determine the correct point in time when the system is at a sufficient stage of development that

– the production costs can be reduced by mass production and that
– the learning curve effects can be exploited,
thus allowing the investment cost target to be achieved.

Blum, L.

Overview of the SOFC development Status

cfi – ceramic forum international, DKG 86 (2009) No. 11-12, E17 - E22, ISSN 01739913

Solid Oxide Fuel Cells (SOFC) show great promise for future employment in electric power production because of their high efficiency and low environmental impact. Moreover, they can be used with a great variety of fuels (hydrogen, carbon monoxide, natural gas, and biogas) and can play an important role in carbon sequestration. However, before they go on the market, some questions have to be answered including long term stability of suitable high temperature materials, low cost designs and manufacturing methods, and efficient plant concepts. This article presents an overview on the essential designs as well as on the most important developers in the field of SOFC technology. Based on the data published in recent years on international conferences a comparison is performed on the status of cell, stack and system development.

Haanappel, V.A.C.; Jordan, N.; Mai, A.; Mertens, J.; Serra, J.M.; Tietz, F.; Uhlenbruck, S.; Vinke, I.C.; Smith, M.J.; de Haart, L.G.J.

Advances in Research, Development, and Testing of Single Cells at Forschungszentrum Jülich

Journal of Fuel Cell Science and Technology, 6 (2009) 021302 / doi:10.1115/1.3080547

This paper presents an overview of the main advances in solid oxide fuel cells (SOFCs) research and development (R&D), measurement standardization, and quality assurance in SOFC testing at the Forschungszentrum Jülich. These activities have resulted in both a significant improvement of the electrochemical performance and a better understanding of the electrochemical behavior of SOFCs. Research and development of SOFCs was mainly focused on two types of anode-supported cells, namely, those employing either $La_{0.65}Sr_{0.3}MnO_3$ (LSM) or $La_{0.58}Sr_{0.4}Co_{0.2}Fe_{0.8}O_{3-\delta}$ (LSCF) cathode materials. In both cases the optimization of processing and microstructural parameters resulted in satisfactory power output and long-term stability at reduced operation temperatures. Standardization and quality assurance in SOFC testing was also addressed with the goal of producing consistent and reliable tests and measurement results. At present, under optimized experimental conditions, SOFCs with LSM or LSCF cathodes can deliver a power output of about 1.0 W/cm^2 and 1.9 W/cm^2 at 800 °C (700 mV), respectively.

de Haart, L.G.J.; Mougin, J.; Posdziech, O.; Kiviaho, J.; Menzler, N.H.

Stack Degradation in Dependence of Operation Parameters; the Real-SOFC Sensitivity Analysis

Fuel Cells, 9 (2009) 6, 794 – 804 / doi: 10.1002/fuce.200800146

The EU Integrated Project Real-SOFC aims at improving the understanding of degradation in SOFC stacks, and extending the durability of planar SOFC stacks to degradation rates suitable for stationary application. As part of the Real-SOFC project, three series of SOFC stacks, each with two or four planar anode-supported cells, were operated for durations of 3,000 h up to 10,000 h under varying fuel and electrical load conditions. The durability tests on these short stacks were conducted

galvanostatically at 800 and 700 °C in dependence of current-density (0.3, 0.5 or 0.7 Acm^{-2}), of fuel composition (hydrogen: H_2 + 3–10% H_2O or methane: CH_4/H_2O (S/C = 2)) and of fuel utilisation (8, 40, 60 or 75 %). A pronounced difference in degradation behaviour was observed between the stacks operated at different current densities. The degradation behaviour was, however, not influenced by the choice of fuel (hydrogen or methane) and was hardly influenced by the fuel utilisation. Lowest degradation rates of about 20 $m\Omega cm^2kh^{-1}$ were determined for the tests of a short stack with cells with LSM cathodes operated at 800 °C and a current-density of 0.3 Acm^{-2} and of a short stack with cells with LSCF cathodes operated at 700 °C and a current-density of 0.5 Acm^{-2}. Post-test characterisation of the cathode with respect to chromium poisoning was performed on cells from several stacks. No clear relationship between the degradation rate of the stacks and amount of Cr incorporated in the cathode could be established. The major difference was a change in microstructure of the cathode in the region near the electrolyte interface; in the stacks operated at lower current densities, the structurally changed zone was clearly thinner than in those stacks operated at higher currents.

Menzler, N.H.; Haanappel, V.A.C.

Influence of anode thickness on the power output of solid oxide fuel cells with (La,Sr)(Co,Fe)-type cathode

Journal of Power Sources, 195 (2010) , 5340 – 5343 / doi:10.1016/j.jpowsour.2010.03.030

The influence of the thickness of the anode (functional layer) on the power output of anode-supported solid oxide fuel cells with a lanthanum–strontium–cobalt–ferrite cathode was investigated. The anode was applied by vacuum slip casting and the thickness varied between 1 and 22 μm. All other material and microstructural parameters were kept constant. Single cells with dimensions of 50 mm × 50 mm and with an active cathode area of 40 mm × 40 mm were manufactured and tested in an alumina housing with air as oxidant and hydrogen with 3 % water vapour as the fuel gas.
Results have shown that SOFCs with anodes between 1 and 13 μm have slightly better performance than those with thicker anodes ($\sim$1.7 A cm^{-2} versus 1.5 A cm^{-2} at 800 °C and 0.7 V). The current densities were discussed with respect to cell area specific resistance, helium leak rate of the half-cell, and microstructure.

Peksen, M.; Peters, Ro.; Blum, L.; Stolten, D.

Numerical Modelling and Experimental Validation of a Planar Type Pre-reformer in SOFC Technology

International Journal of Hydrogen Energy 15 (2009) 6425 – 6436.

A computational model of the Jülich type pre-reformer and its experimental validation used in solid oxide fuel cells (SOFCs) is introduced. A continuum modelling approach has been attended and its feasibility verified. The fluid flow, heat transfer and chemical reacting species transport within the pre-reformer are numerically solved using 3D computational fluid dynamics (CFD) based on the finite volume method. The model considers the typical sub-components of the pre-reformer including the solid frame, air channels, catalyst and the wire mesh structures. Experimental measurements are used to supply appropriate boundary conditions for the simulations. The predicted results of the simulations are experimentally validated using thermocouples and gas chromatography. The results show good agreement, implying that the proposed model is an invaluable tool that can be used to reduce costly experiments in the design and process optimisation of the pre-reformer.

Peksen, M.; Peters, Ro.; Blum, L.; Stolten, D.

Design and Optimisation of SOFC System Components using a Trio Approach: Measurements, Design of Experiments, and 3D Computational Fluid Dynamics

Electrochemistry Society, Vienna, 2009, S.C. Singhal, H. Yokokawa, 1195 – 1200, ISBN 9781566777391

In this present paper, a comprehensive trio approach has been proposed to aid in the optimisation of the pre-reforming process, and to develop a new pre-reformer design. Measurements, design of experiments (DOE), and computational fluid dynamics (CFD) have been employed to determine the effects of several design and material parameters on the pre-reformer performance in detail. The optimisation procedure considers geometrical modifications, material alternatives and the feasibility of the end product simultaneously, in order to achieve efficient reforming rates by reduced component weight.

Steinberger-Wilckens, R.; Blum, L.; Buchkremer, H.-P.; de Haart, L.G.J.; Pap, M.; Steinbrech, R.W.; Uhlenbruck, S.; Tietz, F.

Recent Results in Solid Oxide Fuel Cell Development at Forschungszentrum Juelich

ECS Transactions, 25 (2009) 2, 213 – 220; ISBN 9781566777391

The SOFC group at FZJ has assembled and tested more than 350 SOFC stacks rated between 100 W and 15 kW during the last 15 years. The research topics covered stretch from materials over stack design, manufacturing of cells, stacks and components, mechanical and electrochemical characterisation, up to system design and demonstration. Use of improved steels, cathodes and materials processing has resulted in reduced degradation rates around 6 mV (0.75 %) per 1000 hours at 700 °C and 500 mA/cm² over tested stack lifetimes of over 15,000 hours. However, the target of development is directed at even further lowered degradation for commercial operation in stationary applications. A recent stack displays a degradation of approx. 3 mV (0.4 %) per 1000 hours running at 800 °C and 500 m/cm². This paper gives an overview of some of long-term testing results.

Important patents

Patent applications:

Principal inventor	PT	Description
Ro. Peters	1.2503	Method to operate a High Temperature Fuel Cell System

Patents granted

Principal inventor	PT	Description
Ro. Peters	1.2053	Modularly Built High Temperature Fuel Cell
D. Froning	1.2071	Method for the Modelling of Material Transport and/or Heat Transport Processes in an Apparatus and an Apparatus for carrying out the Method

3.4 Fuel processing and systems

3.4.1 Objectives and fields of activity

The availability of hydrogen is a prerequisite for the use of fuel cells in mobile and stationary applications. At present, however, an infrastructure for hydrogen as a future energy carrier does not yet exist. It is therefore essential that hydrogen is produced from readily available energy carriers. For stationary applications, natural gas and heating oil are suitable sources, while for mobile applications, gasoline, kerosene and diesel are options. Currently, the energy carriers listed above are mainly produced from the fossil primary energy carrier crude oil. In the long term, biomass will be used to produce part of the liquid energy carriers needed today.

At IEK-3, research in the field of fuel processing concentrates on reforming middle distillates such as kerosene, diesel, light heating oil, and diesel-like biofuels. In order to generate electricity or auxiliary power for portable or mobile applications (APU: auxiliary power unit), the same fuel must be used in the fuel cell APU system as is used to power the vehicle. For aircraft applications, kerosene and jet fuel for light aircraft are the only fuels available. They are allowed to contain a high level of sulfur-containing components. In the field of fuel processing, theoretical and experimental studies are therefore being conducted on the desulfurization of liquid fuels and their vaporization.

For auxiliary power supply in the 5–10 $kW_{el.}$ power class, activities concentrate on the autothermal reforming of kerosene, diesel and fuels similar to diesel. Process engineering analysis, component development and system design are important components of the R&D activities. Reformer development concentrates mainly on high-temperature PEFCs (160 °C - 200 °C) as well as on high-temperature SOFC fuel cells.

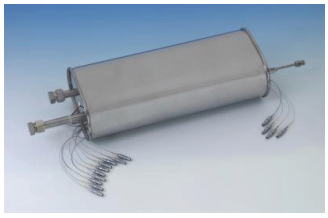

The fuel produced by reforming has a high carbon monoxide content of up to 10 vol.%. In a reactor connected downstream from the reformer, steam is used to convert the carbon monoxide into additional hydrogen and carbon dioxide. The product gas with a carbon monoxide content of 1 vol.% can be fed directly into an HT-PEFC after cooling to 160 °C.

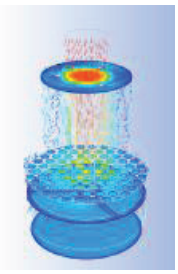

All areas of work are supported by relevant modeling activities. Important tools are CFD simulations on the Jülich supercomputer JUROPA and system simulations using the Simulink program. The aim is to optimize the dynamic performance under load changes and for starting strategies.

3.4.2 Important results

3.4.2.1 Infrastructure for scientific and technical experimints

With regard to a limited range of tests in the past for fuel processing components (reformer, catalytic burner, water-gas shift reactor) and fuel processing systems in the diesel laboratory, the laboratory infrastructure and the storage options were expanded to include a variety of fuels. This allows eight different liquid hydrocarbons to be used for test operation and other fuel grades to be kept in the barrel store. Currently, studies concentrate on the following grades: premium diesel, low-sulfur kerosene, and a low-sulfur GTL fuel free from aromatics.

The fuel storage facility comprises one 25 m³ tank, two 2 m³ tanks and five 1.3 m³ tanks (see Fig. 69). Furthermore, 96 barrels with a volume of 200 l can be stored in a barrel store. The following can be kept in the fuel storage facility: isoparaffin, n-paraffin, petroleum, white spirit, solvent naphtha, xylene, toluene, gasoline, kerosene, diesel fuel, extra light (EL) heating oil and what are known as gas-to-liquid (GTL) and bio-to-liquid (BTL) fuels.

Fig. 69: 25 m³ tank (in the background) and the two 2 m³ tanks on the licensed area. (Licensed according to the Act on Managing Water Resources (WHG))

The fuel storage facility is connected to test boxes via eight fuel lines. Furthermore, nitrogen, air, hydrogen, carbon monoxide, carbon dioxide, methane and argon are fed into the test boxes from the gas store. In addition, a deionized water supply and cooling water supply have been installed. The restructuring of laboratory capacities and the setting up of the fuel store allows IEK-3 to conduct different experiments in four different test boxes on fuel processing and on the coupling of the system with the HT-PEFC. This enables component development, long-term experiments, and system tests with and without fuel cells to be pursued in parallel. Boxes 1–4 have a surface area of 12–29 m^2. They can accommodate modules with a fuel processing system and/or a catalytic burner (box 1), component modules

Fig. 70: **Test modules DeS I, DeS II for desulfurization and modules A–E for testing reformers, shift reactors, burners and HT-PEFC stacks**

for reformers or a water-gas shift reactor (boxes 2–3) and systems including HT-PEFC stacks (box 4). All boxes have coupling systems to connect the modules to the supply and

removal systems. The waste gases from catalytic burners must be disposed of, as must the product gases of reformers in the single test stands and the waste gases from fuel cell stacks. A distinction is made here between combustible residual gases from reforming and combustion gases, which ideally only contain nitrogen, carbon dioxide, water vapor and small quantities of residual oxygen. Furthermore, when these gases are cooled down, condensates are produced which must be removed separately. All boxes are equipped with gas sensors for hydrogen, carbon monoxide and kerosene as well as a ventilation system. If the system is shut down by a gas alarm, then only the box that triggered the alarm is affected. The waste-gas system has a maximum load that is equivalent to a H_2 capacity of approx. 30 kW_{th} (lower heating value for hydrogen) per box.

For a number of years, all test stands have been analyzed in an FMEA and are CE certified. These analyses are used as a basis to derive necessary safety measures in the laboratory for the testing of reformers and fuel cells. Fig. 70 shows the test modules acquired over the last few years for desulfurization and the test modules A–E constructed by IEK-3. These are as follows:

- DeS I: Module for the thermal separation of fuels from middle distillates in the 5 kWe class (Fig. 70, top row, left)
- DeS II: Module for the hydrodesulfurization of middle distillates with presaturated hydrogen in the 5 kWe class (Fig. 70, top row, center)
- Brass board: Module for three HT-PEFC stacks (Sartorius Stedim Biotech) with 3 x 2.3 kWe in hydrogen operation (Fig. 70, top row, right)
- Module A: Module for testing the coupling of reformers (ATR) and shift reactors (WGS) in the 18 kWth class, corresponding to 7.5 kWe (Fig. 70 middle row, left)
- Module B: Module for testing BGS systems with ATR, WGS and CAB in the 28 kWth class, corresponding to 10 kWe (Fig. 70 middle row, center)
- Module C: Module for testing ATRs in the 28 kWth class, corresponding to 10 kWe (Fig. 70 middle row, right)
- Module D: Module for testing catalytic burners (CAB) in the 28 kWth class, corresponding to 10 kWe (Fig. 70 bottom row, left)
- Module E: Module for testing HT-PEFCs in the 5 kWe class (Fig. 70 bottom row, right)

3.4.2.2 Desulfurization

At IEK-3, work began on the desulfurization of liquid fuels in 2005. The focus is on the desulfurization of kerosene and light fuel oil (EL) containing a maximum of between 3,000 ppm and 2,000 ppm sulfur-containing hydrocarbons. The types of kerosene used in European and US infrastructure contain mass percentages of sulfur of less than 500 ppmw. Following a theoretical analysis and the selection of processes that are generally suitable for local desulfurization in fuel cell systems, the individual processes were then examined on a laboratory scale. Using results from experiments, two processes were found to be particularly effective. Hydrodesulfurization with presaturated hydrogen in the liquid phase is the only process that has the potential to be technically implemented in the short term. In the medium to long term, a combination of membranes and adsorbents could also play an important role in desulfurization. However, more research is required in this area.

A variety of processes are currently being considered. These are:

- two-stage desulfurization with pervaporation and adsorption
- three-stage desulfurization with two pervaporation steps and one adsorption step
- multistage adsorption, and
- hydrodesulfurization with presaturated hydrogen

The combination of pervaporation and adsorption in the two-stage process is suitable for kerosene qualities with sulfur volumes between approx. 500–700 ppmw and in the three-stage process for kerosene with 3,000 ppmw according to the specification.

Fig. 71 shows a schematic of how the sulfur-containing components in fuel can be separated using a two-stage process. Commercially available Jet-A1, which is a refinery product made from kerosene and additives, contains significantly reduced concentrations of thiophenes (150 ppmw) and mono- and dimethylated benzothiophenes (100 ppmw each). Trimethyl-benzothiophenes are one of the main constituents with approx. 200 ppmw S. The model substances in Fig. 71 are a trimethyl-thiophene, a methyl-benzothiophene and a trimethyl-benzothiophene.

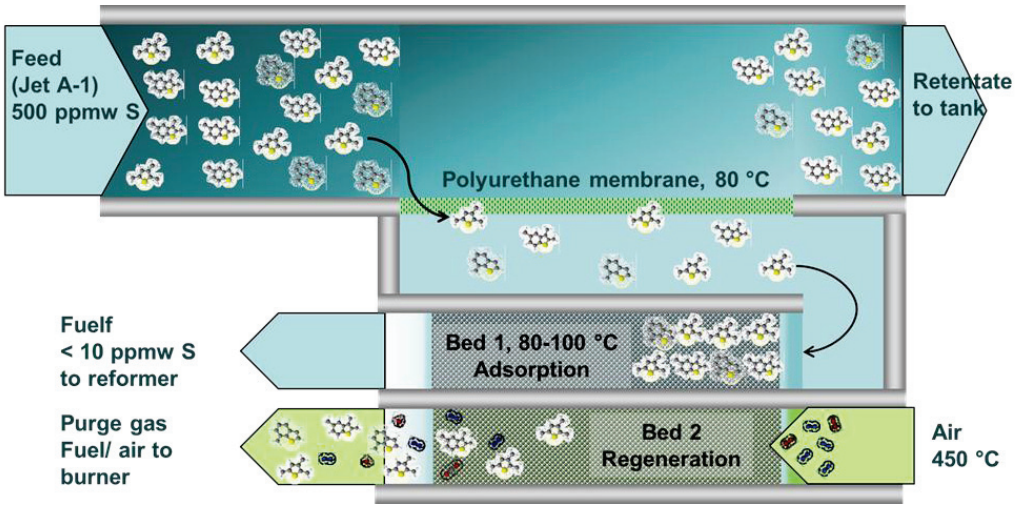

Fig. 71: Schematic of a multistage process for desulfurization using membranes and for deep desulfurization using an adsorbent

As shown by the experimental results in Fig. 72, trimethyl-thiophene preferentially accumulates in the membrane permeate. The enrichment factor shown determines the concentration of a sulfur-containing component in the permeate in relation to the concentration in the feed. Alkylated benzothiophenes, in contrast, remain in the feed flow – referred to as retentate at the membrane outlet. This type of membrane allows the sulfur content to be almost halved and reduced to 250 ppmw S. The sulfur-containing components are subsequently adsorbed by a suitable adsorbing agent. An adsorber bed already loaded with sulfur-containing fuel components must be regenerated with air at temperatures between 400 °C and 500 °C. As the adsorption and regeneration is easier to implement for thiophenes than for benzothiophenes and this in turn is easier to implement than for

dibenzothiophenes, the separation behavior of the pervaporation membrane has a positive effect.

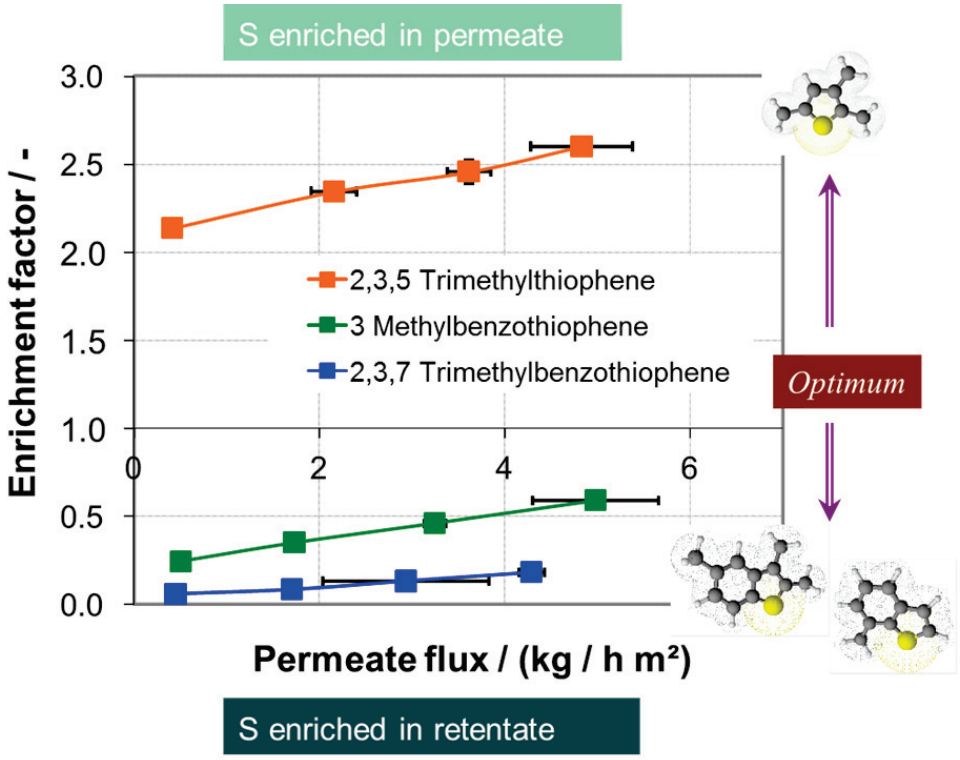

Fig. 72: **Experimental results for the selectivity of a polymer membrane at a feed temperature of 70 °C. The selectivity is characterized by the enrichment factor ß; ß = $m_{S,permeate}$ / $m_{S,}$feed**

In order to assess the suitability of a process, the following criteria must be considered: lifetime, mass flow rate, dimensions, efficiency losses, required thermal and electric energies.

Fig. 73 shows a spider chart for the four different processes in order to assess their suitability for application when kerosene with 3,000 ppmw sulfur is used. Each criterion has been divided by the best value achieved in each of the four processes. The diagram does not provide any information on the absolute suitability of the processes. The target values for the criteria are not currently clearly defined but tendencies are often clear. The consumption of electrical and thermal energy as well as the efficiency losses must therefore be kept as small as possible. The target value for lifetime essentially depends on the application and is between 5,000 - 40,000 h.

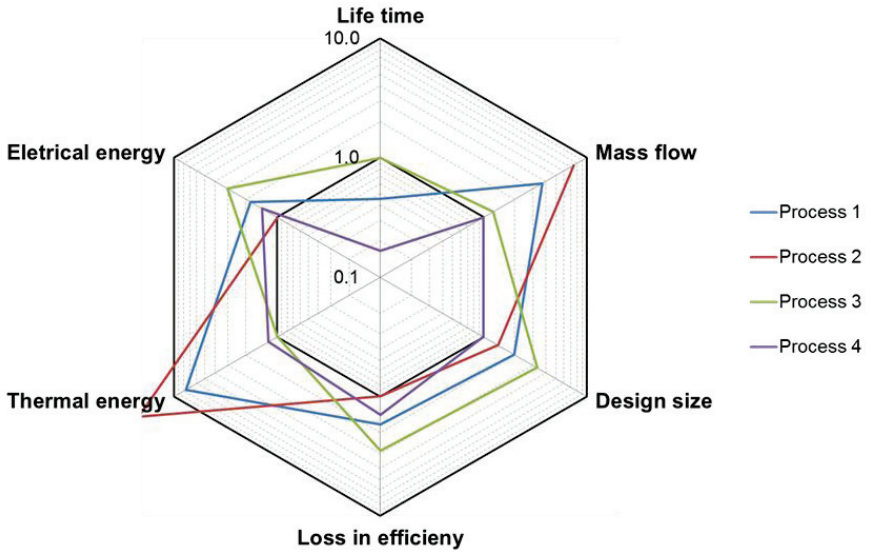

Fig. 73: **Comparison of the evaluation criteria of lifetime, mass flow rates, dimensions, efficiency losses, electrical and thermal energy supplied for an initial mass fraction of 3000 ppmw sulfur in the kerosene. Process 1: two-stage desulfurization with pervaporation and adsorption; Process 2: three-stage desulfurization with two pervaporation steps and one adsorption step; Process 3: multistage adsorption; Process 4: hydrodesulfurization with presaturated hydrogen**

The lowest efficiency losses were exhibited by process 2 with 0.7 %; efficiency losses in process 4 were also in a tolerable range at 1 %. The best lifetime was achieved by multistage adsorption (process 3) with 1,160 h. For many processes, sufficient experience is still lacking. The two membrane processes are characterized by high mass flow rates, which in turn lead to a high consumption of thermal energy to heat the mass flows and high construction costs for the heat exchanger. Processes 1 and 2 are only suitable to a limited extent for fuel grades with 3,000 ppmw S. Multistage adsorption requires a relatively large expenditure of pumping energy and a relatively high efficiency loss (3 %). On the basis of the criteria shown in Fig. 73, it can be concluded that hydrodesulfurization in the liquid phase is preferable for high sulfur contents. An evaluation for fuels with sulfur levels of 500 ppmw S may give rise to different results.

3.4.2.3 Component development

Over the last few years at IEK-3, reformers have been developed for middle distillates and for synthetic fuels made from biomass. These are shown in Fig. 74. This reformer is also capable of using standard diesel fuels to produce a sufficient quantity of hydrogen for fuel cells with a power between 5 kW_e and 10 kW_e. The preferred process for this is known as autothermal reforming. All reformers have a cold-starting device, internal steam generation, and a device for extracting the process heat that arises during reforming. In addition to

hydrogen, autothermal reformers also produce higher levels of carbon monoxide (7 - 10 % (vol.)). In a water-gas shift reactor (WGS), carbon monoxide is converted with water into carbon dioxide and hydrogen. The concentration of carbon monoxide was reduced to 1 %. The hydrogen content rose by approx. 6 - 9 %. The fuel processing efficiency was between 80 % for fossil fuels and 86 % for synthetic fuels based on a Fischer-Tropsch process. The fuel cell uses the hydrogen in the product gas resulting from fuel processing – usually referred to as reformate – at a rate of 80 - 85 %. Residual hydrogen, carbon monoxide and methane, formed in small quantities during reforming, are combusted in a catalytic burner with low emissions. The resulting reaction heat is used together with the heat released during the cooling of the reformate to 400 °C (inlet temperature shift reactor) to generate steam in the reformer. All reactor types were scaled up in 2010 to a reformer thermal capacity of 28 kW_{th} – which is equivalent to a fuel cell capacity of approx. 10 kW_e.

Fig. 74: Overview of component development at IEK-3 between 2007 and 2012

In order to gain a better understanding of the flow and temperature conditions inside the mixing chamber of the reformer, and to be able to predict them more easily, computational fluid dynamics (CFD) modeling is carried out at Jülich. CFD modeling aims to provide precise data on the temperatures reached in the mixing chamber and on the local zones in which the fuel is vaporized under given reaction conditions, such as temperature, flow rates of air, steam and diesel fuel, and the spray pattern of the nozzle. The CFD-based approach used to design the reactor was also adapted for catalytic combustion and the shift reaction. Fig. 75 shows a CFD simulation describing the characteristic flow times. The flow lines and flow times are shown for the steam inlet at 50 % load. The characteristic flow times were determined as follows: for droplet vaporization $t_V < 0.007 - 0.01$ s, for the eddy flow in the front mixing chamber $t_W < 0.02$ s and for the straight through flow $t_D < 0.04$ s.

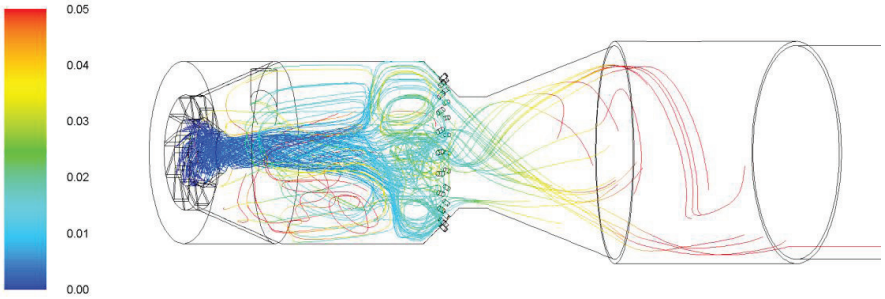

Fig. 75: Flow lines for vapor flow in ATR AH2 at 50 % load; residence time in [s]

The flow calculations for the continuous phase can be validated using glass reactor experiments, as shown in Fig. 76. In the glass reactors, water is used as a fluid substitute and methylene blue is used as a dye tracer. The Mikroskop and Makroskop high-speed cameras are used as analysis tools. The mass flow rates are thus designed with the aid of similarity theory.

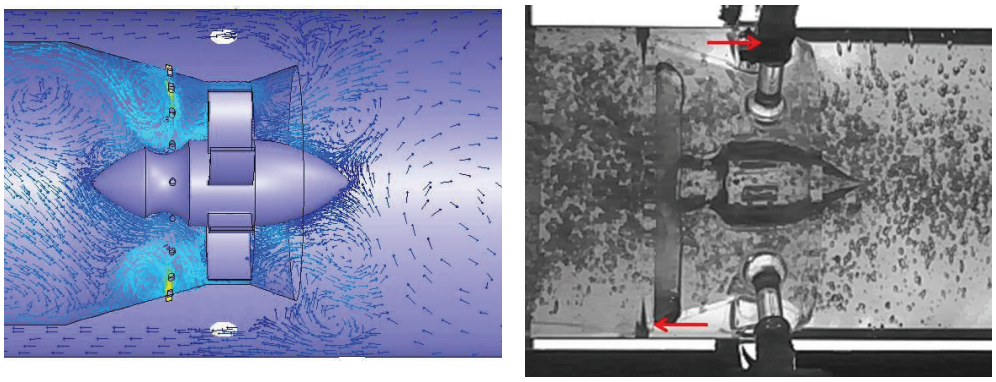

Fig. 76: CFD modeling and flow visualization experiments for model validation in reformer geometry

The glass reactor shown represents the mixing chamber of a reformer in the 50 kW_e class. The flow visualization experiments show good qualitative and quantitative agreement with the calculated and experimentally determined flows. The simulated flow profiles can therefore be considered to be sufficiently accurate. Further visualization experiments and high-speed analyses are planned for the continuous validation of CFD simulations.

A statistical experimental design was derived to characterize the reformer, as exemplified in Fig. 77 by the ATR 9.1. It comprises 11 individual experiments, in which the O_2/C molar ratio is generally varied between 0.43 and 0.47, the H_2O/C molar ratio between 1.7 and 1.9, and the kerosene mass flow rate is varied between 1,215 g/h and 2,025 g/h. The influence of these reaction parameters was investigated on characteristic variables, such as the temperatures in the catalyst, concentrations of reaction products in the reformate and the

efficiency of the reforming process. In the experiments, the temperature of the steam entering the reactor was 460 °C. Fig. 77 shows the impact of the O_2/C and H_2O/C molar ratios on the CO concentration in the reformate of the ATR 9.1 for a kerosene mass flow rate of 2,025 g/h (100 % reformer load) for two different grades of kerosene.

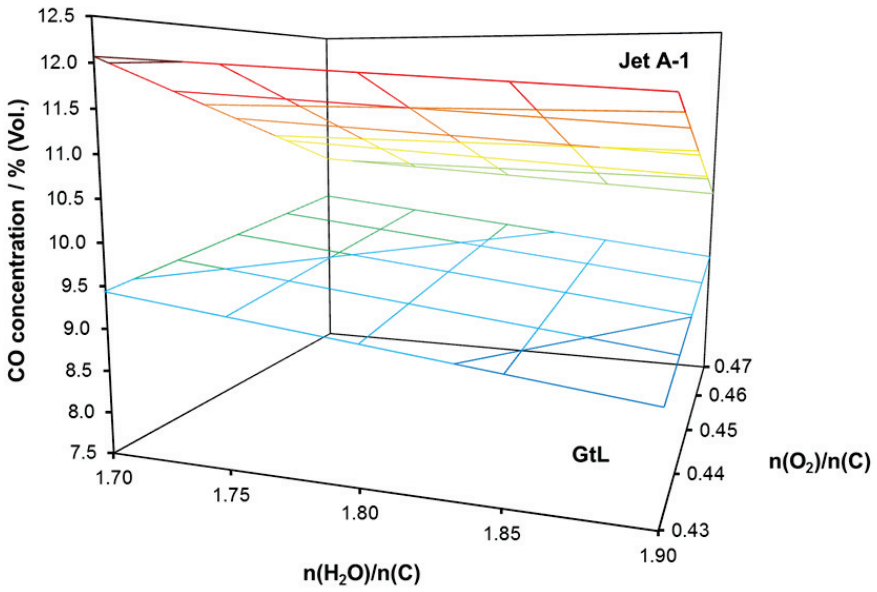

Fig. 77: Comparison of CO concentrations in the product gas of the ATR 9.1 reformer as a function of the oxygen-to-carbon ratio and of the steam-to-carbon ratio at full load for low-sulfur fossil (Jet A-1) and synthetic (GTL: gas-to-liquid) kerosene fuels

Low-sulfur fossil kerosene can be produced in refineries using a “hydrocracking” process. In Fig. 77, it is labeled Jet A-1. It contains approx. 15 - 20 vol.% aromatics and the H/C ratio of the fuel has been reported as very good. The synthetic GTL fuel is produced in a Fischer-Tropsch process using the synthesis gas from natural gas reforming. The summation formula is $C_{10}H_{22}$. GTL kerosene does not contain aromatics or sulfur-containing components. The Jet A-1 reformate contains significantly more carbon monoxide than GTL kerosene: approx. 10 - 12 vol.% CO compared to 9 - 10 vol.% CO. However, the difference was only ΔCO = 1 % at the design point, O_2/C = 0.47 and H_2O/C = 1.9.

3.4.2.4 System development

The development of systems that reform middle distillates involves experimental and theoretical work. On the experimental side, system development for hydrocarbon-based fuel cell systems focuses on HT-PEFCs. One important tool for system development is the modeling of all basic components in fuel cell systems with reforming. This modeling covers SOFCs, PEFCs and HT-PEFCs. The emphasis is on modeling all subcomponents, primarily components with integrated heat exchange and phase change, as well as on static and

dynamic system simulations. The aspects examined are the start-up process and behavior during load change. Within the scope of process analyses, water balances were calculated as a function of external conditions, such as relative humidity and ambient temperature. For more detailed information, see the final report for the ELBASYS collaborative project (see the section on important publications).

Fig. 78 provides an overview of the fuel processing systems constructed from 2007 to 2011 and those currently being tested. The next section will discuss the results that were obtained for a brass board system with the ATR 8V2 reformer coupled to a WGS 3 shift reactor.

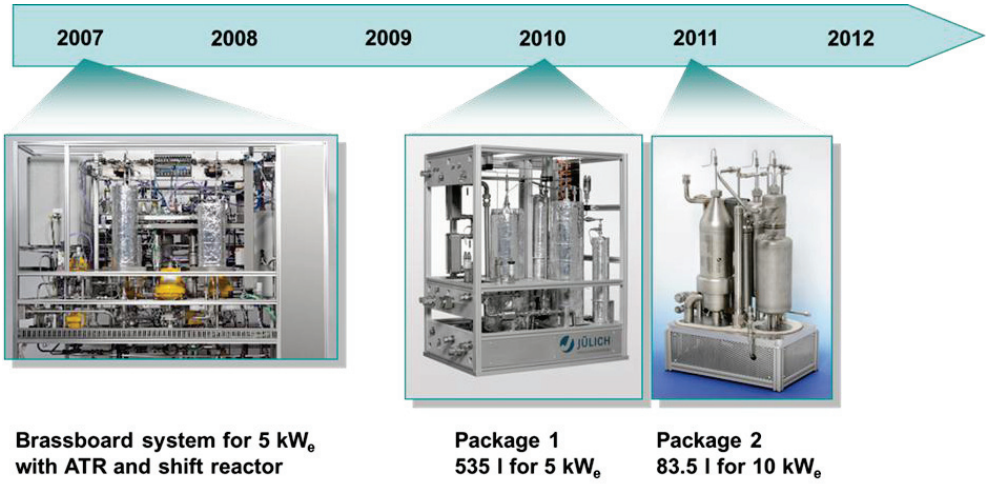

Fig. 78: Overview of system development for fuel processing using diesel and kerosene for the HT-PEFC at IEK-3 between 2007 and 2012

Prior to experiments with the WGS 3 water-gas shift reactor, experiments were conducted in order to characterize the internal steam supply in the fuel processing system. The internal steam supply is one of the most important problems in fuel processing systems. In order to solve it, the system subcomponents must be carefully adjusted in relation to their mass flows and enthalpy flows. The reformer is operated with cold fuel, cold air and superheated steam. For this, the water must be vaporized and superheated with the aid of the reaction heat. The heat is then recovered in the integrated heat exchangers of the catalytic burner and the reformer. Some of the water required for reforming is fed into the catalytic burner and vaporized there. The vaporized water flow is then added to the remaining cold water flow. The resulting wet steam is then fed into the integrated heat exchanger in the reformer, where it is fully vaporized and superheated to the reformer inlet temperature. Fig. 79 shows the design for providing steam in the fuel processing system (left) in comparison with integration in the brass board system (Module A, right in Fig. 79). The biggest difference is that the vaporization function of the catalytic burner (CAB) is performed in module A by an electric evaporator. Moreover, the module provides the option of feeding some of the reforming air together with the water through the evaporator into the reformer. An electric heating cartridge downstream of the reformer heat exchanger allows the temperature of the steam to be precisely set at the inlet into the reformer mixing chamber.

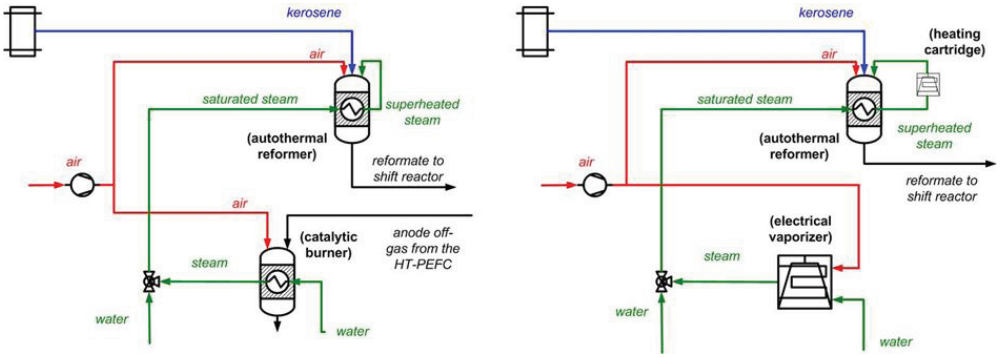

Fig. 79: Comparison of subsystems for providing steam in the fuel processing system (left) and in module A (right)

For normal operation of the fuel processing system, the water must be shared between the catalytic burner and the cold water flow so that the outlet temperature of the reformer corresponds to the inlet temperature of the shift reactor, therefore ensuring that no additional heat exchanger is required. The target temperature at this point is approx. 400 °C. At the same time, the wet steam must be completely vaporized and superheated to around 460 °C. Then, the superheated wet steam can be fed directly into the mixing chamber. System tests aim to characterize the heat recovery in the reformer in order to determine the optimal operating parameters.

For the characterization, a full factorial experiment was designed with 2^3 factors. The ATR reformer was operated at a constant fuel rate of 1,080 g/h GTL kerosene, a H_2O/C molar ratio of 1.9, and an O_2/C molar ratio of 0.47. The temperature of the steam after the heating cartridge was set at 460 °C. As part of the statistical experimental design, the following three variables were varied:

- Water share evaporator/total: 50 % (-) to 70 % (+)
- Outlet temperature evaporator: 200 °C (-) to 300 °C (+)
- Air share in reformer air ring/total: 70 % (-) to 100 % (+)

In all eight tests, the reforming process was very stable with almost constant temperatures and product gas compositions. The effect of the variables will therefore be discussed with respect to the target temperature of the shift reactor reformate and the target steam temperature in the reformer. Fig. 80 shows an overview of the results of the evaluation with a regression function. In order to improve the representation, the third parameter (share of air) was kept constant at its minimum value (top) and maximum value (bottom). The results presented are for an air share of 70 % for the air ring/total air.

The results show that an increasing water flow through the evaporator and an increased evaporator temperature give rise to increased values for both target steam temperature and target temperature for the shift reactor. This can be explained by an increased heat input in the reformer heat exchanger. Both target temperatures also rise in the case where 30 % of the air required for reforming is heated in the evaporator and fed into the mixing chamber via the reformer heat exchanger. An important observation is that the two target temperatures

differ slightly from each other. The target values were 400 °C for the shift temperature and 460 °C for the steam temperature. However, the geometry of the integrated heat exchanger does not appear to allow such a temperature difference of 60 K. The parameter combination of water share 70 %, evaporator temperature 200 °C and air share 70 %, for example, resulted in a steam temperature of 407 °C and a shift temperature of 403 °C.

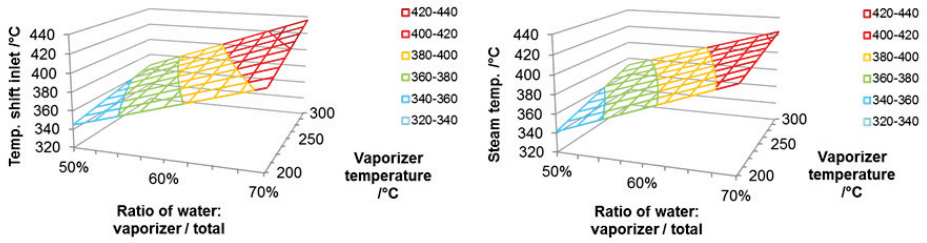

Fig. 80: Evaluation with regression planes for the steam and reformate temperatures at the outlet of the internal heat exchanger of the ATR 8V2 as a function of the evaporator temperature (outlet CAB) and the distribution of the water between CAB and ATR. Air share in reformer air ring/total: 70 %

Further tests revealed that system operation is also possible with no additional components such as heating cartridges. The parameter combination of water share 70 %, evaporator temperature 200 °C, air share 70 % and heating cartridge temperature 400 °C resulted in a steam temperature of 399 °C and the temperature at the reformer outlet was also 399 °C. The temperature of the mixture in the bottom region of the mixing chamber was 320 °C and reforming was stable. This temperature allows a complete vaporization of the GTL kerosene.

In order to test the coupling of reformer and shift reactor, an ATR 8V2 reformer and a WGS 3 shift reactor were connected to each other. The following parameters were varied: the inlet temperature in the high-temperature shift stage was set between 364 °C and 400 °C and the amount of water added between the high-temperature and low-temperature shift stages was varied between 540 g/h and 940 g/h. The addition of water means that the product gas of the high-temperature shift stage could be cooled by means of water evaporation. Varying the amount of water added also altered the inlet temperature in the low-temperature shift stage. The CO concentration at the outlet of the low-temperature shift stage was measured using a mass spectrometer. The mass balances were used to determine the CO concentration in the wet product gas of the shift stages.

Fig. 81 and Fig. 82 show the wet CO concentrations in the product gas of the shift reactor for operation with GTL kerosene and desulfurized kerosene. Both images show the measured values and/or the balanced values as regression planes based on a 3^2 design of experiments. The required outlet concentration was approx. 1 vol.% CO. The graphs show that a large proportion of the parameter variations fulfill this requirement. For low inlet temperatures in the high-temperature shift stage and a large amount of added water, the inlet temperature in the low-temperature shift stage was very low and catalytic activity in the low-temperature shift stage was insufficient to achieve the required outlet concentration. In terms of system operation, an inlet temperature of 400 °C in the high-temperature shift stage is

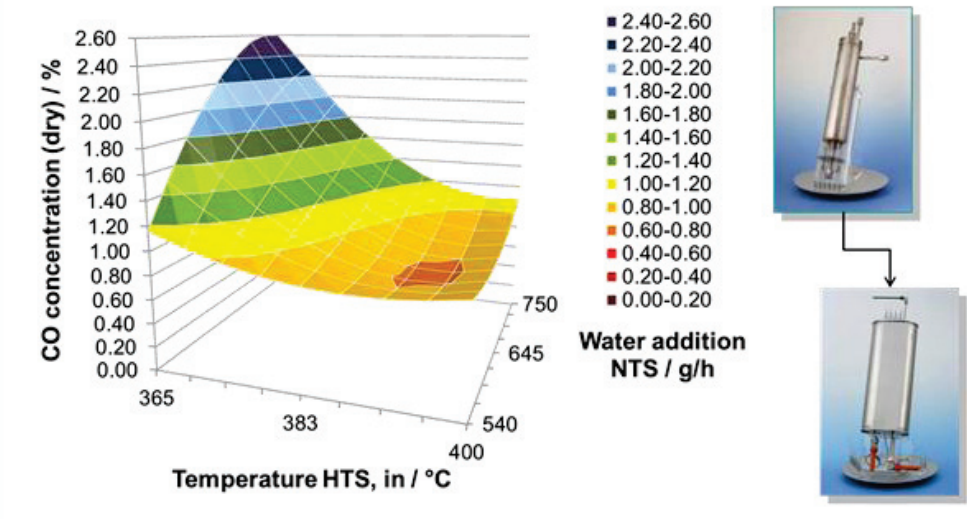

Fig. 81: **CO concentration (wet) in the product gas of the shift reactor as a function of the inlet temperature into the high-temperature shift stage and the amount of water added between the high-temperature and low-temperature shift stages. Regression planes based on a 3^2 design of experiments for GTL kerosene**

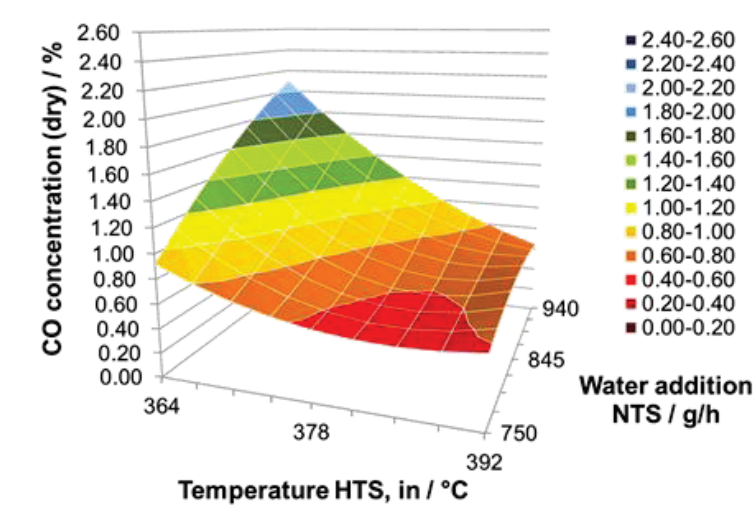

Fig. 82: **CO concentration (wet) in the product gas of the shift reactor as a function of the inlet temperature into the high-temperature shift stage and the amount of water added between the high-temperature and low-temperature shift stages. Regression plane based on a 3^2 design of experiments for desulfurized kerosene**

ideal, as is a low amount of added water. A direct comparison of the two fuels reveals that the achievable outlet concentrations are lower for desulfurized kerosene. This is even more remarkable considering that desulfurized kerosene has a 1 % higher CO concentration than GTL kerosene when it enters the high-temperature shift stage, i.e. when it leaves the reformer (see Fig. 77). The product gas composition of the reformate causes the thermodynamic state of equilibrium to alter and allows the depletion of carbon monoxide to lower concentrations in the shift reactor.

3.4.3 Staff members and fields of activity

Name	Tel. (+49 2461-61-) E-mail address	Field of activity
Prof. Dr. R. Peters	4260 ra.peters@fz-juelich.de	Head of Fuel Processing Systems
Dr. J. Pasel	5140 j.pasel@fz-juelich.de	Head of the Chemistry for Fuel Processing Group
Dr. R. C. Samsun	4616 r.c.samsun@fz-juelich.de	Head of the Systems Engineering for On-Board Power Supply Group
Dr. S. Göll	4394 s.goell@fz-juelich.de	Process engineering systems calculations and analyses
F. Scharf	5322 f.scharf@fz-juelich.de	CFD modeling, diesel reforming
Y. Wang	2779 yo.wang@fz-juelich.de	Desulfurization of kerosene and heating oil
C. Wiethege	6365 c.wiethege@fz-juelich.de	Dynamic modeling, systems engineering for on-board power supply
A. Tschauder	4547 a.tschauder@fz-juelich.de	Reactor development, reforming, system design

3.4.4 Important publications, PhD theses and patents

Important publications

Wang, Y.; Latz, J.; Dahl, R.; Pasel, J.; Peters, R.

Liquid Phase Desulfurization of Jet Fuel by a Combined Pervaporation and Adsorption Process

Fuel Processing Technology, 90 (2009) 458-464

Since the conventional hydrodesulfurization process employed in the refinery industry is not suitable for mobile fuel cell applications (e.g. auxiliary power units, APUs), the present study aims to develop an alternative process and determine its technical

feasibility. A large number of processes were therefore assessed with respect to their application in fuel cell APUs. The results revealed that a two-step process combining pervaporation and subsequent adsorption is the most promising. Six different membrane materials and ten different adsorbents were screened in order to identify the most suitable and promising candidates. Further laboratory experiments were conducted to optimize the operating conditions and to collect data for a pilot plant design. Different jet fuel qualities with up to 1675 ppm sulfur were desulfurized to a level of 15–22 ppm. The aim of developing a suitable process for the desulfurization of jet fuel in fuel cell APUs has therefore been achieved.

R. C. Samsun, C. Döll, R. Peters, J. Pasel and D. Stolten

Start-up Behavior of Fuel Processing Systems

ECS Transactions, 17 (1) 599-610 (2009)

This publication analyzes the start-up behavior of fuel cell systems for on-board power supply. It focuses on the fuel cell types SOFCs, PEFCs and HT-PEFCs. For the dynamic analyses, Jet A-1 is used as fuel – simplified as $C_{12}H_{24}$. The start-up calculation is initially limited to the fuel processing system. Here, the product gas composition was calculated for the reformer, and in the case of low-temperature fuel cell systems, for the shift reactor. Only when the reactor has almost reached its operating temperature can the carbon monoxide be reduced to the necessary level. In the case of a PEFC, reactors or a cascade of reactors are necessary for preferential oxidation. If an ignition burner is used to heat up the entire fuel processing system, then the start-up time is between four and five minutes. Further measures allow this time to be reduced to around 90 s for an optimized HT-PEFC.

Peters, R.; Latz, J.; Pasel, J.; Samsun, R.C.; Stolten, D.

Verbundvorhaben ELBASYS (Elektrische Basissysteme in einem CFK-Rumpf)-Teilprojekt: Brennstoffzellenabgase zur Tankinertisierung –Schlussbericht (*ELBASYS collaborative project – Subproject: Fuel cell off-gases for tank inerting – Final report*)

Forschungszentrum Jülich GmbH, Schriften des Forschungszentrum Jülich, Reihe Energie & Umwelt / Energy & Environment, Band / Vol. 46, ISBN 978-3-89336-587-6, Jülich, 2009

In order to secure a good market position in the future, it is important that the European aviation industry further develops its technological expertise to cover the economic production of light aircraft with correspondingly lower fuel consumption. In order to achieve this objective, work is increasingly concentrating on the application of composite fiber materials. The ELBASYS collaborative project comprises the main aspects for integrating basic electrical systems in a CFRP fuselage. Work at Forschungszentrum Jülich (Jülich) is part of the subproject focusing on the integration of a fuel cell system. Jülich concentrated on the desulfurization of kerosene, the design and construction of a catalytic burner for the generation of inert off-gas flows for tank inerting and on process analyses for different fuel cell systems. Results to date suggest that an option for technically implementing desulfurization in the 5 kWe class in the short term is hydrodesulfurization with the hydrogen presaturation technology. Furthermore, an alternative process was identified for future research work. The catalytic burner developed will be used in the future for low-emission combustion of the off-gases in normal operation under stationary and dynamic conditions. Systems analysis work on PEFC and HT-PEFC systems revealed that HT-PEFC systems with kerosene reforming fulfill the requirements for the multifunctional use of fuel cell technologies better than the corresponding PEFC system.

Peters, R.

Auxiliary Power Units for Light-Duty Vehicles, Trucks, Ships and Airplanes

In Hydrogen and Fuel Cells, Ed. Stolten, D., Wiley-VCH, Weinheim, 2010, pp. 681-714

Fuel cell APUs are one option for generating electricity efficiently with low emissions. In aircraft applications, for example, significant quantities of kerosene and thus CO_2 can be saved compared to conventional gas turbine technologies. In order to use fuel cell APUs, the framework conditions must be taken into consideration. These conditions comprise a combination of the application in question, the required electric power and the fuel to be used. Shipping has the largest power range to be covered from 5 kW_e to 5 MW_e. Most applications, however, have a power ranging from 5 kW_e to 50 kW_e. Fuel cell APUs have a good chance of developing into a marketable product if they are run on fuels for which infrastructures already exist, for example, gasoline, diesel or kerosene. The hydrogen required must then be produced from these fuels by means of a suitable reforming process. In designing a fuel cell APU, a wide range of combinations is possible for different fuel cell types with different reforming processes. This paper provides an overview of the requirements for the use of fuel cells for on-board power supply in different types of transport, such as passenger vehicles, trucks, ships and aircraft. The various steps involved in the production of a hydrogen-rich feed gas are discussed for different fuels. In conclusion, the stage of development of different fuel cell systems is evaluated.

Peters, R.,, Westernberger, A.

Large Auxiliary Power Units for Vessels and Airplanes

In Innovations in Fuel Cell Technologies, Ed. Steinberger-Wilckens, R.; Lehnert, W., Royal Society of Chemistry, Cambridge, 2010, 76-152

This book chapter deals with the use of fuel cells for on-board power supply in the power class 150–500 kW_e. Such fuel cell systems are particularly interesting for applications in ships and aircraft. The operating conditions for these two areas of application, the types of fuel cell available, and the different fuel options are discussed. Maritime applications represent a broad field with a variety of fuel cells and different fuels, although very few systems have actually been realized to date. Aeronautic applications concentrate on two approaches:

- The first involves storing hydrogen in liquid form. This option is particularly suitable for short-range use
- The second approach involves using commercial Jet A-1 or biofuel similar to kerosene for reforming. This solution is preferable for medium-range to long-range flights

The HT-PEFC is ideally suited for use as a fuel cell in both cases. The multifunctional approach for the application of fuel cells in aircraft is emphasized here. In addition to the generation of electricity, the by-products water, heat and off-gas are also considered. Water can be processed and re-used on board the aircraft. The cathode exhaust gas in the fuel cell can be used for tank inerting after moisture has been extracted and it has been dried. The waste heat of the fuel cell can also be used to de-ice the wings during certain flight phases. The analyses for defined combinations of fuels and fuel cell types allow us to draw conclusions on the benefits of such systems for different flight ranges.

Important patents

Patents applications:

Principal inventor	PT	Description
Prof. D. Stolten	1.2392	Process for reduction of sulfur in an liquid sulfur-containing fuel for electric power production

Patents granted

Principal inventor	PT	Description
	1.2281 EP	Device for production of a fuel / air - mixture

3.5 Process and systems analysis

3.5.1 Objectives and fields of activity

Selecting energy systems for the future and developing marketable technologies necessitate systematic and technically sound studies of process chains in terms of energy efficiency, raw material requirements, costs and emissions. For this reason, systems are designed to meet realistic operating conditions, modeled to varying degrees of detail and dynamically simulated. At the moment, the subinstitute is concerned with the topics of electromobility (fuel cell and battery vehicles), hydrogen infrastructure and membrane-based processes for carbon dioxide separation in power plants. The latter topic was integrated into this area at the end of 2010. The institute was also intensively involved in the preparation and follow-up work for WHEC-2010 and ICEPE 2011.

The use of fossil fuels in the energy industry was responsible for 40.8 % of German CO_2 emissions in 2008[10] – corresponding to 352 million tonnes. Carbon dioxide separation and storage are urgently needed in order to reduce the greenhouse effect on the way towards a predominantly renewable energy supply while continuing to ensure the security of supply[11]. Industrial countries now have to demonstrate the feasibility of this approach. Building on past work at IEK-3, which concentrated mainly on the energetic potential of different process flows for coal-fired power plants, future work will assess investment costs and look at minimizing CO_2 mitigation costs. Important process parameters are CO_2 purity and the degree of CO_2 separation. The objective of a high purity is related to the demand for less compression energy, low transport and storage volumes and the prevention of corrosion in pipelines. For this reason, the subsequent energy and cost expenditure must be considered for different purities in a process comparison. The separation efficiency is a simple operand characterizing the separation processes. The crucial factor in evaluating the processes is the derived CO_2 mitigation for an intended constant net power generation. The aim is to achieve a high mitigation

$$1 - \frac{\mathrm{CO_2\ emission\ \ with\,CCS\,(at\ the\,same\ fuel\ heat\ supply)}}{\mathrm{CO_2\ emission\ \ without\,CCS}} * \frac{\eta_{\mathrm{net,\,without CCS}}}{\eta_{\mathrm{net,\,with\,CCS}}}$$

and low mitigation costs, whereby the cost of CO_2 storage and the environmentally friendly disposal of other residues must be taken into account. Low mitigation costs are one of the prerequisites for industrial and social acceptance as well as for the rapid spread of CCS. Along with risk assessments, they are a central criterion for the operator in deciding which technology to use and they can be compared directly with the costs of CO_2 emission certificates.

---

[10] Federal Environmental Agency (ed.): Entwicklung der Kohlendioxid-Emissionen in Deutschland. http://www.umweltbundesamt-daten-zur-umwelt.de (Last updated on 05 March 2011)

[11] Metz, B., Davidson, O., de Coninck, H., Loos, M., Meyer, L.: IPCC Special Report on Carbon Dioxide Capture and Storage, 2005, www.ipcc.ch

3.5.2 Important results

3.5.2.1 Fuel cells and batteries for mobile applications

A decrease in global and local environmental impacts, a reduced dependence on imported energy raw materials, and economic policy-related aspects are the main objectives of the much-needed reorganization of the transport sector. In this context, a modified primary energy mix is discussed in relation to fuels, some of them new, including electricity and the use of new and more efficient drives. A prominent role could be played in future by all-electric fuel cell drives for cars and buses, as well as by battery drives for cars driving short distances. If hydrogen is used in highly efficient fuel cells, renewable power that cannot be utilized due to grid stability issues, especially from wind energy, can be stored temporarily in the form of hydrogen. Liquid fuels with a high energy density will still be required in the long run, predominantly for heavy trucks and long-distance transportation, as well as aircraft and ships. In the future, systems with fuel cells in the power class of between approx. 5 kW and over 1 MW could be used for auxiliary power supply in these types of vehicles, in which a suitable fuel can be produced by reforming the fuel already on board. A renewable basis for liquid fuels is biomass, which can be converted into suitable fuels using biochemical or thermochemical processes.

Vehicle concepts whose drive structure and storage dimensions facilitate all-electric drive operation include:

- *plug-in* hybrids with a combustion engine or fuel cell system (*plug-in hybrid electric vehicles*, PHEVs) with a range of up to 50 km in battery operation
- electric vehicles with fuel cell and battery (*fuel cell hybrid electric vehicles*, FCHVs) with a range of over 400 km and
- electric vehicles with a battery (*battery electric vehicles*, BEVs) with a range of up to 200 km

Such vehicle concepts can be compared to current vehicles with similar payload and total volume on the basis of costs, as well as the performance of the drive in terms of top speed and acceleration, and the range that can be achieved before refueling or battery recharging. The torque curve of their motors shows that electric drives are easy to drive and that manual transmission is no longer required for moderate speeds. For FCHVs in hydrogen operation, PEFCs are currently the only option with operating temperatures between 80 °C and 95 °C. Li-ion technology can be used for BEVs. This technology is best suited to meet requirements such as high specific energy and energy density, as well as a long lifetime and low self-discharge rates.

Detailed simulations based on the New European Driving Cycle (MVEG) were carried out to compare BEVs with a range of 200 km and FCHVs with a range of 400 km. The assumptions for the vehicle were as follows: the transverse area was 2 m^2, the drag coefficient was 0.32 and the vehicle mass excluding the drive, and storage amounted to 900 kg. It was also assumed that the vehicle mass was increased 1.2 fold by additional component masses due to measures for chassis stiffening. The dimensions of the drive components were set on the basis of driving performance requirements: a top speed of 150 km/h and an acceleration time of 12 s from 0 km/h to 100 km/h. Since the energy requirement in the driving cycle and the necessary energy reserve are correlated, the energy requirement is determined in an iterative process. If the specific energy of the BEV battery module is assumed to be

120 Wh_e/kg, this results in a battery mass of 235 kg and an energy requirement of 14.2 kWh_e/100 km [12]. The FCHV has an energy requirement of 27.5 MJ/100 km.

It is difficult to make predictions about the cost of batteries and fuel cell systems today. It is not yet known which materials and manufacturing processes will be relevant for batteries in the future. The target values specified today for the period 2015–2020 are € 250–300/ kWh_e, provided that mass production is implemented. Assuming an average cost of € 275/KWh_e, the cost of a battery module with a battery capacity of 28.3 kWh_e as determined earlier including a reserve capacity of 20 % can be estimated as approximately € 9,700. The cost of fuel cell systems including storage tanks for a range of 400 km is estimated as approximately € 7,400. Here, costs of € 70/kW_e and € 10/kWh_{H2} for 700 bar compressed gas storage are assumed based on the literature.

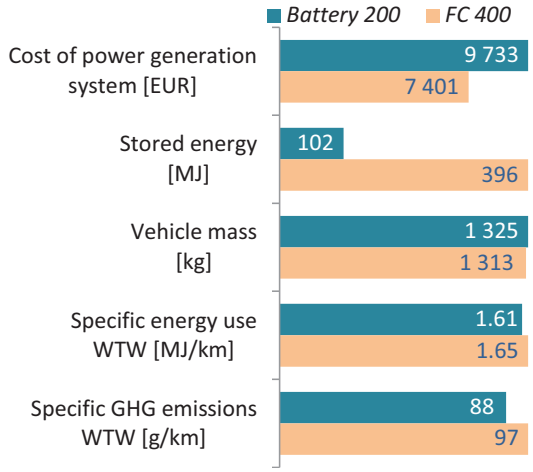

Fig. 83: Comparison of electric cars with batteries and with fuel cells. See text for assumptions; power supply based on the German energy mix (2008) according to [13]; hydrogen provided by means of natural gas reforming and subsequent transport by truck in pressure cylinders (own calculations)

Fig. 83 summarizes the comparison of vehicles with fuel cells and vehicles with batteries. It shows that the costs associated with the power supply system based on fuel cells could be considerably lower for a range that is at least twice as high if the relevant cost targets are met. With respect to the well-to-wheel (WTW) balances for primary energy input and greenhouse gas (GHG) emissions, FCHVs are at a slight disadvantage when natural gas is used to produce hydrogen. By altering the primary energy basis for the generation of electric current and hydrogen in favor of low-GHG primary energies, these values can be reduced further.

---

[12] Grube, Th., Stolten, D.: Bewertung von Fahrzeugkonzepten mit Brennstoffzellen und Batterien (*Evaluation of vehicle concepts with fuel cells and batteries*). Paper at VDI conference “Innovative Fahrzeugantriebe”, Dresden, Nov. 10-11, 2010

[13] AG Energiebilanzen: Energiebilanz der Bundesrepublik Deutschland 2008. www.ag-energiebilanzen.de, last accessed on Sept. 22, 2010

3.5.2.2 Hydrogen infrastructure with a focus on pipelines

One of the most important prerequisites for the emergence of a mass market for fuel cell vehicles is a nationwide, efficient, low-cost and safe hydrogen infrastructure for supplying the vehicles, as illustrated by the various paths shown in Fig. 84. A pipeline system is the most efficient method of transport for most areas provided that market shares are high. A study commissioned by the German Federal Government on where hydrogen in Germany will come from in 2050 ("GermanHy: Woher kommt der Wasserstoff in Deutschland bis 2050") estimated the investment costs for hydrogen production, transport and distribution to be € 125 billion. Of this total, 50 - 80 % will be required for production. This is based on a market share of 70 % and an annual hydrogen requirement of 5 million tonnes.

A research project currently under way at IEK-3 is examining the details of the design, dimensioning and implementation of a pipeline system for Germany, testing its technical feasibility, and looking at component- and material-related issues. This technical review will provide the basis for determining the energy efficiency and costs associated with such a system. A network tool was developed as part of this work. It connects all districts, accounting for any source scenario (location and capacity), and can be adapted to various existing networks. The total length of such a transmission network is estimated to be about 12,000 km. Additional distribution networks connecting all major gas stations are also required. They are also quantified.

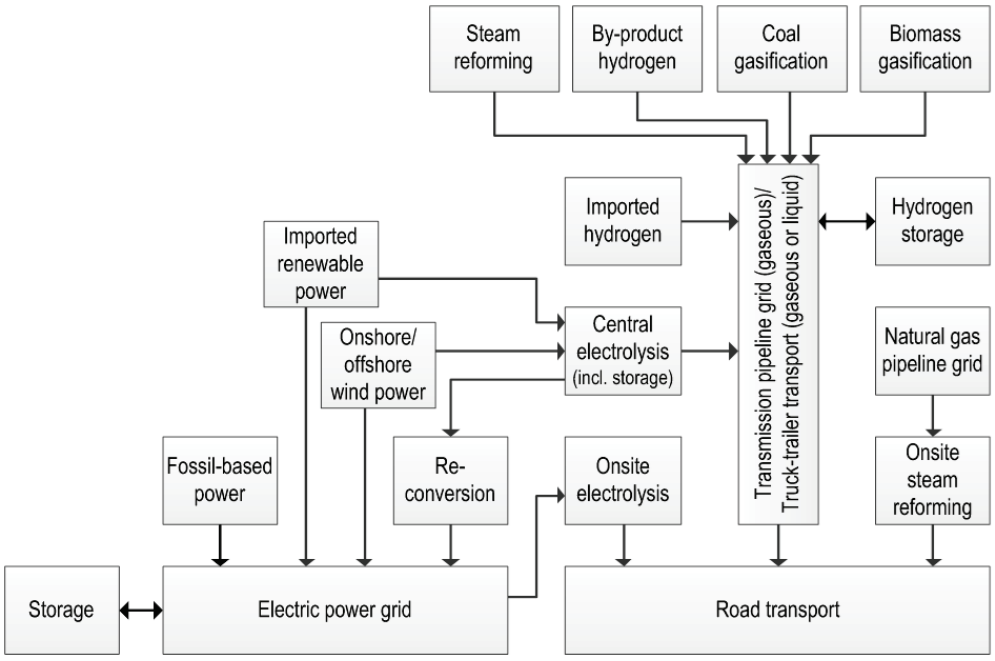

Fig. 84: Simplified structure of a hydrogen infrastructure system

3.5.2.3 Post-combustion capture with membranes

Post-combustion processes are situated downstream of conventional flue gas purification (DeNOx, dedusting, desulfurization). At this stage, the flue gas has approximately atmospheric pressure, a temperature of 50 - 70 °C and a CO_2 level of 13 - 15 mol-%. The low partial pressure (~140 mbar) is challenging for separation using membranes. As sufficient driving forces must be created for post-combustion, the option of low permeate pressures appears most appropriate. However, this places specific demands on the permeate compressors.

Permeate vacuum [mbar]	**CO_2 separation degree [%]**	**CO_2/N_2 selectivity**	**CO_2 purity [mol%]**	**Δη [%-points]**
30	50	200	**95**	-3.4
100	50	3750	**95**	-2.8
100	70	no solution	**95**	-
	90	no solution	**95**	-

Tab. 7: Separation efficiency of a single-stage membrane (HZG: CO_2 permeance = 3 Nm^3/m^2 h bar)

The MEM-BRAIN project aims to achieve a CO_2 separation efficiency of 90 % and a CO_2 purity of 95 mol-% for all concepts. Tab. 7 shows the simulation results for a single-stage membrane where the feed gas comprises 14 mol-% CO_2 and 86 mol-% N_2. Despite a very low permeate pressure, even a low separation efficiency of only 50 % requires a CO_2/N_2 selectivity of 200, which has yet to be achieved. For a technically feasible permeate pressure of 100 mbar and the same low CO_2 separation efficiency, the membrane must achieve a selectivity of 3750, which is unachievable by today's standards. The state-of-the-art polymer membrane POLYACTIVE developed by the Helmholtz-Zentrum Geesthacht (HZG) has a CO_2/N_2 selectivity of only 50. It is therefore essential that multistage membrane concepts be developed.

Ten different multistage concepts were analyzed. It was shown that compressing the exhaust gas (feed gas in the first stage) to achieve an increased driving force for subsequent retentate relaxation cannot be justified in terms of energy. An example of an efficient cascade with recycling of the retentate from the second stage in the flue gas before the first stage is shown in Fig. 85. As the permeate from the first stage already contains a high CO_2 concentration, the energy required to compress it before the second stage is justifiable because the increased driving force allows major savings in membrane area. Fig. 86 shows a key characteristic of the system: for a CO_2 separation efficiency of 90 %, the cascade is unfavorable in terms of energy and effort (Δη= -11.4 percentage points, membrane area 13.2 m^2/kW). Reducing the separation target would therefore lead to considerable improvements. The membrane cascade will be tested further with respect to retrofitting existing power plants.

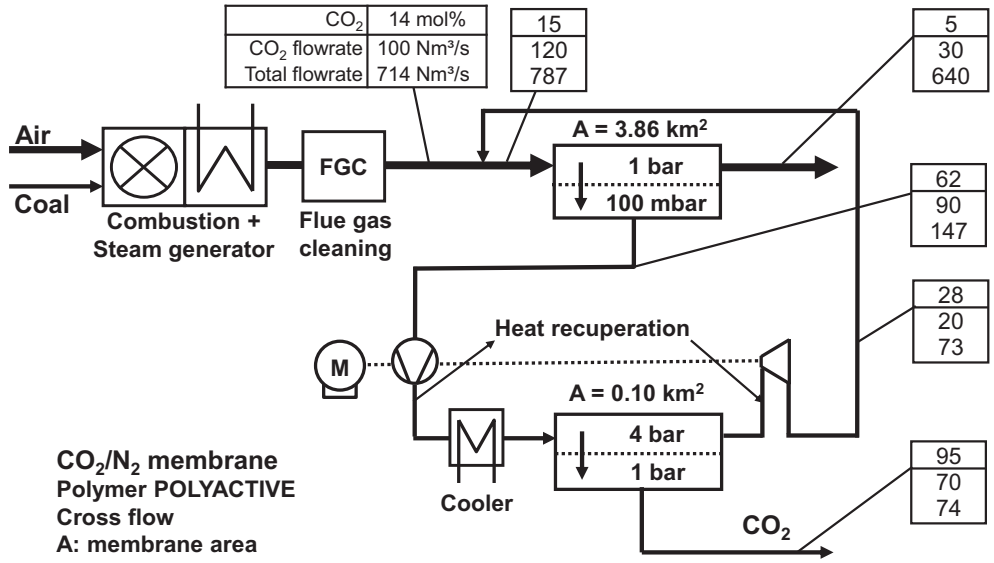

Fig. 85: **Membrane cascade system (values for CO_2 separation efficiency of 70 %, compression in four stages with intermediate and post-cooling to 50 °C, Q_{ab}= 53 MW_{th} [vacuum pump 34, compressor 19], of which 6.5 MW_{th} was recovered in a two-stage expansion. Isentropic efficiency 85 %. No further pressure losses considered.)**

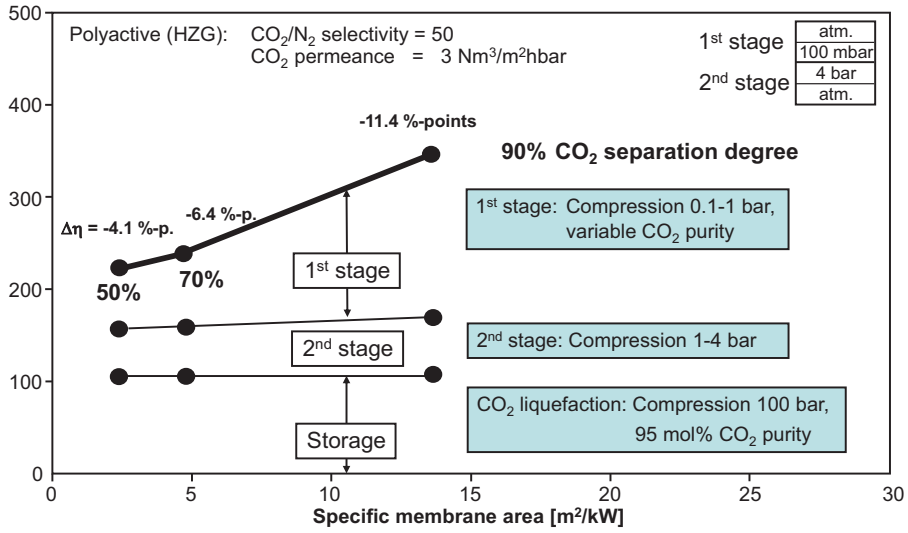

Fig. 86: **Energy profile of the membrane cascade**

3.5.2.4 Precombustion capture with membranes

Combined gas and steam processes with integrated coal gasification (integrated gasification combined cycle, IGCC) offer an alternative way of using solid fuels compared to conventional steam power plants. Due to the higher temperature of the heat input in the primary working medium – over 1,200 °C compared to 600 °C – they facilitate higher power plant efficiencies (see Carnot process). However, this increase is reduced by the energy required for vaporization.

In terms of CO_2 separation, IGCC makes it possible to separate the CO_2 before actual combustion. The synthesis gas, created during vaporization at elevated temperatures (T > 1,200 °C) and pressures (p = 30–40 bar), comprises mainly hydrogen (~33 vol.%) and carbon monoxide (~60 vol.%), which is extremely advantageous for separation with respect to technology and energy. However, steam must be added to the carbon monoxide to convert it into carbon dioxide and hydrogen (water-gas shift reaction) before the carbon dioxide can be separated. As this is an equilibrium reaction, a large excess of steam is required (H_2O/CO ~ 2–2.5) for a high CO conversion (> 98 %). The CO_2 is subsequently absorbed, e.g. by means of physical scrubbing, and after desorption, it is compressed at 1-2 bar for storage. The hydrogen is combusted and relaxed in a gas turbine with a high excess of air. The residual heat contained in the off-gas is transferred to a steam cycle in a waste heat boiler.

The associated efficiency losses compared to IGCC with no CO_2 separation (~11 percentage points [14]) are mainly due to the steam required for the shift reaction (~5.5 percentage points), the pump output and solvent preparation for the physical scrubbing (1.5 percentage points), and CO_2 compression to 120 bar (~2.5 percentage points).

An alternative to CO_2 separation by means of physical scrubbing is the use of hydrogen-selective membranes. In this process, the CO_2 remains in the retentate at high pressure, which considerably reduces the energy required to compress it to the storage pressure. However, energy is needed to compress the separated hydrogen before it can be fed into the gas turbine combustion chamber. In order to better exploit the potential of the membrane, the IGSWEEP-JÜL concept was developed. It recycles a proportion of the flue gas and uses it as a sweep gas for the permeate side of the membrane (see IEF-3 Report 2009, pp. 179f). The large amount of sweep gas causes a high partial pressure difference across the entire membrane area, which in turn allows an even higher H_2 separation efficiency to be achieved even for a limited membrane area. As the total pressure on the permeate side is equal to the process pressure level, recompression is not necessary prior to entering the gas turbine combustion chamber. The effort required for CO_2 compression remains unaffected, i.e. low.

Current conceptual studies concentrate on combining the shift reactor and the hydrogen membrane to form the water-gas shift membrane reactor (WGS-MR), as shown in Fig. 87. This concept has the advantage that hydrogen is continuously extracted from the synthesis gas parallel to the shift reaction. This causes the equilibrium of the shift reaction to continuously alter, thereby allowing new hydrogen to subsequently react. Theoretically, for an infinitely long, perfectly selective membrane and for a H_2O/CO ratio of 1, a CO utilization of 100 % could be possible. In practice, the H_2O/CO ratio is not reduced below 1.3 in order to

---

[14] Prins M., Van der Ploeg, R., Van der Berg, R., Patil, C., Van Dorst, E., Geuzebroek, F., Paul, D.: Technology advances in IGCC with CCS. Presented at CCT2009, Dresden, Germany, May 18-21, 2009

avoid soot formation, but this ratio still corresponds to an enormous reduction in the steam required.

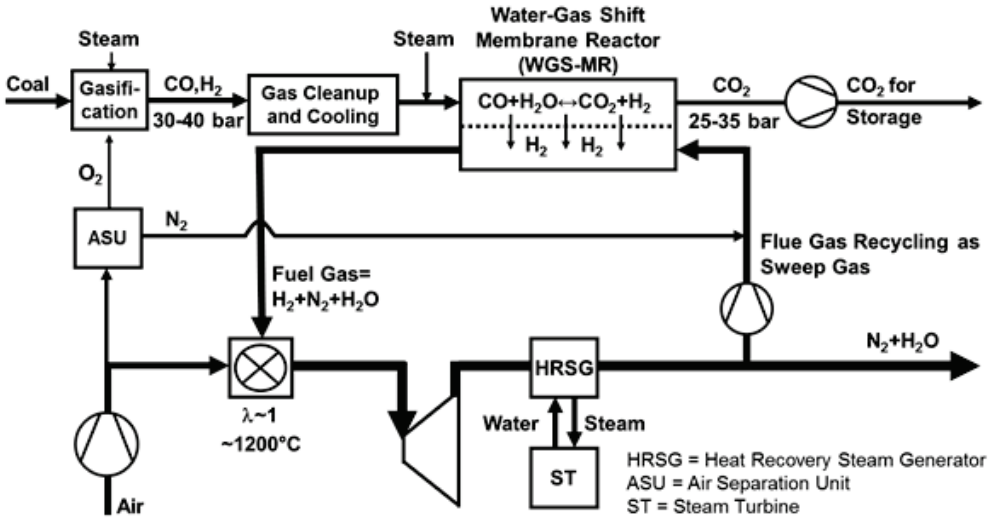

Fig. 87: IGCC with CO_2 separation with flue gas recirculation as sweep gas for WGS-MR

3.5.2.5 Oxyfuel process with membranes

The basic concept of an oxyfuel process is the removal of atmospheric nitrogen from the combustion air with the aim of obtaining a flue gas that after the usual purification steps and condensation of the steam comprises mainly (ideally solely) CO_2. In order to limit the combustion temperature, some of the cooled flue gas is recycled. Due to the necessary excess oxidant, air leaks and coal impurities, the purified flue gas that was largely dehumidified at ambient pressure contains up to 90 vol.% CO_2. The advantage of the oxyfuel process is that it can potentially separate 100 % of the CO_2.

Providing oxygen of normal purity (99.5 vol.%) by means of cryogenic separation has a specific energy requirement of around 0.33 kWh_{el}/kg_{O2} today (Vattenfall “Schwarze Pumpe” pilot plant). For the usual 15 % excess oxidant, this is equal to an expenditure of 0.28 kWh_{el}/kg_{CO2} and an efficiency loss of 9.8 percentage points compared to the NRW reference power plant. The subsequent compression of the CO_2 to 100 bar and its cryogenic purification leads to further efficiency losses of at least 4 percentage points according to Linde [15]. For energetically optimized cryogenic air separation, the corresponding efficiency

[15] Ritter, R.; Kutzschbach, A.; Stoffregen, T.: Energetische Bewertung einer CO_2-Kompressions- und Reinigungsanlage für den Oxyfuel-Prozess am Beispiel einer Demonstrationsanlage. In: Beckmann, M; Hurtado, A. (eds.): Kraftwerkstechnik. Sichere und nachhaltige Energieversorgung. Vol. 1. TK-Verlag Karl Thome-Kozmiensky, 2009. ISBN 978-3-935317-42-9

loss sinks to approx. 6 percentage points. At the same time, the purity of the oxygen decreases to 95 vol.% [16], which leads to increased effort for CO_2 purification.

Alternatively, pure oxygen can be provided, for example, with perovskite membranes. These membranes belong to the group of “dense” ceramic membranes (ion-conducting) and facilitate the selective permeation of oxygen in the temperature range of 700 °C to 1,000 °C. Compared to the energetically optimized cryogenic process, the flue gas is not contaminated with nitrogen or argon. The properties of the presently known membrane-based oxyfuel coal power plant concepts are summarized in Tab. 8 Thermodynamic simulations at IEK-3 concentrate on the concepts with no sweep gas, as the membranes currently available are not suitable for the use of flue gas as sweep gas.

Operating parameters	Membrane side	OXYCOAL-AC	OXY-CLEAN	**OXY-VAC-JÜL**
Provision of driving force	Feed	Compressor & turbine	Compressor & turbine	------
	Permeate	Sweep gas	- / Vacuum suction	Vacuum suction
Total pressure	Feed	10–20 bar	10–20 bar	1 bar
	Permeate	1 bar	1 bar / < 1 bar	< 0.2 bar
Gas composition and contamination	Feed	Air	Air	Air
	Permeate	Flue gas + O_2	O_2	O_2
Flue gas cycle (temperature)		Hot	Cold	Cold
Flue gas cycle (amount)		Large	Small	Small

Tab. 8: Systematization of membrane-based oxyfuel concepts

The process analyses of the OXY-CLEAN and OXY-VAC-JÜL concepts revealed maximum net efficiencies of the power plants for oxygen separation efficiencies of 0.5 - 0.7 (see Fig. 88). Furthermore, the use of the waste heat of the exhaust air is limited in the OXY-CLEAN process. For low oxygen separation efficiencies, losses caused by waste heat of the rising exhaust air flow prevail, while for high oxygen separation efficiencies, the electrical energy required to provide oxygen prevails. Fig. 88 shows the result of design calculations for which the O_2 partial pressure ratio (retentate/permeate) was kept constant. The oxygen flow is in the order of magnitude of 1 ml/min cm² (measured oxygen permeation through a membrane with a thickness of 0.5 mm, OXYMEM project).

The energy expenditure for oxygen separation at a separation efficiency of 0.6 was 0.1 kWh_{el}/kg_{O2} for OXY-CLEAN and 0.13 kWh_{el}/kg_{O2} for OXY-VAC-JÜL. It is significantly lower than the effort required for cryogenic oxygen provision.

[16] Burchhardt, U.; Lysk, S.; Kosel, D.; Griebe, S.; Kass, H.; Preusche, R.: Betriebserfahrungen aus dem Testbetrieb der Oxyfuel-Forschungsanlage von Vattenfall. In: Beckmann, M; Hurtado, A. (eds.): Kraftwerkstechnik. Sichere und nachhaltige Energieversorgung. Vol. 2. TK-Verlag Karl Thome-Kozmiensky, 2010. – ISBN 978-3-935317-57-3

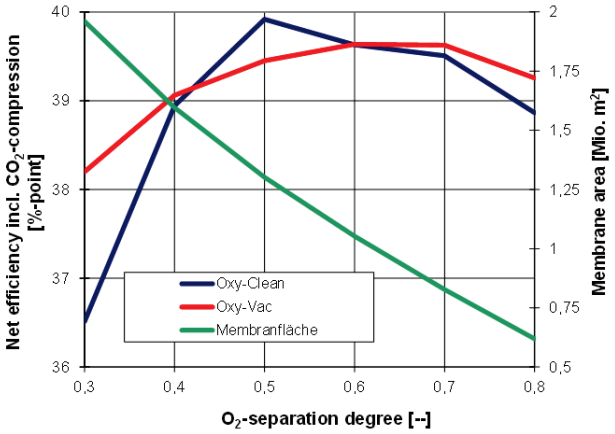

Fig. 88: Net efficiencies and membrane area of the membrane-based oxyfuel concepts

Process integration lowers the efficiency losses (Fig. 89). For economic component design (lower section of the figure), the efficiency loss was around 2.3 percentage points in relation to the NRW reference power plant (no CO_2 compression).

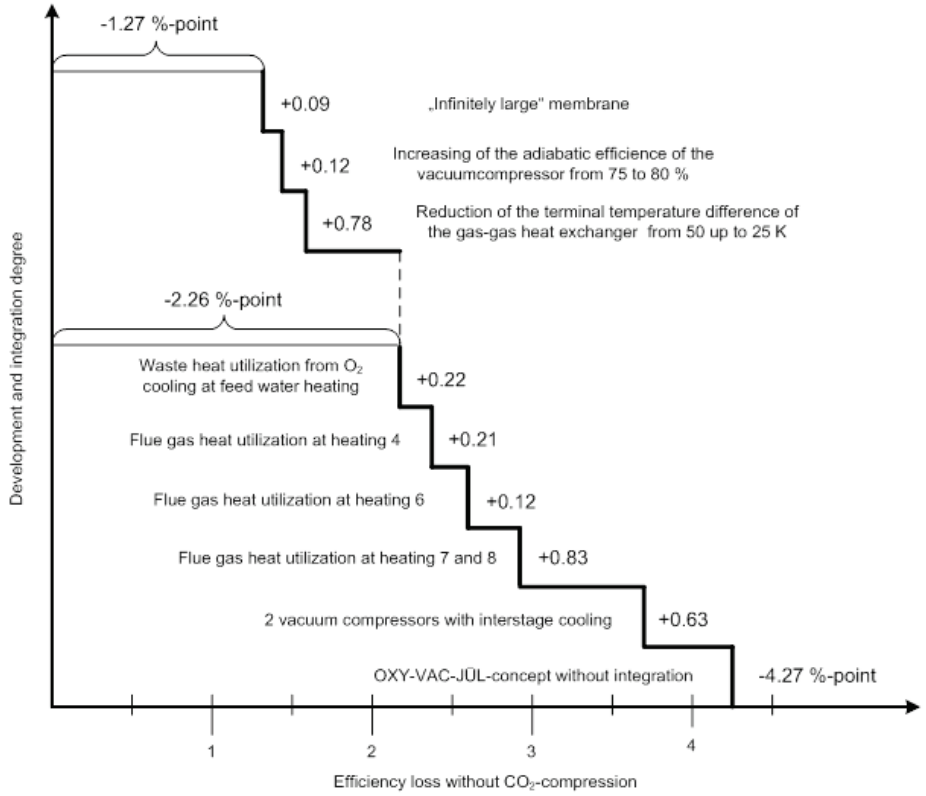

Fig. 89: Reduction in efficiency loss for the OXY-VAC-JÜL concept compared to the NRW reference power plant (oxygen separation efficiency of 0.6; no CO_2 compression)

3.5.2.6 Post-combustion capture with MEA scrubbing

In terms of electricity generation, the downstream separation of CO_2 by means of absorption with monoethanolamine (MEA) has numerous advantages:

- extensive experience from other industrial applications
- availability in the medium term on the required scale
- utilization of the proven technology of a steam power plant
- option of retrofitting existing power plants

Analyzing this benchmark process is necessary in order to compare it to the concepts of membrane-based capture processes.

The process is based on the reversible alteration of the chemical equilibrium with temperature. CO_2 is adsorbed by the aqueous MEA solution at a low temperature in the adsorber (40 - 60 °C) [17] and it is released at a higher temperature in the desorber (100 - 120 °C) [18] and captured separately. The proportion of water that evaporates during this process is subsequently condensed and recycled. The CO_2 loading difference in the MEA solution describes the available cyclic operational capacity (Fig. 90).

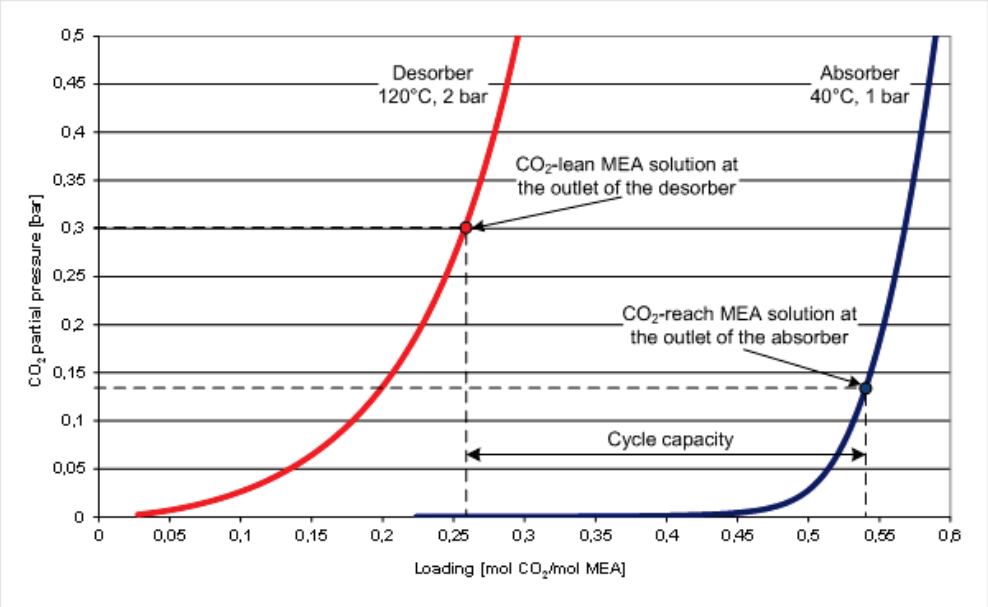

Fig. 90: Equilibrium isotherms and process conditions during MEA scrubbing (30 % MEA solution, simulation in Aspen Plus®, modified electrolyte NRTL model, column algorithm RATEFRAC®)

[17] Whereby 40 °C at the solution outlet can only be achieved using highly complex instruments: for example, by repeatedly intercooling the column trays or by flue gas cooling.

[18] The lower limit is determined by the necessity of adequate stripping and the upper limit by the temperature-dependent degradation of amines.

The heat required to raise the temperature of the MEA solution (if this has not been recuperated) and strip CO_2 is provided by low-pressure steam from the power plant process. This reduces the gross electrical output of the power plant. Other factors affecting the output are the electricity consumed by the CO_2 separator and compressor, additional pressure loss of the flue gas and the increased demand for cooling water. All of these effects together would reduce the net efficiency of the NRW reference power plant retrofitted with MEA scrubbing by up to 13 percentage points at a CO_2 separation efficiency of 90 %. By adjusting the turbo set, this loss can be reduced by up to 1.5 percentage points.

At IEK-3, thermodynamic simulations are being conducted of the stripping, power plant and CO_2 compression processes using PRO II, Aspen and Ebsilon. Several parameters must be reconciled for this. For example, the energetically optimal operating point of the MEA facility alone (in Fig. 91: blue dotted line, desorber pressure 2 bar, loading 0.25 mol CO_2 / mol MEA) is not the same as that of the stripping facility when operated optimally for the power plant as a whole (green solid line, desorber pressure 1.6 bar, loading 0.28 mol CO_2 / mol MEA). The reason for this is the relationship between the regeneration energy required and the electrical equivalence factor of the steam removed. Left of the minimum of the power plant curve, losses caused by providing stripping steam predominate, whereas on the right, losses causes by the increasing mass flow rate of the solvent being heated prevail.

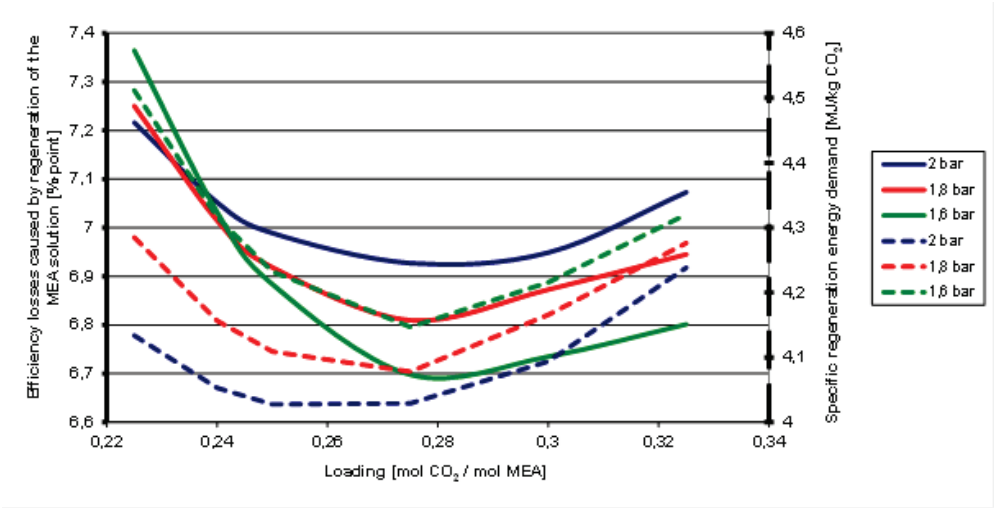

Fig. 91: Specific regeneration energy required and efficiency losses caused by regeneration (reboiler temperature difference: 5 K; pressure loss of the steam removed: 10 % of the saturated steam pressure)

Quantification of the environmental impacts is also part of process analysis. Given current flue gas purification, MEA waste of up to 3 g/kWh$_{el}$ can be expected. According to the current legal situation, this waste would be classed as hazardous or especially hazardous. Improving the desulfurization to 10 ppm would decrease this value to less than 2 g/kWh$_{el}$.

3.5.3 Staff members and fields of activity

Name	Tel. (+49 2461-61-) E-mail address	Field of activity
Dr. Michael Weber	8626 mi.weber@fz-juelich.de	Head of Process and Systems Analysis
Thomas Grube	5398 th.grube@fz-juelich.de	Drive simulation, process and systems analysis
Dennis Krieg	3077 d.krieg@fz-juelich.de	Pipeline infrastructure for hydrogen
Jewgeni Nazarko	3742 j.nazarko@fz-juelich.de	Plant simulation, power plant engineering, amine scrubbing, oxyfuel processes
Dr. Ernst Riensche	6689 e.riensche@fz-juelich.de	Plant simulation, power plant engineering, CO_2 separation
Sebastian Schiebahn	8731 s.schiebahn@fz-juelich.de	Plant simulation, power plant engineering precombustion, membrane processes
Dr. Dr. Li Zhao	4064 l.zhao@fz-juelich.de	Membrane processes, plant simulation, CO_2 storage, post-combustion

3.5.4 Important publications

Important publications

Grube, Th.; Stolten, D.

Bewertung von Fahrzeugkonzepten mit Brennstoffzellen und Batterien *(Evaluation of vehicle concepts based on fuel cells and batteries)*

In proceedings, VDI conference "Innovative Fahrzeugantriebe", Dresden, 10.–11 Nov. 2010

Today, mobility in Germany is almost completely dependent on imported mineral oil and is responsible for a significant proportion of the emission of greenhouse gases and other locally relevant pollutants. Reducing import dependence, decreasing environmental impacts and the issue of global warming in particular demand a strategic reorientation in the transport sector. Modifying the fuel mix for vehicles, incorporating regionally available, renewable, and low-emission primary energies can be realized in the medium to long term. The use of highly efficient fuel cell systems in electric drives combined with the use of hydrogen would then have clear advantages over refined combustion engines. Improved battery technologies and the partially available infrastructure for charging batteries now means that the use of electric vehicles with batteries can significantly reduce the specific energy required and the pollutants emitted by cars.
This paper evaluates the prospects and challenges associated with vehicle concepts based on all-electric operation. The analyses focus on dynamic simulations of cars using different driving profiles and vehicle-specific characteristics. Data on the provision of fuels – including electricity – have been incorporated in order to discuss

the energy requirements and greenhouse gas emissions of the full energy conversion chains of electric vehicles with batteries and fuel cells.

Pastowski, A.; Grube, Th.

Scope and perspectives of industrial hydrogen production and infrastructure for fuel cell vehicles in North Rhine-Westphalia

Energy Policy 38 (2010) 5382–5387

A promising candidate that may follow conventional vehicles with internal combustion engines combines hydrogen from regenerative sources of energy, fuel cells and an electric drive train. For early fleets introduced the refuelling infrastructure needs to be in place at least to the extent of the vehicles operational reach. The question arises which strategies may help to keep initial hydrogen and infrastructure cost low? Industrial production, distribution and use of hydrogen is well-established and the volumes handled are substantial. Even though today's industrial hydrogen is not in tune with the long-term sustainable vision, hydrogen production and infrastructure already in place might serve as a nucleus for putting that vision into practice. This contribution takes stock of industrial production and use of hydrogen in North Rhine-Westphalia based on a recently finalized project. It demonstrates to which extent industrial hydrogen could be used for a growing number of vehicles and at which time additional capacity might need to be installed.

Grube, Th.; Höhlein, B.; Stiller, C.; Weindorf, W.

Systems Analysis and Well-to-Wheel Studies

Erschienen in: Stolten, D. (Ed.): Hydrogen and Fuel Cells - Fundamentals, Technologies and Applications. Chapter 40. 2010. Wiley-VCH Verlag GmbH & Co. KGaA.

Energy systems analyses provide powerful assessment frameworks for research and development projects involving new energy technologies. These analyses rely on the description of state-of-the-art technologies and incorporate scenarios on future developments in the energy sector in order to identify the benefits and weaknesses of the technologies under consideration. This chapter presents selected assessment highlights relating to hydrogen and fuel cell technologies for transportation. With respect to fuel cell system cost, noble metal requirements are of utmost significance. The corresponding balances for fuel cell vehicles will be introduced. Moreover, the relevance of dynamic powertrain simulation for the evaluation of energy process chains in transportation will be discussed. In a further part, the methodology and results of well-to-wheel analyses of energy use and greenhouse gas emissions will be discussed, followed by an assessment of relevant hydrogen-focused well-to-wheel studies of different world regions as well as a comparison and interpretation of key findings.

Stolten, D.; Grube, Th. (eds.)

18th World Hydrogen Energy Conference 2010 – WHEC 2010 Proceedings, Parallel Sessions Book 1 – 6

Schriften des Forschungszentrums Jülich, Energy & Environment Vols. 78-1 tos 78-6, ISBN: 978-3-89336-657-6, Jülich, 2010

Over the past few years, the three major reasons why novel energy technologies will be required in the very next years have become common sense: to mitigate climate change, to secure energy supply, and to foster economic competitiveness. Hydrogen and fuel cells have great potential to meet all three of these societal requirements. Being at the cutting edge of energy R&D, the government of North Rhine-Westphalia

has been supporting hydrogen and fuel cell technologies substantially for many years through the Fuel Cell and Hydrogen Network NRW, by funding research projects, and not the least by hosting the 18th World Hydrogen Energy Conference 2010 in Essen. Although the 18th WHEC was overshadowed by the consequences of the subprime crisis and the subsequent economic downturn, the number of participants was a record high. More than 1,350 eople attended the scientific conference that offered 342 oral presentations in 49 sessions and 183 posters. The technological dimension materialized in an extensive trade fair with 136 exhibitors and a notable share of one third of the presentations being given by industry representatives. Such figures prove that hydrogen and fuel cell technologies are timely and that industry, governments and academia recognize the potential they have of providing viable solutions to the Grand Challenges mentioned above.
In order to ensure that the conference has a long-lasting impact, it was decided to fully document the event in publicly available books. The introductory talks to the sessions are available as full papers in the book entitled Hydrogen and Fuel Cells – Fundamentals, Technology and Applications, edited by D. Stolten and published by Wiley-VCH. These proceedings cover the speeches and technical presentations made on plenary day and the oral presentations and posters in the parallel sessions. They have been published as a set of seven books by the Juelich Research Center.
We gratefully acknowledge the wide-ranging support we had when editing this volume. First of all, we would like to express our gratitude to the authors of the papers in the proceedings who made it possible to promptly publish the talks given in the parallel sessions. Moreover, we are grateful for copy-editing support from the PhD students at the Institute for Fuel Cells in Juelich: Christiane Döll, Ralf Elze, Stefan Hürter, Dennis Krieg, Mirko Kvesić, Fang Liu, Andreas Löhmer, Wiebke Maier, John McIntyre, Florian Scharf, Sebastian Schiebahn, Yong Wang and Christiane Wiethege.

Stolten, D.; Emonts, B. (eds.)

18th World Hydrogen Energy Conference 2010 – WHEC 2010 Proceedings, Speeches and Plenary Talks

Schriften des Forschungszentrums Jülich, Energy & Environment Vol. 78, ISBN: 978-3-89336-658-3, Jülich, 2012

A comprehensive and renowned conference offers the opportunity to extend the scope beyond mere technical issues. It allows for having strategic presentations and discussing aspects of market introduction, industrial and Governmental target setting as well as approaches to and actions for implementation. The 18th World Hydrogen Conference 2010, WHEC2010, succeeded in exploiting this opportunity and satisfied the expectations. Strong political support in Germany and in the State of North Rhine Westphalia in particular made it possible to have high profile decision makers at the conference presenting their strategies first hand.
Hence, a full day was dedicated to plenary speeches and overview talks. The WHEC2010 came handy at a time when fuel cells are developed to suit the requirements for vehicles, except for cost and durability. At a time when the competition with batteries and whether or how a hydrogen infrastructure can be established and afforded were hot topics in the public debate, which needed answers on a well informed basis. Considering fuel cells and hydrogen at a time at one conference and supplementing it with the current knowledge on batteries and hybridization clarity on the future role of these technologies was gained. Very likely fuel cells and batteries will coexist in a future of electrified vehicular transport. Their different technical characteristics will open the doors to different market segments. Implementing hydrogen infrastructure, being a requirement for fuel cells in transport, is considered doable and affordable.
This book presents the speeches and overview papers from the plenary session of the WHEC 2010 on May 17, 2010.
Six further books of this issue contain the papers of the oral and poster presentations, except for the introductory talks of the sessions. The latter are published separately

by Wiley in a book named Hydrogen and Fuel Cells . In total the 18th WHEC is documented on over 3800 pages in a structured way in order to reach the broad spectrum of potential readers.
The editors gratefully acknowledge the strong and sustained support of the State of North Rhine Westphalia and the EnergieAgentur.NRW.

Krieg, D.; Grube, Th.; Stolten, D.

Analysis of the Impact of Hydrogen on Wind Power

In: Stolten, D.; Grube, Th. (Hrsg.), 18th World Hydrogen Energy Conference 2010 – WHEC 2010 Proceedings, Parallel Sessions Book 2, Schriften des Forschungszentrums Jülich, Energy & Environment Vol. 78-2, Jülich, 2010

There are two ways of using electricity generated by wind energy converters. The first is direct sale on the electricity market and the second is indirect use in the form of hydrogen converted by an electrolysis system. This hydrogen may then be used in two ways. On the one hand, it can be stored in order to re-convert it into electricity if needed and, on the other hand, it can be used as fuel in the transportation market. In addition to the well-known influence parameters, e.g. investment cost, maintenance etc.; there are two parameters that have a decisive influence on whether hydrogen should be used and if so, how much should be used. The first factor is the time-variable electricity tariff and the other is the price of hydrogen as fuel. Both aspects depend on the market and the political circumstances, which ultimately influence the market in the form of prohibitions and monetary incentives. This paper will show possible technical progress which might help to make electrolysis more attractive as well as analyzing the parameters affecting the demand side of hydrogen generated by wind power.The goal is to formulate a method which allows us to consider the decisive influence parameters in order to finally conclude the circumstances under which electricity produced by wind power can reasonably be used to generate hydrogen by electrolysis.

Nazarko, J.; Riensche, R.; Blum, L.; Stolten, D.

Optimierung der Oxyfuel-Kraftwerkskonzepte mit der Sauerstoffbereitstellung durch Hochtemperaturmembranen

(Optimization of oxyfuel power plant concepts by providing oxygen via high-temperature membranes)

In: Micheal Beckmann, Antonio Hurtado (eds.): Kraftwerkstechnik. Sichere und nachhaltige Energieversorgung. (Power plant engineering. Safe and sustainable energy supply.) Vol. 2, pp. 147–168. TK Verlag Karl Thome-Kozmiensky, Neuruppin, 2010. – ISBN 978-3935317-57-3

The OXY-CLEAN and OXY-VAC-JÜL concepts have many advantages in terms of the implementation of the membrane-based oxyfuel concept. The use of real heat exchanger temperature differences (50 K) and pressure losses (20 –50 mbar) and real efficiencies of the turbo components (compressor: 80 %, turbine: 85 %, vacuum suction: 75 %) with optimized oxygen separation efficiency can yield net efficiencies of between 39.5 % and 40.0 % depending on the concept, including CO_2 compression. When the results were compared with the corresponding reference processes, a specific energy expenditure of 0.098–0.106 $kWh_{el}/kg\ O_2$ was found for the supply of oxygen. Supplying oxygen for oxyfuel power plant processes using membranes is therefore energetically better than cryogenic oxygen production. Improved components providing the membrane operating temperature and the partial pressure ratio and the optimization of the partial pressure ratio at the membrane further reduced the efficiency loss to 5.27 percentage points including CO_2 compression.

Riensche, E.; Nazarko, J.; Schiebahn, S.; Weber, M.; Zhao, L.; Stolten, D.

Capture Option for Coal Power Plants.

In: Stolten, D.; Scherer, V. (Hrsg.), "Efficient Carbon Capture for Coal Power Plants", ISBN-13: 978-3-527-33002-7 - Wiley-VCH, Weinheim, May 2011

This article provides an overview on the great variety of options for carbon dioxide capture from coal-fired power plants. It focuses on the question of energy efficiency of carbon capture. The capture routes are post-combustion, oxyfuel-combustion and pre-combustion – the latter with selective CO_2 separation and with selective H_2 separation. The basics of gas separation methods like CO_2 absorption with liquids, reaction of O_2 and CO_2 with solids and membrane separation of CO_2, O_2 and H_2 in steam power plants and IGCCs are outlined. Finally, selected capture processes are briefly described and efficiency potentials are discussed.

Blum, L.; Riensche, E.; Nazarko, J.; Menzer, R.; Stolten, D.

Overview on 1st and 2nd generation coal-fired membrane power plants (with and without turbo machinery in the membrane environment).

4th Int. Conf. on Clean Coal Technologies (CCT2009), Dresden, 18-21 May 2009, Proceedings (CD-ROM).

A systematic classification of the capture concepts with conventional separation as well as membrane separation is discussed in a 2-dimensional matrix: The 4 capture principles (post-combustion, oxyfuel, pre-combustion-capture of CO_2 and pre-combustion-capture of H_2), characterized by the 4 separation tasks CO_2/N_2, O_2/N_2, CO_2/H_2 and H_2/CO_2, have to be applied to the 3 different coal power plant (PP) routes: SPP (steam PP), IGCC/standard and IGCC/CO-shift/H_2-turbine.
In case of membrane separation a further dimension of PP concepts is created by the fact, that different measures exist for realization of positive driving forces for permeation. For example the O_2/N_2 separating membranes in oxyfuel SPPs can be operated with feed gas compression, permeate vacuum, application of a sweep gas at the permeate side or combinations of these 3 measures. An overview is given on the actually developed membrane PP concepts (post-combustion and oxyfuel in SPPs, pre-combustion in IGCC). In all cases energy consuming turbo machinery is required for membrane operation or for CO_2 or H_2 recompression in case of pre-combustion (1st generation of membrane coal PPs). Calculated efficiency losses are not significantly below 10%-points.
An outlook is given to a new IGCC concept, where a suitable sweep gas (N_2 with low O_2 content) of sufficient high flow rate is produced (related to the permeated H_2). Now the swept H_2/CO_2 membrane operates without turbo machinery (2nd generation of membrane coal PPs). Lower efficiency losses (between 5 and 10%-points) seem to be possible now.

Schiebahn, S.; Zhao, L.; Grünewald, M

Pre-Combustion Carbon Capture with Physical Absorption

In: Stolten, D.; Scherer, V. (Hrsg.), "Efficient Carbon Capture for Coal Power Plants", ISBN-13: 978-3-527-33002-7 - Wiley-VCH, Weinheim, May 2011

Pre-combustion capture with physical absorption in integrated gasification combined cycles (IGCC) offers a feasible opportunity for separating carbon dioxide with a relatively low efficiency penalty. This article provides an introduction to the IGCC process and the integration of physical scrubbing to separate CO_2. General considerations for process and material selection for physical absorption are explained. Commercially available physical and mixed chemical/physical solvents are described and characterised with respect to the relevant application. Additionally,

current research activities regarding ionic liquids as alternative physical solvents are presented.

Zhao, L.; Blum, L.

Gas Separation Membranes Used in Post-combustion Capture

In "Recent Developments in Capture and Sequestration of CO_2", Editor: R. Hilda Chavez, to be published by Bentham Science Publishers.

Using CO_2/N_2 gas separation membranes for post-combustion capture, the most important problem is how to create the driving force efficiently because the feed flue gas has only ambient pressure and a relatively low CO_2 content. Multi-stage systems are necessary using feasible membranes in order to fulfill the separation target, required by the following pipeline transport, and limited by the storage capacity. The whole work was divided into two steps: a.) energy consumption analysis and b.) capture cost analysis.
This book chapter describes mass and energy balances for single-stage and multi-stage membrane systems used in coal-fired power plant. Using recirculation of flue gas and variation of the feed gas compressor and vacuum pump on the permeate side, two concepts were developed and optimized to achieve minimum energy consumption. In order to evaluate different membrane capture concepts, a comparison with chemical absorption process was carried out, considering different degrees of CO_2 separation. Furthermore, a cost model was developed to make a further analysis of the optimized concept in view of the tradeoff balance between material and energy consumption. The correlation between the membrane parameters (selectivity, permeability) and capture cost was investigated.

Zhao, L.; Riensche, E.; Blum, L.; Stolten D.

How Gas Separation Membrane Competes with Chemical Absorption in Post-combustion Capture

Energy Procedia, 4 (2011), 629-636

This paper describes an investigation for multi-stage systems used in coal-fired power plant. The whole work was divided into two steps: energetic and economic analyses. In the first step: on the basis of a serial concept, through varying the position of compressors and vacuum pumps, recycling the retentate of the 2nd membrane to the feed side of the 1st membrane, a cascade variant was developed and analysed. In the second step: an economic model was developed to calculate the capture cost of the cascade system. The total cost is composed of investment cost, operation and maintenance (O&M) cost and electricity cost. A correlation between the membrane parameters: selectivity & permeability and capture performance: energy consumption & capture cost was built up. Using Polyactive® membrane developed by GKSS with CO_2 permeance of 3 Nm^3/m^2hbar and CO_2/N_2 selectivity of 50, under the separation target of 70% degree of CO_2 separation and 95 mol-% CO_2 purity, adopting the cascade membrane system in the 600 MW NRW-reference power plant, the specific energy consumption including CO_2 compression (110 bar, 30°C) is 256 kWh/tseparated CO_2 with 6.4%-pts efficiency loss. The capture cost is 31 euro/tseparated CO_2, which could be a promising solution as a retrofit for the existing power plants.

Goos, E.; Riedel, U.; Zhao, L.; Blum, L.

Phase Diagrams of CO_2 Gas Mixtures and Their Application in Compression Processes

Energy Procedia, 4 (2011) 3778-3785

Phase diagrams of carbon dioxide, nitrogen and their mixtures with different amounts of nitrogen (e.g. 5 mol-%, 10 mol-% N_2) were calculated with high accuracy with the NIST Reference Fluid Thermodynamic and Transport Properties database program REFPROP® for up to 200 bar, as well as density-pressure diagrams.
Beside the use of carbon dioxide as a solvent for supercritical fluid extraction, increasing interest in physical chemical properties of CO_2 exists as Carbon dioxide Capture and Storage (CCS) starts to play an important role to limit anthropogenic emissions of CO_2 into the atmosphere. Therefore CO_2 processing and pipeline technologies became of considerable commercial importance, especially in the context of future underground storage of CO_2.
As example the CO_2 compression process with gas separation membrane in post-combustion capture was simulated with PRO/II® software. Through adopting several different equations of states, phase diagrams of different CO_2 - N_2 gas mixtures were calculated and compared with the aforementioned accurate thermodynamic and transport properties calculation results. This type of validation is very useful for process engineering analysis.
Further investigations related to the compression process were carried out for the different CO_2 gas mixtures, which are generated from the gas separation membrane capture process. Specific energy of the compression process was analysed for each gas mixture. The energy consumption and the state of the compressed compounds are strongly influenced by the N_2 composition in the mixture.
The impurities in multi-component CO_2 mixtures vary strongly depending on the different capture technologies. The calculation of reliable phase diagrams of CO_2 mixtures provides guidelines for optimization of compression, pipeline transport, and storage processes.

Zhao, L.; Riensche, E.; Blum, L.; Stolten D.

Multi-stage Gas Separation Membrane Processes Used in Post-combustion Capture: Energetic and Economic analyses"

Journal of Membrane Science 359 (2010) 160-172.

Using CO_2/N_2 gas separation membranes for post-combustion capture, the most important problem is how to create the driving force efficiently because the feed flue gas has only ambient pressure and a relatively low CO_2 content. In order to fulfill the separation target – 95 mol-% CO_2 purity and appropriate degree of CO_2 separation – multi-stage systems are necessary using feasible membranes. This paper describes a detailed parametric study for multi-stage membrane systems used in a coal-fired power plant.
According to the above-mentioned boundary conditions, the investigation process was divided into two steps: a) energy consumption and b) capture cost analyses. In the first step, by varying the position of the compressors and vacuum pumps and recycling the flue gas to the feed side, cascade variants were developed and analyzed in detail. The cascade system was integrated in the 600 MW North Rhine-Westphalia reference power plant and compared with the chemical absorption process. In the second step, an economic model was developed to make a further analysis of the cascade system. A correlation was established between the membrane parameters (selectivity, permeability) and system performance (energy consumption, capture cost).

Important patents

Patents applications:

Principal inventor	PT	Description
Dr. E. Riensche	1.2381	IGCC power plant having flue gas recirculation and flushing gas
Dr. E. Riensche	1.2382	Combustion plant and process for its operation
Dr. E. Riensche	1.2405	IGCC power plant with flue gas recycling and sweep gas
J. Nazarko	1.2431	Device and process for removing carbon dioxide (CO_2) from flue gas in a combustion plant after energy conversion
Dr. E. Riensche	1.2437	Power plant and process for operating the same
Dr. E. Riensche	1.2463	CO_2 separation in flue gases using chemical scrubbing and the device for implementing the process
Dr. E. Riensche	1.2501	IGCC power plant having a water gas shift membrane reactor and process for operation of such a power plant using flushing gas

Patents granted

Principal inventor	PT	Description
Dr. E. Riensche	1.2405	IGCC power plant with flue gas recycling and sweep gas

3.6 Analysis

3.6.1 Objectives and fields of activity

The Physicochemical Fuel Cell Laboratory develops and applies analytical methods for the in situ and/or spatially resolved analysis of structures and effects. The fundamental structure-activity relationships of complex processes are determined in fuel cells and reactors and used to improve both. Furthermore, the physical properties of cell components are determined to verify and establish the mechanical and thermodynamic requirements for use in fuel cells. The methods used in the fuel cell laboratory focus on the following areas:

- imaging analysis techniques
- spatially resolved analysis techniques
- physical and electrochemical analysis techniques

3.6.2 Important results

3.6.2.1 Imaging analysis techniques

During the period under review, the microstructures and nanostructures of fuel cell components were investigated in close cooperation with the departments concerned with developing the direct methanol fuel cell (DMFC) and the high-temperature polymer-electrolyte fuel cell (HT-PEFC). The objective was to visualize and document the microstructures according to the various consecutive steps of fabrication, beginning with the starting materials and ending with the complete membrane electrode assembly (MEA).

After electrochemical tests, the next step involved testing the components with different loading profiles or periods of operation. The results were then compared, where possible, with the corresponding starting components in terms of possible changes in the micro- or nanostructure as well as in the material composition. The instruments used were a light microscope (LiMi), a field-emission scanning electron microscope (SEM) with integrated energy-dispersive X-ray spectroscopy (EDX) and a confocal laser scanning microscope (CLSM). The samples, particularly the cross sections of complete MEAs, were prepared using the following methods:

- conventional grinding and polishing process of samples in cold embedding synthetic resin
- ion beam etching
- scalpel cutting

Selected results from these structural studies are discussed in the following as examples.

Fig. 92 shows mechanically manufactured gas diffusion electrodes in their initial state for use in DMFCs. The images were produced using high-resolution SEM focused on the surfaces. The left image shows a cathode and the right image an anode. The noble metal contained in the starting catalyst powder amounted to approx. 70 wt.% Pt for the cathode and approx. 75 wt.% Pt + Ru for the anode.

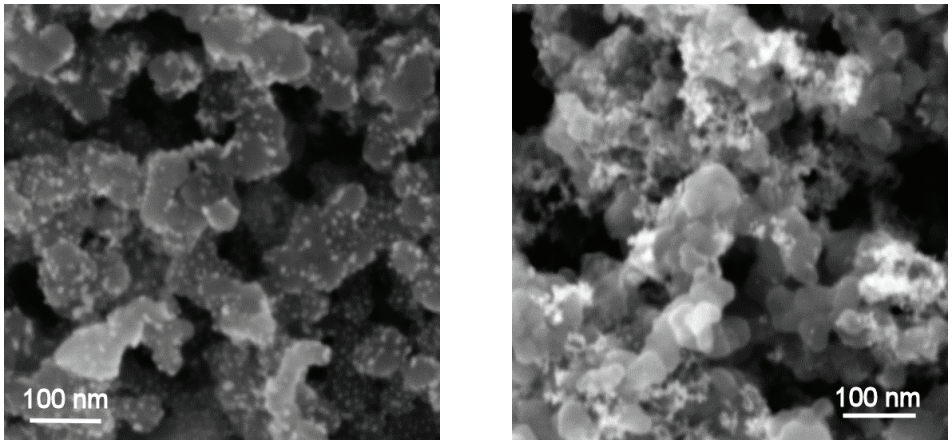

Fig. 92: SEM images of the surfaces of two catalyst layers in their initial state for use in DMFCs in secondary electron mode. Left: cathode; right: anode

The platinum particles in the cathode are ideally finely dispersed on the substrate material, whereas some very large agglomerations of the noble metal particles are found on the anode. These agglomerations can be clearly visualized using the backscattered electron mode (Fig. 93). Such agglomerations reduce the freely accessible surface of the noble metal catalyst, which gives rise to a deterioration in the electrochemical performance of the components.

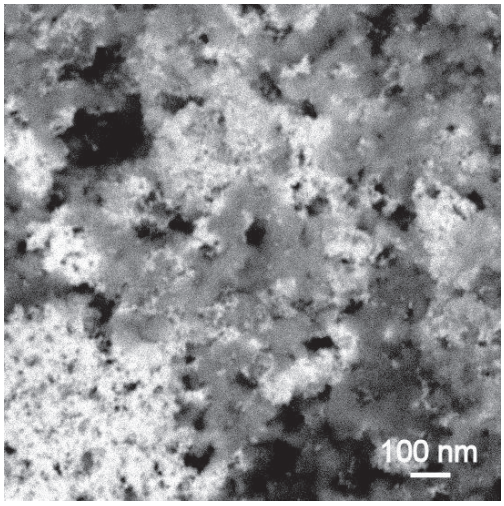

Fig. 93: SEM image of the surface of an anodic catalyst layer on its initial state for use in DMFCs in the backscattered electron mode

Before the mechanically fabricated gas diffusion electrodes are pressed together with the Nafion membrane to form an MEA for use in DMFCs, the GDEs are sprayed with a Nafion suspension in an extra fabrication step in order to improve the connection. This Nafion

spraying step was shown to be advantageous in electrochemical performance tests. After drying, the topography of the GDE often changes. Fig. 94 shows the topography of a GDE taken using a confocal laser scanning microscope before spraying (image from a three-dimensional intensity-weighted series of images) as well as the roughness profile along a line.

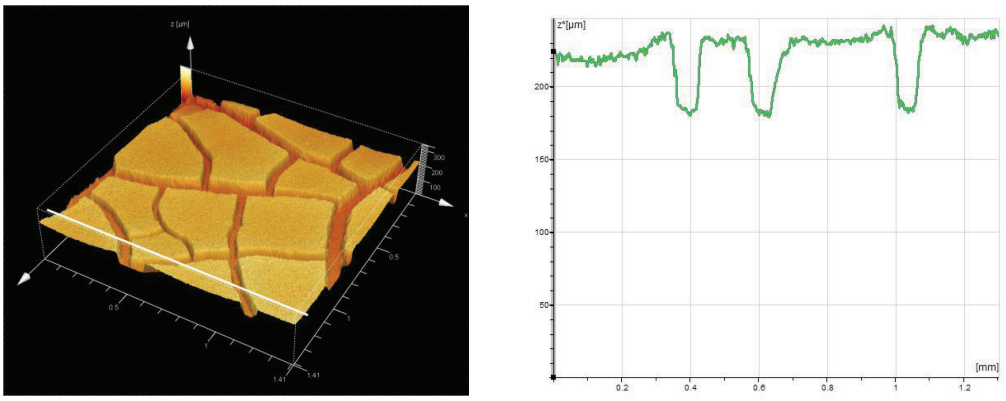

Fig. 94: **Topography of a gas diffusion electrode before spraying with Nafion for use in DMFCs. Left: 3D intensity-weighted series of images; right: roughness profile**

The figure shows a mainly flat topography along the floes, which is only interrupted by the fabrication-induced cracks. In contrast, after spraying with Nafion, the floes are slightly elevated near the edges, as can be seen in Fig. 95. In this case, the height difference near the edges is approx. 60 µm. This can cause discontinuities at the membrane-GDE interface after pressing, which partially counteracts the enhanced performance brought about by spraying.

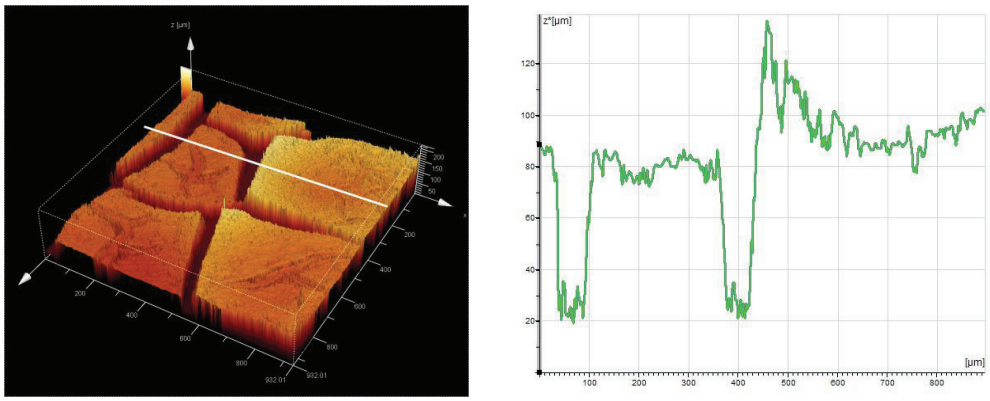

Fig. 95: **Topography of a gas diffusion electrode after spraying with Nafion for use in DMFCs. Left: 3D intensity-weighted series of images; right: roughness profile**

Fig. 96 compares SEM images taken in secondary electron mode of the morphology of the cathodic catalyst layer for use in DMFCs before and after an electrochemical endurance test. The image on the left shows the GDE catalyst layer in its initial state. The image on the right shows a cross-sectional view of the catalyst layer of a whole MEA in the V 3.3 stack after 3,000 h of operation in a DMFC system. The loading profile during the system test was characterized by a large number of start-up and shut-down processes. During operation, a continuous drop in stack performance was measured.

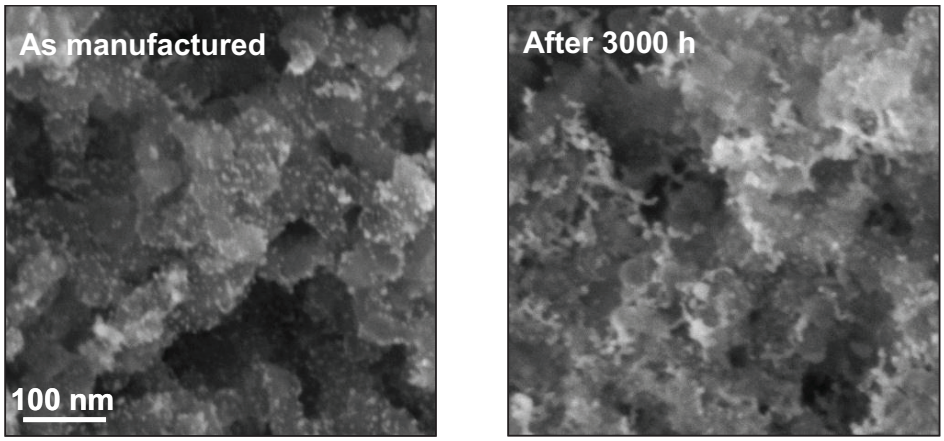

Fig. 96: **SEM images of anodic catalyst layers for use in DMFCs in secondary electron mode. Left: initial state; right: view of the GDE after 3000 h of dynamic operation in a system (MEA cross section)**

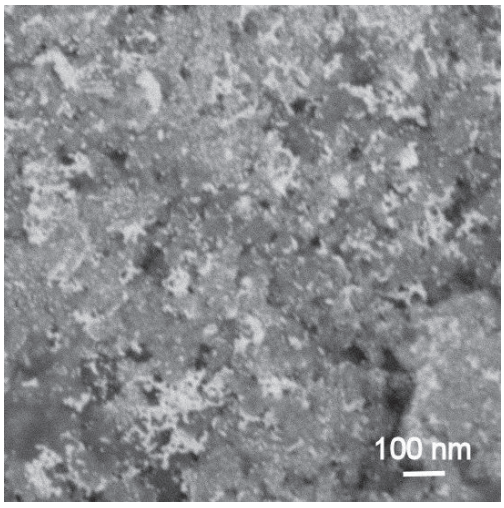

Fig. 97: **SEM image of the cathodic catalyst layer for use in DMFCs in backscattered electron mode after 3000 h of dynamic operation in a system (MEA cross section)**

Here too, the desired fine dispersion of the noble metal particles can be observed in the initial state (see also Fig. 92, left). After dynamic loading, a significant agglomeration of catalyst particles can also be seen on the cathode. This becomes even clearer in Fig. 97 in SEM images of the cathode taken in material contrast. It can be assumed that the drop in performance is partially caused by the decrease in the accessible noble metal surface as a result of agglomeration on the cathode side of the MEA.

On the anode side of MEAs from the V 3.3 stack, after 3,000 h of the operating test, no significant changes were observed in the morphology or the dispersion of the noble metal particles. A strong agglomeration of catalyst particles already present in the initial state remains intact during the loading test. It does not appear to get any worse.

Furthermore, using EDX, a transfer of Ru from the anode to the cathode of the MEAs in the cells of the V 3.3 stack was observed after a test involving 3,000 h of operation. The amount of Ru on the cathode side was approx. 1 - 2 wt.%. From previous investigations, it is known that such Ru transfer has a negative effect on the performance of the MEAs. Whether the transfer of Ru promotes the agglomeration of the platinum particles cannot be conclusively verified at the present time. The strong agglomeration of the catalyst particles containing large quantities of Ru on the anodes in both the initial state and after electrochemical loading does not appear to exclude this.

3.6.2.2 Spatially resolved analysis techniques

Work within the RuN-PEM project

The RuN-PEM project (X-ray and neutron-based test methods for PEM fuel cells) was funded from 2007 to 2010 as a network by BMBF (funding number: 03SF0324D). IEK-3 was responsible for investigating the media and current distribution across the active area of a direct methanol fuel cell using current distribution measurements, neutron radiography and synchrotron radiography. As part of these activities, Mr. A. Schröder completed a PhD thesis in close cooperation with the Institute for Power Electronics and Electrical Drives (ISEA, RWTH Aachen University), the Helmholtz-Zentrum Berlin (HZB) and other project partners. The main objective of this thesis was to identify favorable performance characteristics, material parameters and cell designs for a homogeneous distribution of media in DMFCs. Further details on the motivation, project partners and the research topics can be found in the IEK-3 report from 2009. In the following, the most important research findings from the RuN-PEM project will be presented for 2009 and 2010.

At the CONRAD test facility operated by project partner HZB, neutron radiographic measurements were made with vertically split diffusion layers in order to investigate the influence of the hydrophobization of carbon tissue. No influence was demonstrated for anode hydrophobization. However, for a split cathode diffusion layer, a clear correlation was found between hydrophobization, on the one hand, and the distribution of water and current, on the other. As shown in Fig. 98, the untreated side exhibited a considerable increase in water content and decreased segment currents. On the hydrophobized side, in contrast, almost no water was found in the cathode channels and the local current densities were much higher.

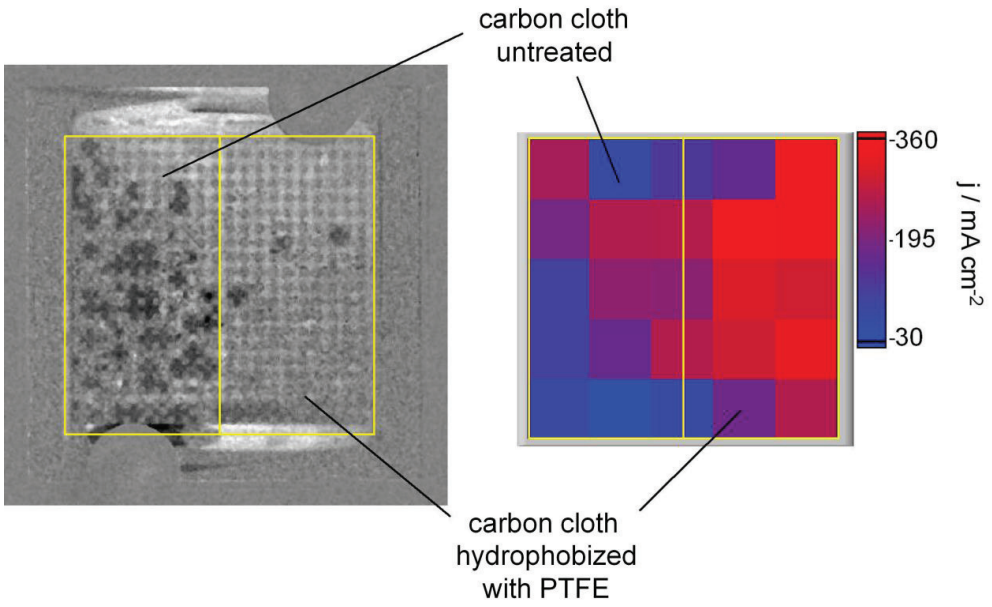

Fig. 98: **Water and current distribution at 300 mA/cm^2, 70 °C, $\lambda_{air} = \lambda_{MeOH} = 4$; splitting of the cathode diffusion layer; left: normalized neutron radiogram (water appears dark, CO_2 bright); right: associated current distribution**

Following this, studies were conducted on how the surface properties of the cathode channels in the flow distributors impact on the water discharge and the cell performance. The flow distributor materials graphite and Sigraflex (expanded graphite) were hydrophilized or hydrophobized by means of a spraying process and characterized at HZB (Dr. G. Zehl) by means of drop contour analysis. Coating with Klingerflon created the smallest contact angle and most hydrophilized surfaces (0 - 30°). The contact angles of the untreated surfaces (90 – 120°) are closer to the values of the hydrophobized materials (110-130°).

Galvanostatic measurements taken for comparison on untreated, hydrophilized and hydrophobized cathode flow distributors made of graphite at various current densities and air stoichiometries revealed that hydrophilic cathode flow distributor plates have several advantages: (i) the water discharge is more uniform, (ii) the pressure difference between cathode inlet and outlet is smaller, (iii) the fluctuations in power output are smaller by one order of magnitude both integrally and locally, which could be favorable in terms of reducing the aging rate, (iv) the mean power is higher for almost all operating conditions. The above-mentioned advantages are particularly pronounced for small air stoichiometries. It is therefore possible in system operation to further increase the power output using appropriately hydrophilized cathode flow distributors, particularly for small air stoichiometries. The advantages of hydrophilized cathode flow distributors become clear when current distribution measurements are compared for untreated and hydrophilized cathode flow distributors. Fig. 99 shows the current densities of two segments from the top and bottom area of the cell as well as the integral power densities for a current density of 150°mA/cm^2.

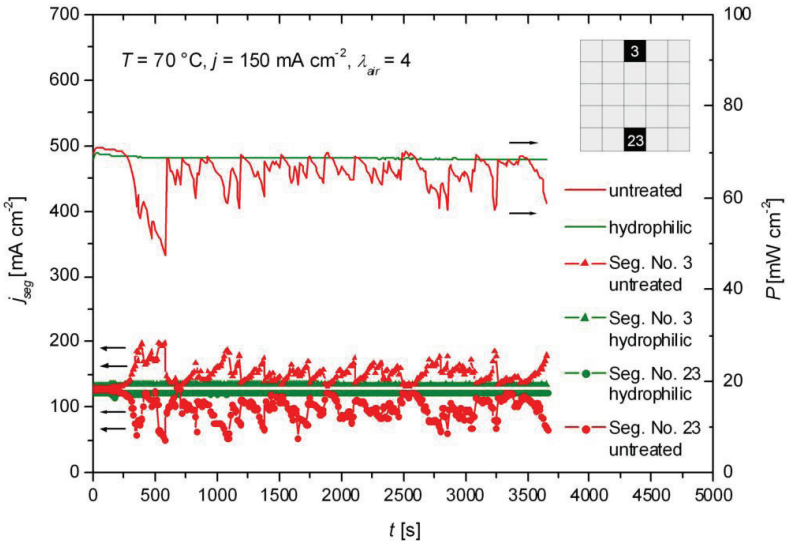

Fig. 99: **Behavior over time of current densities in segments 3 and 23 and power densities for $\lambda_{air} = \lambda_{MeOH} = 4$, 70 °C, 150 mA/cm^2. Comparison of results for untreated and hydrophilized cathode flow distributors (grid structure 1 mm x 1 mm)**

When untreated flow distributors (red curves) are used, strong temporal fluctuations were observed for both power density and segment current densities. The behavior over time of the segment current densities is almost symmetrical. As the total current is constant, the local current densities must increase in the upper cell area, when the local current drops in the lower area as a result of flooding effects, for example. The temporal fluctuations correlate with the power curve: as soon as the segment currents converge, the total power increases and vice versa. On average over time, the power using untreated cathode flow distributors is below that generated with hydrophilic cathode flow distributors (see green curve). The power curves with hydrophilic flow distributors and the current densities of both segments exhibit almost no temporal fluctuations. Overall, the water discharge in the cathode channels appears to be much more uniform for hydrophilization than in untreated flow distributors, which has a positive effect on the total power.

The different water discharge for hydrophilic and hydrophobic cathode channels was verified by neutron radiographic measurements using a double-channel cell specially designed for cross-sectional imaging. The water distribution in the cross section of the cell was visualized and is shown in Fig. 100. The project partners in HZB determined water thickness profiles across the cell cross section from the images. When hydrophilized cathode flow distributors were used, the water droplets on the surface of the GDL filled the cathode channels to a maximum of a third of the channel depth (see Fig. 100, left). Measurements on hydrophobized cathode flow distributors showed that the water droplets filled the channels completely at times, thereby preventing oxygen transport (see Fig. 100, right).

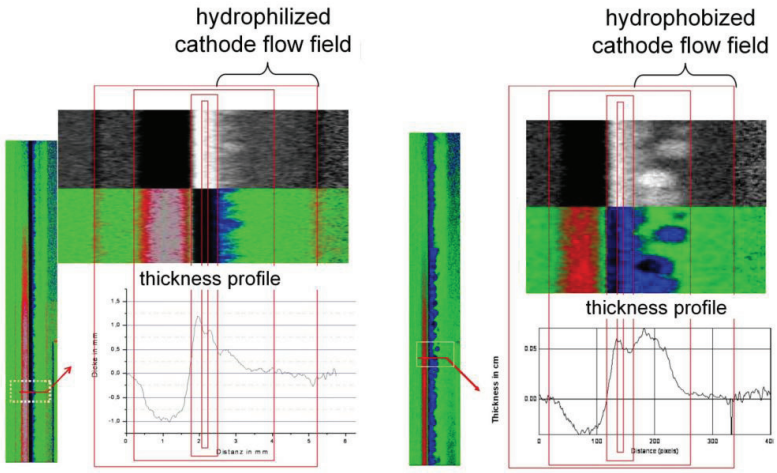

Fig. 100: **False-color cross-sectional neutron radiographs of cells with hydrophilized (left) and hydrophobized (right) cathode flow distributors. The enlarged sections each show the calculated water densities as a profile across the cell cross section. Measurement conditions: j = 150 mA/cm², λ_{air} = 4, λ_{MeOH}= 4, T = 70 °C**

In addition to neutron radiography, synchrotron radiography was also applied to direct methanol fuel cells at the electron storage ring BESSY II. Synchrotron radiography has a much higher temporal resolution than neutron radiography (< 1–5 s compared to 10–15 s) and therefore also provides more detailed insights into dynamic processes such as the formation of water droplets. Due to its higher spatial resolution of 3 μm compared to 60 μm, neutron radiography not only visualized the water and gas distribution in the flow distributor channels but also in the MEA and in the tissue layers. Cross-sectional synchrotron radiographic measurements allow the observation of the formation of water over time in the cathode as well as of water droplets in the cathode channels when current is applied.

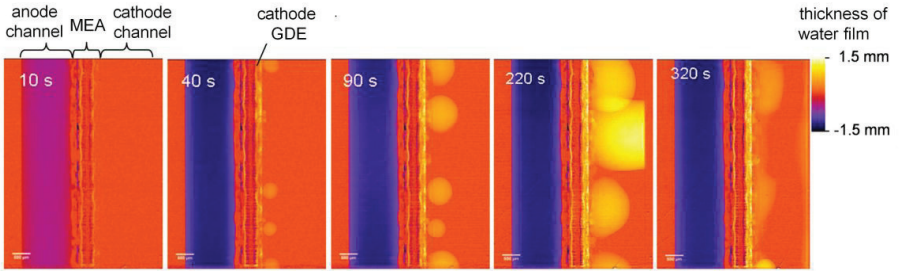

Fig. 101: **False-color cross-sectional synchrotron radiographs of a cell with untreated cathode flow distributors showing the water development in and on the cathode GDE and in the cathode channel; Measurement conditions: T = 70°C, j = 150mA/cm², λ_{air} = λ_{MeOH} = 4**

As shown in Fig. 101, cells with untreated cathode flow distributors begin to form small stationary water droplets on the surface of the cathode GDE after around only half a minute.

Although the number of water droplets hardly changes over time, their size increases. After 220 s, the water droplets have wet the channel walls and fill most of the cathode channels. During the rest of the experiment, although voluminous water droplets continue to form, they only block around half of the channel cross section. The wetting of the channel walls as the droplets grow explains power fluctuations, particularly when a current load is first applied.

In addition to the surface properties, the design of the cathode flow distributors was also varied. Tests were performed on stack cells with an active area of 315 cm^2. The results showed that grid structures offer a more stable and overall higher power output over time than channel structures, particularly for low air stoichiometries and higher current densities. Grid flow distributors with grid dimensions of 1.5 x 1.5 x 1.5 mm^3 and a channel width and depth of 1.5 mm were found to offer the best compromise of all designs tested in terms of power, stability over time and pressure loss in the channels.

Advances in magnetic imaging

Magnetic imaging was developed in order to non-invasively determine the current distribution within a cell and indeed within a stack by measuring magnetic fields at different positions around the cell. This prevents local current density measurements being falsified by measuring instruments positioned directly in the electric circuit. The external magnetic field of the cell is measured in as many positions as possible at a set distance to the edge or surface of the cell. Each point in the cell through which current flows contributes to the whole (magnetic) field in a measuring point – to varying degrees depending on current strength and distance. The magnetic field distribution in the area around the cell can be used to create a reconstruction. This necessitates both the utmost accuracy and a satisfactory resolution of the measurement data.

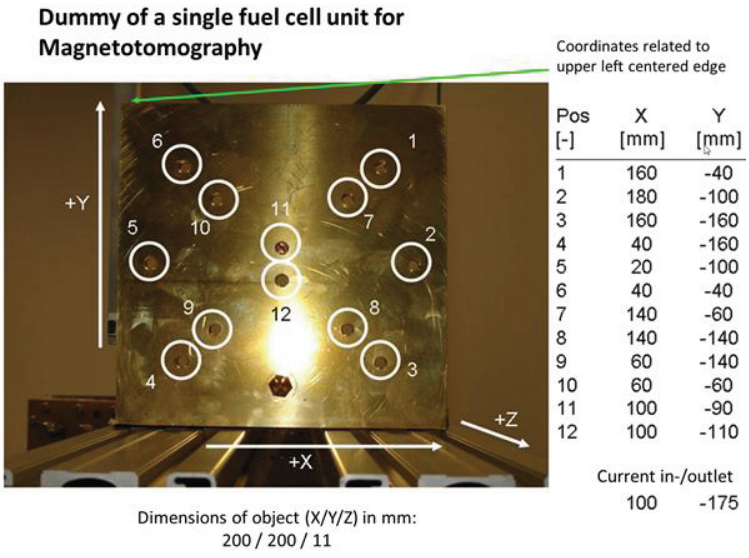

Fig. 102: Test object aiming to improve the magnetic imaging measuring equipment and validate the reconstruction algorithm

However, in the past this proved insufficient for the desired reconstruction quality. As a result, different assemblies and measurement procedures were analyzed in greater detail and accordingly altered and optimized. All of these modifications led to an increase in the effective resolution from some 100 nT to 7 nT for a total area of ±600 µT. The accuracy was also improved to < 20 nT compared to > 1 µT previously. This is close to the physical limits and can only be improved by a new system construction. The measuring time was also shortened considerably for certain types of measurements. This is important as typical measuring times for measurements of large areas with a sufficiently small pitch usually take several tens of minutes, during which time the operating conditions of the object being analyzed (the fuel cell) can change. In order to optimize the system, a test object was fabricated, as shown in Fig. 102. Its magnetic behavior simulates that of a static fuel cell.

This test object comprises two electrically insulated plates, which can be short-circuited at defined spots using electroconductive grub screws. As the flow of current can be predicted and controlled, the reconstruction algorithm can also be verified using the measurement data.

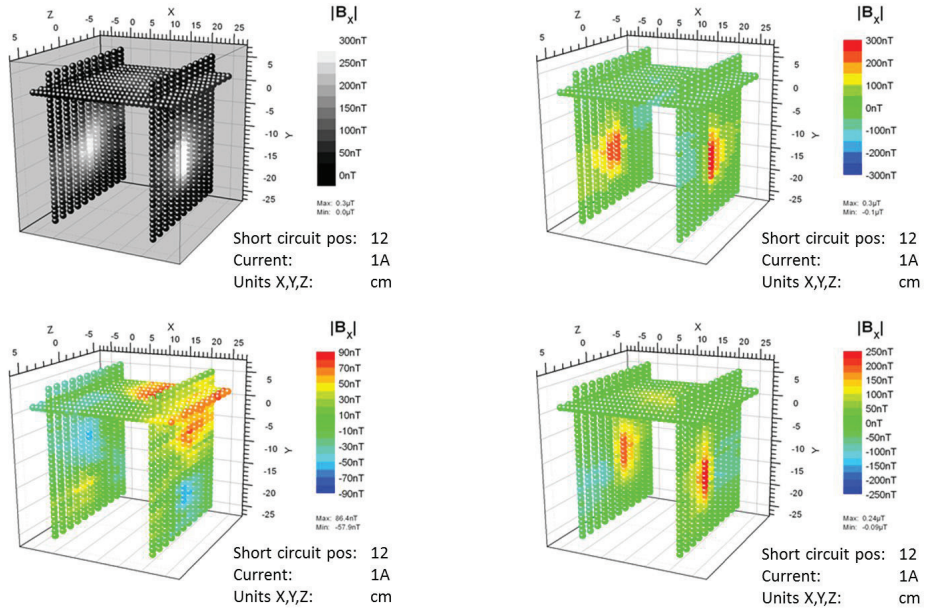

Fig. 103: Total magnetic field strength and single components for a central defect area in the test object

Current densities that are much higher than in real fuel cells can also be generated. Fig. 103 shows an example with a defect current of 1 A, which corresponds to a current density of 3.5 A/cm². Higher local magnetic fields also make it easier to verify the measurement setup. Furthermore, extrapolations can be performed for each short-circuit position in order to gain information on the theoretically resolvable changes in current density. Changes in current density of up to 15 mA/cm² can be resolved at a distance of 10 cm to the sensor. This corresponds to almost 1 mA/cm² at a minimal measuring distance of 5 mm. This sensitivity should also facilitate the use of magnetic imaging for tests on batteries.

3.6.2.3 Physical analysis techniques

Four main methods are available in the field of physical methods: (thermo)gravimetry (TGA/DTA), calorimetry (DSC), porosimetry (ASP) and thermomechanical analysis (TMA). These are predominantly used to determine material characteristics for DMFCs and HT-PEMs as well as for fuel processing. In addition to existing measuring instruments, a precision balance was acquired. It provides essential data supplementing DSC. Using this balance, the starting weight and end weight of DSC samples can be determined down to each 0.1 µg for a maximum mass of 6 g. This is necessary because depending on the type of measurement, the sample masses could be in the range of 1 mg but must nevertheless be known with sufficient precision.

Gravimetry (TGA)

This newly acquired balance can also be used for precise water determination in materials with weak water adsorption such as carbon black.

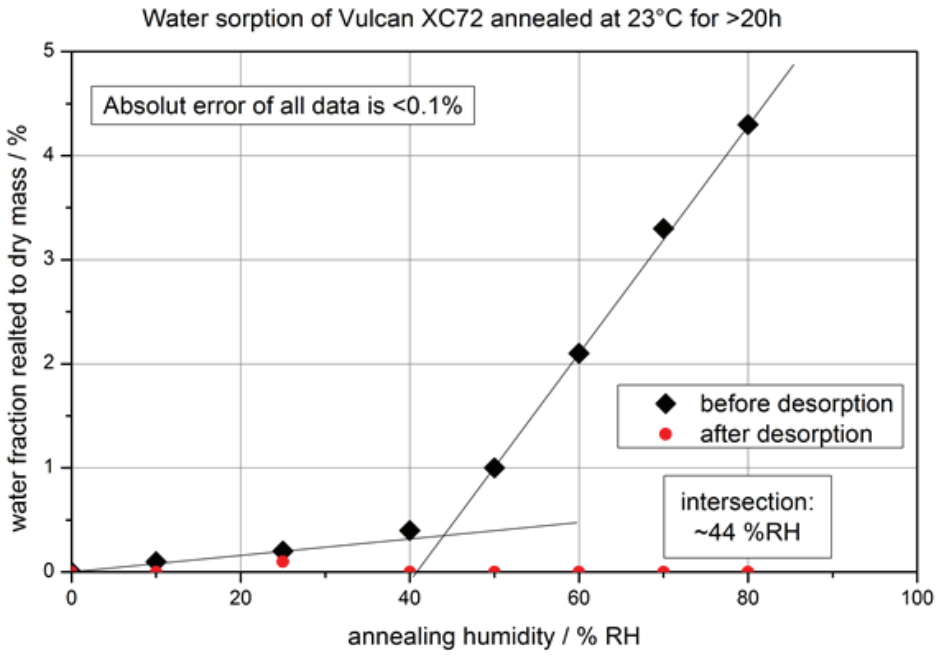

Fig. 104: Equilibrium water adsorption of Vulcan XC72 at 23°C

Fig. 104 shows this using the carbon black Vulcan XC72 as an example. This carbon black is often used as a catalyst substrate. It is interesting to note the split behavior of water adsorption. The carbon black shows a reduced adsorption capacity and a higher hydrophobicity for low humidities than for high humidities. The reason for this is not fully clear but it appears that the (chemical) surface termination of the carbon impacts on this behavior.

Thanks to the high weighing accuracy, the water loading of the carbon black was also reliably determined at low relative humidities despite starting weights of only around 10 mg.

Thermogravimetry (TGA/DTA)

Thermogravimetry with simultaneous differential thermal analysis (TGA/DTA) was mainly used to determine drying parameters and analyze the decomposition behavior of polymer and catalyst materials. Data on polymer materials are relevant for membrane processing in single-cell or stack fabrication. Furthermore, information can be gained on potential operating temperatures. Catalyst powders exhibit, for example, from 200 °C an appreciable mass loss due to oxidation of the carbon substrate. Depending on the activity, this is more or less pronounced. Fig. 105 shows the thermal decomposition of a catalyst material containing > 95 mass percent platinum. A significant mass loss rate is clearly visible from only 200 °C onwards, making it unsuitable for long-term operation in an HT-PEFC.

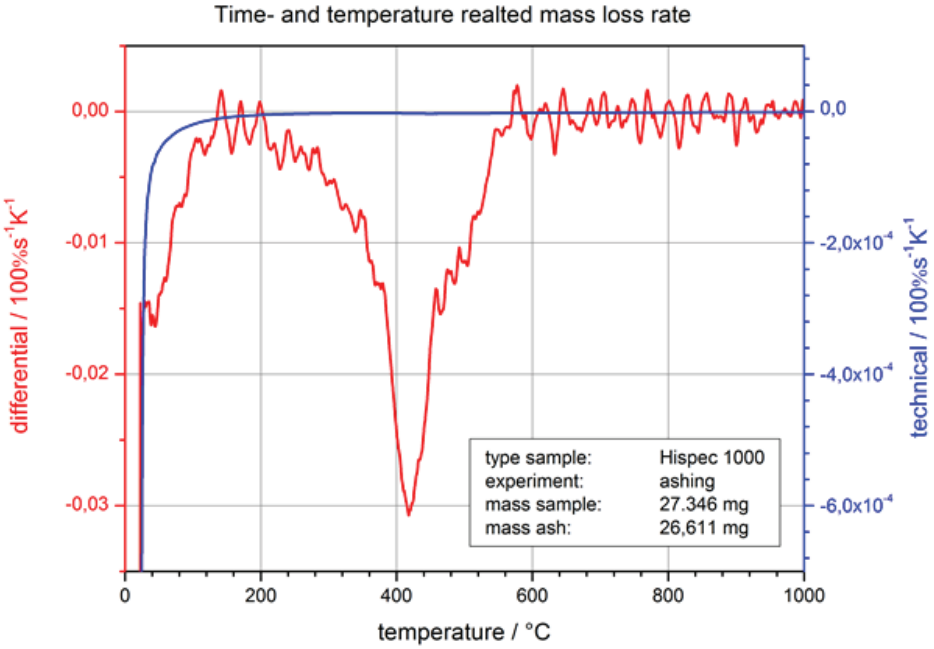

Fig. 105: Mass loss of DMFC catalyst material during thermal decomposition

Calorimetry (DSC)

Differential scanning calorimetry (DSC) provides data on processes in materials that adsorb or release heat (positive or negative reaction enthalpy, respectively). In contrast to TGA/DTA, mass information is not provided. However, this method has a much higher sensitivity. This allows the identification of glass temperatures for polymers or adsorption processes on catalyst materials. In addition, the melting-point depression of the water bound in a material provides us with clues about the inner structure of the material. This was tested on the DMFC membrane material Nafion® for different humidities and the results are shown in Fig. 106. This verified indications from the literature in that the melting enthalpy of the bound water only becomes noticeable for a very strongly humidified membrane.

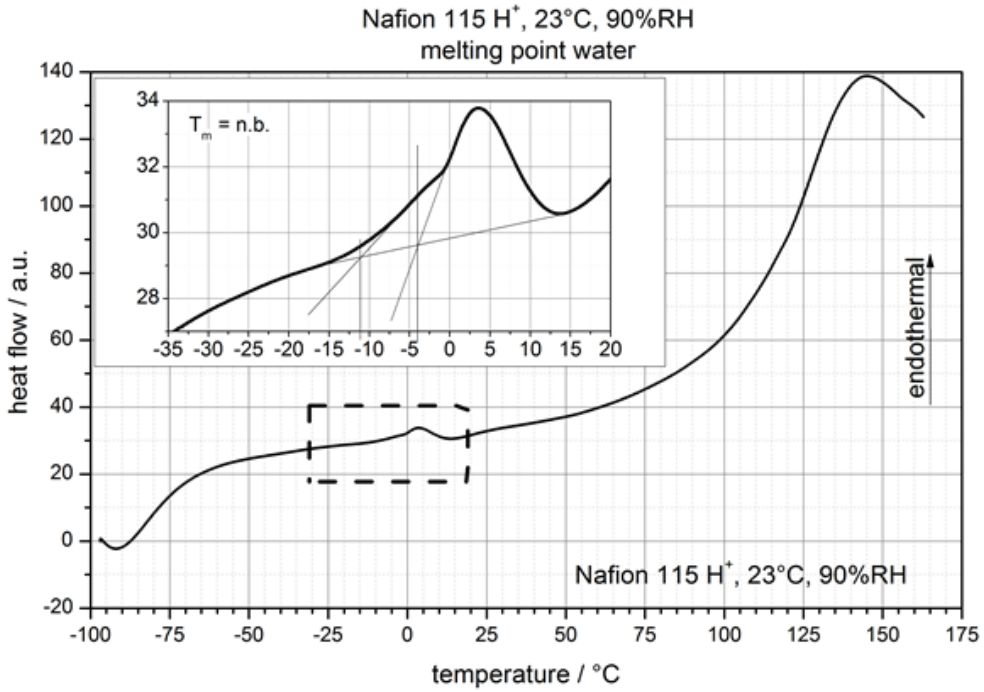

Fig. 106: Melting of water in hydrated Nation® membrane

Automated standard porosimetry (ASP)

In order to demonstrate how reliable the methods are and simultaneously ascertain the impact of different types of sample preparation, extensive measurement series concentrated on a carbon-fiber tissue material using a mesoporous silicia (SBA-15) as a reference.

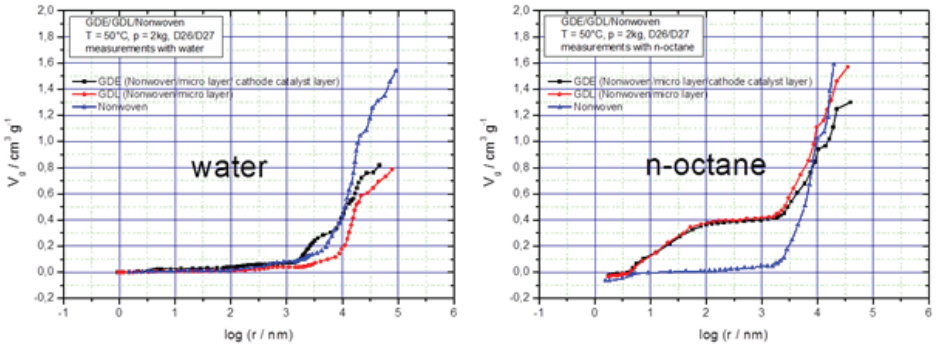

Fig. 107: Comparison of pore radii utilized for both test media water (hydrophilic fraction only) and n-octane (hydrophobic fraction)

Initial measurements were conducted to differentiate between hydrophilic and hydrophobic pores. Fig. 107 shows that pronounced effects emerge with regard to the filling of the various pore radii. This also agrees well with data from the literature and observations from test operation of the cells.

These samples were also investigated using mercury porosimetry. As expected, the fibrous material samples did not show good agreement, as these soft materials change their pore structure under measurement conditions (strong application of pressure). The mesoporous silicia samples, which are not sensitive to pressure under these conditions, showed correspondingly good agreement.

3.6.2.4 Thermomechanical analysis (TMA)

In addition to conventional tensile extension tests on polymer materials, a specially designed measuring technique was developed to determine the shear strength of membrane electrode assemblies (MEAs). By means of a suitable symmetrical configuration, the two most rigid components (tissue and membrane) are sheared against each other.

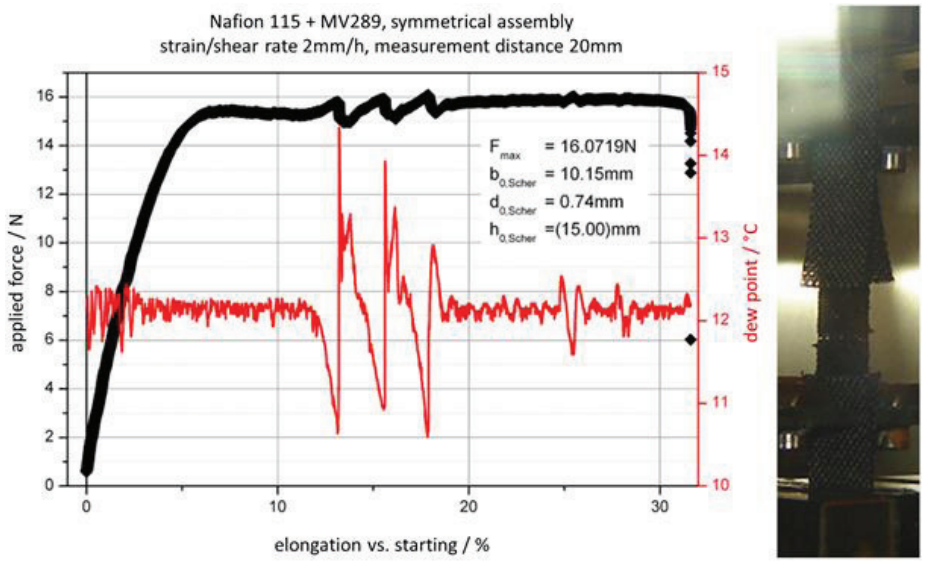

Fig. 108: Tensile shear test on a quasi-MEA

As shown in Fig. 108, the shape of the shear strength curve and the analysis of the sheared areas provide information on the state of the material bond and possible damage mechanisms. The measurements can be used, for example, to determine whether the bonding between electrode and membrane should be optimized or whether it is sufficient. The findings for DMFC-MEAs suggest that the bonding is already adequate.

3.6.3 Staff members and fields of activity

Name	Tel. (+49 2461-61-) E-mail-address	Field of activity
Dr. C. Korte	9035 c.korte@fz-juelich.de	Head of the Physicochemical Fuel Cell Laboratory
Dr. H. Echsler	8710 h.echsler@fz-juelich.de	Imaging analysis techniques
K. Klafki	4832 k.klafki@fz-juelich.de	Conventional sample preparation
A. Schröder	1579 a.schroeder@fz-juelich.de	Studies on media and current distribution in the DMFC using electrochemical neutron-radiographic and X-ray-based methods
W. Sträter	3077 w.straeter@fz-juelich.de	Standard porosimetry
Dr. J. Wackerl	6228 j.wackerl@fz-juelich.de	Physical analysis techniques
M. Wannert	5590 m.wannert@fz-juelich.de	Development of mathematical procedures for magnetic imaging, reconstruction of current density distributions using 2D and 3D models and single cells
Dr. K. Wippermann	2572 k.wippermann@fz-juelich.de	Elucidation of physical and chemical degradation mechanisms, spatially resolved measurements

3.6.4 Important publications

Important Publications

Schröder, A.; Wippermann, K.; Mergel, J.; Lehnert, W.; Stolten, D.; Sanders, T.; Baumhöfer, T.; Sauer, D. U.; Manke, I.; Kardjilov, N.; Hilger, A.; Schlösser, J.; Banhart, J.; Hartnig, C.

Combined local current distribution measurements and high resolution neutron radiography of operating Direct Methanol Fuel Cells

*Electrochemistry Communications **11** (2009) 1606–1609*

The current and fluid distribution in Direct Methanol Fuel Cells (DMFCs) was investigated in situ by means of combined high resolution neutron radiography and locally resolved current distribution measurements. The used neutron radiography set-up allows high spatial resolutions down to 70 μm at the full test cell area. A local formation of water droplets in the cathode flow field channels could be observed. Strongly inhomogeneous current distributions during cathodic flooding processes result in a performance loss of up to 30 % of the initial value. Single CO_2 bubbles can

be observed at low current densities. The water and current distribution during bi-functional operation of a DMFC was measured for the first time.

Wippermann, K.; Wannek, C.; Oetjen, H. F.; Mergel, J.; Lehnert, W.

Cell resistances of poly(2,5-benzimidazole)-based high temperature polymer membrane fuel cell membrane electrode assemblies: Time dependence and influence of operating parameters

Journal of Power Sources ***195*** *(2010) 2806–2809*

Time-dependent measurements of cell impedance of a HT-PEFC based on ABPBI were performed at constant frequencies close to the high-frequency (h.f.) intercept of the corresponding Nyquist plots with the real axis. The h.f. impedances approximate the ohmic resistance of the cell and they decrease, when current (140mAcm^{-2}) is switched on. Steady-state values are attained after 10 min. *Vice versa*, when current is switched off (OCV), the h.f. impedances instantaneously increase but reach steady-state values only after about 1 h. These values rise with increasing gas flow rates. The results are discussed in terms of hydration/dehydration processes, changing the equilibrium between orthophosphoric and pyrophosphoric acid and thus the conductivity of the electrolyte as well as the mobility of molecules and charge carriers. Impedance spectra were recorded after each time-dependent measurement under OCV conditions. The fit of these impedance data based on an equivalent circuit revealed ohmic resistances corrected by h.f. inductances and low frequency impedances associated with the cathode oxygen exchange reaction. The charge transfer resistances deduced from the low frequency impedances strongly depend on both air and hydrogen flow rates.

Schröder, A., Wippermann, K., Zehl, G.; Stolten, D.

The influence of cathode flow field surface properties on the local and time dependent performance of direct methanol fuel cells

Electrochemistry Communications ***12*** *(2010) 1318–1321*

The influence of cathode flow field wettability on the local and time-dependent performance of DMFCs was investigated by galvanostatic measurements of local current distribution, cell voltage and pressure drop along the cathode channels. The cathode flow fields made of graphite were either untreated, hydrophobic or hydrophilic. Drop shape analysis yielded contact angles in the descending order hydrophobic (126.8°), untreated (115.9°) and hydrophilic (26.2°). Especially at low air stoichiometry (λ_{air}=2), hydrophilic cathode flow fields are advantageous with regard to higher power densities, suppression of local current fluctuations and substantial reduction of pressure drop along the cathode channels.

3.7 Quality management

3.7.1 Objectives and fields of activity

Quality assurance measures are regarded as an integral part of work flows and are applied more and more frequently to ensure a high degree of quality in development, production and characterization. The explicit objective of the institute is to introduce quality-assurance measures as the basis of a quality management system (QMS), which can be certified in the medium term.

3.7.2 Important results

3.7.2.1 Quality assurance in the area of standardized electrochemical testing procedures

In the IEF-3 Report 2009, a process-oriented concept was outlined for quality assurance (QAS) for production engineering. The concept as a whole has not yet been fully implemented for financial reasons. As a result, it was decided that the preparation of detailed measures for quality assurance should initially concentrate on a clearly structured sub-area. Electrochemical characterization of DMFC single cells was chosen as a suitable area of work as numerous standardized and automated processes are already in place. These processes comprise sample collection, sample mounting, measuring techniques and evaluation, as well as the maintenance and calibration of the instruments used.

According to DIN EN ISO 9000:2000ff and the framework directives of Forschungszentrum Jülich, measures must be in place for identification, document control, reproducibility and archiving. These elements form the framework for a process-oriented QMS and are currently being compiled and tested in addition to existing processes and will be transferred to other processes.

In order to fulfill the above-mentioned requirements, the following measures have been implemented.

- Conventions were defined and introduced, according to which instruments (test devices, experimental setups), documents (specifications and records), versions (documents, files) must be labeled in a traceable manner
- A document layout was defined and implemented for all QM documents
- The measures for the control of documents laid down in quality procedure VA-RHLQ-01 of Forschungszentrum Jülich were implemented for specifications. Priority was given to reducing the degree of freedom and therefore to avoiding errors. Automated processes were derived to aid the creation of documents. This has not yet been implemented for records
- Measures were implemented to ensure that new standard work instructions are only introduced in combination with the relevant training for the employees concerned
- A system was implemented to record all documents and instruments

In addition, an instrument management system was set up for the registration, identification and monitoring of instruments needed for standard operation of the test stands. Calibration and inspection instructions were compiled for control and monitoring purposes, an evaluation

routine was developed and a calibration certificate developed. A label on the instruments documents the status of the measuring checks.

The FZJ guidelines are still being implemented. Priority is being given to regulating the archiving of documents. Workflows are also being analyzed for MEA fabrication and supplementary QM measures are being implemented. A laboratory will be set up to inspect incoming goods for standard materials.

3.7.3 Staff members and fields of activity

Name	Tel. (+49 2461-61-) E-mail address	Field of activity
D. Kalkreuth	2378 d.kalkreuth@fz-juelich.de	General quality management, quality assurance in the area of standardized electrochemical testing procedures
Dr. Vincent Haanappel	4656 v.haanappel@fz-juelich.de	General quality management, quality assurance in the SOFC area

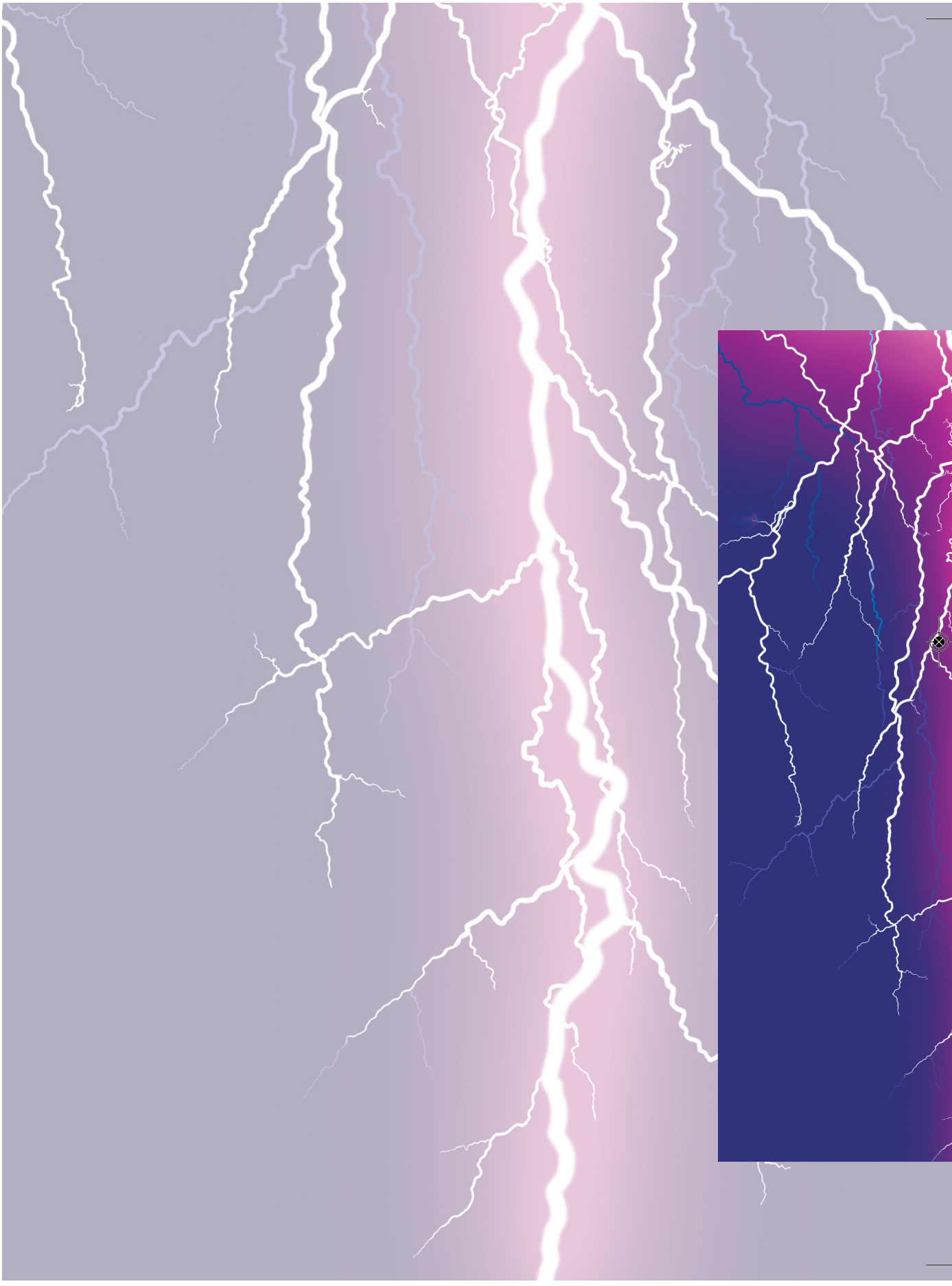

4

Projects

Selected R&D Projects

- Low-cost DMFC systems with long-term stability in the kW class
- Auxiliary power supply with fuel cells for trucks
- Fuel cell APU for aircraft

4.1 Low-cost DMFC systems with long-term stability in the kW class

4.1.1 Project focus and partners

This project, funded by BMWi (funding reference no. 0327769B), aimed to develop and test fuel cell hybrid energy systems based on direct methanol fuel cells (DMFCs) for forklift trucks. For certain applications, these systems have the potential to achieve a cost level that is comparable to conventional battery systems and could therefore be used to launch fuel cell applications on the market. An advantage of such energy systems is that there is no need for the relatively complicated and time-consuming recharging of lead-acid batteries, nor are spare batteries required for multishift operation. DMFC energy systems that are capable of replacing the existing Pb accumulators in terms of structure and energy are therefore required. In order for this to be cost-effective, research and development must be carried out on the service life and power density of the stack as well as the overall development/hybridization of the DMFC energy system.

Within this project, IEK-3 was responsible for investigating long-term stack stability under realistic operating conditions, as well as MEA, stack and system development. Forschungszentrum Jülich also carried out the overall development, the hybridization and the construction of prototypes. Work on hybridization involved modeling and simulating various energy storage media as well as recording long-term profiles and driving cycles for the forklift truck under real operating conditions. Selected energy storage media (batteries, SuperCaps) were also investigated and integrated into a hybrid system.

The project was conducted in cooperation with the following industrial partners: Ritter Elektronik GmbH, Jungheinrich AG, ebm-papst Landshut GmbH and AKG Verwaltungsgesellschaft. The aim was to help *increase service life and power density*, *optimize the systems*, particularly with regard to *simplification and integration* before market introduction. This also involved the automation of production processes, which in turn provided different ways of *reducing costs*.

4.1.2 Long-term test over 3;000 h on a DMFC energy system

At the end of the project, two systems DMFC V3.3-1 and DMFC V3.3-2 (see section 3.1.2.4) were assembled and each subjected to a long-term test lasting 3,000 hours with approximated and realistic load profiles from driving cycles.

The automated long-term test was performed in a special test stand that sets the electrical load profile (not the mechanical loads). In addition to determining stack aging under real load conditions, experience was gained working with the system periphery, the hybridization concept and controlling the energy system. The main targets for data evaluation were efficiencies and utilizations for the system as a whole and system components in relation to operating time.

4.1.2.1 Load profile

Fig. 109 shows the application of the DMFC system discussed here. In warehouses with shelving units, pallets of products are stocked with different goods depending on the commissioned order using forklift trucks. The vehicles move along the rows of shelves and

stop at set positions. The electrical power of the drive motor shows the curves for start-up (peak output approx. 7 kW), braking (energy recovery up to more than 5 kW) and the time waiting for the pallets to be loaded.

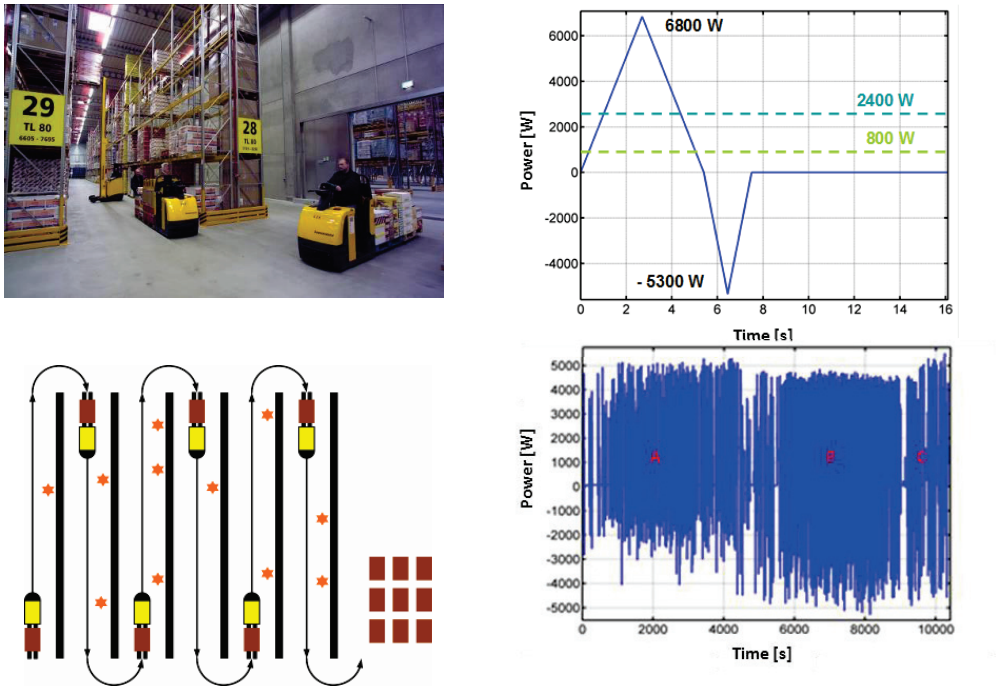

Fig. 109: Vehicle in use (left); load profiles for the long-term test (right); approximated (top) and realistic (bottom) forklift operation

The average power of a cycle typical of this vehicle is approx. 800 W. The motor output at a constant speed is three times as high. The energy system was subjected to two different load cycles during the long-term test. The first involved triangular approximation and cyclic repetition of the above-mentioned characteristic curve. The second involved analyzing measurement data in a real application and combining them in a realistic cycle with three different sections (see Fig. 109, bottom right). Section A with an average power of 360 W and a duration of 1.36 h represents operation with a relatively large number of breaks. Section B (786 W, 1.29 h) is the standard block of operation customary for this vehicle, and section C (982 W, 0.24 h) is a phase with a considerable amount of driving at constant speed. These three phases are repeated cyclically one after the other. The load profiles are specified in the control system for the test stand.

4.1.2.2 Test stand setup

The test stand for the long-term testing of the DMFC energy system comprises two parts. The first part is shown schematically in Fig. 110. The test object (yellow) is placed in a frame with a collecting tray (green), which collects liquids in case of malfunction. In the chamber on the top right, the off-gas of the DMFC energy system is collected and extracted centrally. A feed vessel for methanol is also located here, from which the system can withdraw methanol.

This feed vessel is connected to a hazardous substances cabinet containing 190 liter methanol vessels. In addition to sensors monitoring the system, this is also where an external supply of fully demineralized water can be found (blue). This part of the test stand is coupled electrically to the second part – the hybridization test stand (cf. Fig. 110, right). This hybridization test stand essentially comprises a control cabinet with an electronic current sink that simulates the start-up processes and constant operation, as well as electronic current sources that simulate braking processes. Coupling this to the DMFC energy system allows it to be used for various driving cycles (cf. Fig. 109).

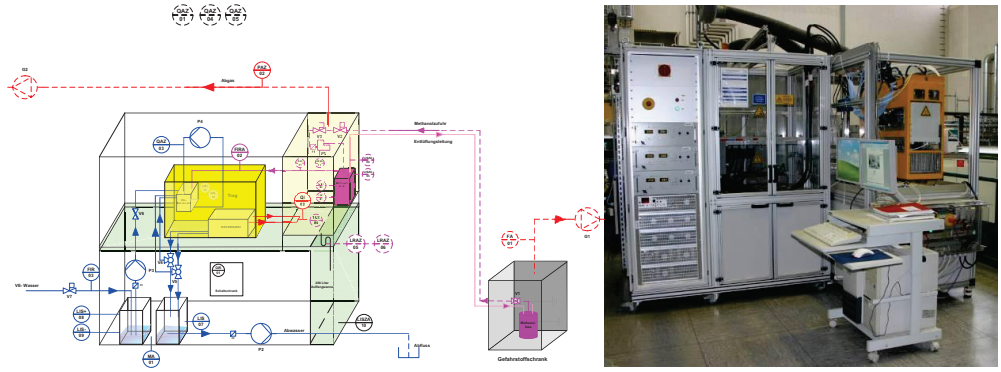

Fig. 110: Test stand for continuous operation of DMFC hybrid systems. Left: schematic. Right: coupling to hybridization test stand

4.1.2.3 Results DMFC V3.3-1

The long-term test comprises different test phases. An overview can be found in Table 9: The first four phases with constant loads of 0 W, 300 W, 600 W and 800 W, respectively, were used to optimize the numerous control parameters. The system was then loaded with the driving cycles from Fig. 109. A large proportion of the 2,225 operating hours achieved in total is accounted for by realistic forklift operation. If the total number of operating hours is compared to the test period from 26 October 2009 to 8 March 2010, system availability is calculated as 69.4 %.

Test phase	Period	Hours of operation
Constant load 0 W	26.10.2009 – 02.11.2009	128 h
Constant load 300 W	02.11.2009 – 04.11.2009	37 h
Constant load 600 W	04.11.2009 – 11.11.2009	84 h
Constant load 800 W	11.11.2009 – 20.11.2009	189 h
Approximated forklift operation	20.11.2009 – 01.12.2009	180 h
Realistic forklift operation	01.12.2009 – 08.03.2010	1,607 h
Total:		2,225 h

Table 9: Overview load cycles and periods of operation

The roughly 30 % downtime during the entire test period resulted from planned outages and various disturbances that led to the system being shut down by the control system (cf. section 3.1.2.4). Fig. 111 shows the disturbance statistics compiled on the basis of the error messages recorded. The majority of disturbances were caused because the permissible single cell voltage was not reached. This applies, for example, when a single cell fails to reach the absolute minimum of 200 mV. Single-cell voltage monitoring is necessary for such measurements, and also protects the DMFC stack from loads that are too high.

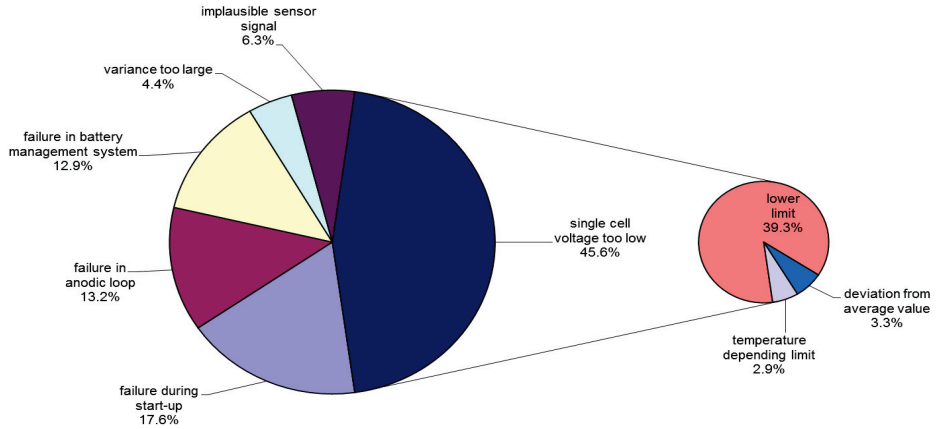

Fig. 111: Disturbance statistics DMFC V3.3-1 (Number of error messages: 272)

In addition to the error messages, the control units in the system and test stand record several different parameters (currents, voltages, methanol concentration, pressure, temperatures, air mass flow rate, methanol volume flow rate), which are saved at different

sampling rates (2 s and 0.1 s) in separate measurement files. The 150 MB of data generated per day gave rise to a total volume of 18.5 GB for the test period. These data are analyzed in the following.

Once the energy system is switched on, it is immediately ready for operation. The vehicle is initially supplied with energy by the hybrid battery, which has a capacity calculated to cover the warm-up phase of the stack when no electrical output is produced. Fig. 112 (left) shows the system behavior after it has been switched on in the cold state. The battery is first discharged by the load cycle (decrease in battery voltage), while the stack still maintains its open-circuit voltage. The stack temperature begins to increase because the system control in start-up mode prompts the controlled addition of methanol in the anode loop, which then leads to the methanol diffusing through the MEA and oxidizing on the cathode side, thereby releasing heat. When a stack temperature of 40 °C has been attained, temperature-limited stack loading is possible according to the following condition:

$$U_{Stack,\,\min} = Cell\ number \cdot \left(0.8\ V - parameter \cdot T_{Stack}\right)$$

This stress limit remains throughout system operation. In this example, the warm-up process took around 40 minutes. The time can, however, be easily influenced by the operating parameters of air and methanol volume flows. A few minutes later, the battery voltage returns to a stationary level, as the stack then has sufficient power reserves.

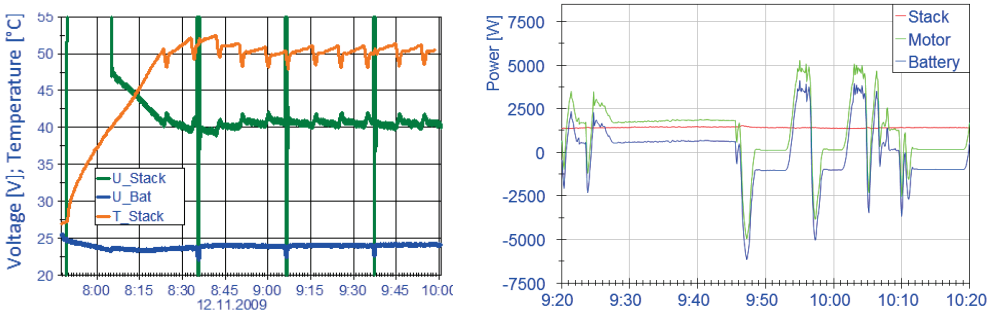

Fig. 112: Behavior over time of the stack warm-up phase (left) and normal operation (right)

Fig. 112 (right) shows the power curves for stack, motor and battery in realistic forklift operation during normal system operation. It can be clearly seen that the dynamic load changes in the motor are almost fully covered by the battery. The controller parameters of the system control as a whole were set to be extremely slow, which resulted in generally constant stack power. This example is taken from section C of the cycle where the stack is operated at its nominal power of 1.3 kW.

During commissioning, a maximum stack power of about 2.7 kW was measured. To facilitate a comparison with MEA data, the measured values were converted into specific values (see Fig. 113). The stack voltage was converted into a mean cell voltage for this purpose. The error bars indicate the values for the highest and lowest voltages in the stack. The same holds for the power curve, which is shown in relation to the right axis.

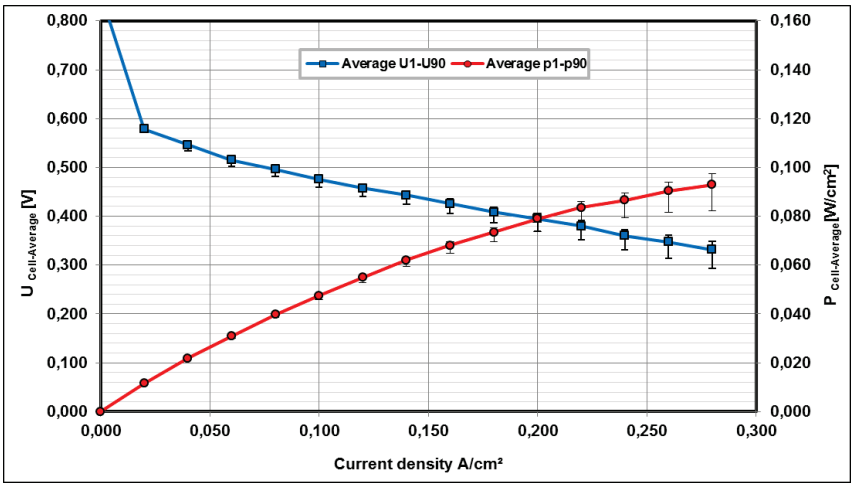

Fig. 113: Current-voltage characteristics for running-in of the stack

The change in stack performance over time is usually determined by periodic measurements of the current-voltage characteristics. This involves keeping the flows constant for three minutes under the most constant operating conditions possible (temperature, methanol concentration, air volume flows (or excess air) and recording the related stack voltage. The measurements are repeated at predefined operating times. The time curve of the mean cell voltage at constant current density represents stack aging. In this case, the reference conditions were defined as a current density of 0.1 A/cm², a methanol concentration of one mole per liter, an anodic inlet temperature of approx. 60 °C and a specific air supply of 28 ml/(cm²min).

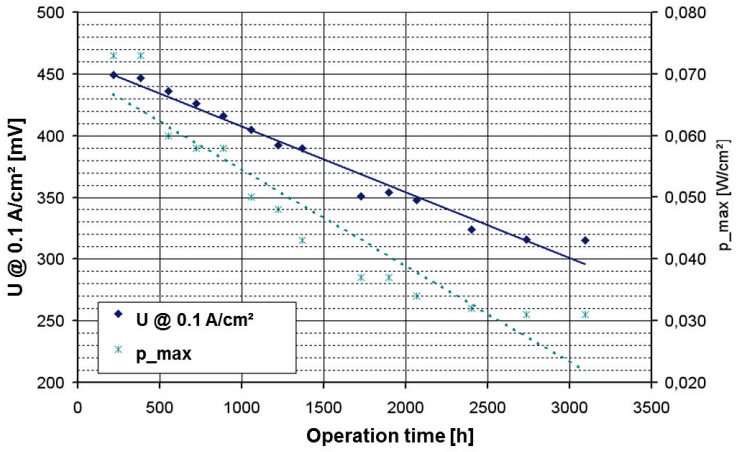

Fig. 114: Time curve of mean cell voltage in the stack at 0.1 A/cm² and the defined conditions

Fig. 114 shows the time curve of the mean cell voltage in the stack as a function of the operating time. The operating time is calculated as the difference between the time of

measurement and the commissioning of the system. The running-in of the stack in another test stand and possible system outages were not considered in this representation. Degradation was found to be around 50 µV/h. This value is higher by a factor of three than that measured in test facilities for short stacks with MEAs of identical design.

Another stack evaluation aspect is the frequency distribution of cell voltages for certain loads after different operating times. The cell voltages during the first curve, which was measured in the test stand at a current density of 0.1 A/cm² fluctuated within a narrow range of 460 mV to 484 mV. After around 77 hours of operation, a slight improvement was observed for some cells. However, a shift to lower voltages was also observed for the weaker cells. The last measurement in the test stand was taken after 173 hours and the cell voltages ranged from 410 mV to 482 mV. This trend continued during system operation (see Fig. 115). After integration into the system (213 h), the cells had a voltage of around 100 mV, whereas after 1893 h, this range rose to 175 mV. This diversity in the cell voltages could have various causes. It could be due to insufficient levels of accuracy during fabrication of the MEA or the bipolar plates or to changes, for example, brought about by the introduction of foreign ions.

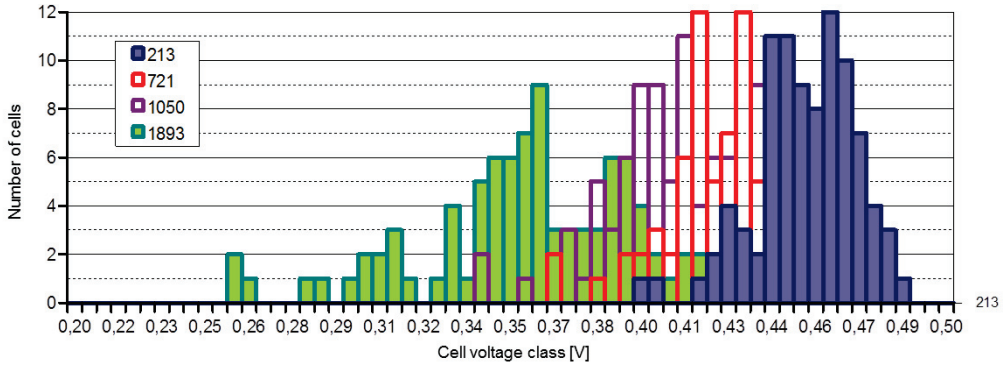

Fig. 115: Cell voltage distribution in the stack as a function of operating time

An alternative procedure for determining stack aging is to filter out the values mentioned above from the measured data of the cyclically loaded system. The essential differences compared to the first method are the dynamic stack loading and the greater scatter of the operating parameters. Fig. 116 shows the result of data filtering. The calendar time is shown on the x-axis. System downtime due to disturbances or planned interruptions is included. Although the voltage values vary considerably within a range of about 30 mV, the slope of the line of best fit at 0.1 A/cm² is 52 µV/h, which is comparable to the result from measurements of the current/voltage characteristics.

An important aim for the evaluation of data from the long-term tests is the determination of individual and overall efficiencies. Different efficiencies and utilizations important for system behavior were calculated, as shown in Fig. 117. They include individual efficiencies of the DMFC stack such as the fuel utilization u and the voltage efficiency η_U. Together, these give the stack efficiency η_{BZ}. On the system level, the DC/DC converter efficiency η_{DCDC}, the energy storage efficiency η_{ESP} and the peripheral efficiency $\eta_{Peripherie}$ were considered; together, they give the electrical efficiency of the system as a whole $\eta_{ges,el}$. The resulting total system efficiency η_{ges} describes the overall losses of the system.

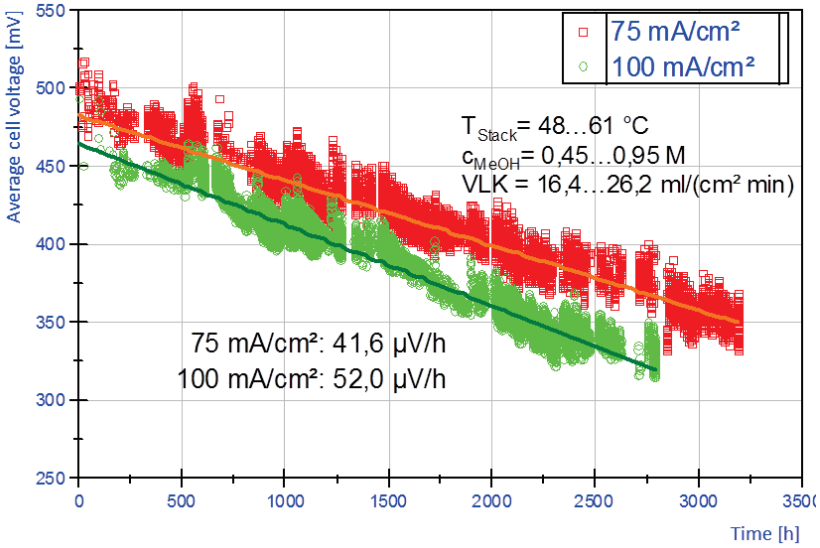

Fig. 116: **Representation of stack aging for DMFC V3.3-1 as voltage loss at a constant current density (filtering of measured data)**

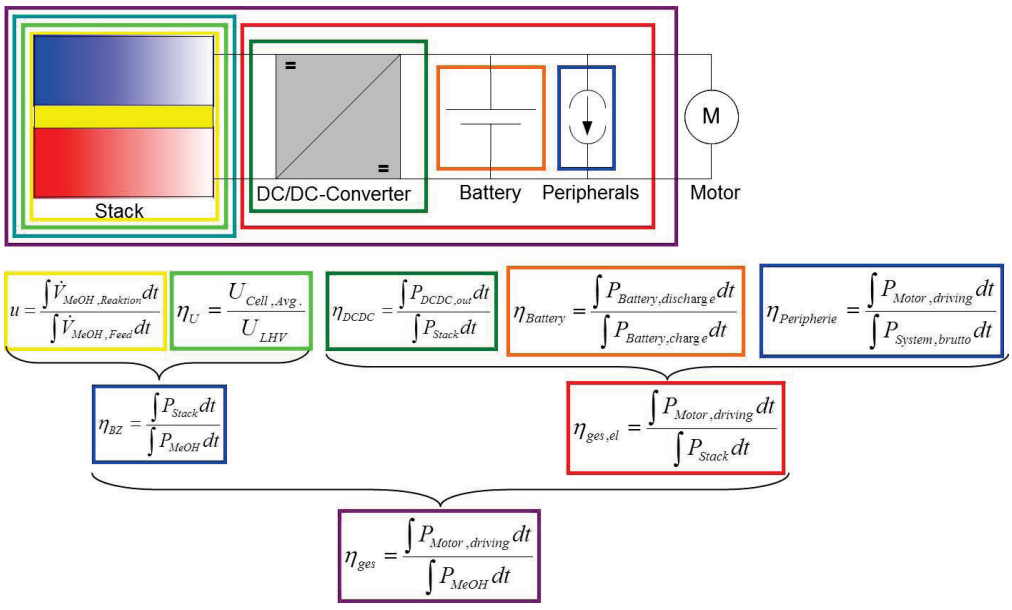

Fig. 117: **Calculation of individual efficiencies and utilizations**

In order to discuss changes in the individual efficiencies over the course of the long-term test, five days were selected from the test phase with realistic forklift operation (cf. Fig. 109).

The calculated mean daily values of the efficiencies and utilizations are shown in Tab. 10. It can be seen that some efficiencies both improved and disimproved over the entire test period, whereas some efficiencies remained almost constant. The reasons for this are summarized in the following:

- u: The fuel utilization improved after the parameters for controlling the methanol feed had been optimized.
- η_U: Degradation of the DMFC stack caused the operating point to shift to smaller voltages, which led to a decrease in voltage efficiency.
- η_{BZ}: The stack efficiency decreased due to degradation of the DMFC stack (cf. η_U).
- η_{DCDC}: When the stack operating point shifts to smaller voltages due to degradation, the voltage difference between the inlet and outlet of the DC/DC converter decreases. This leads to an improved DC/DC converter efficiency.
- η_{ESP}: The energy storage efficiency can be considered almost constant.
- $\eta_{Peripherie}$: The peripheral efficiency decreases as a result of the adjustment of the operating parameters (e.g. activation of the cooling fans), which gives rise to an increased peripheral consumption.
- $\eta_{ges,el}$: The electrical efficiency of the system as a whole can be considered almost constant.
- η_{ges}: The reduction in the overall system efficiency reflects the reduction in the stack efficiency caused by degradation.

Date	u	η_U	η_{BZ}	η_{DCDC}	η_{ESP}	$\eta_{Peripheral}$	$\eta_{total,el}$	η_{total}
01.02.2009	66.8 %	41.4 %	27.2 %	90.2 %	92.7 %	86.9 %	85.7 %	23.3 %
15.02.2009	70.1 %	38.2 %	27.0 %	91.1 %	93.1 %	86.4 %	86.3 %	23.4 %
15.01.2010	68.3 %	36.3 %	24.7 %	91.8 %	94.6 %	82.5 %	84.1 %	20.7 %
25.01.2010	71.5 %	33.9 %	24.3 %	92.7 %	93.8 %	81.3 %	83.4 %	20.3 %
05.02.2010	73.2 %	33.1 %	24.2 %	93.5 %	94.7 %	81.5 %	84.8 %	20.5 %

Tab. 10: Mean daily values of the efficiencies and utilizations for realistic forklift operation

4.1.2.4 Compromises for DMFC V3.3-1

The DMFC system is designed for a triple excess of air (relative to the total amount of methanol) at the nominal operating point (stack power 1.3 kW). A stack temperature of about 70 °C is established. When the stack was put into operation, it proved impossible to achieve stable stack loading at this air mass flow rate (22 kg/h corresponding to 10 ml/cm²/min). Individual cell voltages dropped below a minimum value which led to an emergency shutdown. For long-term testing, the air volume flow was therefore increased by a factor of 2.5 of the design value. This resulted in stack temperatures of between 50 °C and 60 °C.

Under such conditions, water-autonomous operation was not possible because the driving temperature difference in the condenser and the residence time of the stack air was reduced to a greater extent than in the design case. A water deficit of 20 % was determined at the design point. Water compensation was maintained by feeding in deionized water from the domestic supply.

Project partners Ritter Elektronik developed the DC/DC converter and the control system for the application as part of the joint project. The “tailor-made” components for tray integration were not ready at the beginning of the long-term test. As a result, preliminary versions with reduced functionality were used.

4.1.2.5 Lessons learned

The condensers designed by project partner AKG were typically joined by adhesive bonding. It was shown that this form of joining does not solve problems such as leaks and the introduction of adhesive components into the DMFC system. Together with the Central Technology Division (ZAT) at Forschungszentrum Jülich, IEK-3 redesigned the construction and fabricated the condenser block using laser welding (Fig. 118, left). An alternative that is cheaper in the long run is the use of flat tubes for the stainless steel condensation channels, as shown in Fig. 118 (right).

Fig. 118: Welded condenser with channels as flat tubes

In the second system constructed, the stack was modified slightly. When the first stack was disassembled, construction-related problems were encountered removing the water from the cathodic flow distributors. A small cell spacing of around three millimeters can cause a closed film of water to form between two cells, which hinders the supply of air to the cells concerned (see Fig. 119). By introducing comb structures, the wicks can be fixed more securely, thus allowing the water to run off along the comb structure. The principle is shown on the right-hand side of Fig. 119. In order to prevent short circuits, a non-conducting fiber composite material was used.

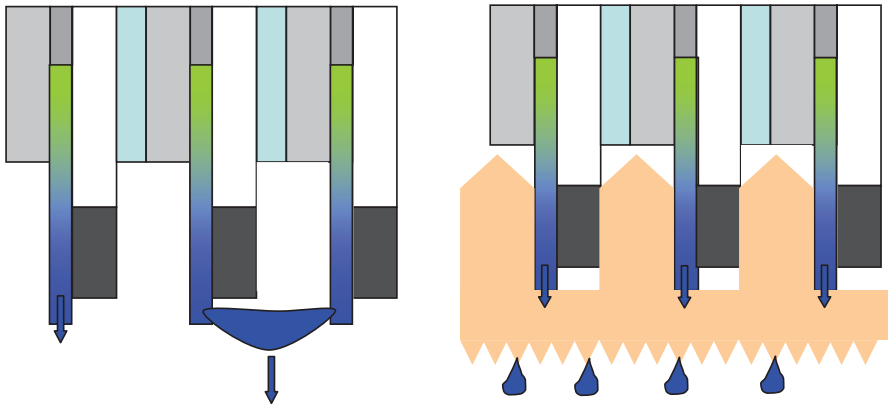

Fig. 119: Droplet formation on the cathode exhaust and the blocking of flow (left); integration of comb structures to improve the removal of water from the cathode channels (right)

The comb structures were incorporated into the stack after assembly. Fig. 120 shows the cathode exhaust of the stack operated. The water droplets can be clearly seen running off from the comb structures. The sealing off of the channels by a water film was no longer observed and operation was also possible for small excesses of air.

Fig. 120: Integration of the comb structures in the cathode exhaust of the stack

The second stack was commissioned in the heated test stand just like the first stack. Typical conditions for the running-in of the stack were chosen once again:

- Specific volume flow rate cathode: 31 ml/(cm²min)
- Methanol concentration: 0.8 mol/l
- Temperature: 68 °C

After this, the current-voltage curves were recorded in order to determine the performance efficiency. It was shown that the stack exceeded the required power output and that the cell voltages did not scatter to the same extent as in the first stack (see Fig. 121).

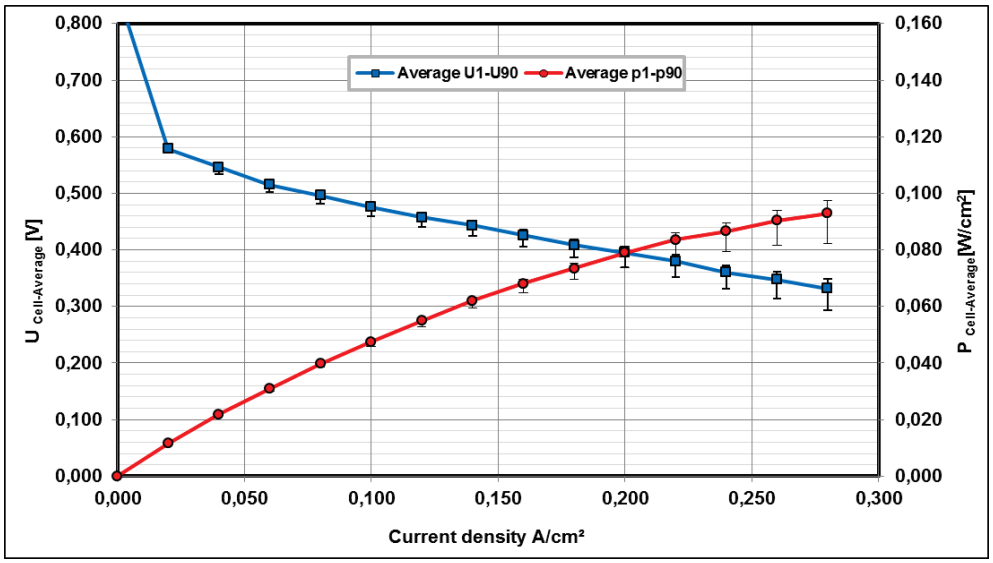

Fig. 121: Current density-voltage curves of the stack when put into operation. Specific volume flow rate cathode 31 ml/(cm²min), methanol concentration 0.8 mol/l, temperature 68 °C

The reduced scattering of the cell voltages and operation at low excesses of air (gamma 3) can primarily be explained by the modified cathode exhaust, whereas the higher cell voltage level was caused by a modified MEA.

4.1.2.6 First results DMFC V3.3-2

At the time of reporting, long-term testing of the successor system DMFC V3.3-2 was still ongoing. The most important improvements in terms of set-up and operation are as follows:

- Condenser designed using welding, very low condenser contamination
- Stack operation at a three-fold excess of air, water-autonomous system operation even for high ambient temperatures (up to 35 °C)
- Driving mode tested in a forklift truck, all components integrated in the battery tray

Fig. 122 shows stack aging compared to the values for the DMFC V3.3-1 system. In contrast to Fig. 116, operating hours are shown here because the two systems have very different downtimes. It is interesting to note that the stack of the successor system was started at a much higher mean cell voltage (520 mV compared to 47 mV at 0.1 A/cm²) and that the degradation is significantly lower.

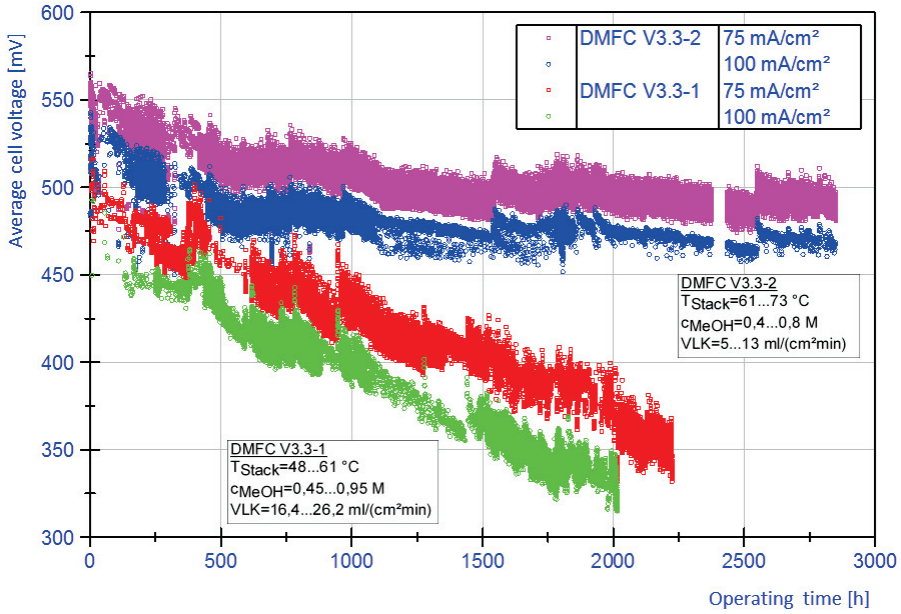

Fig. 122: Degradation DMFC V3.3-1 vs. DMFC V3.3-2

For the second DMFC energy system (DMFC V3.3-2), the efficiencies and utilizations described here were calculated as mean daily values for realistic forklift operation, just as they were for the first system (DMFC V3.3-1).

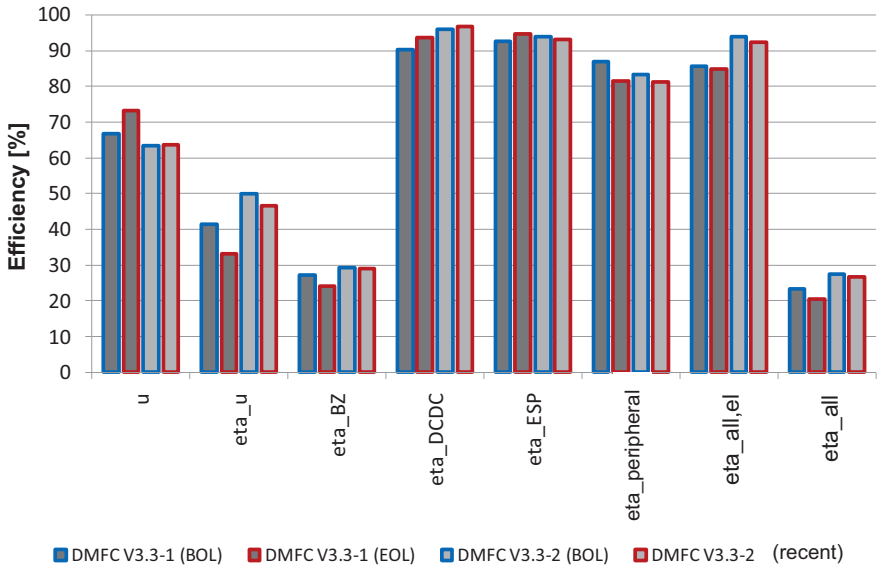

Fig. 123: Efficiencies DMFC V3.3-1 vs. DMFC V3.3-2

Fig. 123 compares the individual efficiencies and utilizations for the two systems. The values shown are those at the beginning of long-term testing (BOL = beginning of life) and the end of long-term testing (EOL = end of life). As long-term testing has not yet been completed for the second system (2850 operating hours as of February 17, 2011), the current values are reported instead of the EOL values. The most important differences were detected for stack efficiency and the overall system efficiency. Both values were better for the second system than the first system at the beginning of the test and at the current point in time of the test. The main reason for this is an improvement of 10 percentage points in the voltage efficiency of the second system. Changes in the fuel utilization can be explained by modified control parameters.

4.1.3 Staff members and fields of activity

Name	Tel. (+49 2461-61-) E-mail address	Field of activity
J. Mergel	5996 j.mergel@fz-juelich.de	Head of Direct Methanol Fuel Cells
M. Hehemann	5431 m.hehemann@fz-juelich.de	Emission measurements on DMFC systems. Component development, setting up and operating test stands
Dr. H. Janßen	5082 h.janssen@fz-juelich.de	Head of the DMFC System Development Group, development of components, system design, construction and testing of DMFC systems
Dr. M. Müller	1859 mar.mueller@fz-juelich.de	Head of the DMFC Stack Development Group, technical and economic optimization of DMFC stacks, selection and testing of materials for stack parts, plant design and verification
Dr. J. Wilhelm	1573 j.wilhelm@fz-juelich.de	Hybridization and control of DMFC systems, modeling and simulation of DMFC systems
W. Zwaygardt	2109 w.zwaygardt@fz-juelich.de	Design and construction of DMFC components, setting up and operating test stands

4.2 Auxiliary power supply with fuel cells for trucks

4.2.1 Motivation for fuel cell systems in trucks

The demand for electrical energy in transport vehicles in the road, shipping and aviation sectors will continue to increase over the next few years. The reasons for this not only include the continually increasing range of comfort, safety and control functions in vehicles. They also include an increasing electrification of auxiliary consumers, which were conventionally supplied with mechanical power from the engine. An advantage of this is the option of mechanically decoupling auxiliary consumers from the drive system so that their power supply can be better adapted to time-dependent requirements.

Consequently, the increasing demand for electric power also requires a more efficient power supply. In passenger cars, this has been realized to date by a conventional AC generator. More powerful systems include innovative crankshaft generators. Aircraft today already contain separate auxiliary power units (APUs), which are based on turbines and burn kerosene. These systems are only employed on the ground and have installed electrical capacities of 150–400 kW_e. APUs provide electric power independent of the drive and can thus relieve the engine. They also facilitate an efficient power supply during downtime phases. The latter is particularly advantageous as operating the engine solely to provide power at generally small partial loads is also connected with a correspondingly low efficiency. The use of systems with particularly low pollutant and noise emissions thus leads to a considerable improvement in the environmental characteristics of vehicles. For example, the emission situation at airports and ports could be improved substantially. In some Scandinavian countries, emission-based (e.g. NO_x and SO_x) fee systems already exist for ships based on the time required to load and unload [19] and similar regulations are in place in European airports [20].

What productions runs are possible? According to Contestabile [21], figures will be somewhere in the region of 400,000 APUs for the “sleeper trucks” in the USA and 100,000 for Europe’s truck sector. Lutsey et al. estimate annual sales of 60,000 APUs to trucks for refrigerated transport in the USA. [22]. This estimate is interesting for IEK-3’s ADELHEID project. Sales of 1,500,000 units to top-end cars in the USA masks the fact that most car manufacturers have implemented APU development based on fossil fuels because of the high standards in this sector. As the ambitious goals in the US DoE program were not achieved, the funding program underwent several modifications [23, 24].

---

[19] Davies, M.E., Plant, G., Cosslett, C., Harrop, O., Petts, J.W.: Study on the economic, legal, environmental and practical implications of a European Union System to reduce ship emissions of SO_2 and NO_x, BMT Murray Fenton Edon Liddiard Vince Ltd., Final Report, Contract B4-3040/98/000839/MAR/B1, August 2000

[20] Flughafen Hamburg GmbH, Flughafenbenutzungsordnung (Airport utilization regulations) of February 10, 2006

[21] Contestabile, M.: Analysis of the market for diesel PEM fuel cell auxiliary power units onboard long-haul trucks and of its implications for the large-scale adoption of PEM FC. Energy Policy, doi: 10.1016/J.enpol.2009.03.044 (2009)

[22] Lutsey, N., Brodrick, C.J., Sperling, D., Dwyer, H.A.: Markets for fuel-cell auxiliary power units in vehicles - Preliminary assessment, in Transport Research Record, 1842 (2003), 118-126

[23] Department of Energy, United States of America, On-board fuel processing go/no-go decision, PDF file downloaded at www1.eere.energy.gov/ hydrogenandfuelcells/ news_fuel_processor.html (2004)

[24] http://www.eia.doe.gov/cneaf/electricity/epa/epaxlfilees1.pdf (November 20, 2009)

More detailed information on the potential and challenges associated with the development of fuel cell APUs can be found in [25]. For the ADELHEID project, transport refrigeration for trucks can be considered a potential application on the European market in the power class of 5–15 kW_e (see Fig. 124). Construction vehicles or other specific APU applications should, however, also be considered. “Sleeper trucks” are a typical and very interesting example of a market in the USA. Internationally, maritime and aviation applications are important. The next section will focus on auxiliary power supply for aircraft.

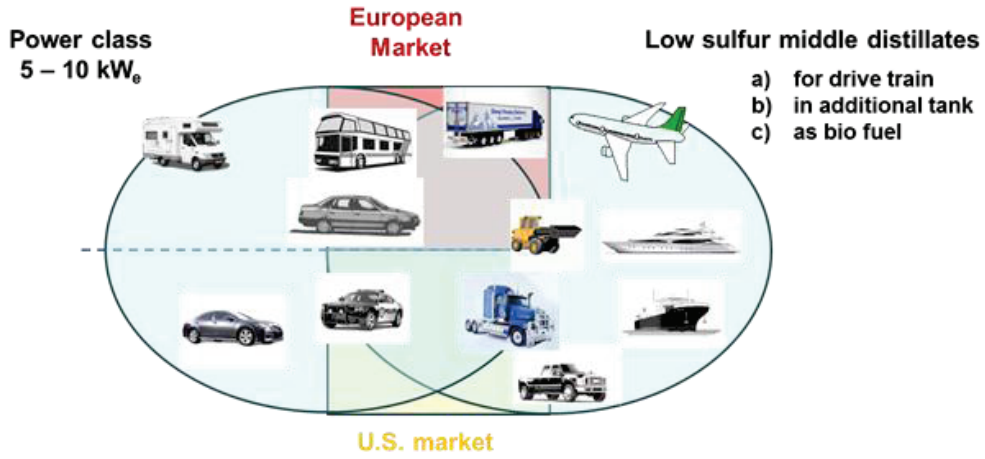

Fig. 124: Defining potential fields of application for APU development in the IEK-3 projects

4.2.2 Need for electrical energy in trucks

Almost all mobile applications require auxiliary power. An overview of the various APU applications can be found in [25]. The most important examples include aircraft, ships, cars and perhaps most notably trucks. Numerous studies in the USA discuss the use of fuel cells in line-haul trucks with sleeping accommodation [26, 27, 28]. In the USA, fuel cell systems for on-board power supply are generally based on SOFC high-temperature fuel cells. The US Department of Energy (DoE) target data have therefore been adapted for SOFC technology. Target values for different APU applications are summarized in Tab. 11. For comparison, target data are also provided for cars and the combined generation of heat and power (CHP). Car applications have the most demanding target values in terms of compact systems. CHP has been included, as an SOFC is also preferable here in most cases. Cost targets are highest for car applications. In terms of lifetime, the most demanding application is CHP.

---

[25] Peters, R.: Auxiliary Power Units for Light-Duty Vehicles, Trucks, Ships and Airplanes, in Hydrogen and Fuel Cells (ed. D. Stolten), Wiley-VCH, Weinheim (2010), pp. 681-714

[26] Lutsey, N., Brodrick, C.J., Lipman, T.: Energy, 32 (2007) 12, 2428-2438

[27] Jain, S., Chen, H.Y., Schwank, J.: Journal of Power Sources 160 (2006) 1, 474-484

[28] Baratto, F. and Diwekar, U.W.: Journal of Power Sources, 139 (2005) 1, 188-196

What are the daily demands on an APU? In many cases, only insufficient analyses of the actual demand exist, particularly in terms of power peaks and general daily demand. Fig. 125 shows the results of a study conducted by Sriramulu et al. [29] These data can be used when designing the system in order to decrease the size of the fuel cell system by means of hybridization with a battery. For application in trucks, approx. 2.5 kW_e are required for 1.5 hours every day to heat the cab. During the day, approx. 2 kW_e are required for 1.5 hours to air-condition the cab. Depending on the study, 5 - 10 kWhe are required. Lutsey et al. [30] determined other values of energy consumption. According to the literature, trucks require between 8 l and 140 l diesel every day and release CO_2 emissions of 19–360 kg CO_2/day when running idle. According to [27] ,[29] and [31], 18 l/day or 19 l/day diesel is consumed, resulting in CO_2 emissions of 45 kg CO_2/day or 49 kg CO_2/day, respectively.

Target value	Car APU [32]	DOE [33], FC drive (H_2), 2015	DOE [34], APU 2015/2020	DOE [34], CHP 2015/2020
Power	10 kW	80 kW	1–10 kW	1–10 kW
Efficiency	< 35 %	50 %	35 %/40 %	42.5 %/45 %
CHP energy efficiency				87.5 %/90 %
Cost for 50,000/100,000 units	€ 40 kW^{-1}	$ 30 kW^{-1}	$ 600 kW^{-1}	€ 450 kW^{-1}
Lifetime	5,000 h	5,000	15,000/20,000 h	40,000/60,000 h
Dynamic aging per 1000 h operation			1.3 %/1 %	0.5 %/0.3 %
Power density	333 W L^{-1}	650 W L^{-1}	35–40 W L^{-1}	
Mass-specific power	250 kW kg^{-1}	650 kW kg^{-1}	40–45 kW L^{-1}	
System availability			98 %/99 %	98 %/99 %
Cold start	< 1 s	5 s @ 20 °C 30 s @ -20 °C	10/5 min	30/20 min
Load change (10 % to 90 % partial load)	< 1 s	1 s	3/2 min	3/2 min
Partial load range	1:50	-40 C		

Tab. 11: Targets for different APU applications and for stationary systems based on natural gas as an energy carrier. CHP: combined heat and power generation

[29] Sriramulu, S., Isherwood, K., Lasher, S., Broderick, C.J., Lutsey, N.: Evaluation of the potential for fuel cell auxiliary power units (APUs), Proc. Fuel Cell Seminar, November 1-5, 2004, San Antonio, Texas, USA

[30] Lutsey, N., Brodrick, C.J., Sperling, D., Oglesby, C: Journal of the Transportation Research Board, 1880 (2004), 29-38

[31] Preliminary Assessment of Planar Solid Oxide Fuel Cells for Transportation Power Applications. Parsons Infrastructure and Technology Group. December 2000. Prepared for Argonne National Laboratory.

[32] Docter, A., Konrad, G., Lamm, A.: VDI-Berichte No. 1565 (2000), 399-411

[33] Department of Energy: Multi-year research, development and demonstration plan, Hydrogen, fuel cells & infrastructure technologies program, Revision 2007, http://www.eere.energy.gov/hydrogenandfuelcells/mypp (November 23, 2009)

[34] http://www1.eere.energy.gov/hydrogenandfuelcells/fuelcells/systems.html (November 22, 2009)

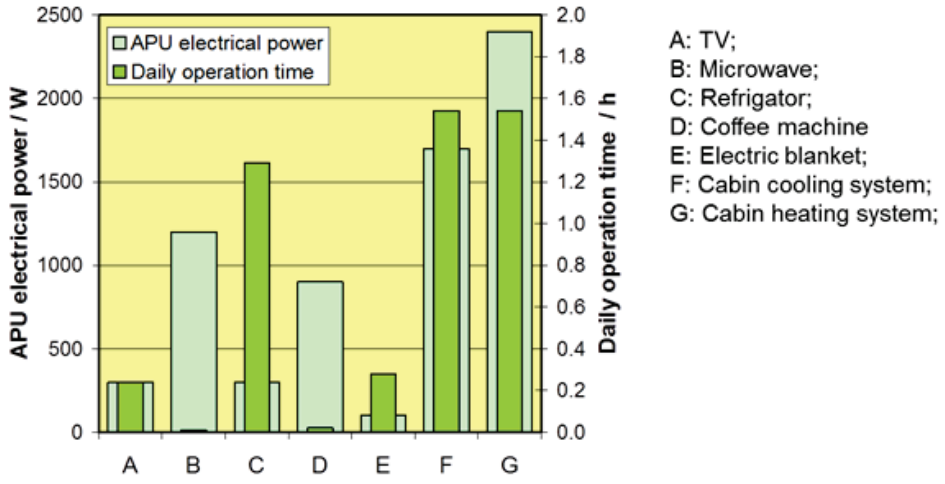

Fig. 125: Consumer-specific APU power and daily operating times for trucks according to [29]

4.2.3 Fuels for fuel cell systems in trucks

What fuels can be used for APUs? Fig. 126 provides an overview of the different options: LPG, alcohols, benzene, kerosene, diesel, heating oil and marine gas oil (MGO) as an example of maritime fuels. Drawing upon the numerous applications, a clear focus is obvious on diesel. The high level of sulfur, the high residue fraction after vaporization, the high concentrations of aromatics – particularly multinuclear aromatics – represent a huge challenge in terms of reforming heating oil and maritime fuels. Kerosene contains a large proportion of sulfur-containing components. Research and development activities in the area of desulfurization are being pursued in other projects [35, 36].

[35] Peters, R., Latz, J., Pasel, J., Stolten, D. (2008) Desulfurization of Jet A-1 and Heating Oil: General Aspects and Experimental Results, in *ECS Transactions,* **12** (1), 543-554

[36] Latz, J., Peters, R., Pasel, J., Datsevich, L., Jess, A. (2009) Hydrodesulfurization of jet fuel by pre-saturated one-liquid-flow technology for mobile fuel cell applications. *Chemical Engineering Science,* 64, 288-293

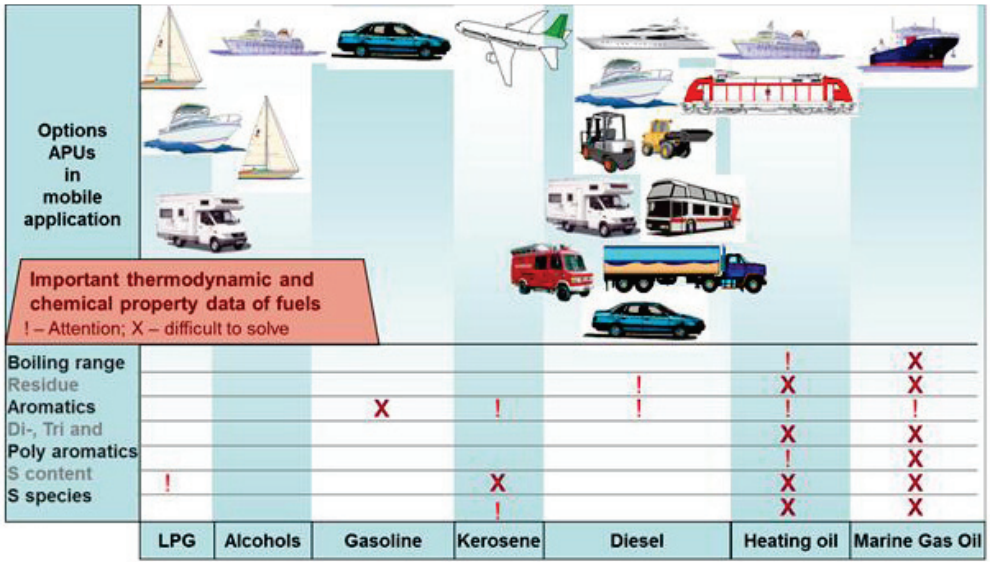

Fig. 126: Fuels and applications for auxiliary power supply

One possible solution for the use of fuel cells for auxiliary power supply in applications that have no suitable fuel available is to install an independent fuel supply system for the APU.

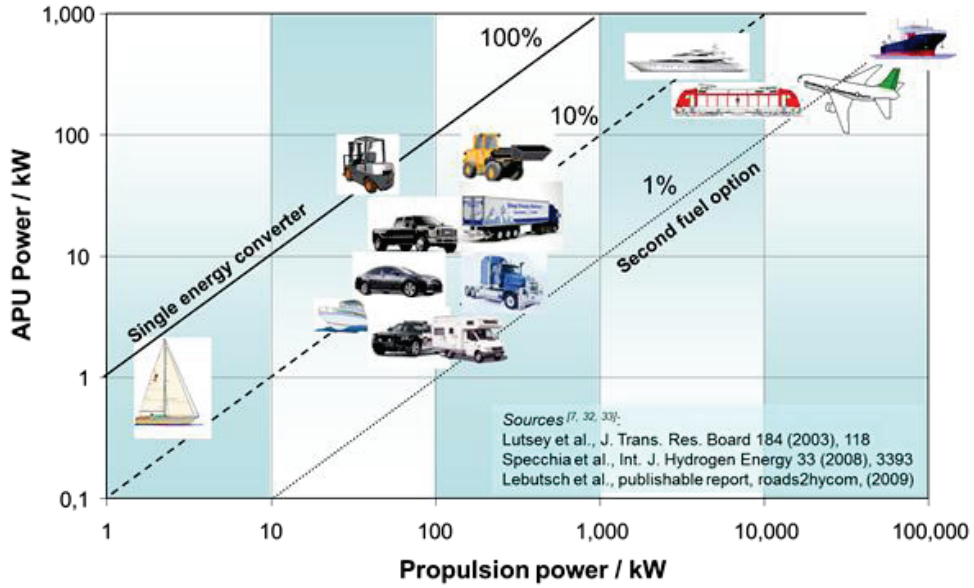

Fig. 127: APU and driving powers for different mobile applications

Fig. 127 shows the ratio of APU to driving power for different applications. If the required APU power is the same order of magnitude as the drive, then an efficient energy converter should be used. If the ratio is approx. 1:10, the fuel used for the drive should also be used for

the APU. If the ratio is 1:100, a second fuel tank can be considered. This solution is often used for maritime applications for MCFC with LNG (liquid natural gas) as an energy carrier [37].

4.2.4 System architectures for fuel cell systems in trucks

What types of fuel cells can be used for system development? In the power class 500 W_e–5 kW_e, for example, DMFCs can be used for sailing yachts [38], PEFCs and DMFCs for light traction and portable applications [39]. For vehicle drives, PEFCs in the power class of 50–100kW_e generally use hydrogen as an energy carrier and are not suitable for operation with reformate. SOFCs in the 5 kW_e power class are being developed by Delphi in the USA [40, 41, 42, 43]. In Europe, development was originally pursued by Webasto [44] before being taken over by Enerday GmbH and finally being terminated in 2010 [45]. From the area of stationary fuel cell development, the MCFC is currently used for maritime fuel cells [37, 46]. The power range of the MCFC is 250–320 kW_e. This cell type is not suitable for use in aviation applications or for small power ranges.

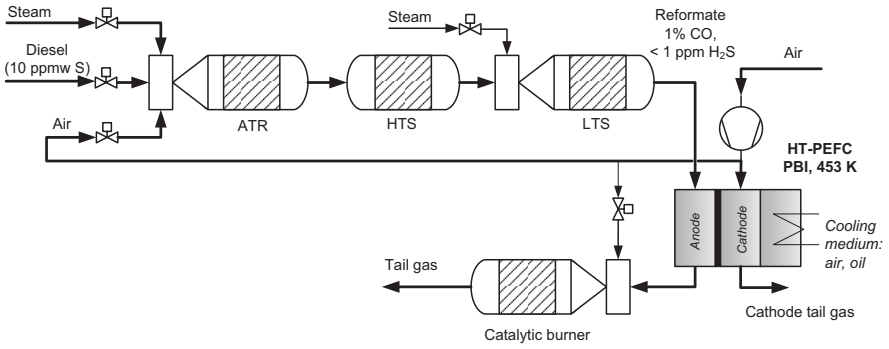

Fig. 128: Flow chart: HT-PEFC system in combination with autothermal reforming of diesel

---

[37] Bordstromversorgung für Schiffe – das HotModule lernt schwimmen, BWK 61 (2009) 11, 20-21

[38] SFC bringt Brennstoffzelle für Segelyachten auf dem Markt, http://www.innovations-report.de/html/berichte/energie_elektrotechnik/bericht-38537.html (January 16, 2010)

[39] Garche, J.: Portable Applications and Light Traction, in Hydrogen and Fuel Cells, (ed. D. Stolten) Wiley-VCH, Weinheim (2010), pp. 715-732

[40] Shaffer, S.: Development Update on Delphi's Solid Oxide Fuel Cell System, 2005 SECA Review Meeting, April 20, 2005, Pacific Grove, CA, USA

[41] Blake, G.D.: Solid Oxide Fuel Cell Development for Auxiliary Power in Heavy Duty Vehicle Applications. DoE Peer Review 2008, http://www.hydrogen.energy.gov/pdfs/review08/fc_44_blake.pdf (November 16, 2009)

[42] Mulot, J., Niethammer, M., Mukerjee, S., Haltiner, K., Shaffer, S.: in Proceedings of Fundamentals & Development of Fuel Cell Conference, December 10-12, 2008, Nancy, France

[43] Kerr, R.: presented at the 2009 SECA Annual Meeting, June 14-16, 2009, Pittsburgh, PA, USA

[44] Stelter, M., Reinert, A., Mai, B.E., Kuznecov, M.: Engineering aspects and hardware verification of a volume producible solid oxide fuel cell stack design for diesel auxiliary power units. J. Power Sources 154 (2006), 448 – 455

[45] http://www.b4bmv.de/Mittelstand/Regionale-Wirtschaftsnachrichten/Mecklenburgische-Seenplatte/arid,50585_puid,14_pageid,657.html (September 01, 2010)

[46] Klinder, K.: Das Leuchtturmprojekt e4ships, Rostock-Warnemünde (2009), www.now-gmbh.de/uploads/.../e4ships_090701_PK-Praesentation.pdf (January 18, 2010)

At IEK-3, the HT-PEFC is used for in-house system development and for funding projects, and the SOFC is used as a component for system developers within funding projects. Fig. 128 shows a simplified process flow chart for HT-PEFC systems in combination with autothermal reforming of diesel. The autothermal reformer produces a product gas (reformate) with approx. 8 - 10 vol.% carbon monoxide. In a two-stage shift process with the addition of water, the amount of carbon monoxide is reduced to around one percent. The gas is fed into the fuel cell at temperatures between 160 °C and 180 °C. The residual gas is combusted in a catalytic burner.

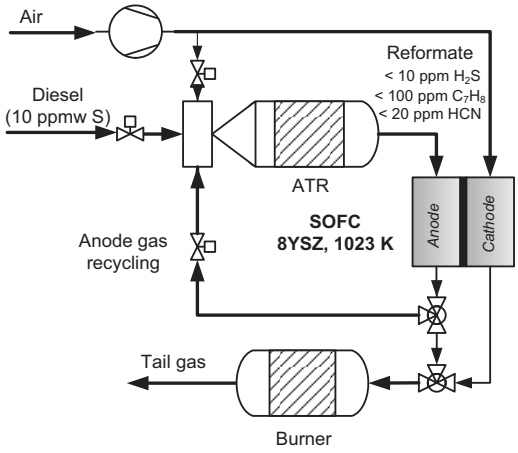

Fig. 129: Flow chart for an SOFC system in combination with diesel reforming. The diesel is reformed by means of partial oxidation. Adding steam from anode gas recycling results in a quasi-autothermal process

Fig. 129 shows a simplified process flow chart for an SOFC system in combination with diesel reforming. When both figures are compared, it becomes clear that the construction of the SOFC system is much simpler. Reforming occurs in principle with air and diesel alone – so-called partial oxidation. If this is performed catalytically, it is referred to as a CPOX process. This process tends to create more carbonaceous deposits. In order to counteract this, the anode exhaust gas is recirculated in a cycle. The anode exhaust gas also contains steam, ultimately giving rise to autothermal reforming.

In the following section, we will look at the SOFC development for application in trucks. The development of HT-PEFC systems will be looked at in more detail for aeronautical applications.

4.2.5 SOFC development for APUs in trucks

4.2.5.1 Optimization off efficiency

Together with industry partners such as Eberspächer, ElringKlinger, Behr, Ceramtec and ThyssenKrupp, BMW has pursued the utilization of lightweight SOFCs for on-board power

supply in passenger cars since 2004. Although progress was made in the development of robust high-performance stacks, BMW came to the conclusion that SOFCs are currently not suitable for use in APUs in passenger cars as they will be unable to fulfill extreme requirements in terms of heating times and dynamics in the near future. Eberspächer then took over as leaders of the system development project (ENSA) with the support of ElringKlinger, who took over as leaders of the stack development project (ZeuS). Both companies have since stopped developing SOFC APUs for use in passenger cars, and have concentrated their development efforts on APUs for trucks and commercial vehicles, which have much lower dynamic requirements. Due to more stringent legislation on idling engines (for example, in parking lots), particularly in the USA, environmentally friendly and efficient solutions for producing the necessary auxiliary power are being sought all over the world. The new consortium comprises Eberspächer, ElringKlinger and Behr – supported by Forschungszentrum Jülich, DLR Stuttgart, the University of Karlsruhe and Oel-Waerme-Institut (OWI) Aachen – and it aims to operate the first demonstration system in a truck within the next few years.

In addition to low noise pollution and no vibrations, efficiency is an important aspect when deciding on an APU system.

For diesel operation, a reformer is connected upstream of the actual fuel cell system. In the reforming process used (partial oxidation with steam from recirculation), the reformer demonstrates an efficiency of around 75 %. This results in the following potential efficiency.

The electrical net efficiency of a fuel cell system can be determined as the product of various individual efficiencies:

$$\eta_{el} = \eta_{Reformer} \times \eta_z \times u_F \times \eta_p \times \eta_{Inv}$$

In addition to the reformer efficiency $\eta_{Reformer}$, the cell efficiency η_z is an important parameter that describes the performance of the cell as the ratio of cell voltage to calorific voltage. The fuel utilization u_F accounts for the proportion of fuel that is converted into electric current. The system's internal electrical consumption is accounted for by η_p and the conversion losses at other voltage levels or for alternating voltage is represented by η_{Inv}.

Fig. 130 assumes an energy input of 9 kW into the system in the form of diesel, which causes losses in the individual efficiency levels. The first clear decrease is caused by the reformer. Of the 9 kW heat originally contained in the diesel, only 6.8 kW are contained in the product gas. Of this, 5.4 kW are used electrochemically in the fuel cell, which at a cell voltage of 700 mV results in an electrical power of 2.9 kW. Inverter losses and the system's own consumption lead to a net power of 2.2 kW, which corresponds to an electrical net efficiency of around 25 %. This clearly shows that the development potential particularly in relation to the cell must be fully exploited.

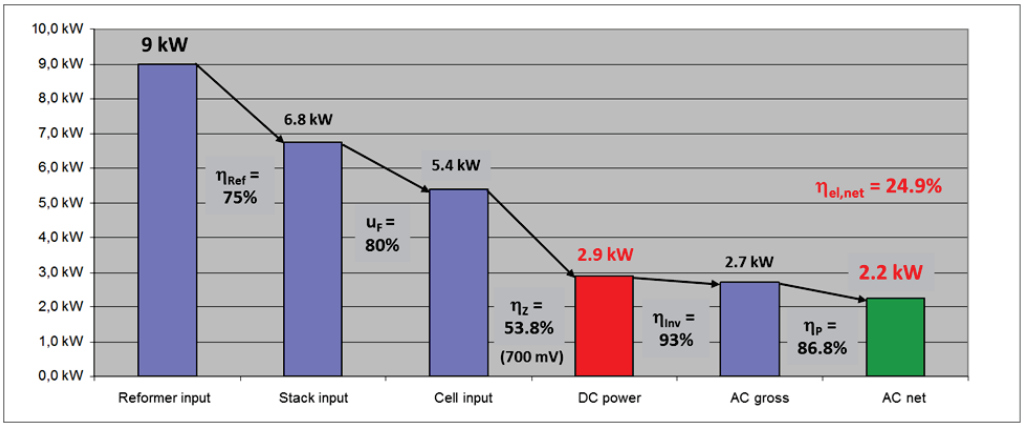

Fig. 130: Power losses in a current APU system based on diesel

What the optimization of the various components can achieve is shown in Fig. 131. In addition to increased fuel utilization and a slight improvement in the inverter efficiency, increasing the cell voltage to 800 mV, in particular, leads to significant improvements. This is also decisive for improving the efficiency of the system's own consumption as smaller losses in the cell mean less waste heat, which in turn means that less air is required for cooling. This then reduces the pressure loss in the system, and both lead to a lower fuel consumption of the air compressor. In this combination, the optimized system can achieve an efficiency of 35 %.

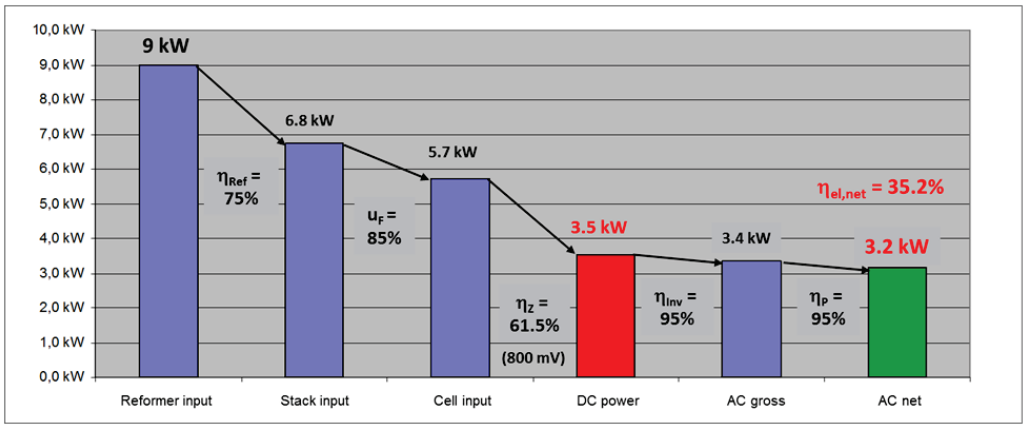

Fig. 131: Power losses in an optimized APU system based on diesel

4.2.5.2 Operating tests on APU SOFC stacks

In the area of APU applications, the demands made on stacks are much more difficult to satisfy than those in the area of stationary applications due to dynamic operation. A new stack design was therefore developed. This CS design for lightweight APU SOFC stacks is based on thin metal sheets, which can be processed using conventional forming techniques.

Two sheets are combined to form a cassette, in which the planar anode substrate cell is integrated. The cassettes containing the cells form the repeating units from which the stacks are assembled. The cassettes are joined together using a glass-ceramic seal. This seal ensures that the gas compartments remain separated and electrically insulates the different layers from each other. A wave profile in the lower section of the cassette distributes the operating gases homogeneously over the cell area. The waves simultaneously fulfill the function of the interconnect, i.e. they electrically connect the cathode of one cell to the anode of the next cell.

The dynamic operation of an APU SOFC system is highly demanding particularly when the stack is rapidly heated to operating temperature and when it is switched off. The fast temperature changes in the stack can cause large temperature gradients and corresponding thermal stresses, which can lead to failure of individual components and interfaces. In addition, starting up or shutting down the system gives rise to a gas exchange on the fuel gas side of the stack. At higher temperatures, in particular, this can damage the anode substrate cells as a result of nickel oxidation in the substrates. In order to test the resistance of the stack to these temperature changes and gas exchange, the stacks were subjected to thermal and redox cycling.

Redox cycling was performed on stack CS05-22 to simulate system sweeping with air on the fuel gas side when the system is started. A set amount of air (0.184 ml/min for a stack with five levels) was supplied to the fuel side of the stack for 10 minutes. For safety reasons, the combustion gas chamber was purged for two minutes with argon in the laboratory both before and after the hydrogen was added. A series of redox cycles were first performed at an operating temperature of 600 °C. The redox cycles were interrupted at irregular intervals for characteristic measurements at 750 °C. After 150 redox cycles had been successfully completed at 600 °C, the temperature was increased to 700 °C for further redox cycling. After 23 redox cycles at 700 °C, the first slight drop in the cell voltage of one level was observed. Further 58 cycles were performed. The experiment was terminated due to a sharp drop in the open cell voltage (OCV) in two of the five levels in the stack.

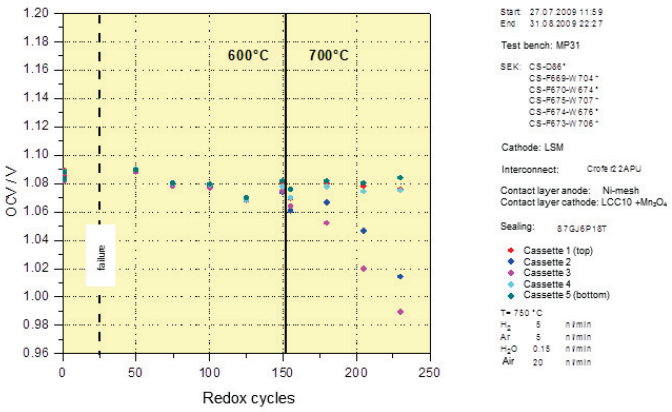

Fig. 132: OCV at the beginning of the characteristic measurements as a function of the number of redox cycles

The characteristics recorded between the various redox cycles were analyzed according to OCV at the beginning of the curves (Fig. 132), ASR (gradient of the characteristic for increasing current between 0.75 V and 0.85 V) (Fig. 133), and the power density at 0.7 V (Fig. 134). The observation of a drop in OCV in cassette 3 is confirmed in Fig. 132. Furthermore, this figure also shows a clear decrease in the OCV of cassette 2. This drop in OCV is a clear indication of a steadily increasing leak. The leakages that occur do not appear to influence the ASR. In relation to the power densities of the cells, only the last characteristic measurements reveal a decrease in power for cassette 3 and to a smaller degree for cassette 2. A malfunction, which automatically shut down the test stand and caused a thermal cycle, had a clearer impact on the ASR and power density. The ASR values after the malfunction are much higher and they drop back to their initial values over time.

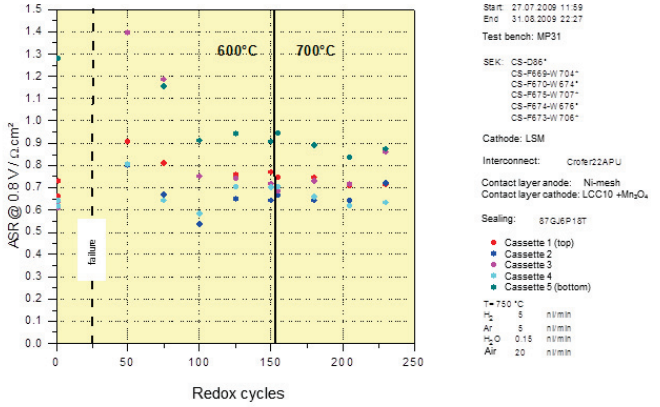

Fig. 133: ASR at 0.8 V as a function of the number of redox cycles

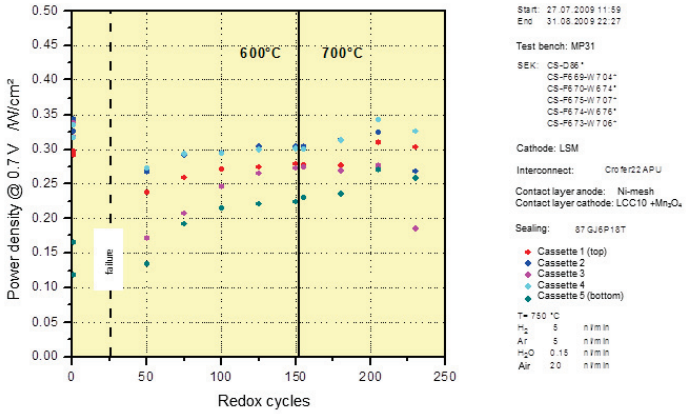

Fig. 134: Power densities of the cells at 0.7 V as a function of the number of redox cycles

Something similar can be seen in Fig. 134. The power density drops after the malfunction and then slowly begins to recover. In similar tests on other stacks, just as was the case for stack CS05-22, no changes were observed in the OCV and ASR values during redox cycling at 600 °C. Redox cycling at 700 °C led to more frequent failures of one or more of the stack levels. Important constraints can be derived from these findings for operating strategies when starting up the system.

Another stack was subjected to thermal cycling. Stack CSII05-04 was thermally cycled 100 times between operating temperature (750 °C) and room temperature (< 50 °C), in line with a procedure derived from the specifications for system start. The system was heated at a rate of 10 K/min. After it was heated up, the stack was then operated at an operating temperature of 750 °C for a period of 2 hours at constant current and characteristic measurements were recorded for each corresponding cycle. The stack was finally allowed to cool down to room temperature in its thermal insulation. The characteristics were recorded for each cycle and they were also analyzed according to OCV at the beginning of the curves, ASR (gradient of the characteristic for increasing current between 0.75 V and 0.85 V), and power density at 0.7 V. These data are shown in Fig. 135 as a function of the number of cycles. The large scattering of ASR values is caused by an artifact in the characteristics that prevents precise determination. Despite this, a slight increase was observed. Accordingly, the power of the stack also decreases with an increasing number of cycles, and the OCV values also exhibit a slight decrease. However, after 100 thermal cycles were completed, the main aim of the experiment had been achieved.

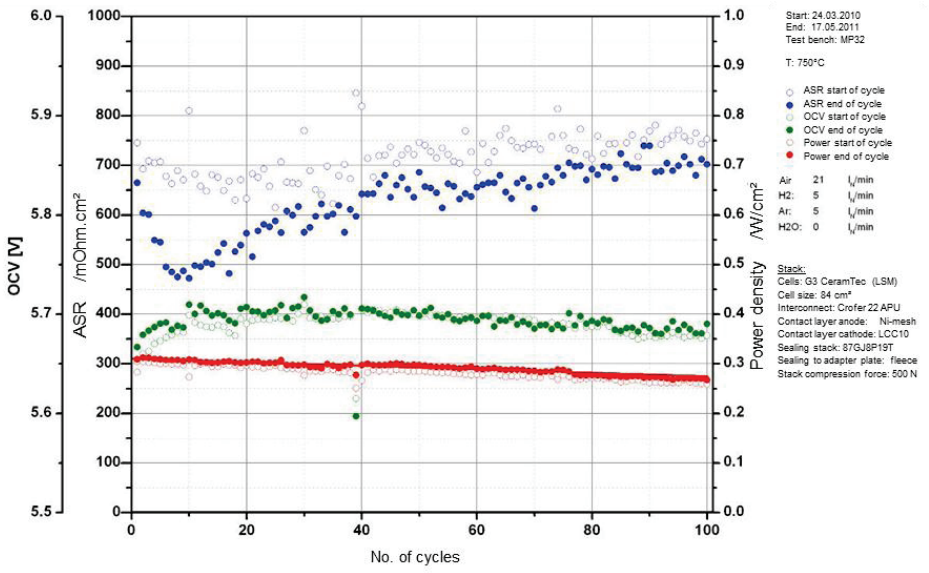

Fig. 135: Characteristics (OCV, ASR and power density) as a function of the number of thermal cycles for the stack CS^{II}05-04

4.3 Fuel cell APU for aircraft

4.3.1 Motivation for fuel cell systems in aircraft

The use of fuel cell systems as auxiliary power units (APUs) in aircraft was suggested in 2001 by Seidel et al. [47]. Conventional APUs based on gas turbines can only achieve a maximum efficiency of 20 % if operated when the aircraft is on the ground. When operated on the ground, fuel cell systems with a potential efficiency of up to 40 % have significant advantages. With efficiencies of 40 %, on-board power supply during the flight using conventional APUs is already extremely efficient [48].

Boeing therefore set high target efficiencies of 75 % for fuel cell systems as they must be able to compete with conventional APUs during the flight [49]. Hybrid systems comprising an SOFC and gas turbines were thus designed and simulated for process analysis [49, 50, 51]. Such systems must be designed for SOFC operation at high operating pressures and temperatures and they must accommodate the use of micro gas turbines. In a series of studies, efficiencies between 32 % and 65 % were calculated [50, 51, 52, 53]. As the technology for realizing such systems is not yet available, no further work was conducted or published.

Airbus Deutschland GmbH is cooperating with project partners, including Forschungszentrum Jülich, on the concept of a multifunctional fuel cell. Conventional systems on board aircraft often have only one single function. Electrical energy is supplied by generators located close to aircraft engines, conventional APUs, and by batteries. A fuel tank inerting system (FTIS) is used to inert the tank. The water required for this task is stored in additional tanks on board the aircraft. These individual systems increase the weight of the aircraft and make their architecture more complicated. The use of fuel cell systems as multifunctional units on board aircraft makes it possible to provide functions such as energy conversion as well as the production of water and inert gas with the aid of one single system. Water tanks, conventional APUs and FTISs could then all be dispensed with and generators and batteries could be downsized. These measures would reduce fuel consumption, increase the overall efficiency of an aircraft and enable the low-emission operation of aircraft

---

[47] Seidel, J.A., Sehra, A.K., Colantonio, R.O.: NASA Aeropropulsion Research: Looking Forward, Proceedings of the 15th ISABE Bangalore, India, June 2-7, 2001, NASA/TM-2001-211087, National Technical Information Service, Springfield, USA

[48] Peters, R. und Westernberger, A.: Large Auxiliary Power Units for Vessels and Airplanes, in Innovations in Fuel Cell Technologies, Eds. Steinberger-Wilckens, R. and Lehnert, W., RSC publishing, Cambridge (2010), United Kingdom, pp. 76 – 148

[49] Daggett, D., Freeh, J., Balan, C., Birmingham, D.: Proceedings of the Fuel Cell Seminar (CD), September 3-7, 2003, Miami, FL, Courtesy Associates, Washington

[50] Srinivasan, H., Yamanis, J., Welch, R., Tilyani, S., Hardin, L.: Solid oxide fuel cell APU feasibility study for a long range commercial aircraft using UTC ITAPS Approach, Vol. I: Aircraft propulsion and subsystem integration evaluation, NASA/CR- 2006- 214458/VOL1, National Technical Information Service, Springfield, USA

[51] Gummalla, M., Pandy, A., Braun, R., Carriere, T., Yamanis, J., Vanderspurt, T., Hardin, L., Welch, R.: Fuel Cell Airframe Integration Study for Short-Range Aircraft, Vol. 1: Aircraft Propulsion and Subsystems Integration Evaluation, NASA/CR- 2006-214457/Vol. 1, National Technical Information Service, Springfield, USA

[52] Mak, A., Meier, J.: Fuel Cell Auxiliary Power Study, Vol. I: RASER Task Order 5, NASA/CR-2007-214461/Vol. 1, National Technical Information Service, Springfield, USA

[53] Dollmeyer, J., Bundschuh, N., Carl, U.B.: Aerospace Science and Technology, 10 (2006), 686-694

in flight and, in particular, on the ground. From an economic perspective, this means that cost-intensive airport equipment such as that required for refilling the water tanks would no longer be necessary. Furthermore, eliminating the above-mentioned systems would reduce the cost of purchasing, maintaining and operating aircraft. The aviation industry also aims to use alternative fuels in fuel cell systems in future generations of aircraft. An example of such a fuel is an alternative synthetic fuel produced using the bio-to-liquid (BTL) process. The relevance of fuel cell technology is therefore high in terms of conserving resources and protecting the environment.

4.3.2 Need for electrical energy in aircraft

Fig. 136 shows details of the electrical energy required in aircraft according to two studies conducted by NASA [50, 51]. Both studies first looked at APU operation on the ground. The profile in NASA/CR-2006-214457[51] assumes a maximal APU power of 260 kW_e and in NASA/CR-2006-214458 [50] of 450 kW_e. In [51], four flights per day and a flight duration of 150 min (taxi out – taxi in) are assumed. In [50], Srinivasan et al. initially assume a flight duration of approx. 1000 min, which is equivalent to a long-haul flight. For the further analyses, two short-haul flight profiles of 500 NM (nautical miles) – corresponding to approx. 926.6 km – and 1,000 NM (1853 km) are considered. The routes are flown four to six times on a daily basis. The respective flight durations are 90 min and 150 min. In Fig. 136, it can be seen that for the 500 NM short-haul flights, two hours of 450 kW_e each are required by the NASA/CR-2006-214458 profile for passenger boarding (E). Using these data, daily energy demands of 1,550 kWh [51], 2464 kWh [1,000 NM, 50] and 3,373 kWh [500 NM, 50] can be derived. Kerosene consumption for conventional APUs at an assumed efficiency of 20 % is then calculated as 865 l/day [51], 1375 l/day [1,000 NM, 50] and 1882 l/day [500 NM, 50]. The corresponding CO_2 emissions are 2 t/day, 3.1 t/day and 4.3 t/day. When an efficiency of 40 % is assumed for an SOFC fuel cell system, the kerosene consumption is halved, as are the CO_2 emissions [50, 51].

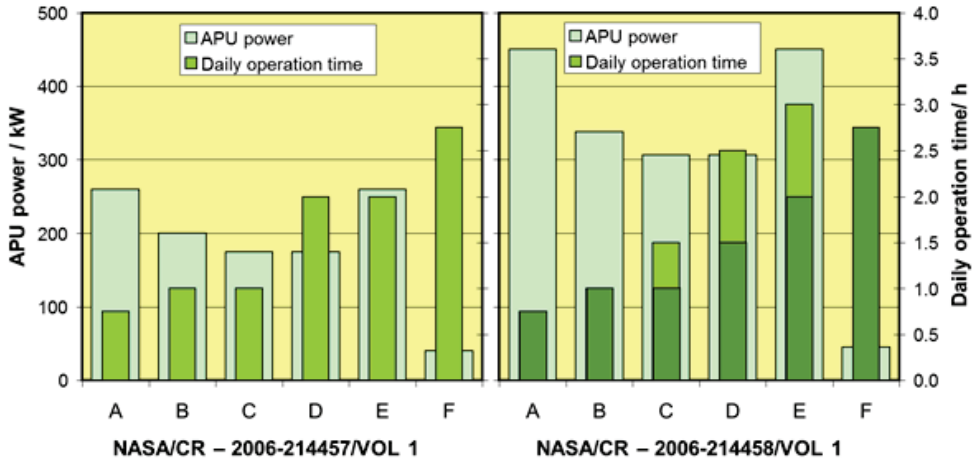

Fig. 136: APU power and daily runtimes for profiles taken from two NASA studies [51 (left), 50, (right)]. A: "Cabin pull down"; B: Maintaining cabin air conditioning; C: Passenger deplaning; D: Service; E: Passenger boarding; F: Maintenance

Fully replacing APUs with fuel cell systems would require an electrical power of 450–550 kW according to [50]. An additional power of up to 425 kW may be necessary to operate an electric “anti-icing” device. In [51], these figures are max. 260 kW for flight operation and another 100 kW for the anti-icing option. According to [50], the effects of more efficient on-board power supply using fuel cell systems on the ground are clearer for short-haul flights than for long-haul flights of 14,720 km. During the flight, similar efficiencies are generated by conventional systems with a turbine and generator and by SOFCs. It therefore does not yet make sense to fully replace conventional methods of power supply with fuel cell technologies. Additional installed APU power in the form of fuel cells can, however, provide auxiliary electric devices such as anti-icing systems with power. Other products such as the water formed in fuel cell systems or its off-gases (tank inerting) would then determine the capacity of the fuel cell APU. In addition, there is a clear advantage in terms of the very low limited emissions for fuel cell APUs [50, 51].

Tab. 12 provides an overview of the achievable amounts of water. Accordingly, a hydrogen system with 240 kW_e (60 % of 400 kW_e) would be required to produce approx. 100 l water per hour. A system with autothermal reforming would have to be operated at 400 kW_e to produce the same amount. For a system with 260 kW_e [51] estimates a usable heat of 325 kW_{th} for an HT-PEFC operated on kerosene and of 260 kW_{th} when it is operated on H_2 [54]. It would therefore make sense to use these heat flows in the existing anti-icing system.

Case	2 x 100 kW_e	4 x 100 kW_e
Operating time	1.5 h	8.5 h
Energy (100 %)	600 kWh	6800 kWh
Mass H_2	18.2 kg	226.0 kg
Volume (1 atm.; 21 K, 90 %)	0.3 m³	3.58 m³
Water production @ 60 % loading of the stack ($\Rightarrow\eta$ = 50 %)	7.3 kg H_2 for 52.4 kg H_2O (1 h)	116.4 kg H_2 for 837.8 kg H_2O (8 h)
Electricity production @ 60 % loading (η = 47.5 %)	7.7 kg H_2 (1 h)	122.5 kg H_2 (8 h)
60 % loading at η = 40.0 %	25.2 kg JET A-1 (1 h)	401.9 kg JET A-1 (8 h)

Tab. 12: Case studies for multifunctional systems with hydrogen as an energy carrier according to [48]

With respect to tank inerting, the off-gas of a fuel cell system with an electrical power of 20 kW is sufficient for an Airbus A320. This power class is equal to that required for the use of ram air turbines (RAT). PEFCs with a H_2/O_2 feed were tested in this regard. As it is expected that electric systems in aircraft will be more efficient in future, APU systems can be

[54] Peters, R., Latz, J., Pasel, J., Samsun, R.C., Stolten, D.: Final report on the ELBASYS (Elektrische Basissysteme in einem CFK-Rumpf) collaborative project, subproject: Brennstoffzellenabgase zur Tankinertisierung (Fuel cell off-gases for tank inerting), Schriften des Forschungszentrums Jülich, Reihe Energie & Umwelt, Vol. 46 (2010), Forschungszentrum Jülich

equipped with lower powers of 100 – 150 kW_e [55]. An essential function of today's APU turbine is the provision of bleed air to start up the turbine. Boeing is currently planning the "Dreamliner 767" without the use of bleed air. The turbines are kick started into operation electrically via starter generator units.

4.3.3 System architectures for fuel cell systems in aircraft

Airbus Deutschland GmbH and Forschungszentrum Jülich GmbH currently favor the use of the high-temperature PEFC as a fuel cell with the energy carriers hydrogen and BTL kerosene [48, 54]. Hydrogen should be stored in liquid form on board the aircraft. In the following, other process variations will be considered with PEFCs, HT-PEFCs and SOFCs.

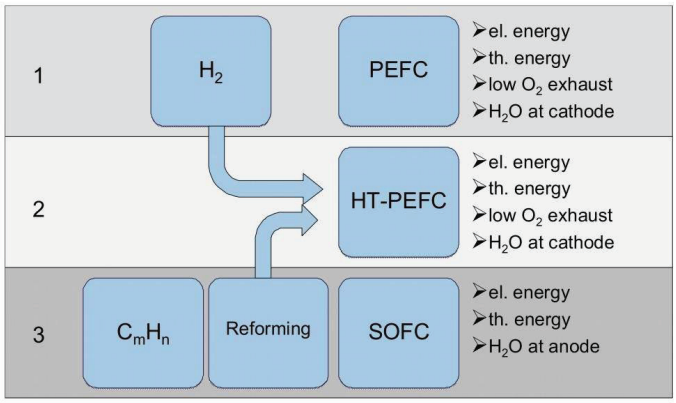

Fig. 137: Options for the use of fuel cells in aircraft [48]

Fig. 137 shows the two favored process chains in a chart. In chain 1, hydrogen is used as a fuel for the PEFC. This design variant is also preferred in vehicles with the difference that Airbus aims to store hydrogen in liquid form, whereas the storage of gaseous hydrogen is preferred in automotive systems. The third chain combines the reforming of kerosene with the SOFC. The HT-PEFC features as the center of the diagram. From a technological point of view, other options are possible. However, in multifunctional systems, they have disadvantages in terms of water production and the use of off-gases for tank inerting.

Peters et al. [54] calculated efficiencies for all fuel cell types considered here – PEFC, SOFC and HT-PEFC – within a range of 20 % to 55 %. Cell voltage and hydrogen utilization had the largest influences on efficiency. The influence of pressure was considered without additional dependences. In this case, an increase in pressure caused by an increasing compression power for cathode air has a negative impact on the efficiency. In the HT-PEFC, however, for constant current density, the individual cell voltages increase significantly with increasing pressure. This enables more compact stacks to be built for higher operating pressures of up to 3 bar for the same efficiencies. Under the same external conditions (p_{sys} = 1.1 bar, U_{Zelle} = 750 mV), the following efficiencies can be achieved:

---

[55] Heinrich, H.J.: presented at Symposium der Wasserstoffgesellschaft Hamburg, October 18 2007, http://www.h2hamburg.de/index.php?page=download (November 18, 2009)

- 38.5 % for the autothermal reforming of kerosene combined with an HT-PEFC with a hydrogen utilization of $\eta_{H2,Nutz}$ = 90 %.
- 42.3 % for the steam reforming of kerosene combined with an HT-PEFC and a hydrogen utilization limited by the heat balance of $\eta_{H2,Nutz}$ = 75 %; (first law of thermodynamics)
- 36.1 % for autothermal reforming of kerosene combined with preferential oxidation (PROX) for CO fine cleaning and a PEFC with a hydrogen utilization limited by the heat transfer of $\eta_{H2,Nutz}$ = 84%; (pinch point; second law of thermodynamics)
- 50.2 % for the HT-PEFC with hydrogen as an energy carrier with a hydrogen utilization limited for comparative purposes to 90 %
- 50.5 % for the PEFC with hydrogen as an energy carrier with a hydrogen utilization limited for comparative purposes to 90 %

4.3.4 Fuels for fuel cell systems in aircraft

According to specifications, the turbine jet fuel Jet A-1 can contain up to 3,000 ppmw sulfur. Reforming catalysts, however, can only tolerate around 10 ppmw S. At the moment, refineries do not desulfurize Jet A-1 to 10 ppmw S. Desulfurization at centralized stations in airports or in small decentralized plants at the gate or on board necessitates technologies other than hydrodesulfurization, which is used in refineries for the desulfurization of benzene and diesel. Desulfurization in the liquid phase is required. A possible process is hydrofining with presaturated hydrogen [56]. Experimental investigations have shown that at a pressure of 24 bar and a temperature of 390 °C, Jet A-1 can be desulfurized from 700 ppmw S to 8.3 ppmw S. The resulting H_2S must be removed via hydrocyclone and combusted in the aircraft turbines. Sulfur therefore leaves the system as SO_2.

Tab. 13 shows the most important material characteristics of the fuel currently used in the aviation sector. As an alternative to Jet A-1, the first and second generation biofuels and liquid hydrogen can be used. Data for other fuels can be found in [48].

[56] Latz, J., Peters, R., Pasel, J., Datsevich, L., Jess, A. (2009) Hydrodesulfurization of jet fuel by pre-saturated one-liquid-flow technology for mobile fuel cell applications. *Chemical Engineering Science,* 64, 288-293

Fuels	Energy densities		Source/Chain	Primary energy consumption	CO_2 emission
	MJ l^{-1}	MJ kg^{-1}		MJ MJ^{-1}_{Fuel}	$g_{CO_2eq.}$ MJ^{-1}_{Fuel}
Kerosene[1]	34.9	43.2	Crude oil	0.13	10.7
Hydrated vegetable oil, NExBTL[4]	34.4	44.0	Palm oil/ *"hydrotreatment"*	1.26	49.6[1]
Fischer-Tropsch middle distillate	34.3	44.0	Wood/FT synthesis gas (2nd generation biomass)	1.19	4.8[2]
"Hydrocracked" middle distillate	n.s.	n.s.	Residual oils/ *"hydrocracking"*	n.s.	n.s.
Hydrogen (LH_2)[3]	7	120	Natural gas/electrolysis	1.28	132.8[4]
Hydrogen (LH_2)	7	120	Wood farming/vaporization	1.50	7.5 (6.6–21.2)
1) Methane emissions from process wastes, 2) Waste wood, 3) Liquid hydrogen stored at 0.5 MPa; 26 K, 4) Transport through a natural gas pipeline (4000 km), n.s.) not stated					

Tab. 13: Energy densities, primary energy consumption and CO_2 emissions for different energy carriers according to a well-to-tank analysis [57, 58, 59, 60, 61, 62]. Sources: Primary energy consumption and CO_2 emissions taken from [57] except for (1) taken from [61]; energy densities taken from [57] except for (1) taken from [60], (2, 3) taken from [62]; (4) taken from [59]

4.3.5 Experimental testing of fuel processing components for fuel cell systems in aircraft

The following equations describe the chemical processes that occur during catalytic autothermal reforming (ATR).

$$C_nH_m + n\,H_2O \longrightarrow n\,CO + (m/2 + n)\,H_2 \qquad \Delta H^0_{298} > 0 \qquad (1)$$

$$C_nH_m + n/2\,O_2 \longrightarrow n\,CO + m\,H_2 \qquad \Delta H^0_{298} < 0 \qquad (2)$$

[57] Concawe: Well-to-Tank report Version 3.0 (2008)

[58] Meinert, M.: Wasserstoff Speichertechnologien für Fahrzeuge (Hydrogen storage technologies for vehicles), presented at Seminar Wasserstoff und Brennstoffzellen im Automobil, Haus der Technik Essen, March 11, 2008, Essen

[59] Aatola, H., Larmi, M., Sarjovaara, T., Mikkonen, S.: Hydrotreated Vegetable Oil (HVO) as a Renewable Diesel Fuel: Trade-off between NOx, Particulate Emission, and Fuel Consumption of a Heavy Duty Engine. 2008 SAE International

[60] Chevron Corporation: Alternative Jet Fuels, Addendum 1 to Aviation Fuels Technical Review (FTR-3/A1) (2006)

[61] Wilson, C.: Environmental assessments/initiatives (life cycle assessment, air quality measurement; international initiatives). Presentation, Workshop on Aviation Alternative Fuels 2009

[62] European Commission: Quantification of emissions from ships associated with ship movements between ports in the European Community. Final report, July 2002

The necessary amount of heat required for endothermic steam reforming in equation (1) is provided by the exothermic partial oxidation of the hydrocarbons according to equation (2). The water-gas shift reaction (3) and methanation (4) occur simultaneously.

$$CO + H_2O \longrightarrow CO_2 + H_2 \qquad \Delta H^0_{298} < 0 \qquad (3)$$

$$CO + 3\,H_2 \longrightarrow CH_4 + H_2O \qquad \Delta H^0_{298} < 0 \qquad (4)$$

The reaction parameters derived from these reaction equations are the O_2/C molar ratio, the H_2O/C molar ratio and the kerosene mass flow rate.

For the experiments in the following section, the alternative fuel “Shell MDS Kerosene” was used. Shell MDS Kerosene is a synthetic fuel fabricated in Malaysia from natural gas using the gas-to-liquid (GTL) process. The GTL process is mainly based on a Fischer-Tropsch synthesis. Shell also uses this process in cooperation with Choren to produce bio-to-liquid fuels. In Choren’s BTL process wood is vaporized in a two-stage process and after suitable synthesis gas cleaning is fed into a Fischer-Tropsch process. BTL fuel could not be procured from Choren in the amounts required for the experimental procedure. GTL fuel is an ideal replacement for this fuel because of its similar production process. It can be assumed that the fuels produced in GTL and BTL processes do not differ significantly from each other. The experiments described in the following were performed using an ATR 9.1 autothermal reformer with a thermal power of approx. 20 kW.

A statistical experimental design was derived to characterize the ATR 9.1. It comprises 11 single experiments, in which the O_2/C molar ratio was varied between 0.43 and 0.47, the H_2O/C molar ratio between 1.7 and 1.9, and the kerosene mass flow rate between 1,215 g/h and 2,025 g/h. The influence of these reaction parameters was investigated on characteristic variables, such as the temperatures in the catalyst, concentrations of reaction products in the reformate, and the efficiency of the reforming process. Some of these dependences are presented and described in the following as examples.

Fig. 138 shows the impact of the O_2/C molar ratio and the H_2O/C molar ratio on the temperature in the catalyst of the ATR 9.1 at 5 mm for a kerosene mass flow rate of 2025 g/h (100 % reformer load). Experiments with earlier reformer generations revealed that the very fast kinetics of the exothermic partial oxidation of the hydrocarbons in accordance with equation (2) give rise to high reaction temperatures after a distance of only few millimeters in the axial direction of the catalyst. Fig. 138 shows that high temperatures were also observed during testing of the ATR 9.1 – at times in excess of 1000 °C – in the upper part of the catalyst. The reaction temperatures were higher the greater the O_2/C molar ratio was and the lower the H_2O/C molar ratio was. The maximum temperature was 1025 °C. Higher oxygen partial pressures appeared to benefit the exothermic partial oxidation of the hydrocarbons, which led to an increase in the catalyst temperature. The lower H_2O/C molar ratios reduced the share of endothermic steam reforming in the reaction process as a whole, which also gave rise to increased temperatures in the catalyst. In addition, lower H_2O/C molar ratios led to the enthalpy flow generated by the heating cartridge being reduced in the reformer.

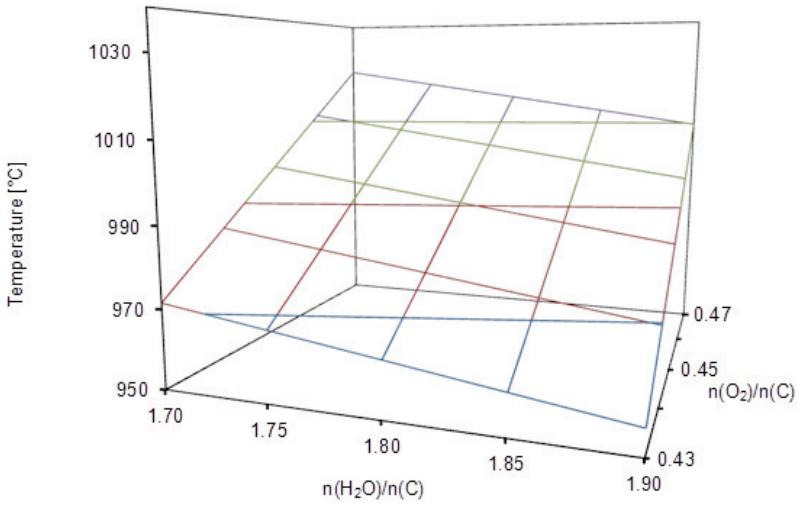

Fig. 138: Impact of the O_2/C molar ratio and the H_2O/C molar ratio on the temperature in the catalyst of the ATR 9.1 at 5 mm for a kerosene mass flow rate of 2,025 g/h (100 % reformer load)

Fig. 138 shows the impact of the O_2/C molar ratio and the H_2O/C molar ratio on the hydrogen concentration in the reformate at a kerosene mass flow rate of 2025 g/h (100 % reformer load). It is clear that the hydrogen concentration in the reformate of the ATR 9.1 is significantly influenced by the O_2/C molar ratio. The average hydrogen concentration was approx. 37.5 vol.% for an O_2/C molar ratio of 0.47 and it increased to an average of 39.0 vol.-% at an O_2/C molar ratio of 0.43. This trend can be explained by the dilution of the reformate with nitrogen at a high O_2/C molar ratio. The impact of the H_2O/C molar ratio in Fig. 139 is not quite as pronounced. Higher H_2O/C molar ratios resulted in higher hydrogen concentrations and vice versa. This trend emerges because higher water partial pressures allow endothermic steam reforming to occur to a much greater extent in accordance with equation (1) than for lower water partial pressures. More water molecules reacted with the hydrocarbon molecules and therefore contributed more strongly to the hydrogen molar flow. This in turn caused the hydrogen concentration to increase. The water-gas shift reaction in accordance with equation (3) was also promoted by a higher partial pressure of water. This had a positive impact on the hydrogen concentration in the reformate.

The experiments described here show that GTL kerosene is suitable for use with ATR 9.1. In all eleven experiments in the statistical experimental design, the hydrocarbon conversion was almost 100 %. The concentrations of organic carbon (TOC) in the aqueous condensate samples from each of the experiments were between 1 mg/l and 1.5 mg/l. This is less than that found in fully desalinated water (2 mg/l).

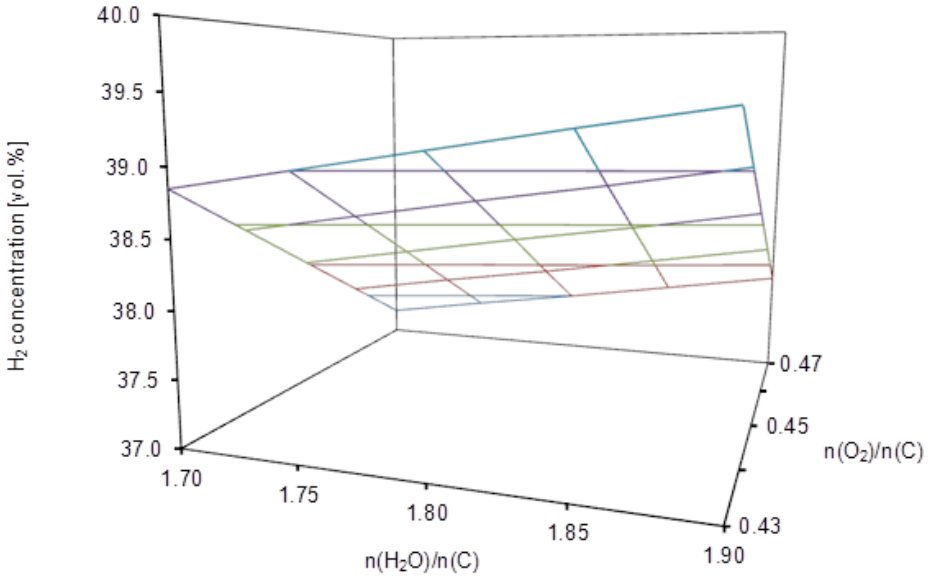

Fig. 139: Impact of the O_2/C molar ratio and the H_2O/C molar ratio on the hydrogen concentration in the reformate of the ATR 9.1 at a kerosene mass flow rate of 2025 g/h (100 % reformer load)

In the 11 experiments, the temperatures in the lower mixing chamber of the ATR 9.1 were identified as being potentially critical. The temperatures there were between 300 °C and 325 °C (not shown in the figures). For synthetic GTL fuel, whose boiling range ends at 200 °C, these temperatures are sufficiently high. However, if the synthetic GTL fuel is used in an aircraft and is mixed with high-boiling aromatic compounds, for example, to ensure that the density value laid down in fuel specifications are met, these temperatures could be too low.

CFD simulations of the mixing chamber for the reformer of the next reformer generation ATR 9.2 therefore aimed to achieve a homogeneous and slightly exothermic prereaction of the fuel with the oxygen in the reformer mixing chamber as this leads to an increase in temperature, which in turn positively affects the targeted full vaporization of the fuel. The prereaction is easier when synthetic fuels are used as these comprise comparatively low-boiling components, which tend to participate in a homogeneous prereaction with oxygen in the mixing chamber.

The ATR 9.2 with a thermal power of 28 kW was also tested experimentally using a statistical experimental design comprising 11 individual experiments. Once again, the O_2/C molar ratio was varied between 0.43 and 0.47, the H_2O/C molar ratio was varied between 1.7 and 1.9, and the kerosene mass flow rate was varied between 1620 g/h and 2700 g/h. The influence of these reaction parameters was again investigated on characteristic variables, such as the temperatures in the reactor, concentrations of reaction products in the reformate, and the efficiency of the reforming process. During tests on the ATR 9.2, particular attention was paid

to whether a homogeneous prereaction occurred and what influence the various reaction parameters had on this reaction.

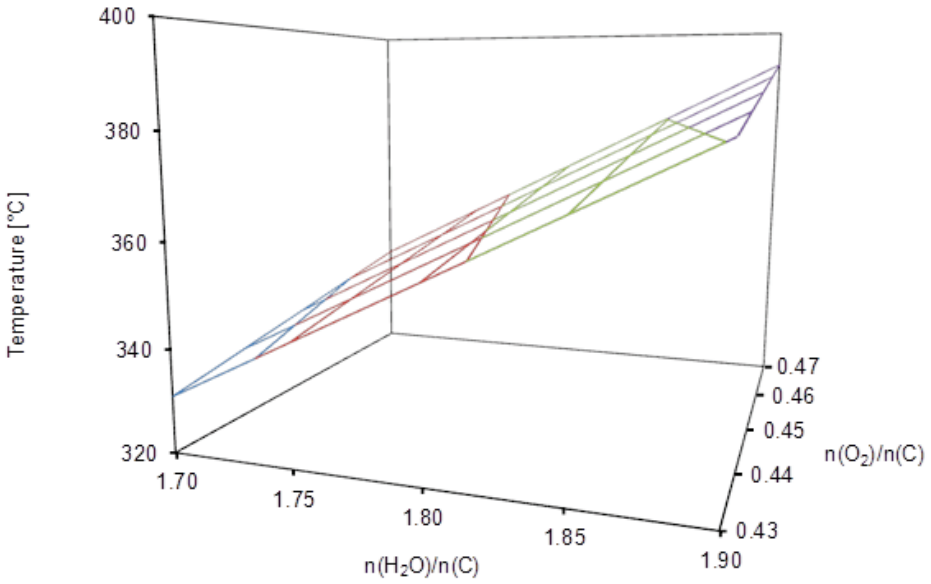

Fig. 140: Impact of the O_2/C molar ratio and the H_2O/C molar ratio on the temperature in the lower mixing chamber of the ATR 9.2 at a kerosene mass flow rate of 2700 g/h (100 % reformer load)

Fig. 140 shows the impact of the O_2/C molar ratio and the H_2O/C molar ratio on the temperature in the lower mixing chamber of the ATR 9.2 at a kerosene mass flow rate of 2700 g/h. In contrast to ATR 9.1, there was a small but clear prereaction of oxygen with the hydrocarbons in the GLT kerosene in the mixing chamber of the ATR 9.2 at a higher water partial pressure. The temperature increased significantly from approx. 330 °C to approx. 380 °C. This observation can be explained by the fact that higher water partial pressures in the educt gas also lead to a higher enthalpy flow entering the reactor. The reduced hydrodynamic residence time of the reactants at a higher H_2O/C ratio had a negative effect on the prereaction. The O_2/C ratio had a very small influence on the temperature in the mixing chamber. Different residence times did not play a role here either.

Fig. 141 shows the impact of the O_2/C molar ratio and the H_2O/C molar ratio on the temperature in the catalyst of the ATR 9.2 beyond 5 mm for a kerosene mass flow rate of 2700 g/h. Similar to the ATR 9.1, the temperatures depended strongly on the oxygen partial pressure. Higher concentrations of oxygen benefited the catalytic partial oxidation of hydrocarbons in accordance with equation (2), while the H_2O/C molar ratio hardly impacted on the temperature in the monolith beyond 5 mm. A clear difference to the experiments with the ATR 9.1 is the temperature level. Depending on the experimental conditions, the temperature varied in ATR 9.1 between 950 °C and 1025 °C. However, for the same experimental conditions, these temperatures in the ATR 9.2 ranged from 820 °C to 880 °C. It

is expected that this much lower temperature level will have a positive effect on the long-time stability of the catalyst in the ATR 9.2. The sintering of the catalyst particles is suppressed by this.

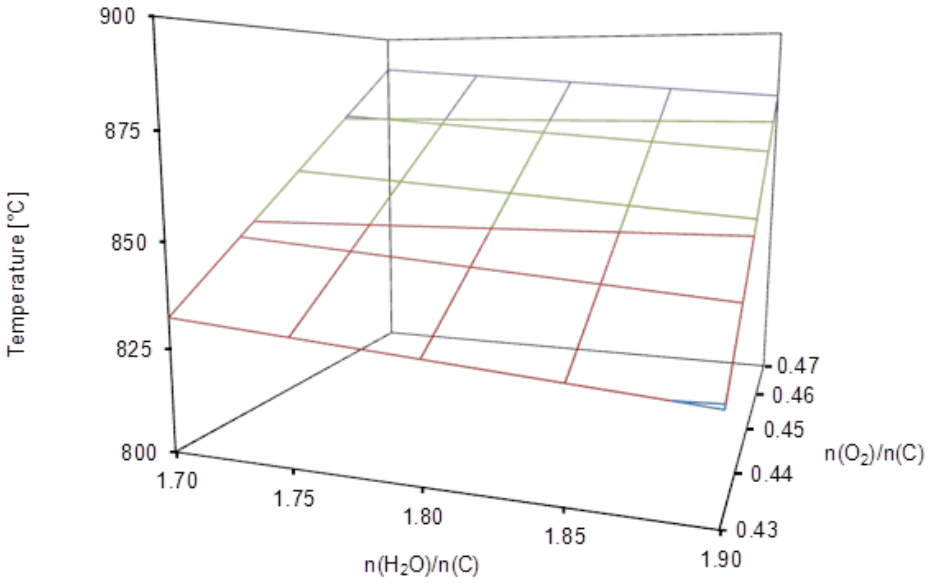

Fig. 141: Impact of the O_2/C molar ratio and the H_2O/C molar ratio on the temperature in the catalyst of the ATR 9.2 beyond 5 mm for a kerosene mass flow rate of 2700 g/h (100 % load)

As the dependences of the hydrogen concentration on the reaction parameters in the reformate of the ATR 9.2 behave in a manner similar to the ATR 9.1 case, they will not be repeated here. Instead, the impact of the O_2/C molar ratio and the H_2O/C molar ratio on the methane concentration in the reformate of the ATR 9.2 will be described and discussed for a kerosene mass flow rate of 2,700 g/h (100 % load). These influences are shown in Fig. 142. A strong influence of the oxygen partial pressure on the methane concentration in the reformate is visible. At an O_2/C molar ratio of 0.47, the methane concentration was found to be 0.5 vol.% This increased to approx. 1.3–1.4 vol.% at an O_2/C molar ratio of 0.43. The causes of this dependence are the temperatures in the catalyst of the ATR 9.2, which also vary strongly depending on the oxygen partial pressure in the educt flow (820 °C – 880 °C), as shown in Fig. 141. Higher oxygen partial pressures led to higher temperatures in the catalyst, which caused a strong shift in the thermodynamic equilibrium of the methanation to the educt side in accordance with equation (4). Higher oxygen partial pressures in ATR 9.2 therefore gave rise to comparatively low methane molar flows and simultaneously higher hydrogen molar flows. This also improved the efficiency of the reforming process. High methane concentrations in the reformate are thus also disadvantageous because methane has to be combusted in the catalytic burner of the fuel processing system and must not be released into the atmosphere. However, methane is a very stable molecule. The amount to be converted is decisive for the design of the catalyst in the catalytic burner and should not

exceed values of more than 1.0 vol.%. Low oxygen partial pressures in the educt flow of the ATR are therefore unsuitable for a fuel processing system. The influence of the water partial pressure on the methane concentration was negligible, as shown in Fig. 142.

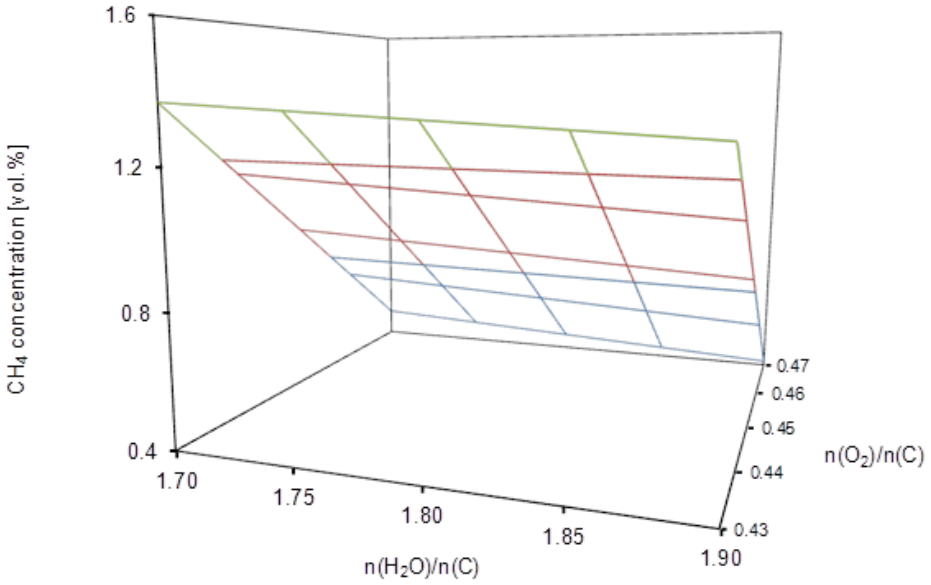

Fig. 142: Impact of the O_2/C molar ratio and the H_2O/C molar ratio on the methane concentration in the reformate of the ATR 9.2 at a kerosene mass flow rate of 2700 g/h (100 % load)

Further experimental testing of the ATR 9.2 involved a load change test at an O_2/C molar ratio of 0.47 and a H_2O/C molar ratio of 1.9. Approx. 40 consecutive cycles were completed in this test. In each cycle, 16 different load points were set between 60 % and 100 %. This corresponds to kerosene mass flow rates of between 1620 g/h and 2700 g/h. The residence time at each of the load points varied between 2 and 10 minutes. The entire experiment took around 70 h. Fig. 143 shows the temperatures in the lower mixing chamber of the ATR 9.2 during the experiment as well as those in the monolithic catalyst beyond 5 mm and 140 mm in the axial direction. For the sake of clarity, only the time interval between 30 h and 40 h is shown here. Depending on the individual load points, the temperature in the lower mixing chamber varied between 370 °C and 410 °C, while the temperature in the catalyst fluctuated between 790 °C and 880 °C. This indicated that only a slight prereaction occurs during the entire load change experiment. The temperature in the monoliths beyond 140 mm in the axial direction remained fairly constant despite the load changes and was between 680 °C and 685 °C.

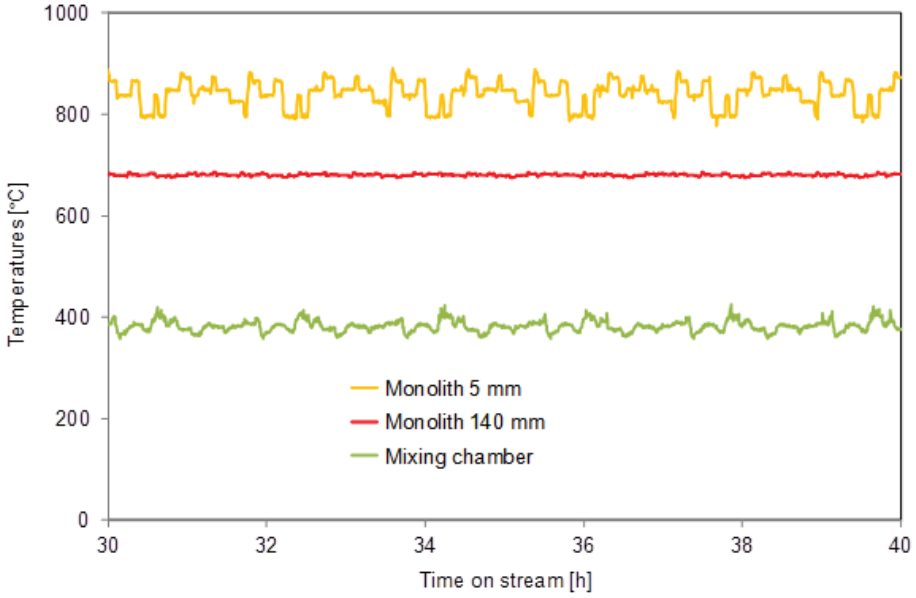

Fig. 143: Temperatures in the monolith and mixing chamber during a load change experiment on the ATR 9.2: O_2/C molar ratio of 0.47 and a H_2O/C molar ratio of 1.9

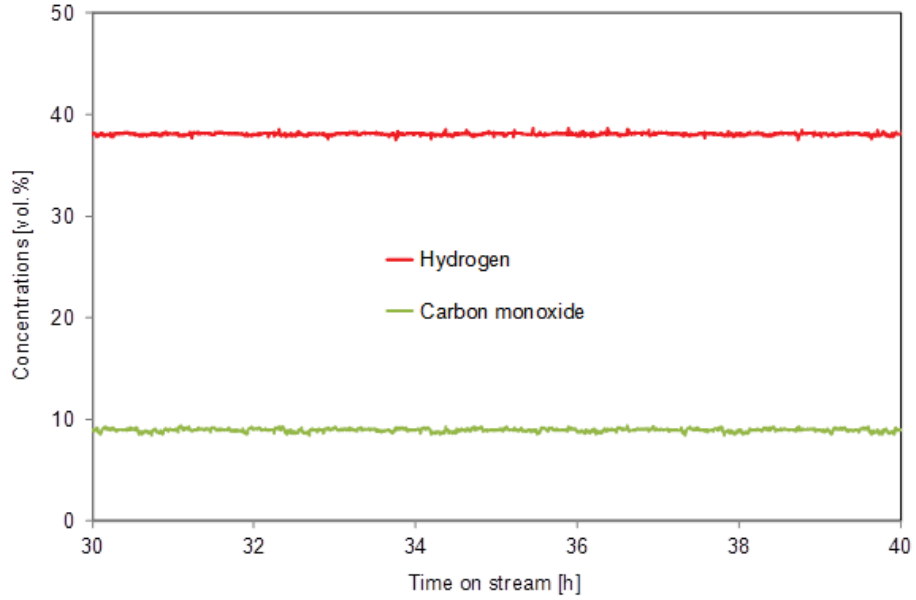

Fig. 144: Concentrations of hydrogen and carbon monoxide during a load change experiment on the ATR 9.2: O_2/C molar ratio of 0.47 and a H_2O/C molar ratio of 1.9

The steam reforming of hydrocarbons in the lower area of the catalyst progresses in accordance with equation (1) and appears to somewhat constrain the temperature fluctuations in the upper area of the catalyst.

Fig. 144 shows the concentrations of carbon monoxide and hydrogen in the same time interval of the load change experiment. The two concentrations were hardly influenced by the load changes. They were 38.2 vol.% for hydrogen and 9.1 vol.% for carbon monoxide. No deactivation of the catalyst as a result of the recurrent load changes was observed throughout the full 70 h of the test (not shown here).

The results obtained for the ATR 9.2 allow the following conclusions to be drawn:

- GTL kerosene is also highly suitable for use with the ATR 9.2. In all eleven experiments in the statistical experimental design, the hydrocarbon turnover was almost 100 %. The concentrations of organic carbon (TOC) in the aqueous condensate samples taken in each of the experiments were between 10 mg/l and 20 mg/l. This is slightly more than that found in fully desalinated water (2 mg/l). For full load, the thermal power of the ATR 9.2 was 27.9 kW for an autothermal reforming efficiency of 86.1 %
- The temperature level in the catalyst of the ATR 9.2 was lower than in earlier reformer generations. At full load, the temperature beyond 5 mm in the axial direction was between 820 °C and 880 °C. This has a positive effect on the long-term stability of the catalyst in the ATR 9.2
- In the mixing chamber of the ATR 9.2, a slightly exothermic prereaction occurs between the oxygen and the hydrocarbons under certain reactions conditions. Its additional enthalpy makes the vaporization of high-boiling hydrocarbons in fuel easier. At full load, a value of 1.9 must be set for the H_2O/C molar ratio. Otherwise, no prereaction occurs
- Low O_2/C ratios of 0.43 are disadvantageous as they promote the formation of methane. The more methane formed, the lower the efficiency of the reforming process and the larger the dimensions of the catalyst in the catalytic burner
- Optimal operating conditions for the ATR 9.2 are an O_2/C molar ratio of 0.47 and a H_2O/C molar ratio of 1.9. The load change experiments showed that the ATR 9.2 can be operated under these conditions without any problems for loads of 60 % to 100 %

A further test involved coupling the ATR 8 to a water-gas shift reactor of the third generation (WGS 3) using the alternative fuel GTL kerosene. The results are presented and described in the following section. Both reactors have a thermal power of approximately 12 kW. In this experiment, the autothermal reformer ATR 8 supplied the educt gas mixture for testing the water-gas shift reactor. Values were chosen for the reaction parameters based on those found most suitable in previous experiments on reactors such as the ATR 9.1 and ATR 9.2, i.e. an O_2/C molar ratio of 0.47 and a H_2O/C molar ratio of 1.9 for 80 % load of the reformer. The ATR 8 was operated during the experiment so that the product gas had a temperature of 400 °C. This temperature is an ideal inlet temperature for the high-temperature section (HTS) of the water-gas shift reactor. Previous experiments showed that at this temperature, the WGS reaction at a space velocity of 90,000 h^{-1} achieves thermodynamic equilibrium with sufficiently fast kinetics. Tab. 14 lists the concentrations of the most important components contained in the reformate of the ATR 8 before it enters the HTS stage of the WGS 3.

Component	Concentration [vol.%]
Hydrogen	29.8
Carbon monoxide	7.2
Carbon dioxide	9.4
Nitrogen	30.7
Argon	0.5
Water	22.3
Methane	0.1

Tab. 14: Concentrations of the components in the reformate of the ATR 8

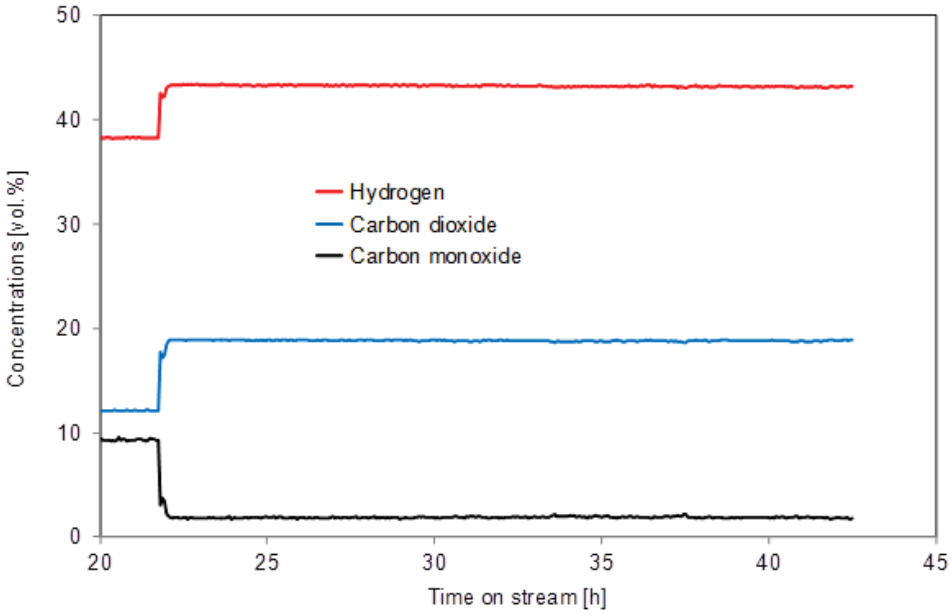

Fig. 145: CO, CO_2 and H_2 concentrations over time in the dry reformate during the experiment testing the WGS 3 in combination with the ATR 8

Fig. 145 shows the behavior of the CO, CO_2 and H_2 concentrations in the dry reformate as recorded during testing of the WGS 3. The CO concentration, which was initially 9.3 vol.% (equivalent to 7.2 vol.% in the wet reformate, cf. Tab. 14), dropped to around 1.8 vol.% after the reformate was fed into the WGS 3. At the same time, the concentrations of the two other products of the WGS reaction increased in accordance with equation (3): CO_2 from 12.1 vol.% (9.4 vol.% in wet reformate) to 18.8 vol.% and H_2 from 38.3 vol.% (29.8 vol.% in wet reformate) to 43.3 vol.%. The concentrations of the individual components remained

constant throughout the experiment lasting approx. 20 h. No deactivation of the catalysts was observed in either WGS stage.

If the value for CO measured with the mass spectrometer of 1.8 vol.% is related to the wet reformate, then we get an initial CO concentration of 1.4 vol.%. The CO conversion, calculated using the given concentrations measured using the mass spectrometer and the flow rates at the inlet and outlet of the WGS-3, was 78 %. If the CO conversion is calculated using the water molar flow, which subsides as the reaction progresses, then the value is found to be 86 %. The concentration of CO in the wet reformate calculated from this is then only 0.9 vol.%.

This finding means that when the WGS 3 is used, the target value for CO concentration in wet reformate of 1.0 vol.% is not achieved. Tests on the combination of the ATR 9.2 with the WGS 4 are due to take place in the near future. They should show whether this is also possible for GTL kerosene in the 28 $kW_{th.}$ power class. Additional information on the results obtained for the coupled ATR-WGS can be found in the section on fuel processing.

5

Outlook

Outlook for New R&D Projects

- Energy storage and hydrogen initiatives in the Helmholtz Association
- Hydrogen system solutions
- Batteries for future energy sectors

5.1 Energy storage and hydrogen initiatives in the Helmholtz Association

As part of the second evaluation of the research area of energy in 2009, the centers involved decided to focus on hydrogen as an interdisciplinary topic and proposed it for funding from the premium budget. The centers take “hydrogen” as a topic to mean the production, storage, transport, safety evaluation and use of hydrogen as energy. The aim was to consolidate and combine activities in this area, incorporate new activities and to define the role of the Helmholtz Association in relation to this topic. In their program applications, the centers proposed establishing new activities or intensifying ongoing efforts. This first stage involved the centers participating in the research programs “Renewable Energies”, “Efficient Energy Conversion and Use” and “Nuclear Safety Research”.

The activities applied for within the hydrogen initiative were evaluated positively by the experts who reviewed the programs, and they were recommended for funding and implementation. The discussion on hydrogen continued and the Helmholtz Senate Commission suggested that the hydrogen initiative be expanded to include the overarching topic of “energy storage”. The existing hydrogen activities were to become part of the new more comprehensive “energy storage and hydrogen initiatives” as a form of chemical energy storage. The initiative was financed out of the premium budget during the second phase of program-oriented funding. In order to highlight the leading role played by the Helmholtz Association’s research area of energy in Germany in the area of energy storage and hydrogen, numerous eligible centers participated in the initiative. These include:

- German Aerospace Centre (DLR)
- Forschungszentrum Jülich (FZJ)
- Helmholtz Centre Berlin for Materials and Energy (HZB)
- Helmholtz Centre for Environmental Research (UFZ)
- Helmholtz Centre Potsdam, German Research Centre for Geosciences (GFZ)
- Karlsruhe Institute of Technology (KIT)
- Max Planck Institute for Plasma Physics (IPP)

As the topic of energy storage has a cross-cutting and interdisciplinary character, and in order to ensure that all storage activities within the Helmholtz Association are brought together, the following Helmholtz centers will also be involved in the initiatives and propose topics:

- GKSS Research Centre Geesthacht

and the Leibniz Association member

- Forschungszentrum Dresden-Rossendorf (FZD)

On 1 January 2011, Forschungszentrum Dresden-Rossendorf became a member of the Helmholtz Association and was renamed Helmholtz-Zentrum Dresden-Rossendorf.

In order to account for the requirements of sustainable mobility and the supply of electricity, which depends on the stability of the grid, more efficient and more cost-effective electrochemical energy storage systems are necessary. Lithium-ion technology plays a key role here. Understanding the electrochemical processes in detail is essential for the development of the next two generations of lithium-ion batteries. This development necessitates a substantial expansion of research activities in the area of electrochemistry for

energy storage systems and in particular a concerted approach within the Helmholtz Association. The six Helmholtz centers – KIT, FZJ, DLR, GKSS, HZB and FZD – involved in the Helmholtz initiative for mobile and stationary energy storage systems contribute the necessary in-depth understanding for rapid progress in the development of lithium-ion batteries thanks to their participation in ongoing and past research activities in other fields, including materials research, process development and fuel cells. In order to establish itself as an important player in the area of electrochemical storage, the Helmholtz Association is selectively combining its competencies in the research areas of energy, key technologies and the structure of matter, and will continue to expand these activities into a new program topic.

Initiative	Hydrogen	Energy storage
Duration	01.2010 – 12.2014	01.2011 – 12.2014
Participating HGF centers	FZJ, KIT, DLR	KIT, FZJ, DLR, HZG, HZB, FZD
Focus	H_2 system solutions	Solid-state batteries
Coordination	REUN program spokesperson	KIT
Total funding [€ k]	4,940	12,000
FZJ share [€ k]	2,072 (42 %)	2,230 (19 %)
IEK-3 share [€ k]	2,072	613
Cost type	100 % free	100 % personnel

Tab. 15: Detailed overview of HGF energy storage and hydrogen initiatives

Tab. 15 summarizes the most important data on the two initiatives. Additional HGF funding is foreseen for the research topics on batteries and electrolyzers. A portfolio topic on “in-system electrochemical storage” over a period of four-and-a-half years and a Helmholtz Energy Alliance on “stationary electrochemical storage and conversion” over three years will consolidate cooperation between Helmholtz centers and universities.

5.1.1 Motivation

Energy storage will considerably decrease consumption in almost all areas of energy technology, and the use of storage systems will allow many processes to be optimized. Examples include heat recovery and temporary storage in industrial processes, decoupling the energy supply from energy demand in the case of renewable energies such as wind and sun by storing electricity, the storage of thermal energy to optimize the use of power plants in grids, and the storage of energy in vehicles using batteries or synthetic fuels. Energy storage systems are a key component in a sustainable energy economy, and they are relevant for all three threads of energy policy:

- decreasing the final consumption of energy,
- increasing the efficiency of energy conversion and provision, and
- increasing the share of renewable energies in the energy mix.

The development of energy storage systems has not been accorded great priority to date. The only notable breakthroughs were in relation to the storage of low-temperature heat from solar collectors and the basic development of safety systems for the handling of hydrogen in the nuclear engineering and chemical industry sectors. All other areas require new technological approaches and new research capacities. The existing activities and newly developed targeted activities will be pooled in the energy storage and hydrogen initiatives. The participating Helmholtz centers aim to focus the topic of energy storage more clearly in the different areas and to cooperate on the various subtopics, incorporating partners from science and industry in so doing. The major tasks will be addressed by interdisciplinary teams and the necessary infrastructure created.

Energy storage can be divided into four general categories:

- thermal energy storage,
- electrical and electrochemical energy storage,
- chemical energy storage, and
- mechanical energy storage.

Completely new concepts and materials must be investigated in all categories, except mechanical storage. The work involved ranges from fundamental aspects to the actual application, and entails the cooperation of different scientific disciplines.

5.1.2 Starting point and existing expertise

Although the topic of energy storage and hydrogen has only been directly addressed in a few subareas within the scope of Helmholtz programs, wide-ranging expertise already exists. Numerous aspects of chemical storage have already been researched by many Helmholtz centers, particularly in combination with hydrogen. These include different processes for hydrogen production, hydrogen storage and hydrogen usage, as well as hydrogen safety issues. Most of the infrastructure for this work has already been set up for different projects. Electrochemical storage (batteries) has not yet been researched as a priority topic. However, existing expertise from the areas of fuel cells and materials research can be exploited to develop batteries. Within the economic stimulus package II, a joint infrastructure initiative involving the Helmholtz centers and their partners saw the creation of extensive infrastructure. The battery associations in the north and south of Germany were granted funding worth € 30 million for investments by the Federal Ministry of Education and Research (BMBF). Work on thermal energy storage began a few years ago focusing on new concepts for high-temperature storage. Extensive infrastructure with large test stands also exists in this area.

In line with the guiding principles of the research area of energy, the HGF centers work in an interdisciplinary manner on technical approaches to improve existing and develop new systems for the conversion and storage of energy in an effort to fulfill the requirements of environmental compatibility, safety, economic viability, and the conservation of resources. With these objectives in mind, IEK-3 researches and develops energy converters based on

the fields of expertise of process and systems analysis, physicochemical analysis, modeling and simulation, electrochemistry, fabrication, and process and systems technology.

The renewable generation of hydrogen on a scale of slightly less than a cubic meter per hour to thousands of cubic meters per hour is a huge challenge in terms of boosting the efficiency of the necessary electrolyzers. Even before PoF-I, IEK-3 researched, developed and verified the core components for advanced water electrolysis with an alkaline electrolyte and equipped prototypes for operation at pressures up to 120 bar. In order to resume these activities, which were completed in 2002, and to adjust the focus in line with current requirements, funds made available within the scope of the energy storage and hydrogen initiatives were used, and further much-needed funding was acquired.

5.2 Hydrogen system solutions

Detailed studies of large-scale energy storage in Germany have shown that the flexible generation of hydrogen in compact electrolysis modules, subsequent storage in salt domes, transport over distances of hundreds of kilometers, distribution to filling stations, and use in fuel cell vehicles represents the best solution both economically and ecologically in terms of substantially reducing CO_2 emissions. In addition to the relevant process and systems analyses, IEK-3 also identified the research and development of electrolyzers with polymer electrolyte membranes (PEMs) and the technical analysis of a future hydrogen infrastructure for storing and distributing energy as appropriate areas of work within the scope of the HGF topic “hydrogen system solutions”. As a result, these topics will be integrated into the topic of hydrogen system solutions within the energy storage and hydrogen initiatives and will be described in the following.

5.2.1 Electrolyzers with polymer electrolyte membranes (PEMs)

The transformation of the energy supply system to include a significant share of renewable energies will only be possible if substantial energy storage capacities are systematically created. In this context, storage in the form of hydrogen, which can be produced using electrolysis from renewably generated electricity, plays an important role. Several companies have already initiated and completed diverse activities aiming to use electrolysis technology to electrochemically convert excess electricity from renewables into hydrogen and oxygen. Systems using a variety of electrolysis techniques have been implemented using existing materials and catalyst technologies. In addition, targeted research and development efforts have tried and are trying to improve alkaline electrolysis and PEM electrolysis for flexible hydrogen production with rapid and frequent load changes for adaptation to renewable energy generation. In addition to overcoming complex technical challenges, these installations must be tailored and made available at low cost for a mass market. As a result, PEM electrolysis is not as advanced as its alkaline counterpart, but it has considerable potential in terms of power density, compactness, and overload capability. IEK-3 therefore intends to create a department dedicated to this research.

In order to be able to use PEM technology for water electrolysis on a mass-market scale after 2020, fundamental technological developments are essential in cooperation with industry and other research institutions. One of the aims is to replace the conventional 175–200 µm thick extruded Nafion membranes with new types of membranes. Nafion membranes are not sufficiently stable for extensive application under high pressure in the planned large-scale systems. Another aim is to reduce the amount of platinum group metals usually employed for catalytic reactions today, such as iridium, ruthenium and platinum, and ultimately substitute them with more economical catalysts. Cost-effective manufacturing processes are also to be identified for metallic bipolar plates and current collectors in order to drastically reduce the costs associated with flow-field and separator plates. At the moment, these costs account for around 48 % of the stack costs and 25 % of the total costs.

IEK-3 has been working on related technology and developing fuel cells with polymer electrolytes for over twenty years. It also boasts expertise from former R&D activities that aimed to refine advanced alkaline water electrolysis at pressures of up to 200 bar (see Fig. 146). In an integrated approach, a specialized scientific and technical department will be set

up for PEM electrolysis to develop, construct and verify new universal and cost-effective PEM electrolyzers to improve the use of renewable energy sources.

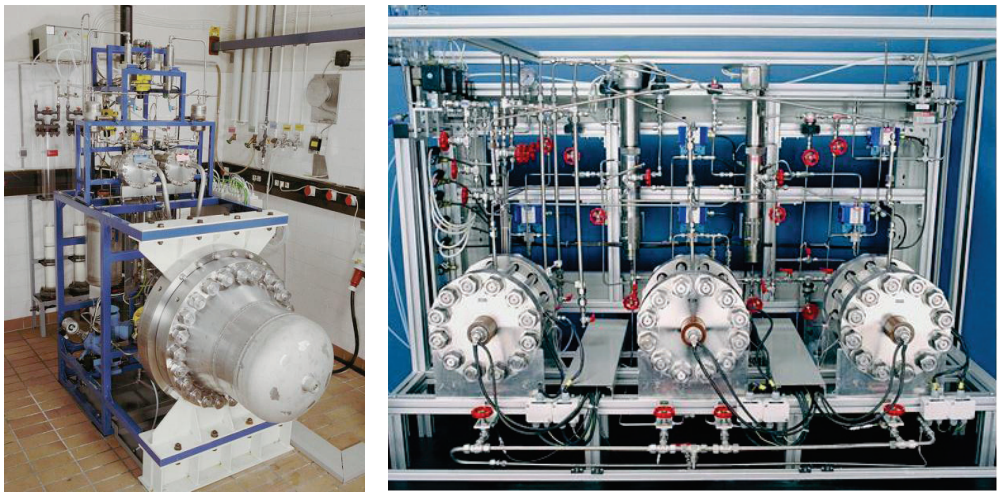

Fig. 146: 120 bar high-pressure electrolyzer (left); 200 bar diaphragm test stand (right)

Using financial support from the energy storage and hydrogen initiative "H_2 system solutions" and the existing expertise in electrochemical process engineering at IEK-3, a broad-based R&D project will be set up. It will be boosted with additional funding and project cooperations. Related R&D measures will involve the comprehensive analysis and evaluation of relevant electrolysis techniques, taking concrete examples of application into account in the context of a predominantly renewable energy supply. The results of these analyses and evaluations will then be transferred to technical specifications for an application-specific PEM electrolyzer. New materials will also be developed for electrolysis cells and stacks and characterized in cooperation with industry and other research institutions. Simultaneous structural investigations, modeling and simulations will allow degradation phenomena and quality defects to be identified. They will also provide a starting point for detailed design modifications in order to improve efficiency. Designing, constructing and testing PEM electrolysis prototypes coupled with fabrication processes for the relevant key operating components will allow efficiency, performance, lifetime, robustness and costs to be verified and demonstrated.

5.2.2 Hydrogen infrastructure for energy storage and distribution

Large-scale handling of hydrogen is standard practice in certain fields of industry and has been for a number of decades. In 1938, a 240 km long hydrogen pipeline went into operation in the Rhine-Ruhr region. After World War II, it was taken over by the chemical company Chemische Werke Hüls before being sold to the British Oxygen Company (BOC). It is currently operated by Air Liquide. Around 1,100 km hydrogen pipelines are in operation throughout the world. In addition, the German gas grid was operated with town gas before the transition was made to natural gas, and town gas is composed predominantly of hydrogen. The systematic creation and large-scale industrial use of a hydrogen distribution

grid, which basically corresponds to our current natural gas grid, is therefore a tried-and-tested option for transporting large quantities of hydrogen over long distances.

To allow hydrogen be used as fuel in passenger cars, a nationwide supply infrastructure must be created. This is very different to supplying gasoline or diesel. Large quantities of hydrogen are best transported as a gas in pipelines similar to natural gas. However, transporting hydrogen in pipelines has not yet been investigated in detail. For example, it is unclear what raw materials should be used as hydrogen impacts negatively on material stability.

Scenario	Climate protection
Motivation	Ambitions climate protection policy
Energy price for crude oil	$ 54 per barrel in 2020 $ 111 per barrel in 2050
Greenhouse gas reduction target	-40 % by 2020 -80 % by 2050
Additional costs for fuel cell vehicles	Decrease in the drive costs for fuel cell vehicles (passenger cars/utility vehicles) to the same level as modern diesel vehicles
Renewable energies	At least 20 % share in primary energy consumption by 2020

Tab. 16: Assumptions and boundary conditions in the GermanHy 2009 study

Planned work aims to develop a technical concept for a pipeline system that will supply the German road transportation sector with hydrogen. The assumptions of the GermanHy study outlined in Tab. 16 will be used, as they are based on a broad consensus. Using Germany as an example, the creation and length of such a pipeline system will be investigated, as will associated economic and ecological aspects. In order to place these findings in the broader context, the production and storage of hydrogen as well as hydrogen filling stations will also be financially assessed. In terms of selecting suitable pipeline materials, innovative solutions will be sought to prevent embrittlement. In addition, the research findings will be used to define concrete approaches for further research and development activities.

It is already clear today that additional knowledge in the following areas is central for the implementation of a hydrogen infrastructure:

- assessment of the suitability of geological storage for hydrogen as a storage medium
- implementing a general concept in a detailed integrated system for cost-effective hydrogen storage and distribution
- evaluation of design and operation variants in terms of grid design and connections as well as operating facilities and parameters

The ongoing PhD project on pipeline systems for a hydrogen supply and conceptual analyses on the implementation of an energy supply with decreased greenhouse gas emissions will be used as a basis to specify further R&D requirements. These will then be transformed into new R&D projects as soon as possible, which IEK-3 will pursue using an integrated approach.

5.3 Batteries for future energy sectors

It is generally agreed that efficient and cost-effective electrochemical energy storage systems are required for both the stationary and mobile sectors. Lithium-ion technology plays a key role here. Understanding the electrochemical processes in detail is essential for the development of the next two generations of such batteries. Building on our partners' broad range of expertise in materials, three priority topics were identified for the participating Helmholtz centers. These topics concentrate on modern materials research for batteries of the third and fourth generations. Overall, the aim is to take an important step within a short time towards developing new battery materials with higher capacity data and to transfer these materials to industrial application and use them in the medium-to-long term for mobile and stationary storage systems. In order to achieve such progress, an in-depth understanding is required of the electrochemical processes in these materials and of the interactions between structure and properties. Work at Jülich focuses on developing solid-state batteries that are inherently safe compared to conventional systems with liquid electrolytes. Suitable solid-state electrolytes are being developed and fabricated as extremely thin films with a high ionic conductivity at the application temperatures. Furthermore, cathode layers with higher voltages and anode materials with lower thresholds have to be fabricated for thin film batteries. On the fabrication side, the processes must be optimized with respect to large-area deposition. The aim is to fabricate a safe solid-state thin film battery with high power densities for mobile and stationary applications.

Work at IEK-3 focuses on material-related issues in line with the character of the Helmholtz initiative for mobile and stationary energy storage systems. For solid-state thin film batteries, this includes issues related to cell and battery characterization and system analyses.

5.3.1 Characterization of the electrochemical behavior

PhD projects on this topic will be used as a basis to develop, set up and apply reliable characterization methods. These projects will be pursued in close cooperation with partner institutes of the Helmholtz centers involved. In order to ensure comparability of the characterization results, existing investigation standards will be used and agreement reached on required standards. This should have a positive influence on the level of quality of the results.

First, the experimental basis for characterizing battery systems will be established in IEK-3. The standard electrochemical methods for battery characterization will first be identified, e.g. methods for determining the behavior of batteries during charge and discharge cycles. The institute already has facilities for impedance spectroscopy and cyclovoltammetry. Specifications of further instruments to be acquired will be defined in consultation with potential suppliers.

The next step will involve applying the developed methods to commercial lithium batteries. Following this, cells fabricated at IEK-1 will be characterized. Particular attention will be paid to relationships between charge and discharge currents, the mean charge level, and lifetime. Another important point involves the heat balance of the battery cells during the charge and discharge cycles.

The electrochemical processes during battery operation will be analyzed using newly developed and existing methods so that a battery system can be described using models. In

addition to electrochemical characterization, the degraded cells will also be subjected to materials chemistry and microscopic analyses. The observed degradation of the cells will be correlated with the morphological and chemical changes in the electrodes and the electrolyte. IEK-3 has a high-resolution scanning electron microscope (SEM) with energy-dispersive X-ray analysis (EDX) and the appropriate sample preparation for such investigations.

Measurement data from an investigated battery system will be used to develop model concepts describing electric behavior and heat balance. These model concepts will then be used to adapt selected batteries for fuel cell systems and to construct a hybridized prototype.

5.3.2 Technical analysis and modeling of thin film batteries

In principle, different batteries are suitable for use as energy storage systems for the hybridization of fuel cell systems. Using characteristic system and operating parameters, potentially suitable batteries will be analyzed and compared. The batteries deemed most suitable will be used to define systems and develop process concepts for efficient operation. These concepts will provide a framework for subsequent system modeling and simulation, the results of which will be compared with the results from the test operation of real systems.

6

Data

Facts and Figures

- Institute of Energy and Climate Research – Fuel Cells (IEK-3)
- Overview of department expertise
- Publications, technology transfer and resources
- Committee work
- Contributions to trade fairsand exhibitions
- How to reach us
- List of abbreviations

6.1 Institute of Energy and Climate Research - Fuel Cells (IEK-3)

The Institute of Energy and Climate Research (IEK-3) focuses on research and development in the field of fuel cells. Priority is currently given to four areas: ceramic high-temperature fuel cells (SOFCs), direct methanol fuel cells (DMFCs), high-temperature polymer electrolyte fuel cells (HT-PEFCs), and the reforming and desulfurization of liquid energy carries that could be used to provide hydrogen in fuel cells.

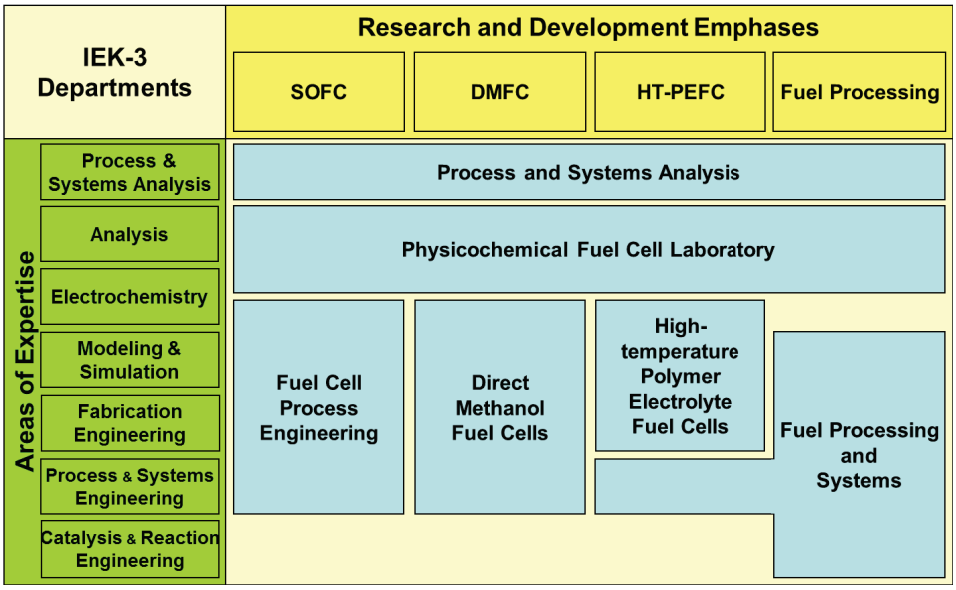

Fig. 147: Departments, areas of expertise and R&D priorities at IEK-3

Focusing intensively on a small number of fuel cells and a restricted power range makes it possible to address these R&D priorities with teams of supercritical size beginning with basic phenomena and ranging up to process engineering for the whole system. The institute's objectives and focal points are unlocking the synergies between the specialized disciplines and putting theory into practice in order to reach a pilot-plant stage. Stationary, portable and mobile applications up to and including complete systems with fuel cells, together with cost aspects, are evaluated by process and systems analysis in terms of their usability. They are also compared to competing systems from a technical, energetic and economic perspective. Furthermore, application-oriented R&D activities are accompanied by basic research aiming to clarify structure-activity relationships using selected advanced analysis methods.

IEK-3 aims to conduct research that is socially, ecologically and economically relevant and thus generate ground-breaking results on an international level. This quality of work is achieved through basic research, which is closely coordinated with technical development work in relevant scientific and technical fields of expertise. International cooperations with partners from research and industry are particularly important in this respect. The institute concentrates on implementing research results in innovative products, procedures and processes in cooperation with industry. It is keen to make a contribution to bridging the gap between science and technology. Collaboration with universities, universities of applied

sciences, training departments and training centers is designed to promote opportunities for further education and training.

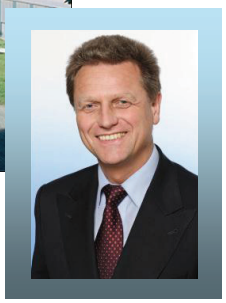

Prof. Dr.-Ing. Detlef Stolten (Head of IEK-3)
Institute of Energy and Climate Research
IEK-3 Fuel Cells
Forschungszentrum Jülich GmbH, 52425 Jülich, Germany
Tel.: +49 2461-61-3076; E-mail: d.stolten@fz-juelich.de

With around 160 employees, Jülich has the largest institutional fuel cell research team in Europe. Of these, around half work on the SOFC, and approx. one-third of these are involved in IEK-3 activities. Another two institutes also work in the field of SOFCs: IEK-1 is responsible for manufacturing materials and IEK-2 tests the materials and conducts steel research. The Central Technology Division (ZAT) is responsible for stack construction. The other 75 or so of the 100 employees at IEK-3 work on advancing low-temperature fuel cells and ceramic high-temperature fuel cells. Each of these two fields has a coordinator for generic topics, and these coordinators also act as initial contacts for information on SOFCs both within and outside of the institutes involved.

Project Leader
Low-Temperature Fuel Cells
and Deputy Head of IEK-3

Dr.-Ing. Bernd Emonts
Tel.: +49 2461-61-3525
e-mail: b.emonts@fz-juelich.de

Project Leader
High-Temperature Fuel Cells
PBZ

Dr. Robert Steinberger-Wilckens
Tel.: +49 2461-61-2052
e-mail: r.steinberger@fz-juelich.de

6.2 Overview of department expertise

Direct Methanol Fuel Cells

High-Temperature Polymer Electrolyte Fuel Cells

Fields of work, range of services

Work on direct methanol fuel cells ranges from membrane electrode assemblies to stacks within the department and in close cooperation with process engineering up to systems. New materials for membranes and catalysts are characterized, facilitating the development and fabrication of innovative membrane electrode assemblies. The structure-activity relationship of the electrode layers is a priority. Stack modeling and design together with new analytical techniques in stack technology, as well as automated fabrication methods on a pilot-plant scale, guarantee the bridging function between science and technology.

Work on the HT-PEFC ranges from the electrode to the stack and is conducted in cooperation with internal and external partners. New electrode structures and preparation methods are developed, and MEAs are fabricated and electrochemically characterized. Moreover, intensive studies are conducted on structure-activity relationships in the electrode layers. This work is accompanied by modeling in order to obtain an in-depth understanding of the processes. In addition, simulation activities are pursued on a cell and stack level. This supports the development of air-cooled and liquid-cooled stacks with high volume-specific and weight-related power densities.

Facilities, processes, methods

Equipment

- Test stands for electrochemical investigations of DMFCs, PEFCs and stacks
- Apparatus for magnetotomographic investigations of current density distribution and single cells and stacks
- Apparatus for characterizing membranes for PEFCs and DMFCs
- Desk coater for the continuous fabrication of MEA components
- Robot facilities for the automated fabrication of cell components (stamping and pressing) and stacks (assembling)

Equipment

- Test stands for the electrochemical characterization of MEAs
- Test stands for electrochemical studies on stacks up to 5 kW_{el}
- Equipment for the fabrication of gas diffusion electrodes

Models

- Simulation models to describe mass, charge and heat transport processes in cells and stacks

Contacts

Dipl.-Ing. Jürgen Mergel
Tel: +49 2461-61-5996
Email: j.mergel@fz-juelich.de

PD Dr. rer. nat.Werner Lehnert
Tel: +49 2461-61-3915
Email: w.lehnert@fz-juelich.de

Electrochemistry and Simulation SOFC **Fuel Processing Systems**

Fields of work, range of services

In Jülich, SOFCs are researched and developed from materials up to entire systems. This department works on electrochemistry and stack tests, as well as modeling from cells to stacks. Cells and stacks are tested under laboratory conditions in order to obtain specific information, and under realistic operating conditions including operation for extended periods of time. In-house models for simulation calculations that take account of the mass, charge and heat transport processes for cells and stacks are applied and refined. The results are used to develop new concepts.

Hydrogen for fuel cells produced from commercially available fuels will make it possible to introduce fuel cell technology in a short space of time. The institute specializes in reforming middle distillates – diesel, kerosene and fuel oil. Work is carried out on the entire system, including desulfurization and CO purification. The focus is on reactors in the 3–50 kW power class, which are integrated into high-temperature PEFC or SOFC systems. Complex, realistic models, which are used to design and construct reactors, are reinforced by the use of glass models in which similarity theory is used to visualize flows.

Facilities, processes, methods

Equipment

- Test stands for electrochemical investigations of solid oxide fuel cells (SOFCs)
- Test stands for electrochemical investigations of solid oxide fuel cell stacks
- Apparatus for measuring permeation and diffusion

Models

- Computer models to simulate operating conditions in SOFCs (membrane, cell and stack) on the basis of the transport processes for heat, mass and charge

Equipment and models

- Test stands for the investigation of reactors for reforming, water-gas shift reaction, preferential oxidation and desulfurization
- Test stands for screening and investigating catalysts with regard to activity and selectivity
- Analytical devices to determine concentrations (GC, GC/MS, NDIR) of reaction gases
- Apparatus for fractional distillation of fuels
- CFD simulation programs for visualizing educt mixing and reactor design

Contacts

Dr. L.G.J. (Bert) de Haart
Tel: +49 2461-61-6699
Email: l.g.j.de.haart@fz-juelich.de

Prof. Dr.-Ing. Ralf Peters
Tel: +49 2461-61-4260
Email: ra.peters@fz-juelich.de

Fuel Cell Process Engineering

Physicochemical Fuel Cell Laboratory

Fields of work, range of services

Designing and building efficient fuel cell systems requires detailed knowledge of the cell and the complete system. The intensive interactions between cells and the system as a whole represent a challenge in terms of development which is fully explored here. Three DMFC test facilities (2 kW) and two SOFC test facilities (1 kW, 20 kW) have been constructed in close collaboration with Cell and Stack Engineering. Work focuses on developing new system concepts, testing and evaluating these concepts, developing components in cooperation with industry, and testing and developing control and regulating concepts.

As technical development becomes more and more advanced, scientific work is becoming increasingly important in terms of understanding future energy systems. This is the reason why this department focuses on determining material and structural properties and their efficiency when implemented in the core components of energy technologies. Imaging, physical and spatially resolved analysis techniques are used to determine chemical and structural changes, mechanical and thermodynamic suitability, and fluid dynamic and electrochemical performance.

Facilities, processes, methods

Equipment and models

Test stands for

- high-temperature heat exchangers up to 850 °C and 200 m^3 air/h
- reformers and afterburners for SOFC stacks with a power of 5 kW
- air compressors up to 100 m^3/h and exhaust-gas-heated steam generators for SOFC systems
- process engineering investigations of DMFC stacks and system components
- CFD models to determine flow distribution in stacks
- simulation models for the design of fuel cell systems

Equipment and methods

- Imaging analysis techniques:
  field emission scanning electron microscope (FE-SEM) with EDX analysis, optical microscopes and confocal laser scanning microscope
- Spatially resolved analysis techniques:
  segmented cell technology (SCT), magnetic imaging and mass spectroscopy (SRMS)
- Physical analysis techniques:
  thermogravimetrical analysis (TG and TGA), dynamic differential calorimetry (DSC), climate cabinet, tensile testing machine with climate chamber, standard porosimeter, particle size measuring unit

---

Contacts

Prof. Ludger Blum
Tel: +49 2461-61-6709
Email: l.blum@fz-juelich.de

PD Dr. Carsten Korte
Tel: +49 2461-61-9035
Email: c.korte@fz-juelich.de

Process and Systems Analysis

Fields of work, range of services

Selecting appropriate energy systems for the future and managing their development requires a systematic approach, which is used here for fuel cells. Investigations are based on observations of energy chains, benchmarks for other application and manufacturing technologies, and economic comparisons. This broad experimental basis and the more extensive modeling in the institute are used to model entire systems and to compare them with competing technologies under realistic conditions. They are also used to identify development potential and shortcomings. Studies are also carried out for industry and confidentiality of information is assured.

Facilities, processes, methods

Methods

- Design engineering for fuel processing and energy systems with fuel cells
- Integrated evaluation methods (life cycle analyses) for energy systems

---

Contacts

Dr.-Ing. Michael Weber
Tel: +49 2461-61-8626
Email: m.weber@fz-juelich.de

6.3 Publications, technology transfer and resources

The scientific and technical results of work carried out at IEK-3 are published in relevant journals and presented to interested specialist audiences at national and international conferences. Important journals in which four or more peer-reviewed papers from IEK-3 were published during the period under review were the Journal of Fuel Cell Science and Technology (2009: 1, 2010: 5), the Journal of Power Sources (2009: 4; 2010: 1), Electrochemistry Communications (2009: 3, 2010: 2), the International Journal of Hydrogen Energy (2009: 2, 2010: 3) and Electrochimica Acta (2009: 2, 2010: 2). The most important conferences in which IEK-3 participated in 2009 were the 11th International Symposium Solid Oxide Fuel Cells (SOFC-XI) in Vienna, Austria, with four contributions, and the European Fuel Cell Forum in Lucerne, Switzerland, with three contributions. In 2010, IEK-3 presented 23 papers at the 18th World Hydrogen Energy Conference in Essen and two papers at the 9th European SOFC Forum in Lucerne, Switzerland. The various departments within IEK-3 also contributed to numerous other specialist conferences with papers and presentations both within Germany and abroad. In addition, four PhD theses focusing on DMFCs, HT-PEFCs and SOFCs were completed during the period under review (2009 and 2010) and one undergraduate dissertation on mathematical problems in physical analysis.

Year		2009	2010
Publications	Reviewed journals[1)]	24	19
	Books and journals	10	13
	Paper in a book	17	33
	PhD theses	0	5
Technology transfer	Ongoing projects with third-party funding	35	39
	Patent applications	11	7
	Patents granted	11	11
Resources[2)]	Personnel (PoF[3)]/third-party funding)	97 (71/26)	93 (66/27)
Explanatory notes	[1)]According to ISI citation index [2)]Data in PY/a [3)]PoF: Program-oriented funding		

Tab. 17: IEK-3 core data for 2009 and 2010

To ensure successful technology transfer, IEK-3 was involved in numerous R&D projects (2009: 35; 2010: 39) which received funding from the European Commission, the Federal Ministry of Economics (BMWi) and that of Education and Research (BMBF), the Ministry of Economics of the State of North Rhine-Westphalia, and projects financed by industry. IEK-3 was also responsible for managing and coordinating some of these projects. The numerous

patent applications (2009: 11; 2010: 7) and patents granted over the two years in question (2009: 11; 2010: 11) were another step towards smooth technology transfer.

IEK-3 has around 100 employees, who are partially financed by program-oriented funding (POF) from the Helmholtz Association of National Research Centres (HGF) and partially by third-party funds. Some of the personnel at IEK-3 are employed on a part-time basis. The effective personnel capacity was 97 PY/a in 2009 and 93 PY/a in 2010.

6.4 Committee work

IEK-3's national and international reputation as leading experts in fuel cells and hydrogen technology is reflected in the fact that several IEK-3 scientists are members of and collaborate with national and international committees. One example of international recognition is the role played by Prof. Stolten as the Chairman of the 18th World Hydrogen Energy Conference 2010 (18th WHEC 2010) and the coordination of WHEC, facilitated by the active involvement of numerous scientists at IEK-3. Furthermore, Prof. Stolten and Dr. Müller hold important positions on the committees responsible for fuel cells within the International Energy Agency (IEA). On a national level, Prof. Stolten is a member of the National Organization for Hydrogen and Fuel Cell Technology (NOW) where he represents the part played by HGF in the German research area. The committee work performed by IEK-3 employees on the various levels is set out in detail below.

IEA Advanced Fuel Cells Implementing Agreement
since 2000, Prof. Dr.-Ing. D. Stolten
Vice-Chairman of the Executive Committee and Head of the German Delegation

since 2004, Dipl.-Ing. J. Mergel
Member of Annex 22 "Collaborative Research on Polymer Electrolyte Fuel Cells"

since 2009, Dr.-Ing. R.C.Samsun
Member of the Executive Committee

since 2009, Dr.-Ing. M. Müller
Operating Agent for Annex 27

GVC Energy Process Engineering Expert Committee/VDI Society for Process Engineering and Chemical Engineering
since 2003, Prof. Dr.-Ing. D. Stolten
Member of the "Energy Process Engineering" Expert Committee

since 2006, Prof. Dr.-Ing. D. Stolten
Vice-Chairman of the "Energy Process Engineering" Expert Committee

since 2008, Prof. Dr.-Ing. D. Stolten
Chairman of the "Energy Process Engineering" Expert Committee

---

Masterflex AG Supervisory Board
since 2004, Prof. Dr.-Ing. D. Stolten
Vice-Chairman of the Supervisory Board

Fuel Cell Qualification Initiative
since 2005, Dr.-Ing. B. Emonts
Member of the Executive Committee

BREZEL Expert Committee of the Association of German Engineers
since 2005, Prof. L. Blum
Member of the Expert Committee

Global Roundtable on Climate Change, Columbia University, New York
since 2006, Prof. Dr.-Ing. D. Stolten
Member

DKE "Portable Fuel Cell Systems" Standardization Working Group
since 2006, Dipl.-Ing. J. Mergel
Member of the Working Group

WILEY-VCH "Fuel Cells" Journal
since 2006, Prof. Dr.-Ing. D. Stolten
Member of the Advisory Board

National Organization for Hydrogen and Fuel Cell Technology Advisory Board
since 2007, Prof. Dr.-Ing. D. Stolten
Member and HGF representative for research

Fuel Cells and Hydrogen Network NRW
since 2007, Dr.-Ing. H. Janßen and Dipl.-Ing. N. Kimiaie
Members of the Complete System and Stack Design and Assembly Working Groups

N.ERGHY in EU FCH Undertaking
since 2008, Prof. Dr.-Ing. D. Stolten
Representative of full member Forschungszentrum Jülich

18th World Hydrogen Energy Conference 2010, Essen
since 2008, Prof. Dr.-Ing. D. Stolten
Conference Chairman, Head of the Executive Board, Vice-Chairman of the Organizing Committee

since 2008, Dr.-Ing. B. Emonts
Organization of "Students' Day", Member of the Organizing Committee

since 2008, Dipl.-Ing. Dipl. Wirt.-Ing. T. Grube
Member of the Organizing Committee

Research Alliance for Renewable Energies (FVEE)
since 2009, Dr.-Ing. B. Emonts
Representative of Forschungszentrum Jülich for Fuel Cells

Advisory Board of h2-netzwerk-ruhr
since 2009, Dr.-Ing. B. Emonts
Member

IEA Experts' Group on Science for Energy (EGSE)
since 2009, Prof. Dr.-Ing. D. Stolten
Co-Chairman

Working Group of Electrochemical Research Facilities (AGEF)
since 2010, Dipl.-Ing. J. Mergel
Member of the Board of Directors

2nd International Conference on Energy Process Engineering 2011: Efficient Carbon Capture for Coal Power Plants, Frankfurt am Main
since 2010, Prof. Dr.-Ing. D. Stolten
Conference Chairman as Chairman of the Energy Process Engineering Groups of Dechema/VDI, Head of the Organizing Committee

since 2010, Dr.-Ing. M. Weber
Member of the Organizing Committee

6.5 Contributions to trade fairs and exhibitions

IEK-3 has set itself the objective of showcasing its capacity for innovation by demonstrating new technologies and pioneering developments made possible by the institute's R&D priorities. The most important annual presentation forum for the highlights of the year is the technology trade fair in Hannover. At the Hannover Messe in 2009, IEK-3 showcased R&D projects in an interactive presentation area with computer animations, on-the-spot analyses and stack assembly kits, which provided visitors with an introduction to system verification, stack assembly, MEA fabrication, analysis, modeling and simulation, as well as process and systems analysis. Photos of the area and the team are shown in Fig. 148.

Fig. 148: Presence at the Hannover Messe 2009

State Secretary Baganz from the Ministry of Economics of the State of North Rhine-Westphalia (shown in Fig. 148, right, second from the left) visited Jülich's stand and was given an overview of the details of R&D by Prof. Stolten. Other interdisciplinary areas of research were included in a small exhibition of the core components from the R&D priorities: membrane electrode assemblies (MEAs), bipolar plates, short stacks and reactor configurations.

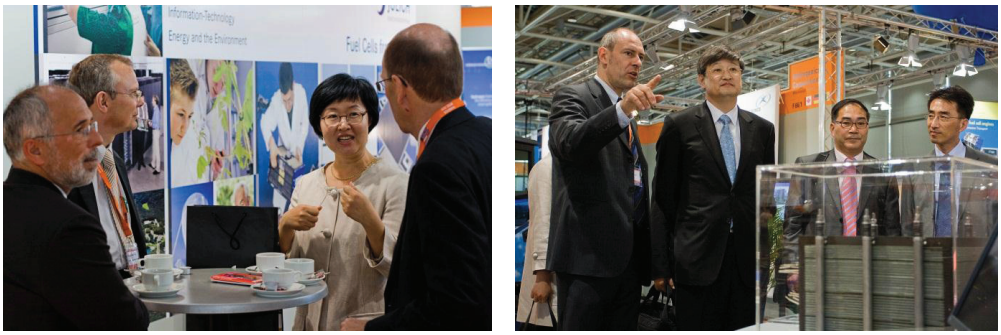

Fig. 149: Representatives of the Korea Institute of Energy Research (KIER) at Jülich's stand at the Hannover Messe 2009

At the official event opening the Hannover Messe in 2009, a memorandum of understanding was signed creating the framework for cooperation between the Korea Institute of Energy

Research (KIER) and Forschungszentrum Jülich in the areas of DMFC and SOFC over the next five years. The memorandum of understanding continues a long-standing tradition of cooperation and comprises joint research projects and workshops, as well as the exchange of information and personnel. The Korean representatives visited Jülich's stand and gained a concrete impression of the R&D results of Jülich fuel cell research (Fig. 149).

Over the course of the year, IEK-3 took part in three other trade fairs and exhibitions in Germany and abroad. Details of these fairs and exhibitions are listed below.

2009

Hanover Messe 20.–24.04.2009, Hannover *Presentation area "Fuel Cell Research and Technology Development"*
Lucerne Fuel Cell Forum 2009 29.06. –03.07.2009, Lucerne, Switzerland *Presentation area "Fuel Cell Research and Technology Development"*
Open Day 2009 06.09.2009, Jülich *Hands-on R&D "The fuel cell on the way from research to application"*
11th International Symposium Solid Oxide Fuel Cells (SOFC-XI) 04. –09.10.2009, Vienna, Austria *Cell and stack fabrication "From ceramic powder to functioning components", components of an integrated stack module*

At the Hannover Messe a year later, IEK-3 showcased the R&D priorities of DMFC, HT-PEFC, SOFC, fuel processing and physicochemical analysis (see Fig. 150). In an effort to attract more visitors, part of the stand was kitted out with an obstacle course with two model vehicles: a battery electric model forklift and a fuel cell electric model forklift. Visitors to the stand had to reach the end of the course as fast as possible with their chosen vehicle. Along the way, they had to lift a pallet off a shelf in one high rack and set it down on a shelf at a height of 35 cm in a second high rack. Those driving the battery electric model forklift also had to pause for five seconds at a make-believe charging station between the high racks and the finish line. The fastest drivers received a souvenir of the event.

Fig. 150: IEK-3 trade fair booths: Hannover Messe 2010 (left) and 18th WHEC 2010 (right)

IEK-3 also had an exhibition area in the German pavilion at the 18th World Hydrogen Energy Conference 2010 in Essen representing a second important development in 2010 (see Fig. 150, left). An overview of the events in which IEK-3 participated in 2010 and the topics concerned is shown below.

2010

Hannover Messe 19. –24.04.2009, Hannover *Presentation area "Fuel Cell Research and Technology Development"*
18th World Hydrogen Energy Conference 2010 15. –21.05.2010, Essen *Presentation area "Fuel Cell Research and Technology Development"*
9th European SOFC Forum 26.06. –02.07.2009, Lucerne, Switzerland *SOFC research and technological development*

6.6 How to reach us

6.6.1 By car

Düren exit, then turn right towards Jülich (B 56). After about 10 km, turn off to the right onto the L 253, and follow the signs for “Forschungszentrum”.

Coming from Aachen on the A 44 motorway (Aachen – Düsseldorf) take the “Jülich-West” exit. At the first roundabout turn left towards Jülich, and at the second roundabout turn right towards Düren (B 56). After about 5 km, turn left onto the L 253 and follow the signs for “Forschungszentrum”.

Coming from Düsseldorf Airport, take the A 52 motorway (towards Düsseldorf/Mönchengladbach) followed by the A 57 (towards Cologne (Köln)) to Neuss-West. Then take the A 46 (towards Jüchen/Grevenbroich), before turning onto the A 44 (towards Aachen). Continue as described in “Coming from Düsseldorf”.

Coming from Düsseldorf on the A 44 motorway (Düsseldorf – Aachen) you have two choices:

1. (Shorter route but more traffic) turn right at the Jülich-Ost exit onto the B 55n, which you should follow for approx. 500 m before turning right towards Jülich. After 200 m, before the radio masts, turn left and continue until you reach the “Merscher Höhe” roundabout. Turn left here, drive past the Solar Campus belonging to the University of Applied Sciences and continue straight along Brunnenstrasse. Cross the Römerstrasse junction, continue straight ahead onto Wiesenstrasse, and then after the roundabout and the caravan dealers, turn left towards “Forschungszentrum” (signposted).

2. (Longer but quicker route) drive until you reach the “Jülich-West” exit. At the first roundabout turn left towards Jülich, and at the second roundabout turn right towards Düren (B 56). After about 5 km, turn left onto the L 253 and follow the signs for “Forschungszentrum”.

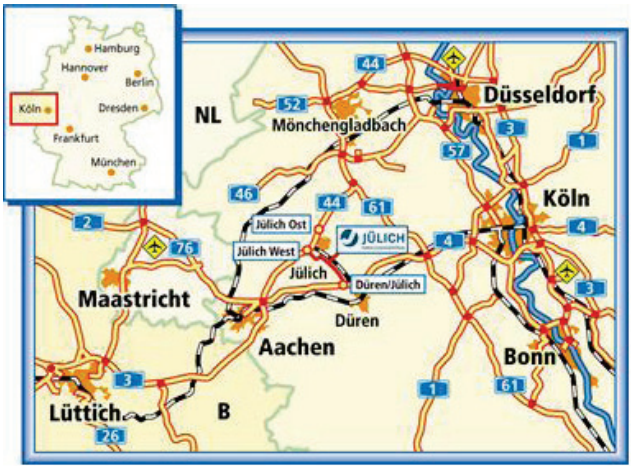

Fig. 151: Map of Meuse-Rhine Euroregion

Sat-nav systems: In your navigation system, enter your destination as “Wilhelm-Johnen-Strasse”. From there, it is only a few hundred meters to the main entrance – simply follow the signs. Forschungszentrum Jülich itself is not part of the network of public roads and is therefore not recognized by navigation systems.

6.6.2 By plane

Cologne Bonn Airport: From the railway station at the airport, either take the S13 to Cologne main train station (Köln Hauptbahnhof) and then continue with the regional express to Düren, or go to Köln-Ehrenfeld by regional express and then take the S12 to Düren. Continue from Düren as described in “By train”.

By train from **Düsseldorf Airport**: From the railway station at the airport, travel to Cologne main train (Köln Hauptbahnhof) station and then continue on to Düren. Some trains go directly to Düren whereas other connections involve a change at Cologne main train station. Continue from Düren as described in “By train”.

6.6.3 By train

Take the train from Aachen or Cologne to Düren’s main train station (Hauptbahnhof). Then take the local train to Jülich (“Rurtalbahn”) and get out at the “Forschungszentrum” stop. From here, you need to keep right and walk towards the main road before turning right towards Forschungszentrum Jülich. The main entrance to Forschungszentrum Jülich is about 20 minutes by foot.

Fig. 152: Location of Forschungszentrum Jülich

Fig. 153: Location of the Institute of Energy and Climate Research (IEK-3: Fuel Cells), Helmholtz-Ring H8, building no. 03.2

6.7 List of abbreviations

ABPBI	poly-2,5-benzimidazole
ACC beku	production and Distribution of Chemical Special Products Ltd (ger.: Herstellung und Vertrieb chemischer Spezialerzeugnisse GmbH)
ACL	catalytic layer on the anode side
AGEF	Group of Electrochemical Research Facilities (ger: Arbeitsgemeinschaft Elektrochemischer Forschungseinrichtungen e.V.)
AKG	Autokühler Company (ger.: Autokühler Gesellschaft)
AP	air preheater
APU	auxiliary power unit
ASP	automated standard porosimetry
ATR	autothermal reforming
BESSY II	electron storage ring at Helmholtz Centre Berlin
BEV	battery electric vehicles
BMBF	German Federal Ministry of Education and Research (ger.: Bundesministerium für Bildung und Forschung)
BMW	Bavarian engine factory (ger.: Bayrische Motorenwerke)
BMWi	Federal Ministry of Economics (ger.: Bundesministerium für Wirtschaft)
BOC	British Oxygen Company
BOL	beginning of life
BP	bipolar plate
BREZEL	Expert Committee Fuel Cells of the Association of German Engineers
BTL	bio-to-liquid
BWK	Journal for Fuel Heat Power (ger.: Brennstoff Wärme Kraft)
CAB	catalytic burners
CALLUX	Light-house project for practical tests of fuel cell heating devices
CCM	catalyst-coated membranes
CCS	carbon dioxide capture and storage
CE	Certification Europe (fr. Conformité Européenne)
CFD	computational fluid dynamics
CGO	cerium gadolinium oxide: $Ce_{0.8}Gd_{0.2}O_{2-\delta}$
CHP	combined heat and power
CL	catalyst layer
CLSM	confocal laser scanning microscope
CO	carbon monoxide
DC/DC	converter from direct current to direct current
DEFC	direct ethanol fuel cell
DES I	Module for the thermal separation of fuels from middle distillates
DES II	Module for the hydrodesulfurization of middle distillates
DIN EN ISO	ISO 9000: family of standards is related to quality management systems
DKE	German Commission for Electrical, Electronic & Information Technologies (ger.:Deutsche Kommission Elektrotechnik Elektronik Informationstechnik)

DLR	German Aerospace Centre (ger.: Deutsches Zentrum für Luft- und Raumfahrt)
DMFC	direct methanol fuel cell
DoE	Department of Energy
DOE	design of experiments
DSC	differential scanning calorimeter
EGSE	Experts Group on Science for Energy
EL	extra light
EDX	energy-dispersive X-ray spectroscopy
ELBASYS	collaborative project electrical basic systems in carbon reinforced plastic body (ger.: Elektrische Basissysteme in einem CFK-Rumpf) Subproject: Fuel cell off-gases for tank inerting
ENSA	project for the development of SOFC APUs
EOL	end of life
EU	European Union
FC	fuel cell
FCH	fuel cell and hydrogen
FCHVs	fuel cell hybrid electric vehicles
FCCT	Fuel Cell Component Technologies (Freudenberg)
FEM	finite element modelling
FE-SEM	field emission scanning electron microscope
FMEA	failure mode effect analysis
FTIS	fuel tank inerting system
FuMA-Tech	Functional Membranes and Plant Technology (ger.: funktionelle Membranen und Anlagentechnologie)
FVEE	Research Alliance for Renewable Energies (ger.: ForschungsVerbund Erneuerbare Energien)
FZD	Forschungszentrum Dresden-Rossendorf
FZJ	Forschungszentrum Jülich
GDEs	gas diffusion electrodes
GDL	gas diffusion layer
GFZ	Helmholtz Zentrum Potsdam, German Research Centre for Geosciences
GHG	Greenhouse Gas
GKSS	Research Centre Geesthacht
GTL	gas-to-liquid
GUS	Commonwealth of Independent States (ger: Gemeinschaft unabhängiger Staaten)
GVC	Society for Process Engineering and Chemical Engineering (ger.: Gesellschaft Verfahrenstechnik und Chemieingenieurwesen)
HGF	Hemholtz Association of National Research Centres
HT-PEFC	high-temperature polymer electrolyte fuel cell
HT-PEMFC	high-temperature polymer electrolyte membrane fuel cell
HT-PEM	high-temperature polymer electrolyte membrane
HTS	high-temperature section
HZB	Helmholtz-Zentrum Berlin
HZG	Helmholtz-Zentrum Geesthacht

IAHE	International Association for Hydrogen Energy
ICEPE	International Conference on Energy Process Engineering
IGCC	Integrated Gasification Combined Cycle
IEA	International Energy Agency
IEK-1	Instiute for Material Synthesis and Processing
IEK-2	Mictrostructure and Properties of Materials
IEK-3	Institute of Fuel Cells
IGSWEEP-JÜL	Jülich process for application in zero-CO_2 power plants
IPHE	International Partnership for Hydrogen and Fuel Cells in the Economy
IPP	Max Planck Institute for Plasma Physics
ISEA	Institute for Power Electronics and Electrical Drives (ger.: Institut der Stromtrichtertechnik und Elektrische Antrieb) RWTH Aachen University
IQ-BZ	Fuel Cell Qualification Initiative (ger.: Initiative Qualifizierung Brennstoffzelle)
KIER	Korea Institute of Energy Research
KIT	Karlsruhe Institute of Technology
LiMi	light microscope
LSC	lanthan-strontium-cobaltite
LSCF	lanthanum-strontium-ferrite cobaltite cathodes
LSM	lanthanum strontium manganese oxide: $La_{0.65}Sr_{0.3}MnO_3$
LT-PEFC	low temperature polymer electrolyte fuel cell
MATLAB	programming language for technical calculations
MCFC	molten carbonate fuel cell
MDS	middle destilates synthesis
MEA	membrane electrolyte assembly
MeOH	methanol
MEM-BRAIN	HGF project: Membrane technologies for clean coal-burning power plants (ger.: Membran-Technologien für saubere Kohlekraftwerke)
MGO	marine gas oil
MOR	Methanol Oxidation Reaction
MVEG	Motor Vehicle Emissions Group - New European Driving Cycle
NDIR	nondispersive infrared adsorption analyser
N.ERGHY	New European Research Grouping on Fuel Cells and Hydrogen
NIST	National Institute of Standards and Technology
NRW	North Rhine-Westphalia
OCV	Open Cell Voltage
O&M	Operating and Maintenance
OWI	Oel-Waerme-Institut
OXY-CLEAN	concept for CO_2 separation within power plant processes
OXY-VAC-JÜL	concept for CO_2 separation within power plant processes
OXYMEM	Project for CO_2 separation via membranes
PBI	polybenzimidazole
PBZ	Project Fuel Cells (ger.: Projekt Brennstoffzellen)
PEFC	Polymer Electrolyte Fuel Cell
PEM	Polymer Electrolyte Membrane
POF	program-oriented funding
PPs	Power Plants

PRO/II	process analysis software
PSC	process-specific criterion
pSOC	partial state of charge
PTFE	polytetrafluroethylene
PVD	physical vapor deposition
QA	quality assurance
QAS	quality assurance system
QM	quality management
QMS	quality management system
RAG	company name (ger.: Ruhrkohle Aktiengesellschaft)
REUN	efficient energy conversion and use program (ger.: Rationelle Energieumwandlung und –nutzung)
R&D	research and development
RuN-PEM	X-ray-based and neutron-based test methods for PEM fuel cells (ger.: Röntgen- und neutronenbasierte Untersuchungsmethoden für PEM-Brennstoffzellen)
RWE	a leading European electricity and gas company
RWTH	RWTH Aachen University (ger.: Rheinisch-Westfälische Technische Hochschule Aachen)
S++	Simlation Services, Murnau, Germany
SCT	segmented cell technology
SFC	company name: Smart Fuel Cells
SEM	scanning electron microscope
SPP	steam power plant
SRMS	magnetic imaging and mass spectroscopy
SOFC	solid oxide fuel cell
TG	thermogravimetrical analysis
TGA	thermogravimetry analyzer
TGA/DTA	Simultaneous thermal analyzer (ger.: Simultanes Thermoanalysengerät)
TMA	thermomechanical analysis
TOC	total concentration of total organic carbon
UFZ	Helmholtz-Zentrum für Umweltforschung
VA-RHLQ-01	database for documents with regard to quality management
VBZ	fuel cell process engineering
VDI Verlag	Publishing company (ger.: Verein Deutscher Ingenieure)
WBZU	Fuel Cell Education and Training Centre, Ulm (ger.: Weiterbildungszentrum Brennstoffzelle Ulm)
WGS	water-gas shift reactor
WGS-MR	water-gas shift membrane reactor
WHEC	World Hydrogen Energy Conference
WILEY-VCH	Publishing company (ger.: WILEY-Verlag Chemie)
WHG	managing water resources
WTW	well-to-wheel
YSZ	yttria-stabilized zirconia
ZAT	Central Technology Division (ger.: Zentralabteilung Allgemeine Technologie)

ZBT	The Fuel Cell Research Center (ger.: Zentrum für Brennstoffzellentechnik)
ZeuS	SOFC stack development project

Band / Volume 135
Untersuchung der Ladungsträgerkonzentration und -beweglichkeit in mikrokristallinen Siliziumlegierungen mit Hall-Effekt undThermokraft
C. Sellmer (2012), 159 pp.
ISBN: 978-3-89336-778-8

Band / Volume 136
Development of thin film inorganic membranes for oxygen separation
H. J. Moon (2012), XII, 118 pp.
ISBN: 978-3-89336-781-8

Band / Volume 137
Influence of Material and Testing Parameters on the Lifetime of TBC Systems with MCrAlY and NiPtAl Bondcoats
P. Song (2012), V, 126 pp.
ISBN: 978-3-89336-783-2

Band / Volume 138
Strömungsmechanische Modellierung eines Brenngaserzeugungs-systems
F. Scharf (2012), vi, 223 pp.
ISBN: 978-3-89336-784-9

Band / Volume 139
Clouds and aerosol in infrared radiative transfer calculations for the analysis of satellite observations
S. Grießbach (2012), viii, 169 pp.
ISBN: 978-3-89336-785-6

Band / Volume 140
Untersuchung zum Thin Film Low Pressure Plasma Spraying (LPPS-TF) Prozess
A. Hospach (2012), 165 pp.
ISBN: 978-3-89336-787-0

Band / Volume 141
Development of thermal spray processes with liquid feedstocks
A. Guignard (2012), 128 pp.
ISBN: 978-3-89336-788-7

Band / Volume 142
Herstellung uranbasierter Keramiken mittels interner Gelierung zur Konversion trivalenter Actinoiden
H. Daniels (2012), 154 pp.
ISBN: 978-3-89336-794-8

Band / Volume 143
Experimental and numerical studies on solute transport in unsaturated heterogeneous porous media under evaporation conditions
M. Bechtold (2012), xviii, 131 pp.
ISBN: 978-3-89336-795-5

Band / Volume 144
Konzept und Kosten eines Pipelinesystems zur Versorgung des deutschen Straßenverkehrs mit Wasserstoff
D. Krieg (2012), 228 pp.
ISBN: 978-3-89336-800-6

Band / Volume 145
Mechanistic studies on the OH-initiated atmospheric oxidation of selected aromatic hydrocarbons
S. Nehr (2012), viii, 129 pp.
ISBN: 978-3-89336-804-4

Band / Volume 146
Electron Spin Resonance Investigation of Semiconductor Materials for Application in Thin-Film Silicon Solar Cells
L. Xiao (2012), VIII, 147 pp.
ISBN: 978-3-89336-805-1

Band / Volume 147
Untersuchungen zum Sicherheits- und Transmutationsverhalten innovativer Brennstoffe für Leichtwasserreaktoren
O. Schitthelm (2012), V, 150 pp.
ISBN: 978-3-89336-806-8

Band / Volume 148
IEK-Report 2011. Klimarelevante Energieforschung
(2012), ca. 250 pp.
ISBN: 978-3-89336-808-2

Band / Volume 149
IEK-Report 2011. Climate-Relevant Energy Research
(2012), 238 pp.
ISBN: 978-3-89336-809-9

Institute of Energy and Climate Research – Fuel Cells (IEK-3)

IEK-3 is one of nine sub-institutes within the Institute of Energy and Climate Research at Forschungszentrum Jülich GmbH. IEK-3 aims to conduct research of social, ecological and economic relevance and thus generate groundbreaking results on an international level. This quality of work is achieved through basic research in close coordination with technical development work in relevant scientific and technical fields of expertise. Special significance is attached here to international cooperations with partners from research and industry.

By implementing research results in innovative products, procedures and processes in cooperation with industry, IEK-3 hopes to help bridge the gap between science and technology. Cooperation with universities, universities of applied sciences, training departments and training centers is designed to promote opportunities for further education and training.

With a staff of approximately 100, IEK-3 concentrates on the basic topics of electrochemistry and process engineering for fuel cells. In an integrated approach, the four key areas worked on in the institute – direct methanol fuel cells, high-temperature polymer electrolyte fuel cells, solid oxide fuel cells and fuel processing systems – are accompanied by systems analysis and theoretical investigations, basic modeling and simulations, and by experimental and theoretical systems evaluations. The information generated in these areas is used to design and verify functional systems. In addition, particular attention is given to the development, configuration and application of special measuring techniques for the structural analysis of membrane electrode assemblies, for flow simulation and visualization, and for the characterization of stacks.

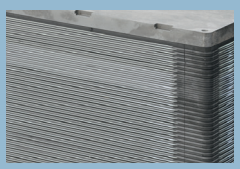

The solid oxide fuel cell (SOFC) stack pictured comprises 36 cells, each with an active cell area of 360 cm². The nominal power at a mean cell voltage of 800 mV is approximately 5.5 kW. The stack is operated on natural gas, which is directly reformed on the anode to hydrogen and CO.

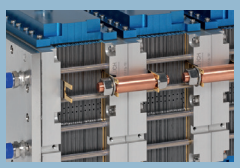

The high-temperature polymer electrolyte fuel cell (HT-PEFC) stack pictured comprises a total of 30 cells. With an active cell area of 320 cm², the maximum electric power is approximately 2 kW. Two distinctive features are the modular construction and the split bipolar design with integrated temperature control.

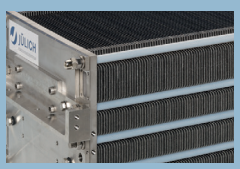

The direct-methanol fuel cell (DMFC) stack pictured is part of a hybrid system that will replace batteries in the light traction sector. The nominal electric power is 1.3 kW (peak: 3 kW). The stack comprises 90 cells, each with an active area of 315 cm². The bipolar plates are made of expanded graphite. The cathodic pressure loss is less than 2 mbar, thus allowing the use of an air compressor to supply air.

Energie & Umwelt / Energy & Environment
Band / Volume 149
ISBN 978-3-89336-809-9

JÜLICH
FORSCHUNGSZENTRUM